



Assessing the Wind Energy Potential in Bangladesh

Enabling Wind Energy Development
with Data Products

Mark Jacobson, Caroline Draxl, Tony Jimenez, and Barbara O'Neill
National Renewable Energy Laboratory

Taj Capozzola
Harness Energy

Jared A. Lee, Francois Vandenberghe, and Sue Ellen Haupt
National Center for Atmospheric Research

Technical Report
NREL/TP-5000-71077
September 2018

A product of the USAID-NREL Partnership
Contract No. IAG-17-2050

NOTICE

This work was authored in part by the National Renewable Energy Laboratory, operated by Alliance for Sustainable Energy, LLC, for the U.S. Department of Energy (DOE) under Contract No. DE-AC36-08GO28308. Funding provided by the United States Agency for International Development (USAID) under Contract No. IAG-17-2050. The views expressed in this publication do not necessarily represent the views of the DOE or the U.S. Government including

This report is available at no cost from the National Renewable Energy Laboratory (NREL) at www.nrel.gov/publications.

U.S. Department of Energy (DOE) reports produced after 1991 and a growing number of pre-1991 documents are available free via www.OSTI.gov.

NREL prints on paper that contains recycled content.

Cover photo: Meteorological tower installed at Rajshahi, Bangladesh. Photo from Harness Energy

Acknowledgments

We would like to extend a special thank you to the USAID Bangladesh Mission—Sher Khan, Shayan Shafi, Karl Wurster, and Kerry Reeves—for invaluable guidance and support and to the project team from the Government of Bangladesh—Bazlur Rahman, Md. Atiqur Rahman, and team—for consistent assistance with travel logistics, intergovernmental communications, and landowner relations. Without their devotion to the project’s success, we could not have completed this work. We would also like to thank Jennifer Leisch of USAID Washington for her guidance and support throughout this project.

Special thanks to Harness Energy LLC, which installed all nine of the meteorological stations across Bangladesh. Enduring unique installation challenges with the environment and effectively communicating with government officials, local leaders, landowners, and subcontractors ensured successful implementation of the measurement equipment. Thanks to Ben Schloesser, Wade Grewe, and Will Everhart for their work. We also thank Sarfarez Ahmed for assistance with numerous in-country challenges.

We extend our gratitude to the National Center for Atmospheric Research (NCAR) team—in particular Wanli Wu—for their major contribution to the modeling part of the project. Their expertise, work, and willingness to help access NCAR’s computing resources were invaluable for the successful completion of this report.

We would like to acknowledge the use of computational resources at NCAR-Wyoming Supercomputing Center, provided by the National Science Foundation and the State of Wyoming and supported by NCAR’s Computational and Information Systems Laboratory.

The boundary conditions for the modeling were provided by the Data Support Section of the Computational and Information Systems Laboratory at NCAR. NCAR is supported by grants from the National Science Foundation.

We also thank the following people: Billy Roberts from the National Renewable Energy Laboratory (NREL) for creating the wind resource maps; Ted Kwasnik, Paul Edwards, and Michael Rossol from NREL for help with data analysis and the Renewable Energy Data Explorer; and Heidi Tinnesand from NREL for her support with data analyses.

List of Acronyms

ADP	Asia Development Bank
AGL	above ground level
CFSR	Climate Forecast System Reanalysis
ECMWF	European Centre for Medium-Range Weather Forecasts
ERA-Interim	European Re-Analysis Interim
FDDA	Four-Dimensional Data Assimilation
GFS	Global Forecast System
GIS	geographic information system
GOB	Government of Bangladesh
GOB-PD	Government of Bangladesh, Power Division
IEC	International Electric Commission
MAE	mean absolute error
ME	mean error or bias
MERRA	Modern Era Reanalysis for Research and Applications
MET	meteorological
MYJ	Mellor-Yamada-Janjic
NCAR	National Center for Atmospheric Research
NCEP	National Centers for Environmental Prediction
NREL	National Renewable Energy Laboratory
NWP	numerical weather prediction
PBL	planetary boundary layer
QC	quality control
QF	quality factor
RE Data Explorer	Renewable Energy Data Explorer
RFP	request for proposal
RMSE	root-mean-square error
SODAR	sonic detection and ranging
SOM	self-organizing map
USAID	United States Agency for International Development
UTC	Coordinated Universal Time
WMO	World Meteorological Organization
WRF	Weather Research and Forecasting
YSU	Yonsei University

Executive Summary

USAID Bangladesh and the U.S. Department of Energy's National Renewable Energy Laboratory partnered with the Government of Bangladesh to develop a national wind resource assessment. The assessment used sophisticated resource modeling that was validated by a ground measurement campaign. Results from the project included a long-term, correlated wind data set; validated high-resolution wind resource maps; and publicly available data accessible through the RE Data Explorer (<https://www.re-explorer.org/>). The Renewable Energy (RE) Data Explorer allows users to access and download the Bangladesh wind resource assessment data and related geographic information system (GIS) data sets and perform customized technical potential analyses. Figure ES-1 is an example wind resource map for Bangladesh that can be created with the RE Data Explorer.

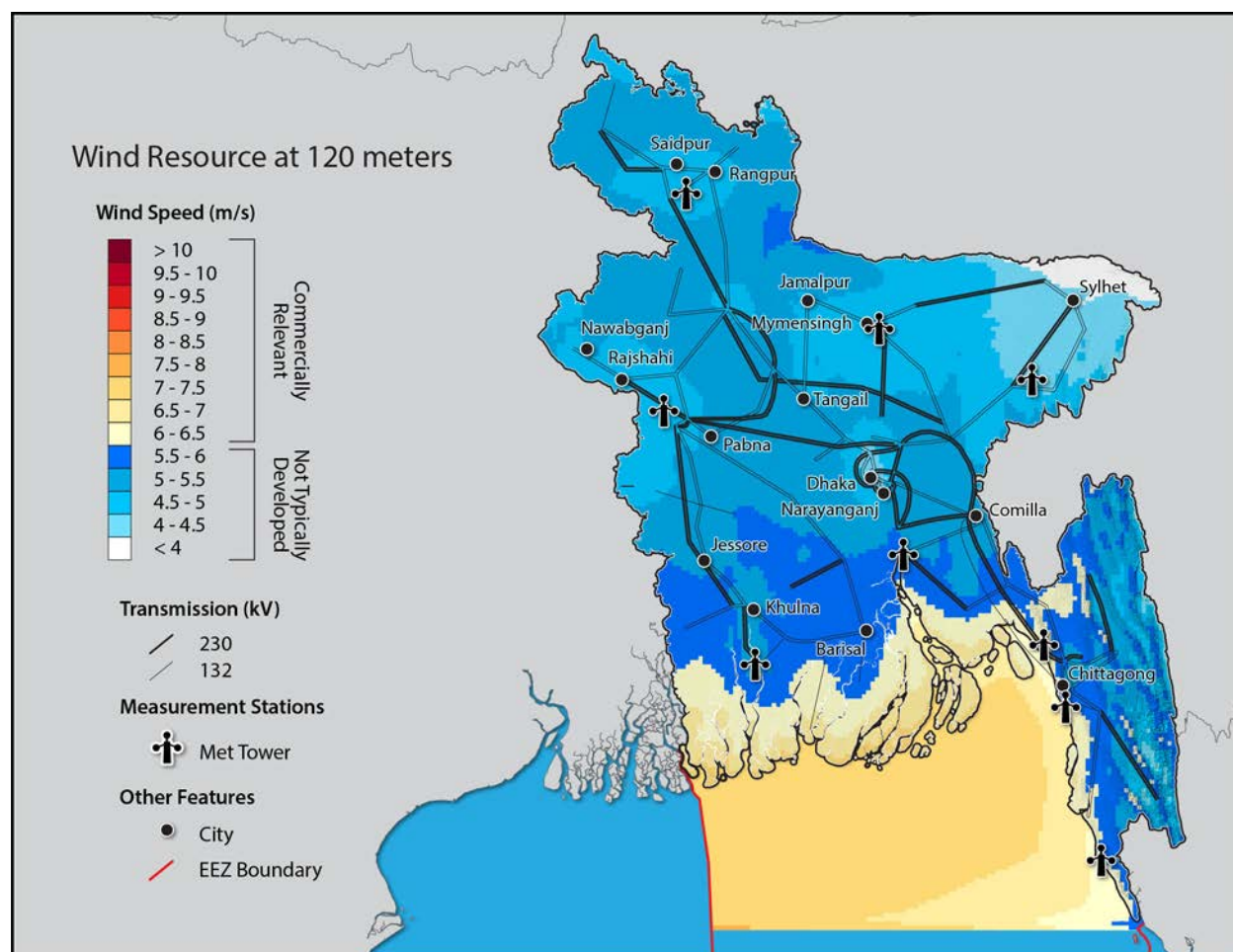


Figure ES-1. Wind resource map of Bangladesh and measurement locations

This project improved upon existing global data sets by using best-in-class modeling techniques and analysis. Global models are good first steps in predicting wind resources in various parts of the world, but they do not generate the accuracy needed to reduce project risk and stimulate renewable investment. This project improved the quality of modeled wind resource data for Bangladesh. In addition to the modeling effort, the project team used a multi-year, local data-collection campaign to validate the model and further improve the accuracy of the data sets. The measurement campaign consisted of nine meteorological sites representing all geographical regions of the country. Seven meteorological towers and one remote-

sensing, sonic detection and ranging unit (deployed at two sites) collected the data. Site-selection criteria focused on geographic diversity and proximity to existing transmission lines. Figure ES-1 shows measurement locations. The measurement campaign spanned June 2014 through December 2017.

The results of the Bangladesh wind resource assessment will help Bangladesh overcome significant energy challenges. Its energy sector suffers from power shortages, increasing demand, decreasing domestic natural gas reserves, and inadequate transmission infrastructure. As part of a comprehensive plan to overcome these challenges, Bangladesh has committed that 10% of the total generation capacity will be renewable energy by 2021 (Power Division 2016). High-quality renewable energy resource data and other GIS data, such as those developed in this assessment, are important if Bangladesh wishes to reach its 10% renewable energy capacity target. These data support informed decision making, ranging from policy and investment decisions to reliable power sector planning. Specifically, the Bangladesh wind resource assessment will help reduce technical risk and encourage private-sector interest in the nascent wind market in Bangladesh. In addition, the Government of Bangladesh may use the results of the wind resource assessment to develop well-designed policies that could encourage investment in wind energy.

This report provides a comprehensive description of the Bangladesh wind resource assessment, including details on the modeling approach and methods, instrumentation, data quality-control techniques, and resulting data sets.

Table of Contents

1	Introduction	1
1.1	Wind Resource Assessment Scope	1
1.2	Using Data Products to Expand Market Opportunities for Wind	3
2	Approach	5
3	Siting	9
3.1	Measurement Site Selection	9
3.1.1	Step 1. Desktop Analysis	9
3.1.2	Step 2. Micrositing	11
3.1.3	Step 3. Land Lease	12
3.2	Landowner/Community Relationships	12
4	Instrumentation	14
4.1	Tower Evaluation and Selection	14
4.2	Sensor Evaluation and Selection	18
4.2.1	Horizontal Wind Speed	19
4.2.2	Wind Direction	20
4.2.3	Mounting	20
4.2.4	Air Temperature	21
4.2.5	Barometric Pressure	22
4.2.6	Relative Humidity	22
4.2.7	Solar Insolation	22
4.3	Data Logger and Communications	23
4.4	Remote Sensing	24
5	Data Collection, Quality Control, and Preparation for Modeling	26
5.1	Data Collection, Transmission, and Recovery	27
5.1.1	Data Collection	27
5.1.2	Data Transmission	27
5.1.3	Data Recovery	27
5.2	Data Quality Control	29
5.2.1	Tower Shadow	29
5.2.2	Consistency Checks (Sensor Pair Comparison)	30
5.2.3	Instrument Failure	31
5.2.4	Corrected Transfer Function	31
5.2.5	QC Data Flagging	31
5.3	Data Preparation for Modeling	31
6	Modeling the Wind Resource in Bangladesh	34
6.1	Numerical Weather Prediction Simulations	34
6.2	Reanalysis Data Sets	35
6.3	Simulation Method	36
6.4	Sensitivity Study	38
7	Results	40
7.1	Validation of the Model Simulations	40
7.1.1	Validation Methodology	40
7.1.2	Value of Assimilating NREL Special Observations	41
7.1.3	Validation Results	45
7.2	Extension of 3-Year Simulations to 15 Years to Create a Long-Term Reference	49
8	Products/Tools	54
8.1	Measured Data Sets	54
8.2	Maps	56
8.3	Modeled Data Sets	57

8.4 Renewable Energy Data Explorer	58
9 Conclusions	62
References.....	64
Appendix.....	67

List of Figures

Figure ES-1. Wind resource map of Bangladesh and measurement locations.....	iii
Figure 1. Connections across geospatial data, analyses, and decisions to support renewable energy development.....	4
Figure 2. Low-resolution wind map, circa 1980s.	5
Figure 3. High-resolution wind map, circa 2010.	6
Figure 4. The project’s approach of using observational data to inform the model simulations.	8
Figure 5. Layout for the Sitakunda tower	12
Figure 6. Site visit to Mongla.	13
Figure 7. Abdullah (left), engineer at Construction BD, and Ifteekhar Ayub (right), president of Construction BD.	15
Figure 8. 80-m tower at Rajshahi.	15
Figure 9. Safety training seminar in Dhaka.	16
Figure 10. Hard hat notice.	17
Figure 11. Local tower technician working on the tower in Sitakunda.	17
Figure 12. Typical MET tower configuration with sensors attached to boom extensions.	19
Figure 13. Anemometer at Mymensingh.	19
Figure 14. Wind vane at Rajshahi.	20
Figure 15. Mounting boom testing.....	21
Figure 16. Temperature sensor at Chandpur	21
Figure 17. Insolation sensor at Mymensingh.	22
Figure 18. Typical base configuration at Mymensingh.	23
Figure 19. Enclosure with data logger.	23
Figure 20. Transporting Triton to the Rajshahi platform.	24
Figure 21. Triton deployed at Rajshahi.....	24
Figure 22. Triton deployed at Inani Beach.	25
Figure 23. Overview of data collection, quality control, and preparation for modeling.....	26
Figure 24. Data recovery.....	28
Figure 25. Tower shadow	30
Figure 26. Sensor pair comparison	30
Figure 27. Visual data inspection at Rajshahi.....	31
Figure 28. Schematic for the concept of NWP models.....	34
Figure 29. WRF simulation domain setup	37
Figure 30. Schematic demonstrating the nudging technique	38
Figure 31. Scatterplots of WRF versus observed wind speed at the NREL MET tower locations.....	41
Figure 32. Scatterplots of WRF versus observed wind speed at the NREL SODAR locations.....	42
Figure 33. Scatterplots of WRF versus observed wind speed at the WMO radiosonde locations between 10 m and 200 m AGL	42
Figure 34. Scatterplots of WRF versus observed wind speed at the NREL SODAR locations at 80-m AGL height only	43
Figure 35. Binned histograms at the NREL MET tower locations	44
Figure 36. Binned histograms at the NREL SODAR locations	44
Figure 37. Binned histograms radiosondes	45
Figure 38. Annual cycle of mean wind speed.....	46
Figure 39. Annual cycle of the ME (bias).....	46

Figure 40. Annual cycle of the RMSE.....	47
Figure 41. Wind roses at the Rangpur SODAR.....	48
Figure 42. Wind roses at the Rajshahi MET tower.....	48
Figure 43. Wind roses at the Sitakunda MET tower.....	49
Figure 44. Wind roses for most representative regimes identified during the classification.....	51
Figure 45. Wind roses for regimes downscaled with the WRF model to 3-km grid spacing.....	52
Figure 46. Four most frequently occurring 200-m wind regimes.....	53
Figure 47. Bangladesh’s wind resource map at 120 m.....	57
Figure 48. RE Data Explorer sample analysis.....	59
Figure 49. RE Data Explorer sample analysis identifying excluded zones and promising zones.....	60
Figure 50. RE Data Explorer sample analysis with detailed information for one cell.....	60
Figure 51. RE Data Explorer sample analysis with available query delimiters.....	61
Figure 52. Illustrative map showing Bangladesh’s wind resources at 120 m (left) and 160 m (right).....	61

List of Tables

Table 1. Wind Resource Assessment Approaches.....	2
Table 2. Bangladesh Measurement Sites.....	9
Table 3. Typical Tower Instrumentation.....	18
Table 4. Data Recovery.....	28
Table 5. Explanations for Major Data Gaps.....	29
Table 6. Data Preparation for Modeling (Tower).....	32
Table 7. Data Preparation for Modeling.....	33
Table 8. Evaluated Reanalysis Data Sets, Origin, Resolution, and Available Period.....	36
Table 9. Error Metrics for Wind Speed, Wind Direction, Temperature, and Relative Humidity for the Experiments in the Sensitivity Study.....	39
Table 10. Dates and Times of the Most Representative Regimes for 200-m Hourly Wind Vectors at the 29 x 32 Grid Points of WRF Domain 1 (27 km) Covering Bangladesh.....	50
Table 11. Raw Data.....	55
Table 12. Processed Data Files.....	56
Table 13. Modeled Data Available via the RE Data Explorer Tool and Globus Connect.....	58

1 Introduction

Bangladesh is one of the most densely populated countries in the world, with more than 160 million people living in an area the size of the U.S. State of Louisiana. Approximately 64% of the population has access to electricity, and the price of energy is subsidized. With limited natural gas resources waning and a costly energy subsidy system, the Government of Bangladesh (GOB) is evaluating multiple paths to ensure reliable and affordable power. Under its 2016 Power System Master Plan, Bangladesh set a goal to generate 50% of its electricity from coal by 2030. An alternative path being evaluated by the GOB involves identifying, quantifying, and exploiting the country’s domestic renewable energy resources to support the 2016 Power System Master Plan’s goal of generating 10% of electricity from renewable energy by 2021. In support of this low-emission development strategy, this project seeks to unlock one natural resource that has been largely unexplored in Bangladesh—wind.

One of the prime challenges to the expanded use of wind and other renewable energy technologies globally is understanding regional renewable energy potential. The variable nature of the wind resource and its strict location dependency impose additional—and often new—challenges compared with traditional energy technologies. Annual wind maps developed for Bangladesh over the last 15 years have been useful in demonstrating national wind potential, but the measurement and modeling methodologies used to create these maps do not adequately represent the wind resource available to modern wind turbines. Consequently, they are not sufficiently rigorous to attract investors and spur growth in the wind technology sector. Today’s much more sophisticated tools and techniques, such as validated wind resource models based on years of actual wind data measured at turbine hub height, reduce uncertainty and generate a wealth of data products—including annual, monthly, seasonal, and hourly wind-distribution data and annual wind-speed maps—needed to attract private and government investment. This partnership between the United States Agency for International Development (USAID) and the National Renewable Energy Laboratory (NREL) is helping the GOB use state-of-the-art methodologies to collect and analyze detailed, regional wind resource data that will pave the way for future wind power deployment.

1.1 Wind Resource Assessment Scope

Since 2011, the USAID Bangladesh Wind Resource Assessment Project has provided technical assistance to support the GOB’s goal of promoting wind development as a low-emission, domestic energy resource that will meet growing energy needs and stimulate rural economic development within the country. Assessing the deployment of utility-scale wind technologies requires a large investment in measurement campaigns and a high level of technical knowledge to identify and prioritize potential development opportunities. Wind experts from NREL worked with GOB experts and partners to install, operate, and maintain state-of-the-art wind-measurement systems in nine strategic and geographically diverse locations across Bangladesh. Once these measurement systems became operational, over 3 years of wind data were collected and put through a rigorous quality-control (QC) process. The results of the data collection were used to validate a sophisticated (and open-source) weather-prediction model. To ensure generation of investment-quality wind resource data, the project team used internationally recognized best practices and state-of-the-art measurement and modeling tools to assess Bangladesh’s coastal and inland wind power potential.

Table 1 outlines tasks and best practices in wind measurement and how these have been applied in Bangladesh. The fourth column describes how these practices and data contribute to better policy design, reduced risk for investors and developers, and more efficient and accurate project siting.

Table 1. Wind Resource Assessment Approaches

Task	Best Practice	Wind Resource Assessment Project	Role in Advancing Growth in the Bangladesh Wind Sector
Identify wind-measurement sites	Available wind and meteorological (MET) data and models are used to create a preliminary wind resource assessment map. This provides an initial indication of potential wind speeds and direction and seasonal wind variability and can be used to identify appropriate sites for more detailed wind measurement.	Nine sites were selected for collecting wind measurements based on these criteria: potential reflected in existing wind resource maps, proximity to transmission lines, geographic diversity, and developability (as determined by individuals experienced with wind development, modeling, and MET tower installation).	With relatively few wind farms in operation in Bangladesh, measurement sites were selected to ensure an accurate national wind map but also target zones where access to existing transmission would be optimized. Engagement with the GOB and local partners in this effort raised awareness for local policymakers to understand the potential for wind opportunities.
Perform multi-year wind measurement campaign	Instrumented MET towers and remote-sensing equipment are used to gather wind resource data at various heights at selected sites across a region. One to three years of actual wind data (wind speed and direction) are required to validate preliminary modeling results and confirm viability of potential project sites.	Once wind measurement equipment was installed, 2 years of measured wind resource data (at heights of 20–200 m) were collected from nine MET sites strategically located across the country. Measuring wind speeds at the turbine rotor’s hub height and beyond (up to 200 m) using remote-sensing equipment reduces uncertainty in annual energy production forecasts.	Modern, utility-scale wind turbines access wind resources at hub heights of 80 m and higher. Wind shear data at multiple hub heights allow for better system design to maximize power production based on turbine type and height. Higher hub height data often reveal much greater wind resource potential at any given location that is attractive to both developers and potential investors (DOE 2013, Global Energy Concepts 2005).
Model the regional wind resource and generate data-rich wind resource products	Computer models based on historical data on atmospheric conditions combined with actual measured wind data are used to update regional wind resource assessments. These wind resource models provide an overview of the climatological wind conditions of a region (e.g., wind speeds, direction, and seasonal variability) and are useful as a screening tool for the identification and preliminary evaluation of potential wind project sites.	A national wind resource model was created based on the state-of-the-art global Weather Research and Forecasting (WRF) model and adapted for wind forecasting applications. The resulting web-based access to diverse data sets will enable industry analysis, integration into other models and tools, and development of visualization products for policy analysis.	The data products generated from a Bangladesh wind resource model provide a wealth of information, including annual, monthly, and hourly climate data such as wind speed, shear, frequency distribution, and air density. These detailed data sets enable system operators to forecast how the developed resource will address seasonal demand and other grid-integration issues. Developers and investors are better able to define the capacity values of potential power plants, improving the economic analysis of the project. As the industry matures and the developers/investors make decisions about where to invest capital, markets that have more information to answer such questions surrounding grid integration and economic value will be more attractive.

1.2 Using Data Products to Expand Market Opportunities for Wind

High-quality renewable energy resource data and other geographic information system (GIS) data are essential for the transition to a clean energy economy that prioritizes local resources, improves resiliency, creates jobs, and promotes energy independence. These data are crucial for making informed decisions—ranging from policy and investment decisions to reliable power sector planning. Decisions that are data driven reflect appropriate ambition, maximize cost effectiveness, and enable successful implementation of renewable energy investments. Renewable energy resource assessment and techno-economic analysis can help inform integrated power sector planning, policymaking, and investment opportunities. Figure 1 provides an overview of the connections across geospatial data, analyses, and decisions to support renewable energy development that are described in this report.

For the project development and finance sector, the risk-return profile of a project is the key determinant of whether a project should be financed or not. Project developers, lenders, and investors want to make a return proportional to the level of risk they undertake. Quantifying and managing the elements of risk (political, technical, commercial) associated with renewable energy projects, particularly in developing countries, represents a key challenge in obtaining financing. Because Bangladesh is in the relatively early stages of wind market development, improved resource data will specifically address aspects of technical risk by providing improved insight on the actual wind potential with a significant degree of temporal and spatial detail. While potential political risk is much harder to measure or address through a technical program like this wind measurement campaign, commercial risk is also mitigated through improved access to high-quality data that may allow for power-purchase agreements and financing arrangements to be negotiated on a more transparent basis using data that all partners agree are valid.

The Bangladesh Wind Resource Mapping Project is helping to reduce the development and investment risk by providing high-quality comprehensive wind resource data products needed to encourage public- and private-sector wind energy development and increase investor confidence in the viability of wind energy projects. The validated high-resolution wind maps and associated data products will provide the tools for wind developers looking to find opportunities, reduce wind prospecting timelines, and demonstrate to government officials the wind potential that might aid in future energy policy decisions. Specifically, the data products allow potential developers to conduct detailed pre-feasibility studies, focused on evaluating how the wind resource in a particular region matches up with the local utility's seasonal demand, generating credible estimates of wind production, and predicting the overall potential of a site. Positive results from these studies can be used to justify further investments in project-specific, on-the-ground wind resource assessments, expediting the development process and stimulating the wind market.

Over the long term, the improved wind data products will reduce development risk, increase public and private stakeholder confidence in wind energy projects, and expand potential opportunities for wind power by providing the data needed to evaluate wind projects and incorporate wind resources into a national energy strategy.

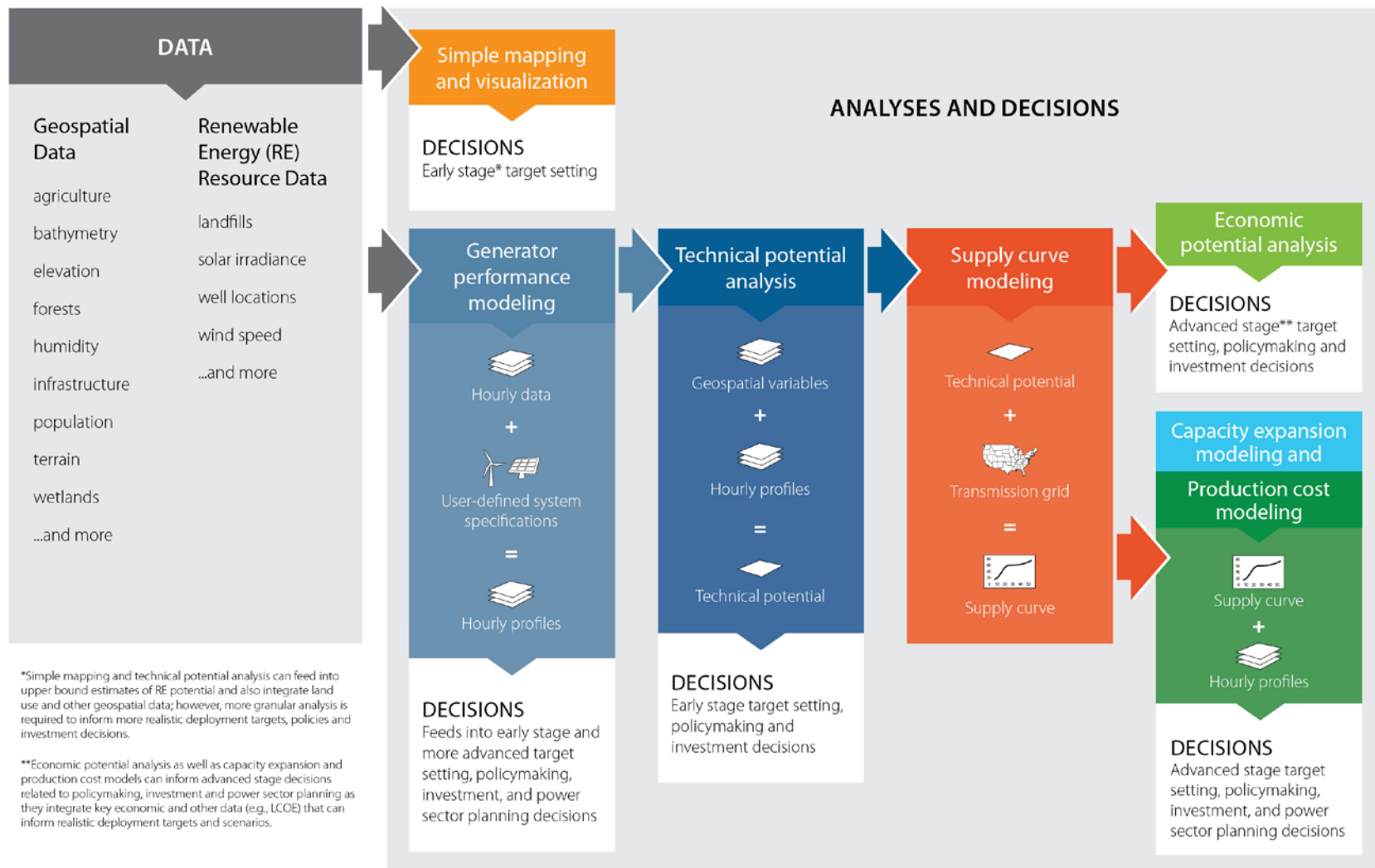


Figure 1. Connections across geospatial data, analyses, and decisions to support renewable energy development

2 Approach

Wind resource estimates can be developed in several ways (Clifton et al. 2018). Historically, static maps have been created to show the wind resource across a region. Wind maps are a common tool for providing resource data for a given area to governments, private companies, stakeholders, and the public. Wind maps can help wind farm developers identify potentially promising locations, aid utilities with long-range planning, and assist governments in formulating policy.

The first generation of wind maps—created in the 1970s and 1980s—suffered from low resolution. Figure 2 is an example. Starting around 2000, higher-resolution wind maps provided greatly increased resolution and accuracy (Figure 3). Despite the improved resolution and accuracy, the utility of wind maps (at least those that were publicly available) was somewhat limited because they were static. Another significant limitation was that the wind resource portrayed with these static representations was at a lower elevation above ground level (AGL) relative to modern turbine hub heights.

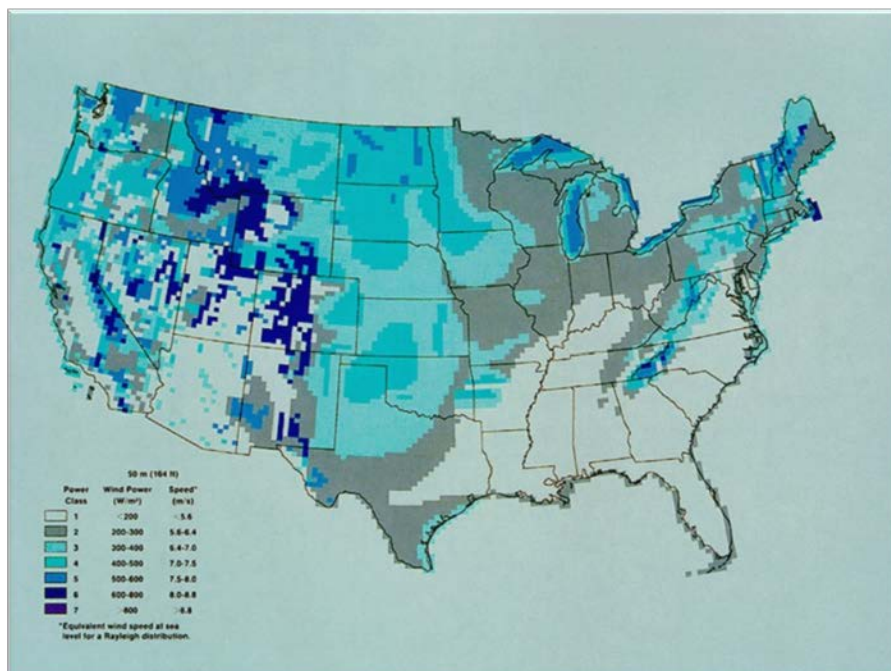


Figure 2. Low-resolution wind map, circa 1980s.
(Elliott et al. 1986)

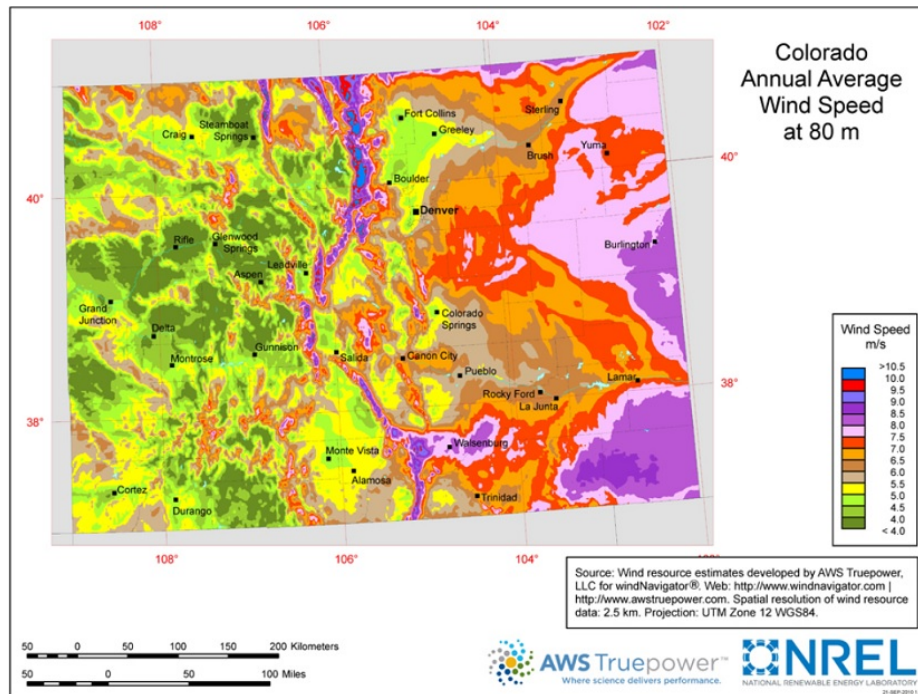


Figure 3. High-resolution wind map, circa 2010.
(AWS Truepower and NREL 2010)

To best support wind energy development, facilitate prospecting by developers, and enable grid-integration studies, high-resolution spatial and temporal data sets are needed. A best practice is the use of GIS tools that combine wind resource data with other data layers. These GIS-based tools—of which the Renewable Energy Data Explorer (RE Data Explorer) for Bangladesh is an example (see Section 8.4)—enable users to dynamically explore and display wind data in conjunction with other data, such as electrical transmission infrastructure, populated areas, political boundaries, and environmentally sensitive areas.

Usually wind resource estimates are created by combining observations and simulated data. Because observations at common wind turbine hub heights (80 m and higher) were not previously available in Bangladesh, NREL acquired a limited number of measurement systems—seven wind towers and one sonic detection and ranging unit (SODAR) that was mobilized at two sites—and strategically deployed them across Bangladesh (see Section 4). Even though observations provide “ground truth” measurements for their location and for the monitoring period, they are sparse and available only at certain locations that might or might not be representative of the regional wind climate. Monitoring data at a specific site over a certain period might not reflect the long-term wind resource. Thus, modeled wind speeds are utilized to provide an estimate of the wind resource over a region for an extended period.

To meet the objective of assessing long-term wind resources in Bangladesh, we used both observations and high-resolution simulations to create a high-resolution data set that achieves the current state of the art in resource data sets. The modeling team conducted modeling and analysis of the long-term annual, monthly, and daily wind resources. We further quantified the model uncertainty by validating the model-based wind resource with measurements collected over a 3-year period. Uncertainty estimates provide decision support for stakeholders, such as government agencies, investors, and private developers. Finally, we statistically expanded the 3-year model simulations to a 15-year data set. The resulting fine-scale climatology, with its known associated uncertainty, provided valuable material for a new assessment of Bangladesh wind resources.

More specifically, the team created high-resolution (3-km) wind resource data sets with the WRF model (Skamarock et al. 2008) during the 3-year period (2014–2017) for which wind tower observations were collected by NREL. We began with a detailed study of the WRF model performance in the region and a carefully designed model configuration tuned to local climate specificities, atmospheric features prevailing in Bangladesh, and wind energy applications. The National Center for Atmospheric Research (NCAR) WRF-based Four-Dimensional Data Assimilation (FDDA) is an efficient tool to generate large databases of atmospheric parameters at high resolution. The FDDA was applied to dynamically downscale a global reanalysis data set and create 3 years of hourly gridded data over Bangladesh at a 3-km grid resolution. Global reanalysis data sets are coarse data sets (~30 km to 100 km horizontal resolution) and freely available. To ensure accuracy, observational data (e.g., surface reports, radiosondes, aircraft reports, satellite winds) from NCAR’s historical database were used wherever available (i.e., India) along with the local observations in the regions of Bangladesh where NREL collected wind data. The observational data were input into the FDDA algorithm to constantly nudge the model analysis toward observations (more detail is provided in Section 6). To extend the 3-year modeled wind data to a 15-year period, the self-organizing map (SOM) clustering method was applied to both the long-term global reanalysis data set and the FDDA simulations. The correlation between the synoptic situations identified in the global reanalysis with the regional weather regimes found in the FDDA data was assessed by using SOMs.

The methods used to create the wind resource estimate for Bangladesh are open and freely available. The high-resolution wind resource data are publicly available through interactive maps in the RE Data Explorer toolkit¹ and through download with Globus Connect² (Section 8). The measured data are available through the RE Data Explorer. Figure 4 illustrates how the project’s approach of using observational data to inform the model reduces the uncertainty in the final data set.

¹ For access to the RE Data Explorer, please visit <https://www.re-explorer.org/bangladesh-data.html>.

² For access to Globus Connect, please visit www.globus.org.

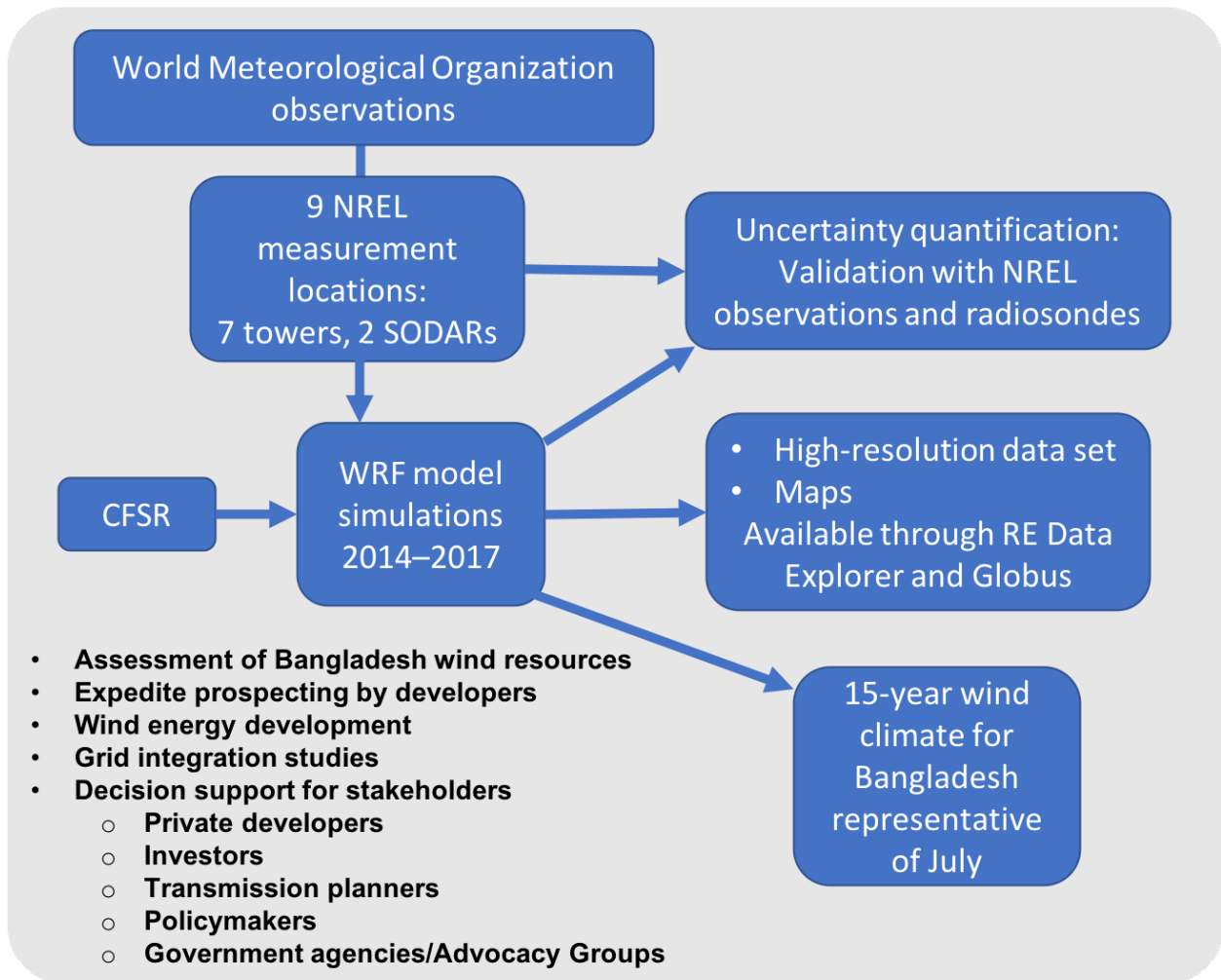


Figure 4. The project’s approach of using observational data to inform the model simulations.
The applications of the data product are bulleted in the lower left. CFSR = Climate Forecast System Reanalysis data set.

3 Siting

Meteorological (MET) towers were placed across the country for this measurement process and to support and enhance the modeling of the wind resource over Bangladesh. Having measurements for this effort is crucial to model wind resources more accurately. The modeling is only valuable if the errors are known. To have confidence in the collected data and create a high-quality wind resource data set and accurate wind prospecting tools, it is important to start with high-quality inputs from the instrumentation. The first step to creating high-quality input is appropriately siting the data-collection equipment.

Altogether, this campaign included seven MET towers and one SODAR instrument that collected measurements at two sites for 1 year each. Six of the MET towers are 80 m tall, and one is 60 m tall. The location of each tower and the two SODAR locations are provided in Table 2.

Table 2. Bangladesh Measurement Sites

Site	Site Type	Installation Date	Monitoring End Date	Latitude (N)	Longitude (E)
Rajshahi	80-m Tower	06/11/14	12/20/2017	24.17035	88.90734
Chandpur	80-m Tower	06/11/14	12/04/2017	23.21116	90.64237
Sitakunda	80-m Tower	12/18/14	12/20/2016	22.60416	91.6601
Parkay Beach	80-m Tower	12/24/14	07/14/2017	22.18513	91.81767
Mymensingh	80-m Tower	08/13/15	12/13/2017	24.71546	90.4668
Mirzapur	80-m Tower	10/19/15	11/22/2017	24.37778	91.57462
Mongla	80-m Tower	10/31/15	12/25/2017	22.47342	89.56826
Inani Beach Triton	SODAR	07/25/14	08/02/2015	21.14732	92.07575
Rangpur Triton	SODAR	08/05/15	04/19/2017	25.60641	89.06877

3.1 Measurement Site Selection

The process of determining the final locations for the towers and SODAR equipment began with a desktop analysis, was followed by micrositing in the field, and was concluded after final land-lease agreements were executed.

3.1.1 Step 1. Desktop Analysis

The first step in the site-selection process was a desktop analysis using computer-based mapping tools to determine potential site areas for further inspection. The desktop analysis began by superimposing layers that represented each level of the site-selection criteria to Bangladesh's map. After all layers were added to the map, it became more straightforward to identify the most effective locations (based on criteria noted below) for the modeling effort while continuing to meet the access and construction requirements for the installation and maintenance of the MET towers and remote-sensing equipment.

3.1.1.1 Selection Criteria

When considering the selection criteria for this project, three primary goals were established to inform the final list of layers used to isolate potential measurement locations.

1. Represent many geographic regions. The measurement sites should represent as many geographic regions of the country as possible and add as much value to the country-wide modeling effort as

possible. A key objective of the overall project was to create a resource tool that could be trusted to inform investment decisions accurately for Bangladesh. Knowing about low-wind-speed areas could be just as important as knowing about high-wind-speed areas if it reduced the potential for investment in underperforming projects.

2. Properly position the towers, considering terrain and nearby obstacles. Proper positioning minimizes air disturbance and improves the site-representativeness of the measured data. The locations must be capable of hosting the measurement asset and providing high-quality data. This meant meeting construction space requirements but limiting environmental impact, meeting established budgets, and ensuring that the area was safe for crews to stay and work. Where possible, the tower was located away from any significant trees or manmade obstacles. This was especially important if the tower was similar in height to the trees or obstacles nearby. Any obstacle at a height similar to that of the instrumentation has the potential to influence the speed and direction of the wind before it is measured. This could lead to a data set that misrepresents the available resource with undervalued wind speeds or overestimated turbulence.
3. Provide project areas with potential development. Go beyond the development of a wind resource data product for Bangladesh and provide areas of potential project development, assuming the wind speeds are sufficiently strong. A potential developer for any new wind site needs site data to verify investment decisions. Using site data from this project instead of setting up new measurement assets could reduce development costs and shorten development timelines. For the terrain, the sites were located in areas representative of future proposed turbine locations. If a proposed future wind project was located in an area having diverse slope angles, hills, and ridges, then it was important to place MET towers in several areas that represent the diversity of terrain present on the site. Additionally, to improve development potential, the sites were located near a utility-scale transmission line.

Considering these goals, a list of selection criteria was established to focus the search. The following factors were considered:

- **Geographic diversity.** Ideally, these sites would meet the diversity requirement, and all eight divisions of Bangladesh would receive at least one measurement site.
- **Proximity to major load centers.** Sites near city centers with the highest populations or major industrial zones (e.g., Dhaka, Chittagong, Sylhet, Jessore, Mymensingh) were prioritized in an attempt to match electricity supply to the areas with the greatest demand. This opened up the potential for distributed projects.
- **Proximity to existing high-voltage transmission.** The construction of transmission equipment can be cost prohibitive. The potential for utilizing existing transmission infrastructure could help those areas with lower wind speeds meet internal rate of return limits.
- **Primarily open areas.** To capture the best data, the sites had to be clear of obstructions, both natural and manmade. Areas near rivers, open agricultural zones, ocean shorelines, and ridgelines were considered.
- **Limited environmental impact.** Tree clearing and significant impact to the area beyond the disturbance necessary to install the measurement asset were avoided.
- **Sufficient tower area.** The clearing had to be large enough to accommodate the tower footprint.
- **Wind turbulence reduction.** The clearing in the north/south directions had to be large enough to provide uninhibited wind flow.
- **Access.** The existing roads had to be large enough to allow transport of crew and materials to and from the site.

- **Safety.** The area had to be physically safe for the crew.

After all of the criteria were applied, the remaining areas represented potential measurement locations that would be acceptable for project execution. With a target of nine measurement locations, the team needed to select nine areas from the map for further investigation.

A site area was selected in each division except Barisal. The Barisal Division posed some logistical challenges for construction. Given its close proximity to Khulna to the west and Chittagong to the east, the team decided that the Barisal site could be moved east without negatively affecting the overall modeling effort. The final site was placed in the Chittagong Division, along the coast further to the south. With most of the expected high winds coming from the south off the Bay of Bengal, it was important to make sure the coastline was well represented.

3.1.2 Step 2. Micrositing

After potential locations were targeted during the desktop analysis, a field team was deployed to inspect the sites, confirm the information that was identified during the desktop analysis, apply the next layer of more-detailed site requirements, and begin the process of establishing lease agreements (led by the GOB) with the landowners. During this process, the team was looking for the following:

- **Good exposure.** The available wind rose for these areas showed that the predominant winds come from the south in the summer and from the north in the winter. Thus, the areas to the north and to the south of the site had to be clear of obstructions to allow for uninterrupted wind flow from these predominant directions.
- **Clear area.** The open land area had to be large enough to host the footprint of the tower and guard house or the SODAR platform and guard house. It also had to allow for the orientation of the equipment to maximize the data availability and quality.
- **Access.** The site had to have existing transportation routes in place to allow vehicles to bring tower materials, concrete materials, and crew members to and from the site.
- **Appropriate land use.** Most of the open land in Bangladesh is used for agriculture or aquaculture activities. Land used for rice cultivation is flooded during the summer months but dry during the winter months. Land used for fish farming is flooded year-round. Land used for tea or fruit farming is often dry year-round. It is difficult to use satellite imagery to determine how the land is used or how conditions change seasonally at that specific location. Ideally, the site area had to be dry for most of the year for construction and continued site access.
- **Safety.** There are inherent risks of working in Bangladesh that applied to the entire project, but each site could pose a unique set of risks. It was important that each site was free from aggressive or dangerous wildlife and that the area was politically stable, supported the project, and was hospitable for a team from the United States.
- **Minimal number of landowners.** The land area for the tower footprint (base and anchors), the guard house, and the access right of way often covered the land owned by more than one entity. For fewer complications during the land-lease negotiation process, it was important to try to find an area with the fewest landowners.
- **Supportive landowners.** It was critical that the landowners supported the project. The landowners would become the local project representatives and provide ongoing support and critical information throughout the project. They needed to be respected as stakeholders from the beginning of the process.

Experience had proven that it was critical to have at least one representative from the data team, the construction team, and the land-acquisition team on each micrositing trip. The data and construction representatives confirmed that the site met all of the requirements to make it a good data-collection location, and then the land-acquisition team immediately started speaking with landowners and began the process of establishing lease agreements. This approach gave the team the flexibility needed to find a new site quickly if land negotiations stalled.

3.1.3 Step 3. Land Lease

After the final site was selected and the site-selection criteria had been verified, the process of reaching a lease agreement between the GOB, Power Division (GOB-PD) and the landowner was initiated. The land-acquisition process was led by the GOB-PD and occurred at all nine measurement sites. Drawings that detailed the areas impacted during construction and the areas occupied during the measurement period were provided to the GOB-PD and used to identify the total area of impacted land for the lease agreement. The GOB-PD representative would start the negotiation during the micrositing visit and would travel between the site area and Dhaka until the final formal contract was executed. We found land deeds and proof of land ownership difficult to find and verify. Figure 5 demonstrates the typical layout map used to communicate with the contractor in charge of tower installation (Harness Energy), the GOB, NREL, and the landowner.



Figure 5. Layout for the Sitakunda tower

3.2 Landowner/Community Relationships

Getting through the final step of the process and executing the lease agreement proved to be the most difficult and time-consuming part of the project, but it also was the most critical factor for the long-term success of each measurement location. The landowners were often the best stewards of their land and understood the local politics. It was critical to start with the support of landowners and then to build on that with the larger community.

Gaining the trust of the landowner required multiple visits to the landowner's home to meet the extended family and friends and share meals. During these visits (Figure 6), efforts were made to alleviate fears and debunk any myths about wind power that were common in some communities. Once we had gained the support of the landowner and had established a baseline of mutual respect, we could move forward knowing we had support in the community. Based on our experience going through this process at nine locations around the country, the sites where this baseline of respect was established early resulted in sites without many problems.



Figure 6. Site visit to Mongla.
Photo by Harness Energy.

It was also critical to build a network of support with other community leaders. Local political representatives and religious leaders could generate positive support if they were included as stakeholders in the process.

4 Instrumentation

The precision of the instrumentation and the mounting and orientation of the sensors were important considerations. The goal was to design a measurement campaign that met or exceeded the characteristics of measurement campaigns used by sophisticated wind developers around the world, so the data set from the MET towers could be of sufficient quality to be utilized by any potential developer. It was important to think about each site as a potential long-term measurement location. Although the measurement period for the project was defined as 2 years, it was important that the sites could be maintained for 10 or more years if the GOB was interested in establishing and maintaining long-term reference stations.

4.1 Tower Evaluation and Selection

Preliminary wind-speed modeling in Bangladesh indicated that higher-hub-height, low-wind-class turbines would likely be a good fit for the existing wind regime. Because higher hub heights were likely, it was critical to get data up to at least 80 m AGL. Collecting data at various measurement heights up to 80 m AGL required choosing an 80-m tower capable of supporting the instrumentation and meeting the following criteria:

- Meet local building codes and withstand potential cyclonic winds along the coast.
- Enable cost-effective maintenance during the measurement period.
- Have a working life of at least 10 years so the tower can remain in place past the project period if local stakeholders show interest in taking ownership and maintaining it as a long-term reference station.
- Ensure the structure will not negatively impact data and will meet International Electric Commission (IEC) standards.
- Keep cost down to allow for more measurement locations.

The two tower options were a guyed lattice tower locally manufactured in Bangladesh and a tilt-up tubular tower manufactured in the United States. The guyed lattice tower was selected for the following reasons:

- The tower could be designed by a local engineer to meet specific building codes at each site and to last for at least 10 years.
- The cost and difficulty of shipping tower hardware from the United States to Bangladesh were eliminated.
- Once installed, the tower could be quickly and easily maintained by a small group of trained local climbing technicians.
- The design minimized the number of technicians needed to travel to Bangladesh from the United States. This choice reduced travel and maintenance budgets, providing room in the budget for more measurement locations.
- The tower provided an immediate positive economic impact to Bangladesh and a positive long-term impact to the individuals that were trained to install and maintain the measurement equipment.

Construction BD, based in Dhaka, Bangladesh, was contracted to design, fabricate, install, and maintain the towers with the assistance of Harness Energy (Figure 7). The final design was a three-sided, guyed lattice structure with a 24-inch face width (Figure 8). The towers were engineered to meet or exceed local building codes and designed for ease of transport to remote areas, ease of erection without the use of a crane, and ease of future maintenance with an open column positioned up the middle of the tower and large enough to accommodate a climber.



Figure 7. Abdullah (left), engineer at Construction BD, and Ifteekhar Ayub (right), president of Construction BD.
Photo by Harness Energy.



Figure 8. 80-m tower at Rajshahi.
Photo by Harness Energy.

Harness Energy worked with Construction BD to develop a safety and training program to integrate a culture of safety into the project and provide the local technicians with the skill set necessary to install and maintain the towers independently moving forward. Prior to starting tower construction, meetings were held in Dhaka to go over project safety rules and ensure that the construction team was comfortable with the new safety standards being implemented (Figure 9). The changes initially were not met with acceptance. Through open communication and hands-on training, however, a new set of standards was enacted and implemented. Figure 10 shows a required hard hat notice. Figure 11 shows a local tower technician outfitted with safety equipment.



Figure 9. Safety training seminar in Dhaka.

Photo by Harness Energy.

In addition to the safety of the crew, the safety of the community had to be considered. The project generated a considerable amount of publicity, and an interested audience could be found daily at each site. A perimeter was established around the construction zone with notices to keep non-construction personnel at a safe distance. The guards were an invaluable resource for keeping the local community at a safe distance and keeping materials secure throughout the construction process.



Figure 10. Hard hat notice.
Photo by Harness Energy.



Figure 11. Local tower technician working on the tower in Sitakunda.
Photo by Harness Energy.

4.2 Sensor Evaluation and Selection

Instrumentation was standardized across all tower sites to maintain a consistent standard of measurements across the country. Each of the instruments selected for this measurement campaign was highly accurate and calibrated to ensure quality data. The instruments were installed at four heights—three along the top half of the tower (Figure 12) and a cluster near the ground level. The mounting configurations for the sensors are shown in Table 3.

Table 3. Typical Tower Instrumentation

Application	West	East	Direction N/A
Level 1, ~80 m			
Anemometers	NRG Class 1	NRG Class 1	
Wind Vane, ~78 m	NRG #200P		
Temperature 1			RMYoung 1k RTD
Temperature 2			Vaisala HMP-155
Relative Humidity 1			Vaisala HMP-155
Pressure 1			Setra 278
Level 2, ~60 m			
Anemometers	NRG #40C ³	NRG Class 1	
Wind Vane, ~58 m	NRG #200P		
Level 3, ~40 m			
Anemometers	NRG Class 1	NRG Class 1	
Wind Vane, ~38 m	NRG #200P		
Level 4, ~4 m			
Temperature 3			RMYoung 1k RTD
Temperature 4			Vaisala HMP-155
Relative Humidity 2			Vaisala HMP-155
Pressure 2			Setra 278
Solar Insolation			Huskeflux LP02
Precipitation			Decagon Leaf Wetness

³ The 60-m west anemometers were NRG #40C anemometers at all sites except Rajshahi and Chandpur. All NRG Class 1 anemometers were used at Rajshahi and Chandpur.



Figure 12. Typical MET tower configuration with sensors attached to boom extensions.
Photo by Harness Energy.

4.2.1 Horizontal Wind Speed

Wind speed is the most important component of the available resource. A calibrated Class 1 anemometer from NRG Systems was used to measure wind speed (Figure 13). Two anemometers were mounted at each of the three measurement levels. Multiple anemometers at each level provided redundancy in the case of single sensor failure and also allowed for a consistent data set when one sensor was being shadowed by the tower structure. Anemometers at multiple heights allowed the meteorologist to understand the wind shear at the site.



Figure 13. Anemometer at Mymensingh.
Photo by Harness Energy.

4.2.2 Wind Direction

Wind direction measurements were used to optimize the layout of a wind farm and to understand the distribution of the wind resource across the project area. One wind directional vane from NRG Systems was mounted under each set of anemometers (Figure 14).



Figure 14. Wind vane at Rajshahi.
Photo by Harness Energy.

4.2.3 Mounting

The primary consideration for mounting and orienting the sensors was to ensure that the tower and booms did not interfere with the measurement. If booms were too short, then the anemometers measured wind speeds that were either artificially high or low, depending on the precise length. This is true for both the vertical and horizontal booms. International standards have been established to specify recommended dimensions for each of these booms. To orient the booms properly, it is best to have a general understanding of the prevailing wind direction at the site so that the instrumentation is not shadowed by the tower in the prevailing wind direction, because this would cause excessive data to be filtered out during the QC (i.e., data-scrubbing) process. See Section 5 for a detailed description of the QC process.

The mounting booms were designed specifically to work with the towers provided by Construction BD. The guyed design enabled the use of longer booms, thus increasing the distance between the tower face and the instruments. The booms were designed with future maintenance in mind and could be easily adjusted for instrument replacement. Figure 15 shows mounting boom testing.



Figure 15. Mounting boom testing.
Photo by Harness Energy.

4.2.4 Air Temperature

Air temperature was used to estimate air density, which affects power output. It was measured at the top of the tower and near ground level (Figure 16) using two different sensors: the Vaisala HMP155 and the RM Young 1k RTD. The RM Young sensor was used for the delta temperature measurement—or temperature differential measurement—which measures the thermal stability of the atmosphere.



Figure 16. Temperature sensor at Chandpur.
Photo by Harness Energy.

4.2.5 Barometric Pressure

Barometric pressure along with air temperature can improve the air density estimates. The Setra 278 was mounted in an enclosure at the top of the tower and in the logger enclosure at the base of the tower.

4.2.6 Relative Humidity

Relative humidity can impact air density estimates. The Vaisala HMP155 was mounted at the top and at the base of the tower.

4.2.7 Solar Insolation

Solar radiation measurements can assist with the prediction of atmospheric stability. The Huskeflux LP02 pyranometer is used to measure solar radiation and was mounted on the horizontal plane at the base of the tower (Figure 17). Figure 18 shows a typical tower base configuration.



Figure 17. Insolation sensor at Mymensingh.
Photo by Harness Energy.



Figure 18. Typical base configuration at Mymensingh.
Photo by Harness Energy.

4.3 Data Logger and Communications

The sensors on the towers terminated at a data logger (Figure 19), which collected the raw signals from each of the sensors and converted the data to standard MET units. The data were stored on the data logger and emailed to a server in the United States daily for processing using a cellular gateway. Quarterly site visits were completed to retrieve manually any data that were not sent to the remote server owing to local cellular outages or data logger issues. Section 5 provides a detailed description of the data-processing methodology.

The Campbell Scientific CR3000 data logger was chosen for this application because it is capable of handling a great number of sensors, can perform differential measurements for the temperature measurements, allows for programming different averaging intervals for each sensor, and is capable of remote communication for data collection.



Figure 19. Enclosure with data logger.
Photo by Harness Energy.

4.4 Remote Sensing

A Vaisala Triton Wind Profiler was used at two locations. The Triton uses SODAR technology to capture wind data, including speed, direction, and turbulence at heights ranging from 40 m to 200 m AGL. The Triton has been used extensively around the world at various stages of wind project development. It can be deployed quickly and collects data at heights well above most MET towers. This makes the Triton a valuable solution for early-stage site prospecting, reducing spatial uncertainty and improving the understanding of wind shear, which is why it was selected for this measurement campaign.

The Triton was validated against the MET tower at Rajshahi for a 30-day period (Figure 20, Figure 21). Once the validation period was complete, the Triton was moved to Inani Beach, where it was deployed for 1 year (Figure 22). At Inani Beach, the Triton was mounted on a concrete mounting platform to protect the machine from potential storm surge flooding. After a year of measurement at Inani Beach, the Triton was moved to Rangpur in the northern part of the country.



Figure 20. Transporting Triton to the Rajshahi platform.
Photo by Harness Energy.



Figure 21. Triton deployed at Rajshahi.
Photo by Harness Energy.



Figure 22. Triton deployed at Inani Beach.
Photo by Harness Energy.

5 Data Collection, Quality Control, and Preparation for Modeling

This section covers three related topics:

- The data collection, transmission, and recovery from each site
- The QC process used to scrub invalid and low-quality data points from the raw data sets to create the processed data sets
- The process used to create data sets specifically for the modeling team.

Figure 23 shows this entire process graphically.

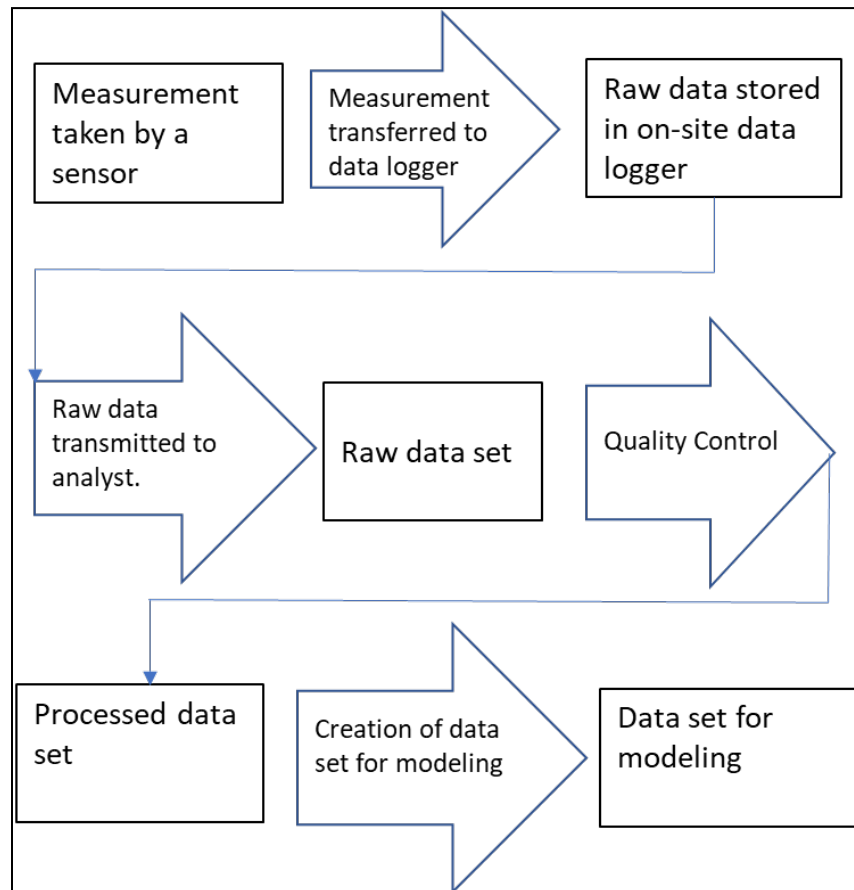


Figure 23. Overview of data collection, quality control, and preparation for modeling

Although raw data sets with time steps of 1 minute, 10 minutes, and 60 minutes were created by the data logger, only the 10-minute data went through the QC process for two reasons: only the 10-minute data were required for the modeling effort and using 10-minute time steps is the industry standard for wind data. All the graphs and tables in this section refer only to the 10-minute data. All the data sets—raw and processed—are available through the RE Data Explorer tool.

5.1 Data Collection, Transmission, and Recovery

A key part of any wind resource monitoring effort is taking measurements, storing the resulting data in the onsite data logger (data collection), and transferring the data sets from the monitoring site to the wind resource analyst (data transmission). Issues occurring during either of these steps—as occasionally occurred with this effort—cause loss of data.

5.1.1 Data Collection

Measurements were taken (usually at multiple heights) for wind speed, wind direction, temperature, barometric pressure, relative humidity, and solar insolation. Data sets were collected with three different time-step intervals: 1 minute, 10 minutes, and hourly. The 10-minute data sets are the most comprehensive, with readings on wind speed, wind direction, temperature, humidity, and barometric pressure. The 1-minute data sets contain the solar insolation data. The hourly data sets contain data-collection system status data. The tables in the Appendix list each data stream taken at each monitoring site.

Several unique challenges during this project caused data collection to cease for shorter or longer periods. These challenges included, but were not limited to, red ants infesting a data logger, an animal biting through an exposed wire, PV system theft, vandalism, data logger failure, and political unrest.

5.1.2 Data Transmission

Data transmission was hampered by the lack of direct connection with the MET towers. There were issues navigating local communication protocols set by the Bangladesh Telecom Regulatory Agency while attempting to enable a two-way connection between the sites and a foreign server. As a result, instead of the (U.S.-based) server retrieving the data packet from the site, the cellular modems from each tower were configured to turn on once per day and push a data packet to the (U.S.-based) data server. This packet contained data from the previous 24 hours. If the cellular modem was not able to connect to the server within a certain period, that data packet was stored in the data logger at the tower but was not transmitted to the server. As a backup, Harness Energy personnel would download the data from the logger during their periodic site visits. Between the daily data push and the periodic downloading of data from the loggers, most of the available data were eventually collected and transferred to NREL.

For the SODAR unit, the process was somewhat different. The data packet from the unit was pushed to a server multiple times throughout the day. The server was maintained by the manufacturer, where the data were compiled, cleaned, and then made available for retrieval by NREL.

5.1.3 Data Recovery

Data recovery—data on hand with the analyst—is the ultimate result of data collection and transmission. The recovery ratio is the amount of data recovered (and on hand with the analyst) as a percentage of the maximum amount of possible data. For example, if monitoring occurs at a given site for 10,000 hours, but ultimately only 9,000 hours of data are available, then the recovery ratio is 90%.

Table 4 summarizes data recovery for each site. Figure 24 graphically shows data recovery, illustrating gaps in the data for Chandpur, Mirzapur, Parkay Beach, and the Rangpur SODAR site. These gaps are explained in Table 5. Note that the data-recovery percentages in Table 4 show overall recovery; therefore, if there is even a single measurement within a time step, then that time step is considered recovered. Recovery percentages for individual sensors or data streams typically are less than the values shown. Data-recovery values (for the 10-minute data) for each sensor on each tower, as well as for each data stream from the SODAR, can be found in the Appendix. The Appendix is a copy of the final quarterly report produced by the project team.

Table 4. Data Recovery

Site	Site Type	Installation Date	Monitoring End Date	Data Recovery (%)	Data Quantity (Months)
Chandpur	60-m Tower	6/11/2014	12/04/2017	80.07	33.5
Mirzapur	80-m Tower	10/19/2015	11/22/2017	63.40	19.1
Mongla	80-m Tower	10/31/2015	12/25/2017	98.59	25.4
Mymensingh	80-m Tower	8/13/2015	12/13/2017	97.45	27.3
Parkay Beach	80-m Tower	12/24/2014	7/14/2017	89.03	27.3
Rajshahi	80-m Tower	6/11/2014	12/20/2017	94.58	40.0
Sitakunda	80-m Tower	12/18/2014	12/20/2016	91.54	22.0
Rangpur (SODAR)	SODAR	8/04/2015	4/19/2017	73.80	15.1
Rajshahi (SODAR)	SODAR	5/28/2014	7/22/2014	100.00	1.8
Inani Beach (SODAR)	SODAR	7/25/2014	8/02/2015	95.92	11.6

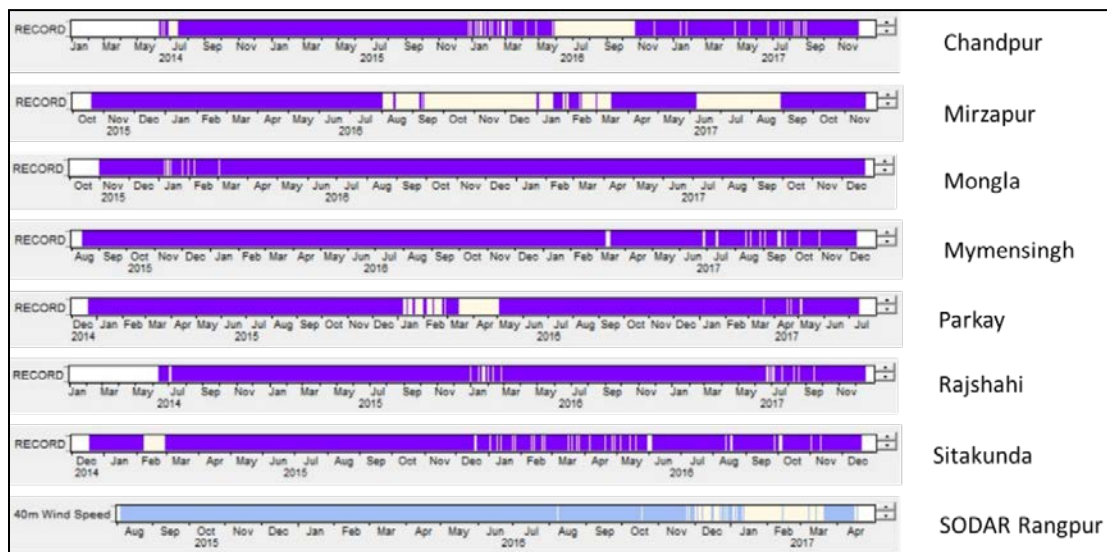


Figure 24. Data recovery

Table 5. Explanations for Major Data Gaps

Tower and Gap Date	Explanation
Chandpur (June–Sept. 2016)	Data logger failure
Mirzapur (Sept. 2016–Jan. 2017)	Vandalism
Mirzapur (Feb.–Mar. 2017)	Data logger failure
Mirzapur (June–Aug. 1 2017)	Data logger failure
Parkay (Mar.–Apr. 2016)	Power system failure
Rangpur (SODAR) (Dec. 2016–Mar. 2017)	Progressive failure of a SODAR unit component

5.2 Data Quality Control

For any number of reasons (e.g., sensor failure, tower shadowing), a proportion of the data points in the data set will be “bad” and not accurately characterize the physical property that is being measured. The purpose of QC is to scrub the raw data set of bad measurements to create a processed data set that accurately characterizes the physical properties at the site during the monitoring period. Rigorous QC of the collected data is vital for correctly characterizing the wind resource at the monitoring sites. This accurate characterization of the measured data is important for the follow-on wind resource modeling effort, because the results of the modeling only can be as good as the data used to inform it. Lastly, a wind resource model with less uncertainty allows for lower-cost financing of wind projects (due to higher investor/lender confidence) and, thus, a lower cost of energy.

Data QC is not an exact science. Therefore, good practice calls for both preserving the raw data and documenting the QC process. This allows the QC process to be revisited later and allows use of a different QC process if desired.

The data QC for this project was conducted using the Windographer wind data analysis software (version 3.310).⁴ As part of the QC process, a series of filters were applied to the data to screen out invalid or suspect data points. These data filters included tower shadow, consistency checks, and visual inspection. The filtering methods are described in more detail below.

5.2.1 Tower Shadow

Data were removed in a 30-degree area centered on the axis of each anemometer’s boom. These data exhibit wind-speed readings lower than the actual wind speeds, because the tower was blocking part of the wind that should have been acting on the instrument. This is shown in Figure 25, which depicts 80-m wind-speed data from Mongla.

⁴ See the Windographer website at <https://www.windographer.com/>.

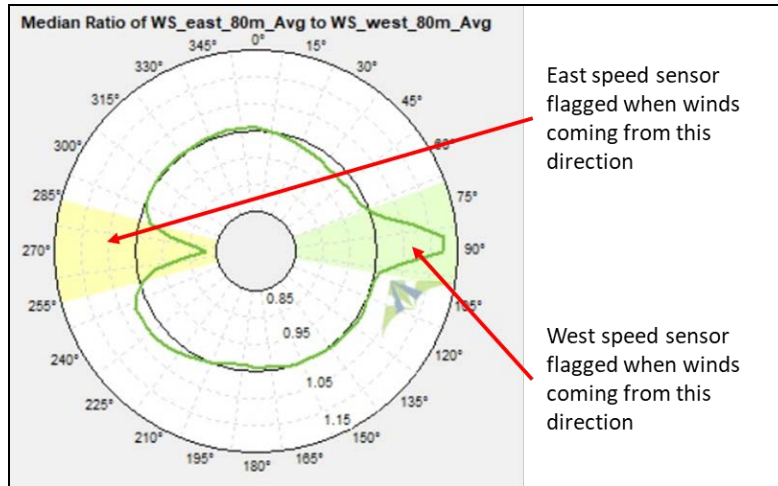


Figure 25. Tower shadow

5.2.2 Consistency Checks (Sensor Pair Comparison)

Whenever possible, it is useful to look at instruments relative to one another. For example, the two wind-speed sensors at each level were compared to ensure that there were no issues with any of the sensors. This filter often identifies problems with sensor configurations and sensor failure. This is shown in Figure 26, which uses the data from the Mymensingh 80-m sensor pair.

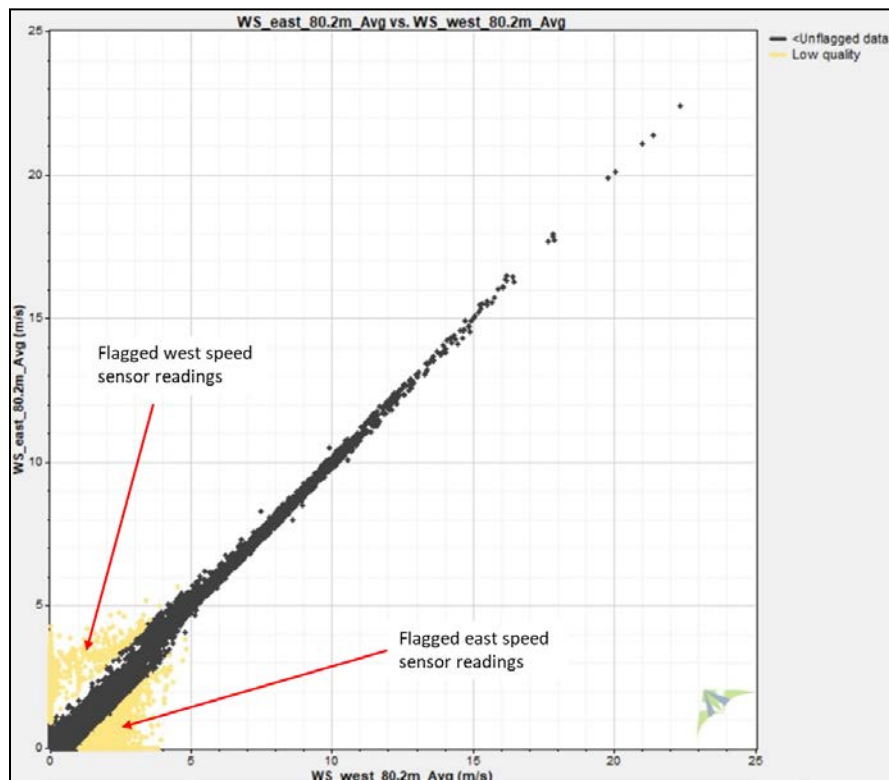


Figure 26. Sensor pair comparison

5.2.3 Instrument Failure

Sometimes instruments drop out for various reasons, and these data points are typically filtered out manually by visual inspection, as shown in Figure 27, which is a time-series plot of temperature from Rajshahi.

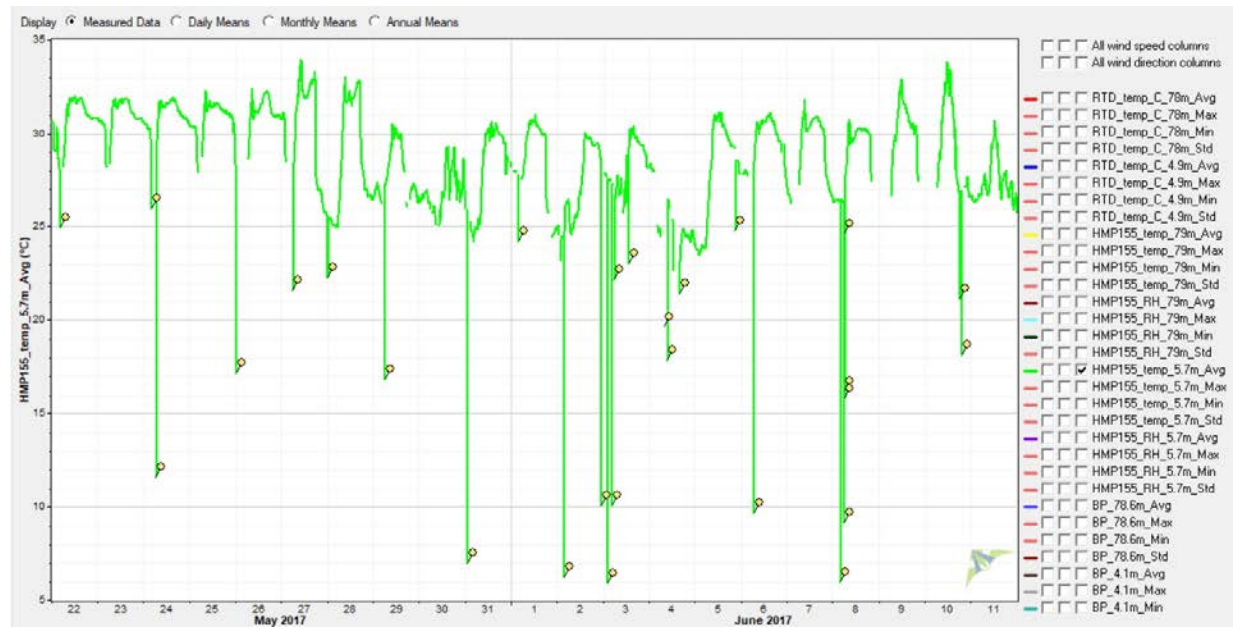


Figure 27. Visual data inspection at Rajshahi

5.2.4 Corrected Transfer Function

The pressure sensors used at Rajshahi were a different model than those used at the other tower sites, and thus an incorrect transfer function was entered into the logger. To correct this transfer function, during the QC process, a corrective transfer function of $y = 0.5x + 300$ was applied to the barometric pressure readings for this site.

5.2.5 QC Data Flagging

- **Quality factor (QF) (SODAR only).** Data points with a QF of less than 90% were excluded.
- **Rain (SODAR only).** SODAR units perform poorly when it rains. All wind-speed, vertical wind-speed, and wind direction data were flagged when the relative humidity exceeded 95%.
- **Vertical wind speed (SODAR only).** When the vertical wind speed at a given height exceeded 0.5 m/s, the (horizontal) wind-speed reading for that height was flagged.

5.3 Data Preparation for Modeling

The modeling effort only required a subset of the data channels collected, because the FDDA code only can assimilate wind speed, temperature, and water vapor. Additionally, the FDDA code requires only one data channel per measurement. The following general procedures were used to prepare data sets prior to handoff to the modeling team. For measurements including two data streams (e.g., wind speed at a given height), a composite data stream was created by averaging the (unflagged) readings of the two data streams. For measurements using only one data stream, that data stream (after QC) was used as is. Table 6 summarizes the procedures used to prepare the data sets from the towers for the modeling team. The data were then further converted by the modeling team into a format that can be read by the FDDA system. The procedure used for the data sets from the SODAR units is shown in Table 7.

Table 6. Data Preparation for Modeling (Tower)

Data Stream	Procedure
80-m wind speed	Average of the 80-mE and 80-mW sensors
60-m wind speed	Average of the 60-mE and 60-mW sensors
40-m wind speed	Average of the 40-mE and 40-mW sensors
20-m wind speed (Chandpur only)	Average of the 20-mE and 20-mW sensors
80-m wind direction	80-m direction sensor
60-m wind direction	60-m direction sensor
40-m wind direction	40-m direction sensor
20-m wind direction (Chandpur only)	20-m direction sensor
80-m temperature (60 m for Chandpur)	Average of 80-m HMP 155 and 80-m RTD (Chandpur: only used the HMP 155 due to issues with the RTD)
4-m temperature	Average of 4-m HMP 155 and 4-m RTD (Chandpur: only used the HMP 155 due to issues with the RTD)
80-m barometric pressure (60 m for Chandpur)	80-m barometric pressure sensor
3-m barometric pressure	3-m barometric pressure sensor
80-m relative humidity (60 m for Chandpur)	80-m relative humidity sensor
4-m relative humidity	4-m relative humidity sensor

Table 7. Data Preparation for Modeling

Data Stream	Procedure
40-m wind speed	sensor @ 40 m; SODAR/Doppler
50-m wind speed	sensor @ 50 m; SODAR/Doppler
60-m wind speed	sensor @ 60 m; SODAR/Doppler
80-m wind speed	sensor @ 80 m; SODAR/Doppler
100-m wind speed	sensor @ 100 m; SODAR/Doppler
120-m wind speed	120-m sensor, SODAR/Doppler
140-m wind speed	extrapolating wind shear from 120-m sensor, SODAR/Doppler
160-m wind speed	extrapolating wind shear from 120-m sensor, SODAR/Doppler
180-m wind speed	extrapolating wind shear from 120-m sensor, SODAR/Doppler
200-m wind speed	extrapolating wind shear from 120-m sensor, SODAR/Doppler
40-m wind direction	40-m wind direction
50-m wind direction	50-m wind direction
60-m wind direction	60-m wind direction
80-m wind direction	80-m wind direction
100-m wind direction	100-m wind direction
140-m wind direction	140-m wind direction
160-m wind direction	160-m wind direction
180-m wind direction	180-m wind direction
200-m wind direction	200-m wind direction
2.5-m temperature	temperature sensors
1.5-m barometric pressure	pressure sensors
1.5-m relative humidity	relative humidity sensors

6 Modeling the Wind Resource in Bangladesh

As stated in Section 2, wind resource estimates are usually created using a combination of observations and simulated data. Although observations can be regarded as the most accurate descriptions of a location if their quality is sufficient, observation locations are sparse and available only at certain sites that might or might not be representative of the regional wind climate. Therefore, model simulations of wind speeds and other atmospheric parameters typically are used to describe the wind climate over a given region.

This section describes how numerical weather prediction (NWP) models work and provides information on reanalysis data sets, followed by a discussion of our modeling methods and a sensitivity study of various model parameters.

6.1 Numerical Weather Prediction Simulations

To generate a preliminary estimate of the wind potential in Bangladesh at the beginning of the project, NREL conducted the NWP simulations described in this section. The NWP simulations calculate atmospheric processes on a 3D grid (Figure 28). Atmospheric motions are calculated on a grid with a defined horizontal extent (grid points are separated by a distance dx) and vertical extent, up to several thousand meters above ground.

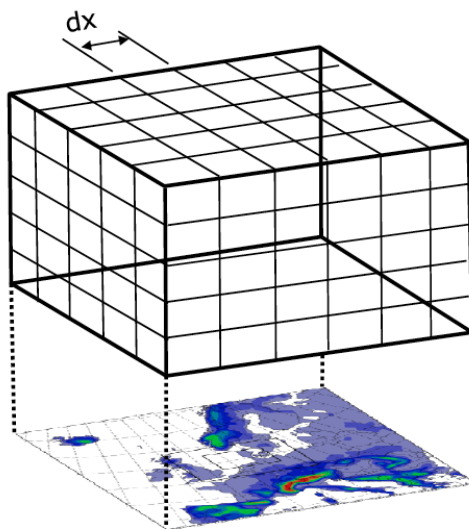


Figure 2

Figure 28. Schematic for the concept of NWP models

NREL's work began with a detailed study of the NWP model (WRF model) performance (Skamarock et al. 2008) (www.wrf-model.org) in the region and a carefully designed model configuration tuned to both local climate specificities and wind energy applications. The WRF setup was tuned by working with the University of Dhaka in Bangladesh, which both uses WRF and understands the climate in Bangladesh. In turn, NREL used their model setup.

The WRF model is a community NWP model maintained by NCAR in the United States. The advantage of a community model is that many users contribute with code updates and experiences. The WRF model serves a wide range of MET applications across scales ranging from meters to thousands of kilometers. The WRF is used operationally in the United States at the National Centers for Environmental Prediction (NCEP), the Air Force Weather Agency, and other centers. It has been successfully applied to wind-energy-related studies and wind resource assessments (e.g., Draxl, Purkayastha, and Parker 2014; Draxl et al. 2012; Draxl et al. 2013; Storm and Basu 2010; Dvorak et al. 2012; Carvalho et al. 2013; Carvalho et

al. 2014; Santos-Alamillos et al. 2013; Garcia-Diez et al. 2012; Li, Guo, and Wang 2014; Lundquist et al. 2014). The WRF model allows for accurate simulations of winds near the surface and at heights that are important for wind energy purposes. The WRF's ability to downscale to required resolutions enables the modeling of small-scale features, such as fronts, sea breezes, and winds influenced by orography, which are all important factors in characterizing the wind resource. The WRF is thus an optimal tool to predict the distributions of the wind over a given area—in this case Bangladesh.

The WRF simulations are controlled by the user, who can choose from many different physical models that describe the interaction and processes between and in the land surface, the atmospheric boundary layer, and the middle and upper atmosphere.

The present research used the WRF-based FDDA system (see Section 2). Running NWP models is computationally expensive, and finding the appropriate setup for a region and climate of interest is time consuming. Storing many gigabytes of data is not trivial; therefore, at the beginning of the project, the team limited the preliminary analysis to a sampling of the current data set (total of approximately 3 months of simulations).

6.2 Reanalysis Data Sets

The WRF model requires input from reanalysis data sets, which are available from large weather centers and have a relatively coarse horizontal resolution of approximately 30 km to 100 km. The data sets usually extend over several decades or longer and cover the entire globe—from the Earth's surface to well above the stratosphere. The data sets use weather observations from around the globe for a combined modeled-observed estimate of atmospheric states. The WRF model downscales the information in these data sets to a more accurate representation of atmospheric processes at a much finer horizontal resolution—3 km in the present case. This means that information about these processes, such as wind speed and direction, is available at points 3 km apart. For non-complex areas like Bangladesh, this resolution is usually sufficient to describe wind distributions with satisfactory accuracy. In fact, current research suggests that model runs at a horizontal resolution of about 1 km or less do not necessarily produce more accurate results than 2- to 3-km runs (Wyngaard 2004). In a study in Gujarat, India, NREL found that using a grid spacing of 1.1 km did not improve the wind resource estimates compared with a 3.3-km grid (Draxl, Purkayastha, and Parker 2014). Further, because running an NWP model at higher resolutions is computationally more expensive, a horizontal resolution of less than 3 km might not be justified.

Reanalysis data sets can be used to get a first impression of the wind resource in a country. For that purpose, and also to select the best reanalysis product among the many available, NREL compared the publicly available global reanalyses. These lower-resolution reanalyses were used to map the annual average wind speeds around common hub heights for a first assessment of the wind climate in Bangladesh. A study of annual average wind speeds and frequency distributions, as well as seasonal and diurnal cycles at the measurement sites, was conducted based on these data.

The reanalysis data sets evaluated in this project were the European Re-Analysis Interim (ERA-Interim) from the European Centre for Medium-Range Weather Forecasts (ECMWF), the NASA Modern Era Reanalysis for Research and Applications (MERRA), and the NCEP Climate Forecast System Reanalysis (CFRS) (Table 8).

Table 8. Evaluated Reanalysis Data Sets, Origin, Resolution, and Available Period

Product	Center	Resolution	Period
ERA-Interim	ECMWF	0.75° x 0.75° x 37 levels, up to 0.1 hPa, 6 hourly	Jan. 1, 1979, to present
MERRA	NASA	0.5° (latitude) x 0.666° (longitude) x 42 levels (up to 0.01 hPa), hourly (surface), 6 hourly (upper-air)	Jan. 1, 1979, to present
CFSR	NCEP	Surface: 0.3° x 0.3°, 6 hourly; upper-air: 0.5° x 0.5°, 37 levels, up to 0.1hPa, 6 hourly	Jan. 1, 1979, to present

The CFSR data set was selected as the best choice (which was confirmed by the sensitivity study in Section 6.4). It has the highest horizontal resolution, the data are updated daily, and it is unified with NCEP’s Climate Forecast System, which has been shown to be the best choice on the Indian Subcontinent (Draxl, Purkayastha, and Parker 2014).

The reanalysis comparison showed that, among the three data sets, ERA-Interim generally showed weaker wind speeds than did CFSR and MERRA. The annual wind speeds at all the sites were greater at 100 m than at 30 m, as expected. The wind speeds tended to get stronger from the interior sites toward the coastal sites. The average 100-m wind speeds did not appear to change significantly from year to year.

6.3 Simulation Method

The model simulations were carried out with the WRF model, which is run at several different horizontal scales. These include an outer domain, intermediate domains, and a finer-resolution inner domain. Weather patterns inherited from the reanalysis data sets are passed down to finer resolutions through so-called “nests.” We used a nested setup to dynamically downscale to 3 km in the finest domain (Figure 29). The grid spacings for each of the three domains were 27 km, 9 km, and 3 km. In the finest domain, the number of grid points was 256 x 280.

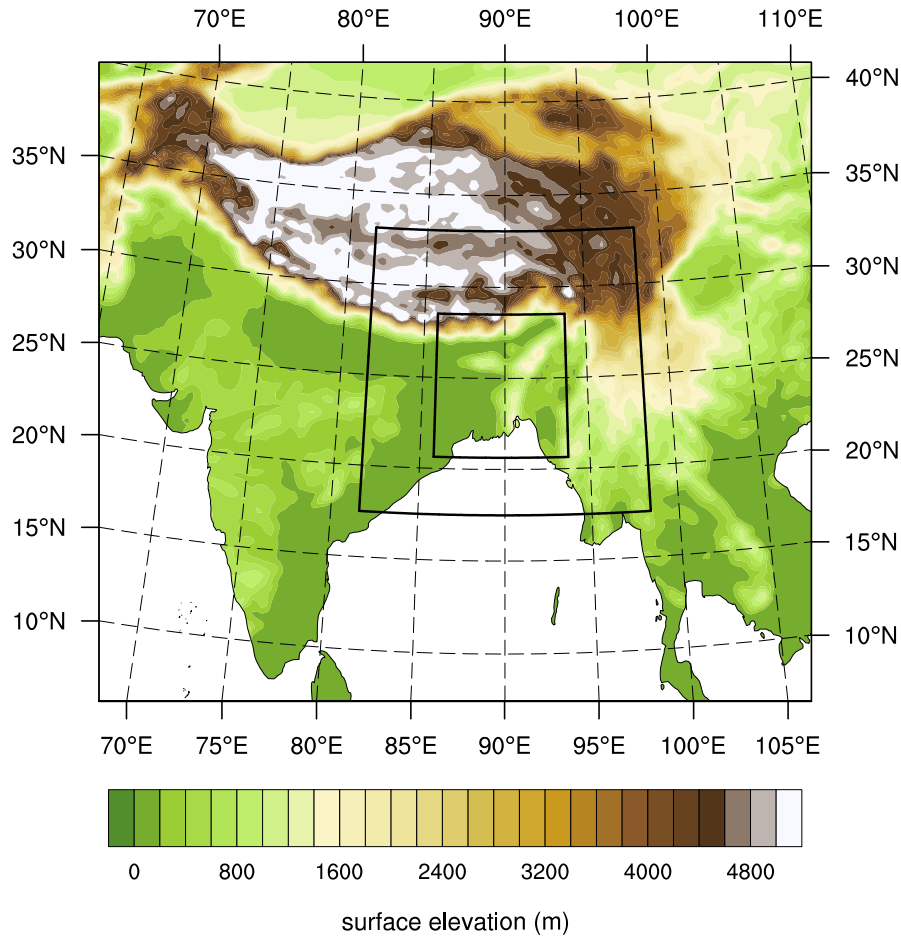


Figure 29. WRF simulation domain setup

As mentioned previously, we dynamically downscaled the selected global reanalysis data set to create hourly gridded data over Bangladesh at a 3-km grid spacing. To ensure accuracy, observational data (i.e., surface reports, radiosondes, aircraft reports, and satellite winds) from NCAR’s automated data processing historical database were used, wherever they were available (India), together with the local observations collected by NREL. The observational data served as input for the FDDA algorithm to constantly nudge the model analysis toward observations.

The concept of nudging the model toward observations is shown in Figure 30. The green line is assumed to be an observed quantity—an observed time series of wind speed—which represents the truth at a certain location. The red dots represent the initial conditions of modeled wind speeds, assumed to be as accurate as possible. They are never completely accurate, however (i.e., they do not coincide with the green line), because of incomplete data fed into the model. These red dots represent the values taken from the coarse reanalyses. When the model is integrated forward in time, the model solution arrives at a certain estimate of the atmosphere (blue dot), which usually is less accurate than the initial condition owing to non-linear error propagation with time. Then data are assimilated, the model is bent toward measured site conditions, and another best guess for the atmospheric state (second red dot) is produced. From that, the model again is integrated forward in time, and the cycle repeats itself.

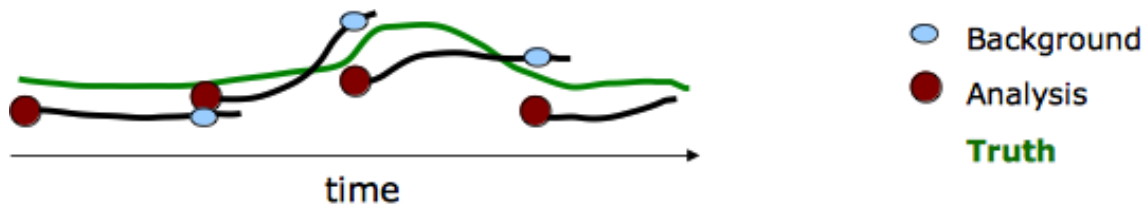


Figure 30. Schematic demonstrating the nudging technique

For the final wind resource data set, all the observations (historical and local) were ingested into the model. For the preliminary modeling described here, only the historical data were ingested, and the local observations measured by NREL were used to validate the model output. These SODAR measurements were extremely valuable for wind energy purposes, because they measured the wind up to 200 m, which is the layer of the atmosphere where wind turbines operate. Measurements at these heights have not been available in Bangladesh so far and, therefore, constitute a unique and very important new data asset. Model validation not only shows whether the simulated winds are true, but also it can be used to assess model uncertainty and, most importantly, adjust the modeled values to a more accurate solution.

6.4 Sensitivity Study

The more confidence there is in the configuration of the NWP model, the more valuable the wind resource assessments. Because WRF model simulations are set up by the user, the results of a simulation depend on the inputs or the choices made by the user. Therefore, for the present research, the team carried out a sensitivity study for several model input parameters to yield the best possible model setup. The main setup was motivated by the experience of experts from NCAR and NREL and by WRF model simulations in India (Draxl, Purkayastha, and Parker 2014). The analysis of these simulations was tuned to both local climate specifics and wind energy applications.

The week of August 15–23, 2015, was chosen for this study owing to the availability of local measurements at all the sites. Eight different experiments were chosen to determine the best setup. In column 1 of Table 9, the simulations are described, specifying the reanalysis data set that was used to force the model at the boundaries and provided initial conditions, whether World Meteorological Organization (WMO) data were assimilated in domain 1 (“WMO assimilated” or “no WMO assimilated”), which planetary boundary layer (PBL) scheme was used (Yonsei University [YSU] or Mellow-Yamada-Janjic [MYJ]), the number of vertical levels (63 or 41), the version of WRF (3.6.1 or 3.7.1), and the radiation scheme (4 or 1).

Among the many parameterizations in WRF, the PBL scheme is basically responsible for the calculation of wind speeds. The treatment of physical processes in the boundary layer is empirically described in these schemes, and that description is different in each scheme. We therefore tested two commonly used approaches and further tested two commonly used radiation schemes. Because numerical modeling is time consuming and radiation scheme 4 contributes to much more computing time than does radiation scheme 1, those were included in the analysis. We found that the ERA-Interim boundary conditions yield very poor wind-speed estimates (Draxl, Purkayastha, and Parker 2014) and therefore did not include this data set in the sensitivity study.

The results from the sensitivity study are summarized in Table 9, which shows bias and root-mean-square error (RMSE) for wind speed and wind direction as well as bias for temperature and humidity. Measurements were taken from the towers deployed through this project. The error metrics represent the combined error metric for all heights available. Two simulations show the lowest error metrics: CFSR WMO assimilated MYJ 63 Levels v3.7.1 rad4 and CFSR WMO assimilated MYJ 63 Levels v3.7.1 rad4. The latter was selected for its lower errors in humidity (important in Bangladesh) and lower wind direction RMSE as compared to the former. The shaded cells in Table 9 represent the lowest error for each column which represents the best simulation. This setup was used to create the final Bangladesh data set.

Table 9. Error Metrics for Wind Speed, Wind Direction, Temperature, and Relative Humidity for the Experiments in the Sensitivity Study

Simulation	Wind Speed Bias	Wind Speed RMSE	Temperature Bias	Wind Direction Bias	Wind Direction RMSE	Relative Humidity Bias
CFSR WMO assimilated YSU 63 Levels v3.7.1 rad4	0.3	2.4	-1.1	11.7	59.2	4.5
MERRA no WMO assimilated YSU 63 L v.3.6.1	0.6	2.1	-2.3	6	51.1	10.7
CFSR WMO assimilated YSU 41 Levels v3.7.1 rad4	0.4	2.4	-1.1	9.7	58	4.4
CFSR WMO assimilated MYNN 63 Levels v3.7.1 rad4	0	2.5	-0.9	11.1	65.4	4
CFSR WMO assimilated MYJ 63 Levels v3.7.1 rad4	0	2.3	-1	12.7	46.3	3
CFSR no WMO assimilated YSU 63 Levels v3.7.1 rad4	-1.1	2.2	-2.4	2.4	44.5	9.2
CFSR no WMO assimilated YSU 63 Levels, v3.7.1 rad1	-0.5	2.3	-2.2	6.3	48.1	9.4
CFSR no WMO assimilated YSU 63 Levels v3.6.1 rad1	-0.5	2.2	-2.2	1.1	49.3	9.5

7 Results

The model setup that was chosen based on the results of the sensitivity study (Section 6.4) was used to conduct the 3-year numerical simulations that ingested the observations set up during the measurement campaign. The simulations were compared with observations; that is, a validation was performed to assess the accuracy of the model simulations and to estimate the uncertainty of the resulting wind resource assessment.

7.1 Validation of the Model Simulations

7.1.1 Validation Methodology

To validate the multi-year simulations with the WRF model and FDDA, we used the above-surface wind-speed observations from the seven NREL MET towers set up around Bangladesh, the NREL SODAR that was set up in sequence at two primary measurement locations (after being co-located for a month near the Rajshahi tower) around Bangladesh, and any publicly available radiosondes within the third domain. Radiosondes generally were available twice per day, at 0000 Coordinated Universal Time (UTC) and 1200 UTC. To focus on validation of rotor layer winds, only observations between 10 m AGL and 200 m AGL were used. A secondary validation was performed against observations that were taken at 80 m AGL (+/- 5 m) to assess model performance at hub height.

The WRF-FDDA simulations began at 0000 UTC on June 1, 2014, and continued to 2300 UTC on December 29, 2017, to encompass the full operational period of every NREL MET tower and the NREL SODAR and to guarantee that at least 2 full years of data were collected from each MET tower and 1 full year of data from both primary sites at which the SODAR was deployed (the initial deployment of the SODAR at Rajshahi was for testing purposes and only lasted for about 1 month). All available observations within the simulation window were used for assimilation.

The FDDA assimilated all publicly available WMO observations (e.g., radiosondes, surface observations, aircraft observations) plus the special NREL observations. This experiment is called “WMO+NREL.” To assess the impact of the special NREL observations, another WRF-FDDA simulation was run that assimilated only the standard WMO observations. This experiment is called “WMO_only.” For both experiments, the same set of observations was used for validation.

Prior to assimilation, the observations were passed through the “wrfqc” QC program (Liu et al. 2004), where they were processed for QC against a first-guess model field and compared to the expected error of the type and height of the observation. The expected observational error is based on static statistics from NCEP’s operational Global Forecast System (GFS) model and data assimilation system. Based on this evaluation, observations were assigned an integer value from 0 (bad) to 10 (excellent); the nudging coefficient was made proportional to this QC value. Thus, observations that received a QC value of 0 were given no weight and were not assimilated, but observations with a QC value of 10 were given maximum weight in the assimilation. For this validation, observations with a wrfqc value of 0 were withheld from the validation. Less than 0.1% of the MET tower, SODAR, and radiosonde observations received a QC value of 0, and more than 90% of the observations received a “good” QC value of 8, 9, or 10.

The WRF-FDDA simulations were validated using the metrics RMSE, mean absolute error (MAE), and mean error (ME), all of which are commonly used. In addition to the RMSE, MAE, and ME, we also explored the distributions of the WRF and observed wind speed through both scatterplots and binned histograms.

At each observation location, the WRF wind speeds first were interpolated horizontally using inverse distance weight interpolation from the surrounding grid points. Then the model wind speeds were interpolated linearly in height to the observation heights. Model levels generally were spaced about 20–25 m apart in the rotor layer; thus, linear interpolation is deemed an acceptable approximation, especially in regions of relatively flat terrain such as Bangladesh (e.g., Drechsel et al. 2012). Once the model/observation pairs were calculated, these pairs were aggregated into monthly and yearly groups before calculating means, standard deviations, or any of the metrics. For the scatterplots and binned histograms, the full 3.5-year set of model/observation pairs were aggregated. All validation was done separately by observation platform (MET tower, SODAR, radiosonde) to allow more granular analysis.

7.1.2 Value of Assimilating NREL Special Observations

The first aspect of the modeling runs analyzed is the benefit attained by assimilating the NREL MET tower and SODAR observations. This is accomplished by examining scatterplots and binned histograms from both the “WMO_only” and “WMO+NREL” experiments. Scatterplots for the two experiments for validation against the MET tower, SODAR, and radiosonde observations are shown in Figure 31, Figure 32, and Figure 2Figure 33, respectively. For those three figures, the scatterplots were validated against all observation heights between 10 m and 200 m AGL. A scatterplot for the two experiments only validating against the 80-m AGL SODAR observations is shown in Figure 34, which indicates that similar results are found when examining the 80-m height only as when including all heights. For each of these scatterplots below, a linear regression fit was calculated. The thin black line is the 1:1 line, the regression line is shown in red, and the regression coefficient (r) is printed in the upper-right corner of each scatterplot.

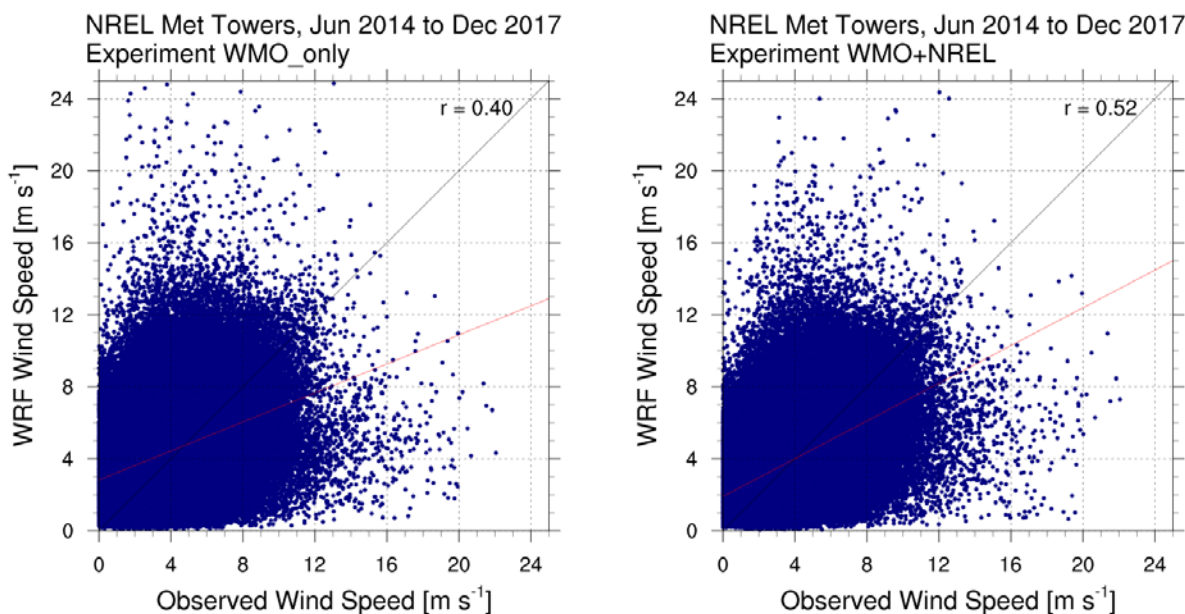


Figure 31. Scatterplots of WRF versus observed wind speed at the NREL MET tower locations

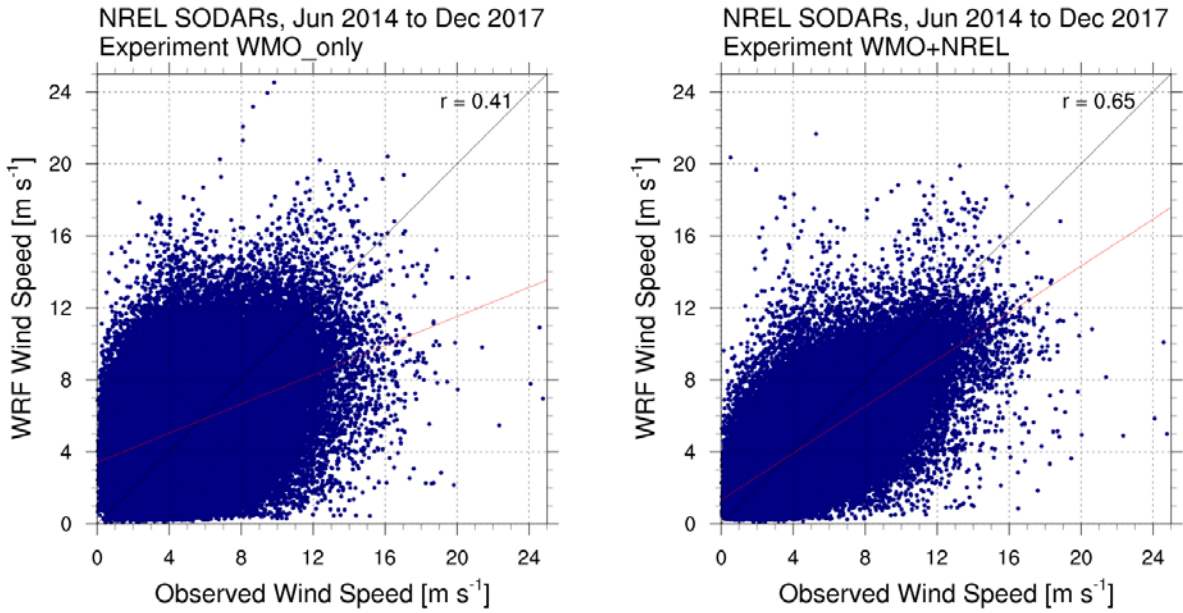


Figure 32. Scatterplots of WRF versus observed wind speed at the NREL SODAR locations

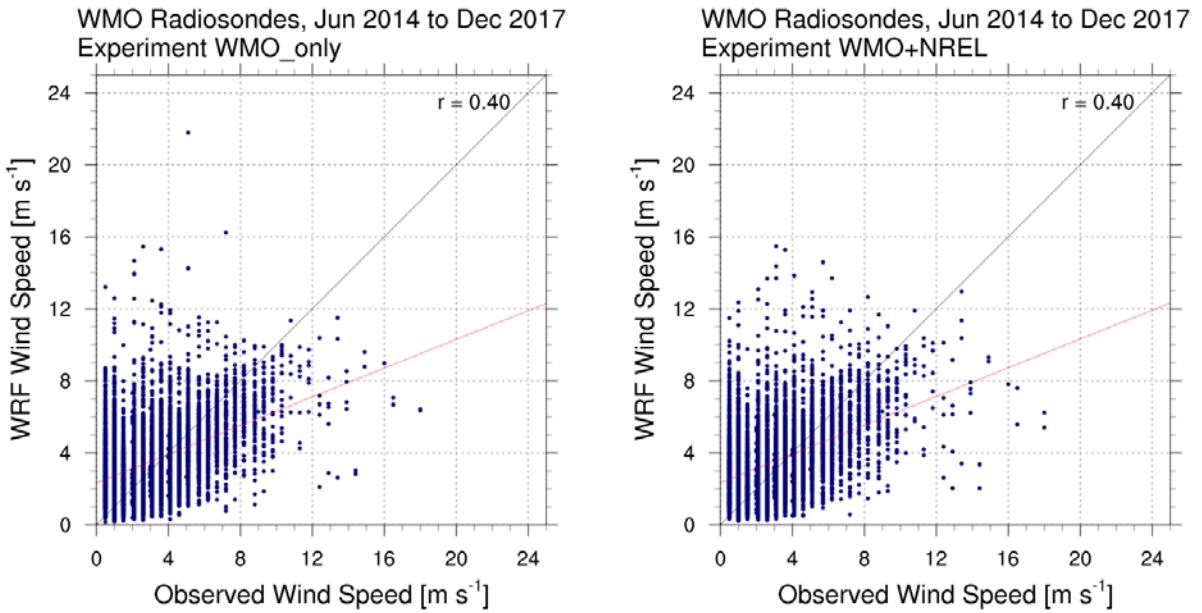


Figure 33. Scatterplots of WRF versus observed wind speed at the WMO radiosonde locations between 10 m and 200 m AGL

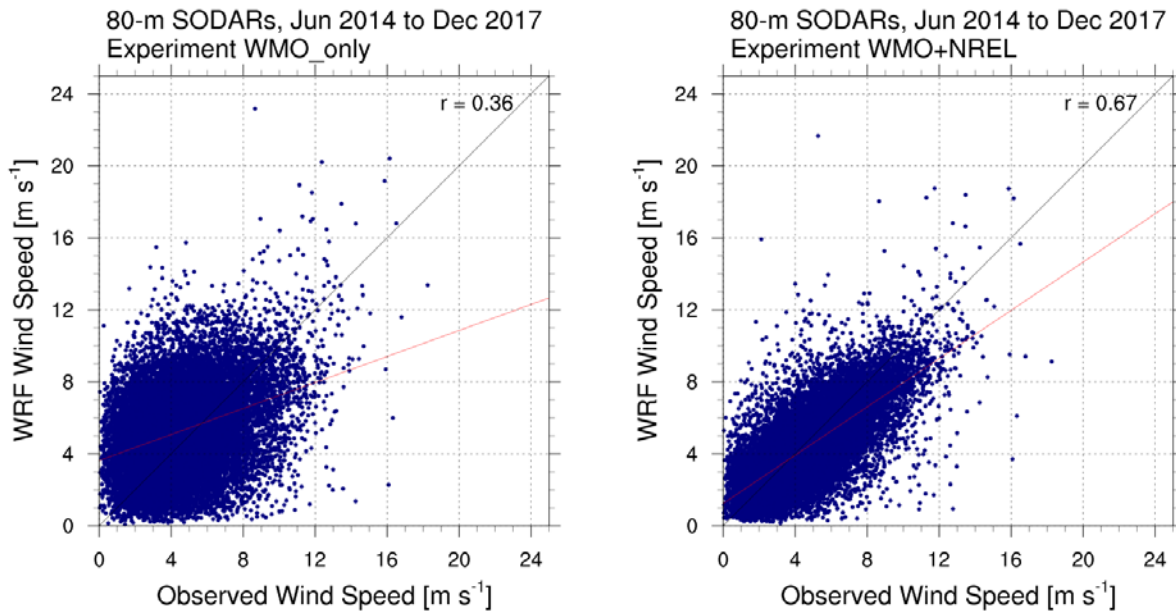


Figure 34. Scatterplots of WRF versus observed wind speed at the NREL SODAR locations at 80-m AGL height only

For the plots validating against MET tower and SODAR observations, the “WMO+NREL” experiment had both a larger regression coefficient and a regression line that was closer to the 1:1 line than did the “WMO_only” experiment. For instance, the regression coefficient increased from 0.41 to 0.65 at the SODAR sites when all the NREL observations were assimilated (Figure 32). This is expected, because the “WMO+NREL” experiment nudged the WRF simulation toward those observations and the “WMO_only” experiment did not. This result showed that assimilating these observations yielded an improved wind-speed analysis, at least in the vicinity of these observation locations.

For the rotor-layer radiosonde scatterplots (Figure 33), the regression coefficient was 0.40 for both experiments. The correlation between the WRF forecasts and observations at these locations illustrates one of the limitations of FDDA—that assimilating near-surface observations has limited impact on simulations at locations that are relatively distant from the observation. It is also interesting to note the vertical stripes on the radiosonde scatterplots. Those are artifacts resulting from the instrument on the radiosonde reporting wind speed to the nearest 0.5 m/s. WRF has much greater numerical precision (as do the MET tower anemometers and the SODAR), although that does not necessarily imply greater accuracy.

Another way to more closely examine the distributions of the WRF and observed wind speeds is through binned histograms, which are shown for the two experiments for the MET towers (Figure 35), SODARs (Figure 36), and radiosondes (Figure 37).

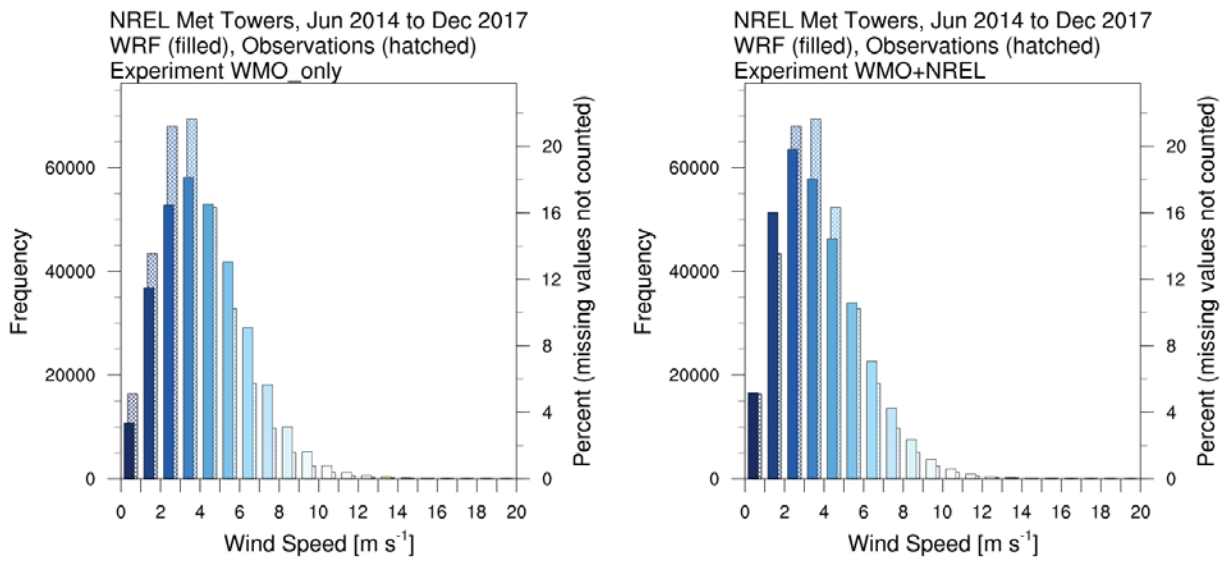


Figure 35. Binned histograms at the NREL MET tower locations

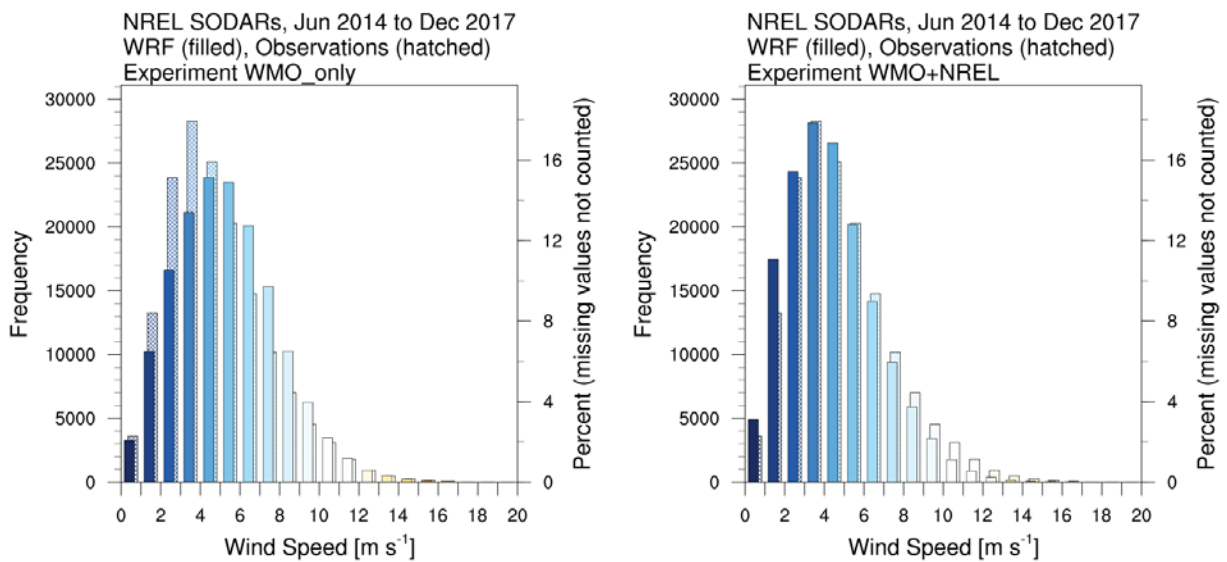


Figure 36. Binned histograms at the NREL SODAR locations

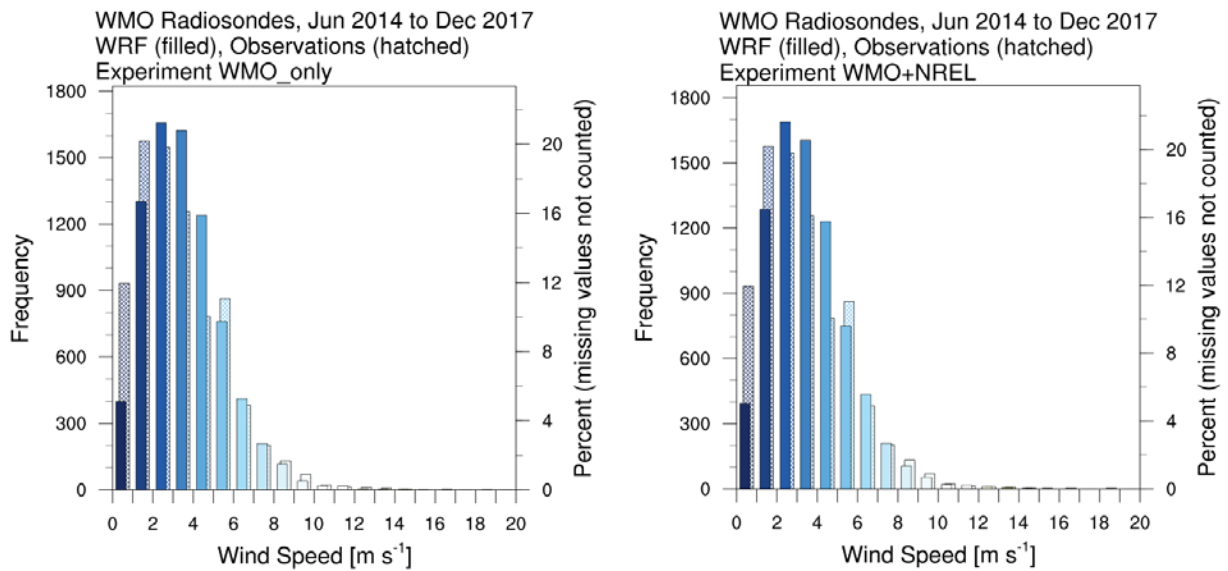


Figure 37. Binned histograms radiosondes

These binned histograms show that, for the MET towers and SODARs, the WRF wind-speed distribution more closely matches the observed wind-speed distribution for the “WMO+NREL” experiment than for the “WMO_only” experiment. For the radiosondes, the WRF and observed distributions are similar between the two experiments. Thus, the binned histograms also confirm the benefits to the WRF-simulated wind speed when assimilating all available observations. Further, the binned histograms reveal that, at the MET tower and radiosonde locations, more than 50% of the observed wind speeds are less than 4 m/s; at the SODAR locations, more than 40% of the observed wind speeds are less than that threshold.

Because assimilating the observations from the NREL MET towers and SODAR improved the WRF wind-speed analysis overall, all remaining plots and discussion include only the WMO+NREL experiment.

7.1.3 Validation Results

The mean wind speed for both WRF and observations was plotted, both as a series of monthly averages and a series of annual averages. The same information was averaged into an annual cycle, which sketches out the long-term averages through the year over the course of this 3.5-year modeling study. Figure 38 shows the annual cycle for mean wind speeds for WRF and observations at all heights (left panel) and at only 80 m AGL (right panel). These plots indicate a clear annual cycle in the winds, with a peak in the spring and summer of generally 4–6 m/s, and a low in the autumn and winter of generally 2–4 m/s. Although a 3.5-year observational and modeling study is insufficient to characterize the range of interannual variability in the wind speed, the annual cycle in the average wind speed is important information for estimating the expected power and viability of potential wind farms.

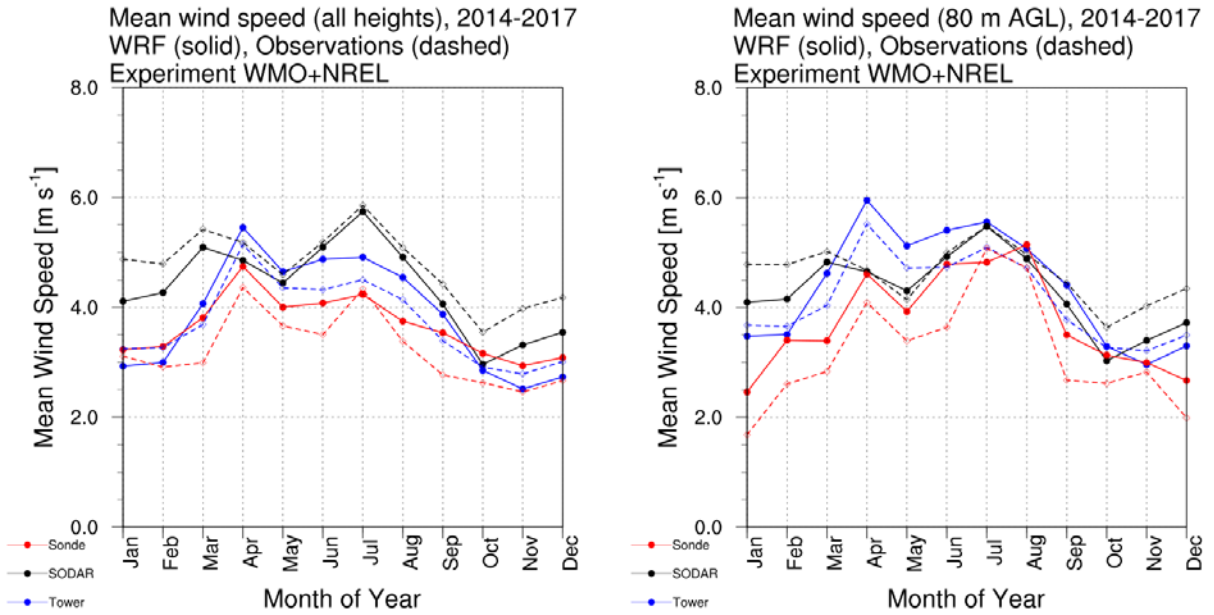


Figure 38. Annual cycle of mean wind speed

Figure 38 shows that WRF slightly underpredicted the observed wind speed at the SODAR locations year-round but with near-zero bias in the summer, underpredicted the observed wind speed at the MET towers in winter and overpredicted it the rest of the year, and overpredicted the observed wind speed at the radiosonde locations year-round. This is also borne out more clearly in the annual cycle of the ME (bias), defined as WRF minus observations, in Figure 39. For most months for all three observation platforms, both at all heights and at 80 m AGL only, the absolute value of the bias is less than 0.5 m/s.

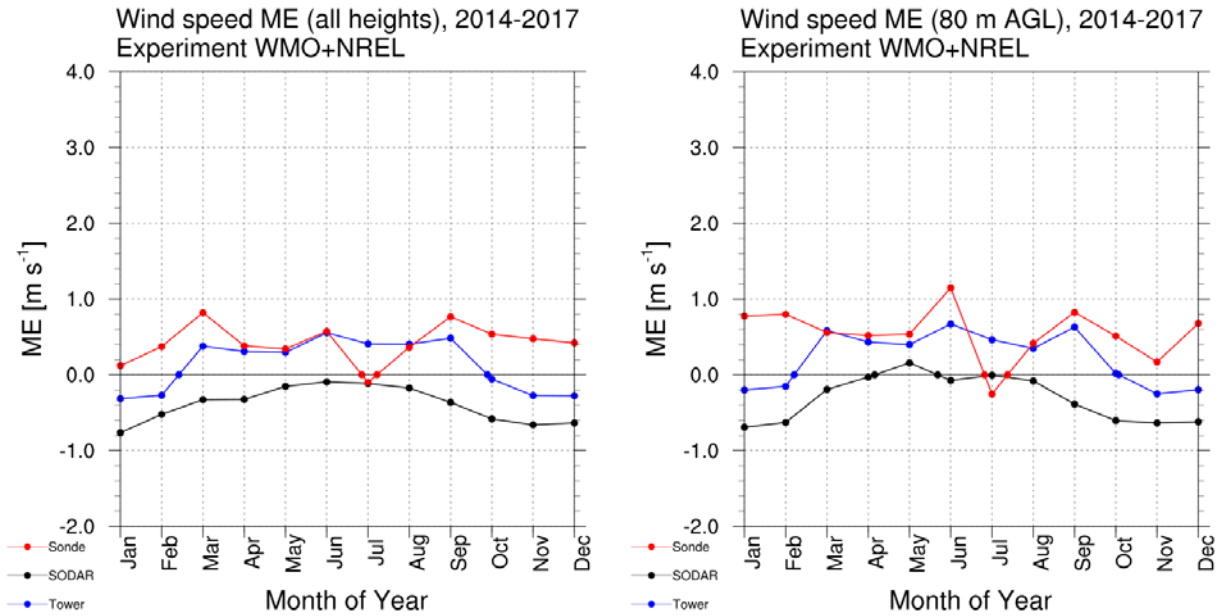


Figure 39. Annual cycle of the ME (bias)

The annual cycle of the RMSE (Figure 40) is remarkably similar for all three observation platforms when validating against all observation heights (left panel), tracking far more closely together than for the ME, with a peak value of the RMSE in April and May. The RMSE signal becomes noisier for the radiosonde observations at 80 m AGL (right panel), because the sample size is comparatively small, with only a few dozen model/observation pairs in each month as compared to a few thousand in each month for the SODAR and MET tower data series. The RMSE for all data series typically is 1.5–3.0 m/s, both when validating against observations at all heights and observations at only 80 m AGL.

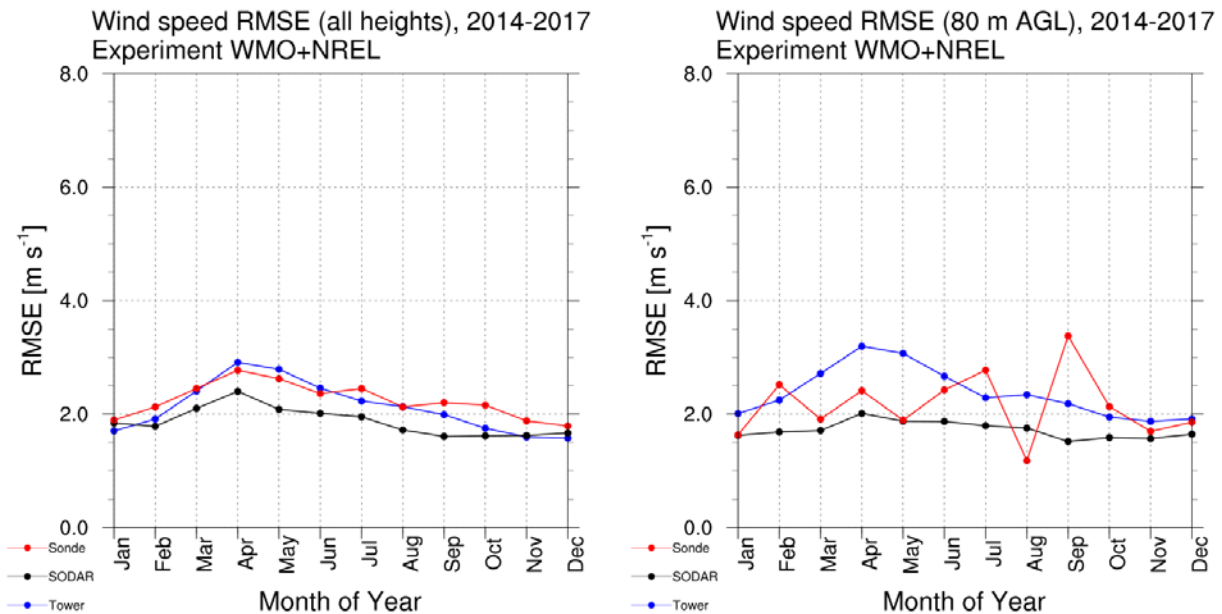


Figure 40. Annual cycle of the RMSE

In addition to the above metrics, wind roses for the observed and WRF-modeled MET towers that had measurements at 80 m AGL as well as those for the SODAR at its locations were plotted. For instance, for the Rangpur SODAR (Figure 41), the observed and WRF wind roses are fairly similar overall. The WRF correctly captures that winds from the east, southeast, and northeast were the three most dominant wind directions during the period that the SODAR was located in Rangpur, although WRF underpredicted the frequency of winds from the northeast and somewhat overpredicted the frequency of winds from the west, as compared to observations. Similarly, good agreement was found for the SODAR while it was located in Inani and Rajshahi (not shown). The agreement between the observed and WRF wind roses for the Rajshahi MET tower also was generally good (Figure 42). The wind roses for the Sitakunda MET tower (Figure 43) show the WRF model doing a poorer job of replicating the observed wind rose. At Sitakunda, the WRF most notably underpredicted the frequency of winds from the north and overpredicted the frequency of winds from the south and southwest. The WRF also overpredicted the highest wind speeds for winds coming from the east and north, with at least some instances of 20–25 m/s wind, as compared to the highest observed wind speeds from those directions being 10–15 m/s. It is unclear why the WRF performed better compared to observations at some locations than at other locations, but, in general, the WRF model reasonably reproduced the statistics of the observed winds across Bangladesh at 80 m AGL.

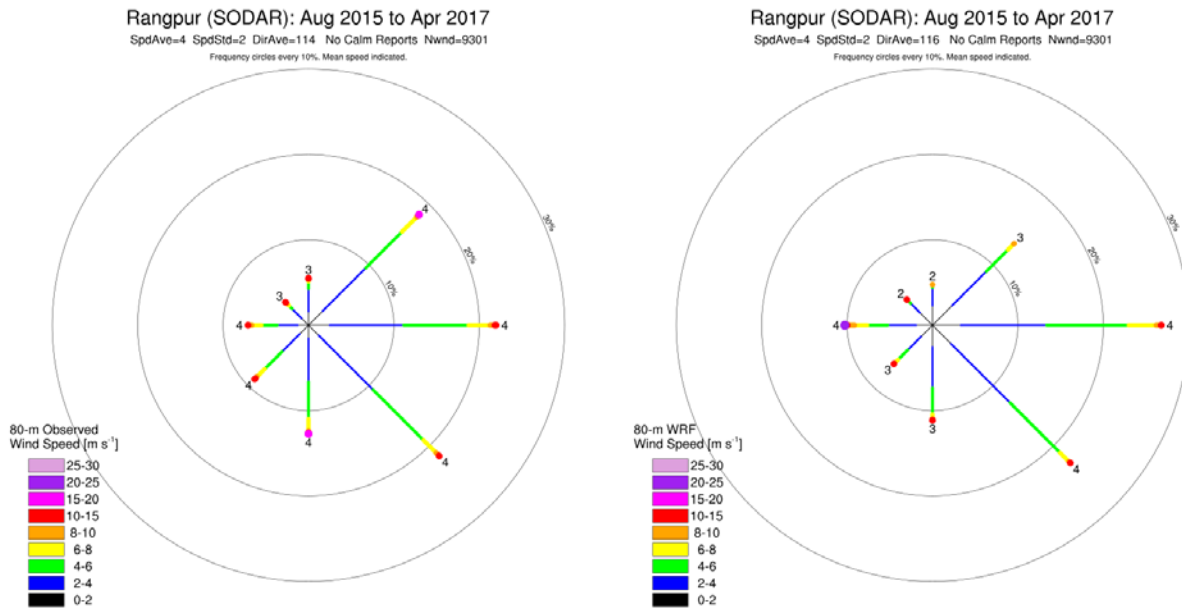


Figure 41. Wind roses at the Rangpur SODAR

Colors denote wind-speed ranges (see legend), and circles denote frequency in intervals of 10%. Wind direction is defined by MET convention—for example, 90° is a wind coming from the east. The average speed for winds coming from a particular direction is given at the end of each “petal” of the wind rose.

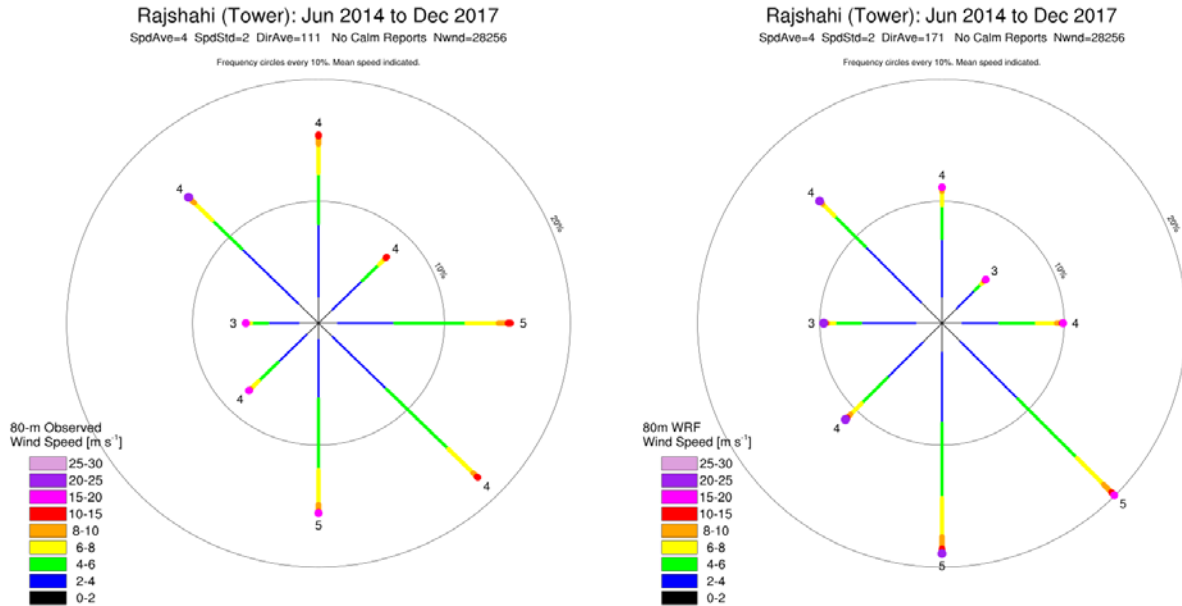


Figure 42. Wind roses at the Rajshahi MET tower

Colors denote wind-speed ranges (see legend), and circles denote frequency in intervals of 10%. Wind direction is defined by MET convention—for example, 90° is a wind coming from the east. The average speed for winds from a particular direction is given at the end of each petal of the wind rose.

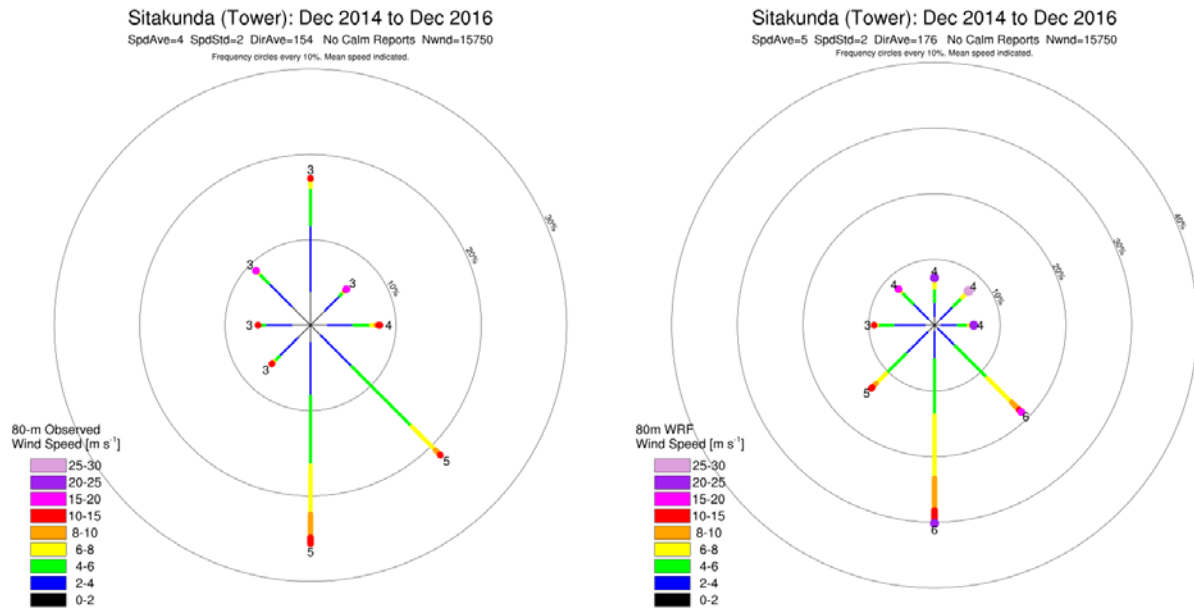


Figure 43. Wind roses at the Sitakunda MET tower

Colors denote wind-speed ranges (see legend), and circles denote frequency in intervals of 10%. Wind direction is defined by MET convention—for example, 90° is a wind coming from the east. The average speed for winds from a particular direction is given at the end of each petal of the wind rose.

7.2 Extension of 3-Year Simulations to 15 Years to Create a Long-Term Reference

The dynamical downscaling over Bangladesh of CFSR (Saha et al. 2014) global data with the WRF regional model requires about 730 core hours and 15 GB of disk space per day of climatology. The computing resources required to downscale 15 years to create a climatology are immense. Statistical methods to downscale wind fields at a fraction of the cost of dynamical downscaling have been proposed and successfully applied. The main idea is to selectively downscale certain days representative of the climate of the region under study. The approach tends to statistically identify those regimes from the global analyses. The WRF dynamical downscaling is then applied to representative samples of the global analysis, hence saving computing time.

Rife et al. (2013) demonstrated the potential of the method for hub-height wind resources assessment and showed that 180 days could be sufficient to represent a full year of data. This approach is based on a Monte Carlo method coupled with stratified sampling and is purely statistical. Monaghan et al. (2012) applied similar concepts in combination with the WRF regional model to create a 2-km 1999–2009 climatology of precipitations over East Africa using 10 years of WRF data at 18-km grid spacing and a single year of WRF output data at 2-km grid spacing. The authors performed 1 year of WRF simulations (2006) with four embedded domains (56 km/18 km/6 km/2 km); the additional 10 years of simulations (1999–2009) were performed on only the outer two domains (56 km and 18 km), hence saving a significant amount of computing resources. A statistical technique, the bias-correction spatial disaggregation method of Wood et al. (2004), was employed to downscale 18-km WRF output to 2-km grid spacing for the 15-year period in which the WRF inner domains were not used. This statistical/dynamical downscaling hybrid method—like its companion technique, the analog (Keller, Monache, and Alessandrini 2017)—requires a training data set, usually a subset of the full data set at higher resolution, and a test data set, usually the main portion of the data at lower resolution. The

overlapping period (year 2006) (Monaghan et al. 2012) when both low- and high-resolution data are simultaneously available is used for calibration.

A technique similar to that of Monaghan et al. (2012) and Keller, Monache, and Alessandrini (2017), although simpler, was applied in this study. This technique is illustrated for the generation of a 15-year wind climatology at about 200 m AGL for 15 years of Julys in Bangladesh, which is the windiest season. To be general, NREL’s local observations were not used, but the WMO data were assimilated in all the WRF simulations performed in this downscaling study.

We began with the generation of 15 years of July’s (2003–2017) WRF hourly output data for the outermost domain (D1, $dx = 27$ km), masked to include only the portion of D1 that encompasses the finest domain (D3). Figure 44(a) shows the wind rose at 200 m for all the grid points of D1 covering Bangladesh (i.e., grid points common to both WRF domains 1 and 3). The resulting data set is composed of 15 years times 31 days times 24 hours, which equals 11,160 WRF hourly output files. Each file contains 928 (29 x 32) grid points covering Bangladesh. We used the wind speed at those 928 grid points valid at vertical level 11 (~200 m). Each file constitutes a vector data point on which we applied a classification based on SOMs to determine the most predominant regimes for the 200-m wind speed. An SOM analysis (Kohonen 1982) is a particular application of an artificial neural network that can be used to conduct unsupervised classification. It therefore is not necessary to know which regimes to look for; the SOM analysis finds those regimes and sorts the output files according to those regimes (Hewitson and Crane 2002). The number of sought regimes, however, must be specified by the user. Based on previous experience, we chose six regimes, as this provides a sufficient number of regimes to cover most of the variability but leads to a manageable number of regimes. The SOM analysis provides the data maps that are most representative of each regime identified. As a result, we obtained six WRF output files that are the most representative of the predominant regimes present in the 11,160 WRF hourly output files for July of the years 2003 to 2017. The corresponding days and times are listed in Table 10. Figure 44(b) shows the wind rose similar to Figure 44(a) but for the six most representative regimes identified during the classification.

Table 10. Dates and Times of the Most Representative Regimes for 200-m Hourly Wind Vectors at the 29 x 32 Grid Points of WRF Domain 1 (27 km) Covering Bangladesh

Valid for the months of July 2003–2017, with the frequency of occurrence of the corresponding regime.

WRF domain 1 output date and time of most representative regimes	Frequency of occurrence of the regime
2007-07-11 / 12 UTC	24%
2003-07-08 / 06 UTC	21%
2005-07-28 / 06 UTC	20%
2011-07-03 / 12 UTC	19%
2008-07-31 / 06 UTC	9%
2008-07-16 / 12 UTC	7%

Figure 44(a) was constructed from $11,160 \times 928 \approx 10 \times 10^6$ wind vectors, and Figure 44(b) uses only $6 \times 928 \approx 5 \times 10^3$ wind vectors, or about 1,800 times fewer data points. Nonetheless, the graphs look very similar. The frequency of occurrence presented in Table 10 indicates that the first four regimes represent nearly 85% of all weather situations occurring in July between 2003 and 2017. This outlines the very low wind variability over Bangladesh at this time of the year. This lack of variability presents an additional argument for employing statistical downscaling.

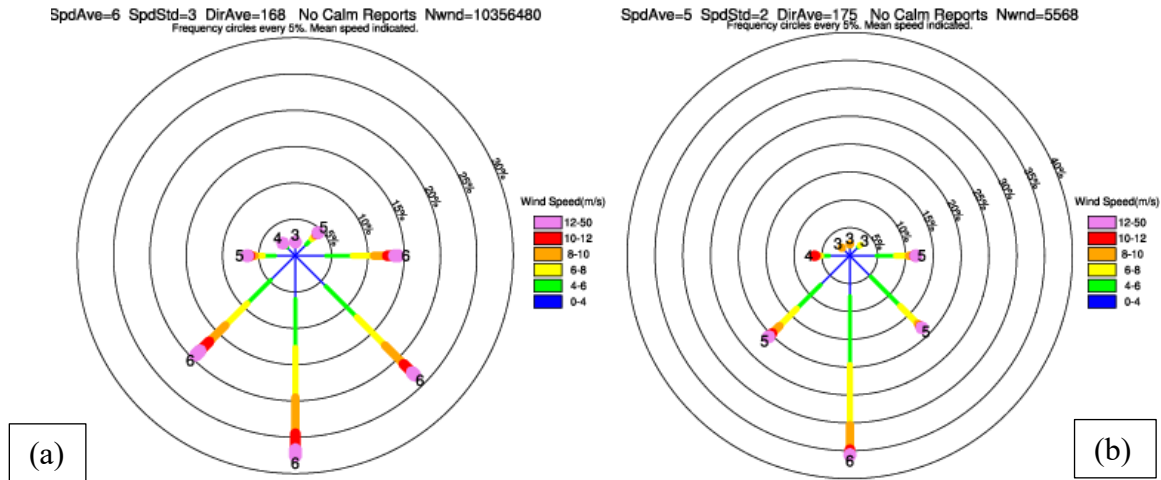


Figure 44. Wind roses for most representative regimes identified during the classification

- (a) Wind rose at 200-m height from WRF hourly wind vectors at the 29×32 grid points of WRF Domain 1 (27 km) covering Bangladesh, valid for the months of July 2003–2017;
- (b) wind rose at 200-m height from WRF hourly wind vectors at the 29×32 grid points of WRF Domain 1 (27 km) covering Bangladesh, valid for the most representative dates of the main regimes (listed in Table 10).

The six identified regimes were downscaled with the WRF model to 3- km grid spacing, and the wind rose for those six regimes was assembled in Figure 45(b). This wind rose uses the same wind data as the wind rose shown in Figure 44(b) but for the WRF Domain 3 instead of Domain 1. To evaluate how well the six regimes identified using the lower-resolution grid can represent the higher-resolution winds, we constructed the wind rose from the 3-km downsampled data valid for the months of July 2014, 2015, 2016, and 2017. This wind rose is shown in Figure 45(a). The two wind roses look remarkably similar. In particular, they share the same mean wind speed (6 m/s) and standard deviation (3 m/s). The mean directions differ by only 13° . This similitude between the downsampled winds from the six SOM regimes and 4 years of fully downsampled data provides confidence that those same regimes can well represent the full 15-year distribution.

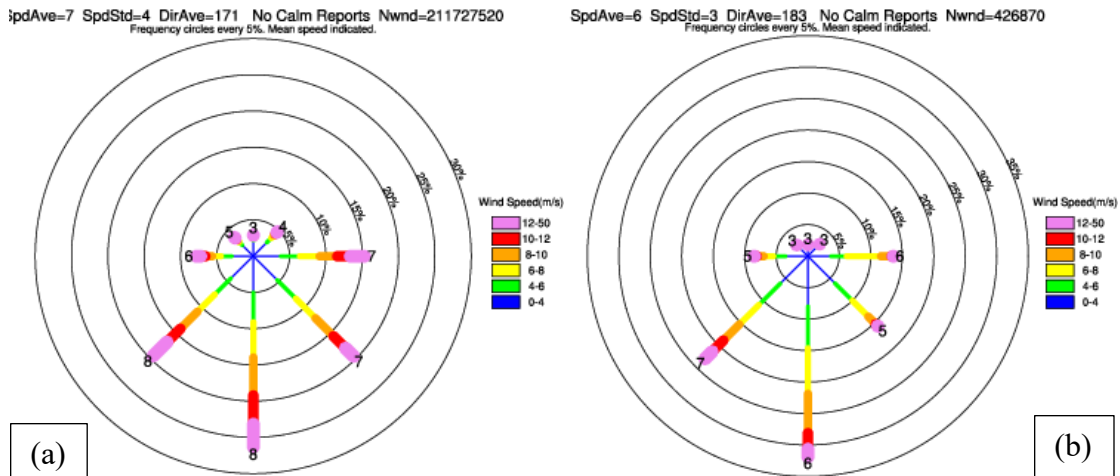


Figure 45. Wind roses for regimes downscaled with the WRF model to 3-km grid spacing
 (a) Wind rose at 200-m height from WRF hourly wind vectors on WRF Domain 3 (3 km) valid for the downscaled months of July 2014–2017; (b) wind rose at 200-m height from WRF hourly wind vectors on WRF Domain 3 (3 km) valid for the six most representative dates of the main regimes (listed in Table 10).

The 200-m winds representative of the four most predominant regimes, as represented by the dates and times listed in Table 10, are plotted in Figure 46.

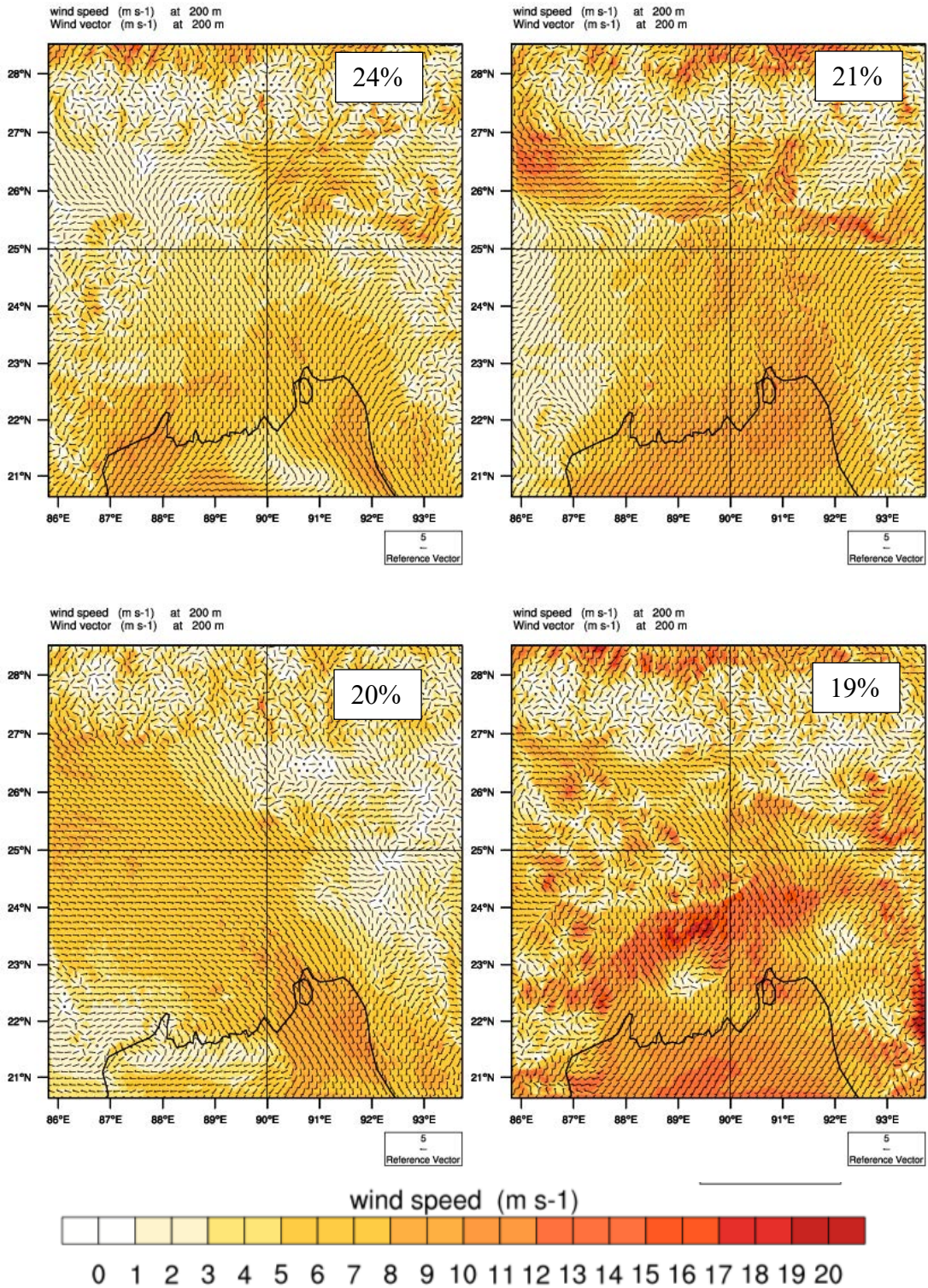


Figure 46. Four most frequently occurring 200-m wind regimes
Each regime frequency of occurrence is indicated as a percentage.

8 Products/Tools

The measured data in raw format, as a formatted and quality-controlled data set, and the model simulations are tools that were created through the project and are freely available. The model simulations are available through the RE Data Explorer tool (www.re-explorer.org) and Globus Connect,⁵ as formatted data or as maps.

8.1 Measured Data Sets

The data sets containing the measured data are publicly available via Globus Connect. Two different types of measured data sets are available: raw data and quality-controlled data.

The raw (text) data files are available via the RE Data Explorer. The raw data files from the towers are available in different types and time-step intervals. The daily files are the data packets pushed daily from the data logger to the server; these files typically contain a day's worth of data. Occasionally, a daily file is less than a full day's data, either due to collection/transmission errors or because the file is from the first or last day of monitoring. Daily data files are available with either 1-minute or 10-minute time steps. To make identification easier, the daily files are named using the follow convention: four-character site code then time step (oneMin or tenMin), then eight-digit date, and then a letter (if more than one file is available for a given date). For example, the file from Parkay Beach for October 12, 2015, has the filename PKAY_tenMin_2015_10_12.dat.

The other type of raw files from the towers are the “logger” files. These files are data that were downloaded from the data loggers during site visits by Harness Energy personnel. These files each generally contain several months of data. The data in these logger files have a time step of either 1 minute, 10 minutes, or 1 hour. These files are named using the following convention: Site name-(time step)-start date-end date. An example is “Mongla (Ten Min)-20160313-20160806.”

The SODAR raw data files are different from the tower raw data files. The data from the SODAR unit are pushed several times a day to the SODAR manufacturer's server. The analyst can then download the data from the server by selecting data from a specific period. The analyst also can choose to only download data with a QF equal to or greater than a specified minimum. Values for QF can range from 0 (worst) to 100 (best). The SODAR raw data files in the RE Data Explorer contain the data for the whole monitoring period and with no minimum QF. The QF for each data point is provided within the file, allowing users to filter the data to whatever value of QF desired. There are two raw data files for each SODAR site. One file has the wind speed and direction measurements. The other file, dubbed the “operational” file, contains additional measurements, such as temperature, as well as data streams regarding the status of the SODAR unit.

Table 11 provides details of the raw data files for each monitoring site. In contrast to the raw data files, there is only one processed data file for each site. The processed data file names are listed in Table 12. The situation for the files created for the modeling team is the same as for the processed files; there is one file per site. Details are provided in Table 12.

⁵ Please contact NREL (windtoolkit@nrel.gov) for details on how to access the wind data for Bangladesh.

Table 11. Raw Data

Site	File Type	Notes
Chandpur	Daily, 1 minute	449 files
	Daily, 10 minutes	513 files
	Logger Files	
Mirzapur	Daily, 1 minute	161 files
	Daily, 10 minutes	178 files
	Logger Files	
Mymensingh	Daily, 1 minute	532 files
	Daily, 10 minutes	594 files
	Logger Files	
Parkay Beach	Daily, 1 minute	250 files
	Daily, 10 minutes	250 files
Rajshahi	Daily, 1 minute	697 files
	Daily, 10 minutes	790 files
	Logger Files	
Sitakunda	Daily, 1 minute	530 files
	Daily, 10 minutes	566 files
	Logger Files	
Inani (SODAR)	Data from server	
Rangpur (SODAR)	Data from server	

Table 12. Processed Data Files

Site	File Name—Processed	File Name—For Modeling
Chandpur	Chandpur(QCd)_20140611-20171204.txt	Chandpur(MOD)_20140611-20171204.csv
Mirzapur	Mirzapur(QCd)_20151019-20171122.txt	Mirzapur(MOD)_20151019-20171122.csv
Mongla	Mongla(QCd)_20151031-20171225.txt	Mongla(MOD)_20151031-20171225.csv
Mymensingh	Mymensingh(QCd)_20150813-20171213.txt	Mymensingh(MOD)_20150813-20171213.csv
Parkay Beach	Parkay_Beach(QCd)_20141221-20170714.txt	Parkay_Beach(MOD)_20141221-20170714.csv
Rajshahi	Rajshahi(QCd)_20140611-20171220.txt	Rajshahi(MOD)_20140611-20171220.csv
Sitakunda	Sitakunda(QCd)_20141218-20161220.txt	Sitakunda(MOD)_20141218-20161220.csv
Inani (SODAR)	Inani(QF90)(QCd)_local_time_20140725-20150802.txt	Inani(QF90)(MOD)_local_time_20140725-20150802.csv
Rajshahi (SODAR)	Rajshahi(QF90)(QCd)_local_time_20140508-20140722.txt	N/A – Data not used for modeling due to short monitoring period and overlap with Rajshahi tower data
Rangpur (SODAR)	Rangpur(QF90)(QCd)_local_time_20150804-20170418.txt	Rangpur(QF90)(MOD)_local_time_20150804-20170418.csv

8.2 Maps

Developing resource maps is an important step in any wind resource assessment campaign. Increasing the distance away from the collection station increases the uncertainty of the data used to validate the model. Financing entities will probably require additional testing depending on factors such as distance from the MET tower, size of project, and complexity of terrain. However, in the initial prospecting or feasibility stage, developers and financiers may want to evaluate the wind resource from a macro perspective. As an example, Figure 47 demonstrates the wind resource in Bangladesh at 120 m. In this figure, the MET stations are identified by an anemometer icon. More maps may be generated using the RE Data Explorer, as explained below.

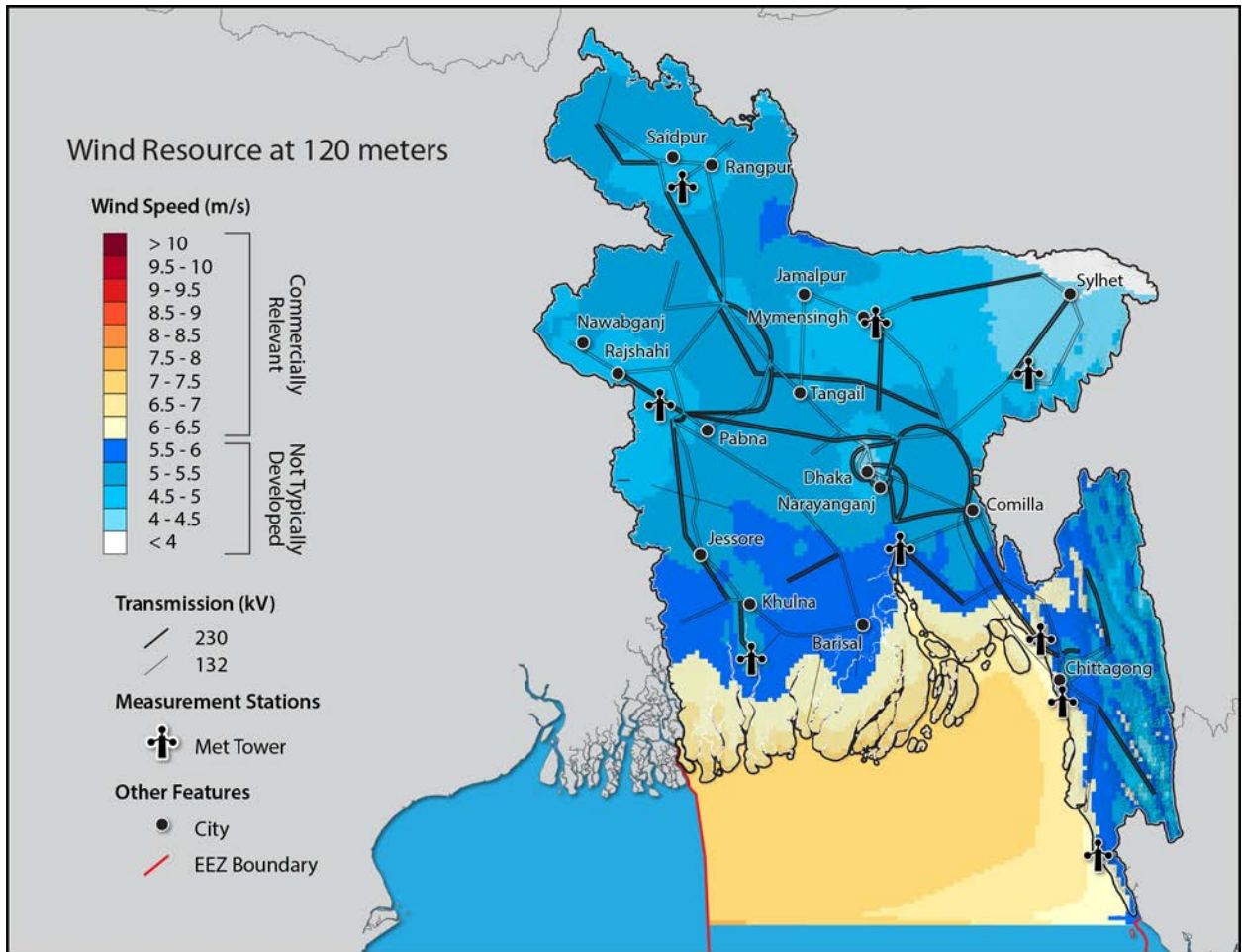


Figure 47. Bangladesh's wind resource map at 120 m

8.3 Modeled Data Sets

The raw model output was converted to a format similar to the WIND Toolkit data (Draxl et al. 2015). This format is very useful for users and can be easily integrated into the RE Data Explorer tool. Users can download data for specific sites via the RE Data Explorer tool but also can download the entire hourly time series for every grid point at once via Globus Connect. This allows analysts to perform their own studies for any application they wish, such as statistics over an area or the whole country, preparation of files to be read by other software, or even preparation for applications other than wind energy. Note that the entire time-series data set has a size of 3 TB. The final converted model output includes the variables described in Table 13, at 10 m, 30 m, 40 m, 60 m, 80 m, 100 m, 120 m, 140 m, 160 m, and 200 m on a 3-km grid.

Table 13. Modeled Data Available via the RE Data Explorer Tool and Globus Connect

Data	Available Through RE Data Explorer	Available Through Globus
Time [UTC]	Yes	Yes
Wind speed [m/s]	30 m, 80 m, 100 m, 120 m, 140 m	10 m, 30 m, 40 m, 60 m, 80 m, 100 m, 120 m, 140 m, 160 m, 180 m, 200 m
Wind direction [°]	30 m, 80 m, 100 m, 120 m, 140 m	
Temperature [K]	2 m	
Relative humidity [%]	10 m	2 m, 10 m
Barometric pressure [Pa]	Surface	Surface, 100 m, 200 m
Precipitation rate	—	Surface
Solar radiation	—	Global horizontal shortwave irradiance
Atmospheric stability	—	1/L (Monin-Obhukov length)
Skin temperature	—	Surface
Upward heat flux	—	Surface
Boundary layer height	—	Yes
u^* in similarity theory	—	Yes

Access to the data via the RE Data Explorer tool, as well as the data structure within the RE Data Explorer tool, are discussed in the next section.

8.4 Renewable Energy Data Explorer

The final model simulations are available at no cost online in the RE Data Explorer, which is a dynamic, web-based geospatial analysis tool that facilitates renewable energy decision making, investment, and deployment.

From the RE Data Explorer homepage (www.RE-Explorer.org), users can click on “Bangladesh.” Users next have the option to watch a tutorial on the tool and/or read the user guide. Users can also visually display data for specific geographic areas or points within the RE Data Explorer.

The following exercise demonstrates how the RE Data Explorer might be used for a preliminary identification of potential wind energy development sites. Circled locations overlaying the screenshot in Figure 48 depict possible areas for development.

1. Select the data layers of Transmission Lines, Wind Resource (choose the height), and Meteorological Stations so that you may consider:
 - A. Strength of wind resource
 - B. Proximity to transmission line (and size of transmission line)
 - C. Proximity to MET station.

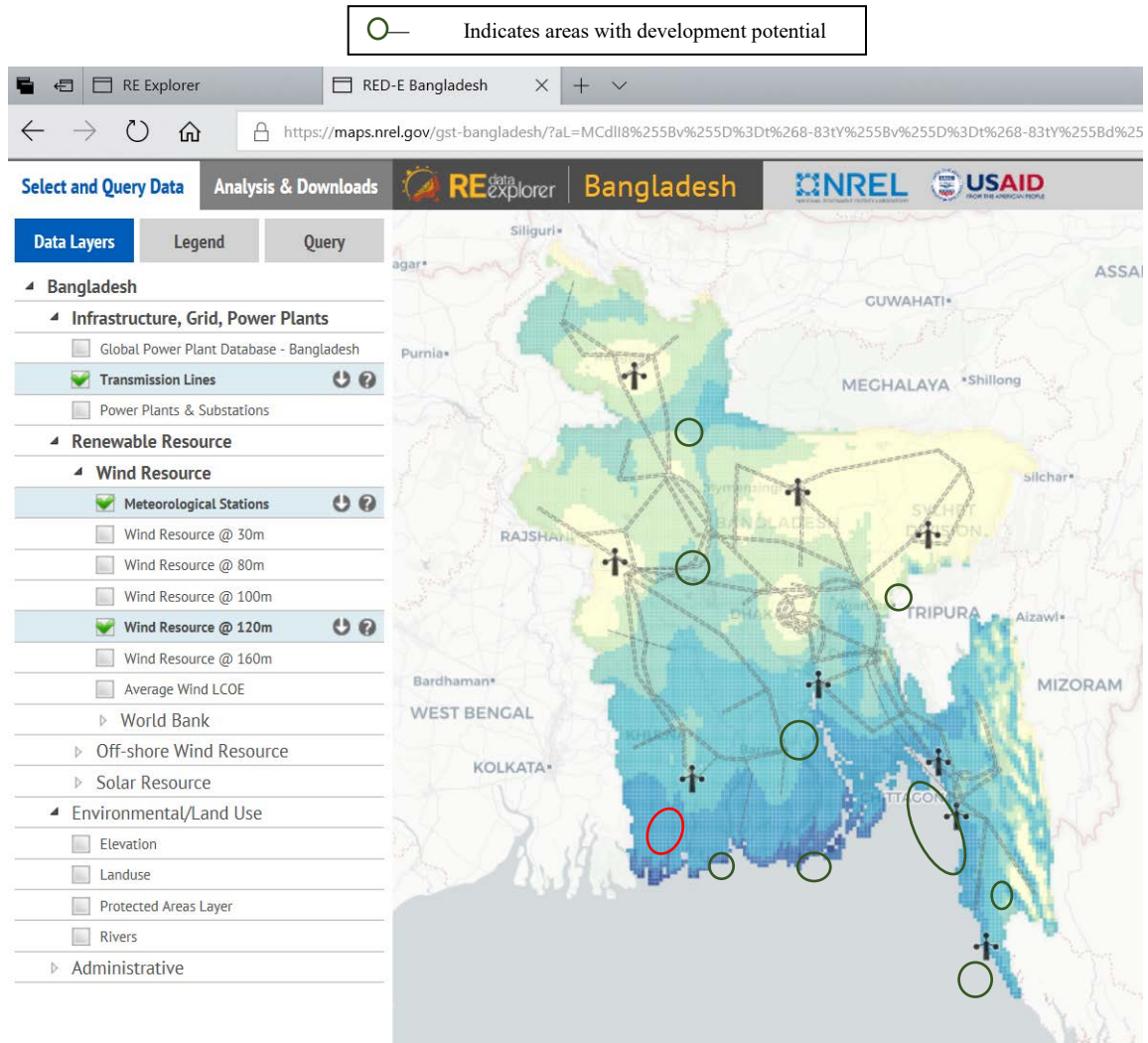


Figure 48. RE Data Explorer sample analysis

2. Evaluate land use and environmentally sensitive areas preliminarily by turning on the land-use layers and protected areas to determine if the area is suitable for development. Zoom in on the southwest area of the map near the red circle. It will help to turn off the wind resource layer. Use the transparency button to focus on land use and better understand issues, such as:
 - A. Environmentally protected areas
 - B. Water bodies vs. actual land
 - C. Urban areas vs. agricultural areas
 - D. Road layers to evaluate ease of transport of turbine components.

Figure 49 shows that the red selected area is in an environmentally protected area, and development would not be recommended. However, the dark green selected area to the southeast is outside of this protected zone and is worthy of further consideration.

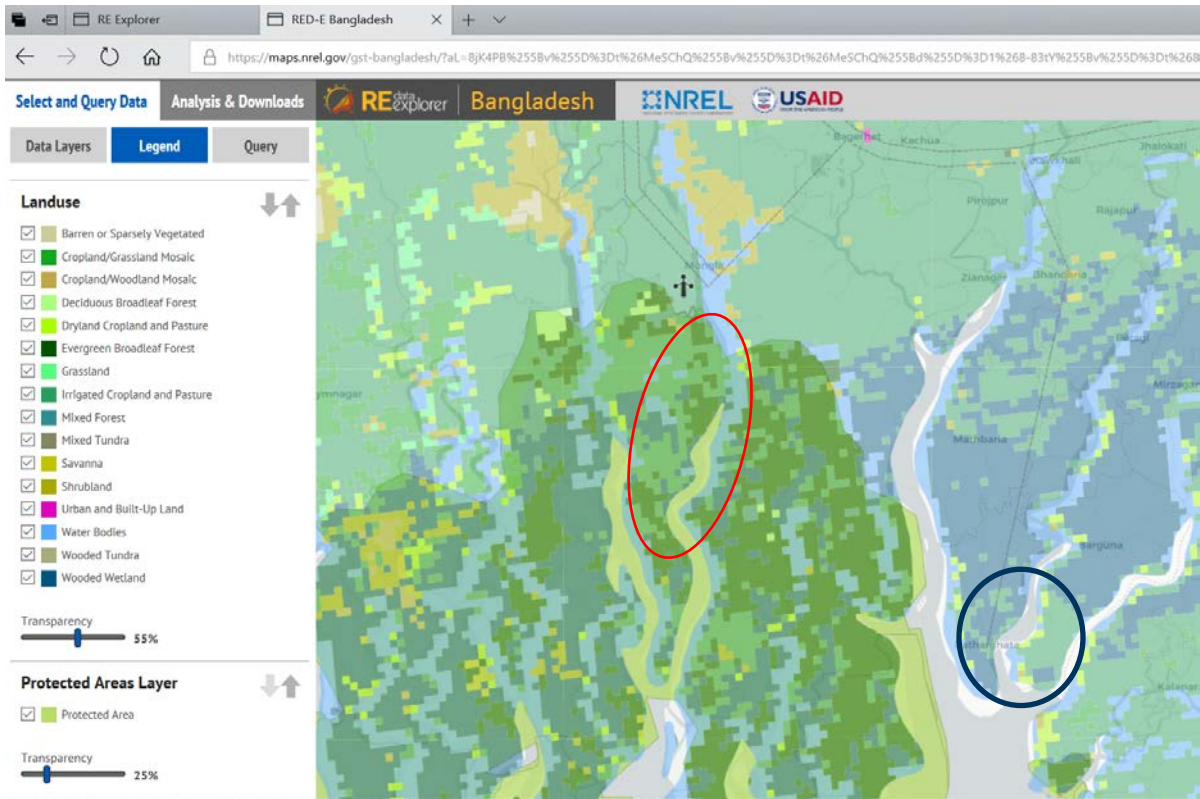


Figure 49. RE Data Explorer sample analysis identifying excluded zones and promising zones

If you click on a cell, you can obtain additional information on the transmission size and the strength of the wind resource at those specific location coordinates (Figure 50).

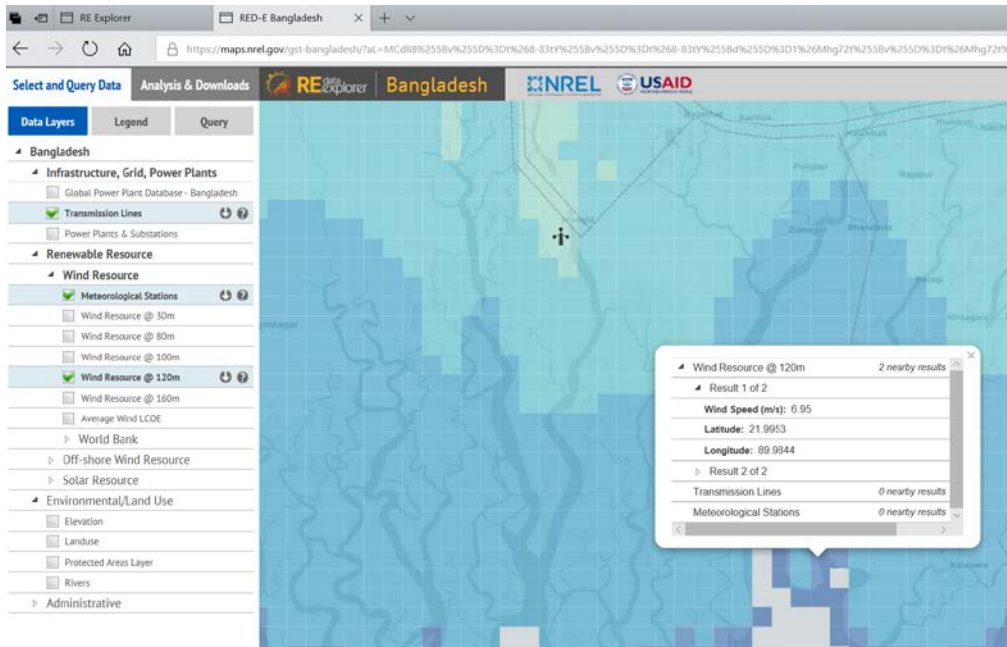


Figure 50. RE Data Explorer sample analysis with detailed information for one cell

For more information, you can use the query tool to download the information and view it on your computer (Figure 51). It is also possible to download a layer by clicking the down-arrow icon to the right of a layer name. This tool supports CSV, Shapefile, KML, or GeoJSON formats. Hourly time-series data also can be downloaded to provide analysis of how the wind resource varies temporally.

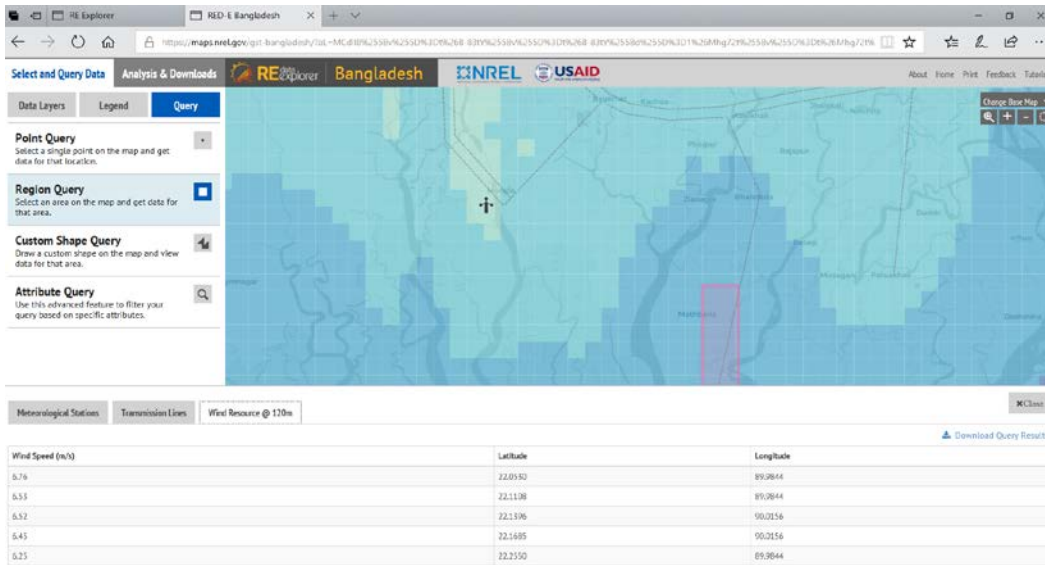


Figure 51. RE Data Explorer sample analysis with available query delimiters

View the wind resource at different hub heights by selecting layers such as 30 m, 80 m, 100 m, 120 m, and 160 m (Figure 52).

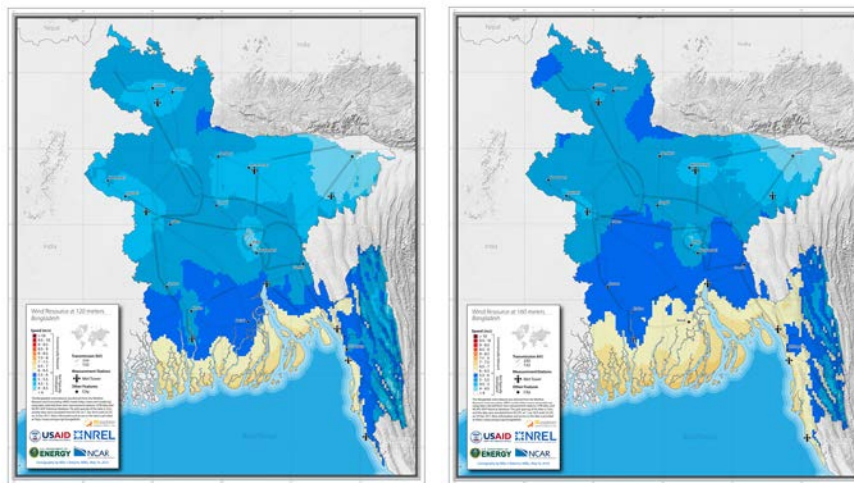


Figure 52. Illustrative map showing Bangladesh’s wind resources at 120 m (left) and 160 m (right)

9 Conclusions

This report provides a detailed discussion of the modeling approach, methods, instrumentation, and data-collection QC techniques used in the Bangladesh Wind Resource Assessment. High-quality instrumentation, proper siting, and detailed installation commissioning reports are the required first steps to generate high-fidelity models producing high-quality data products that can be used in decision making. These high-quality data products are used to develop proper tools for varied audiences to ensure usability and accessibility of the data for the public. This report describes our methods, documents the work completed, and demonstrates what types of data products are now available following completion of a 3.5-year resource-assessment campaign. In support of the USAID Bangladesh Mission, NREL, in collaboration with the GOB, completed the project, which included the following components:

- Development of a national wind resource assessment that involved creation of a preliminary and final wind resource model. As a result of this project, the wind profile and specific attributes are now well understood. A clear annual cycle in the winds was identified, with a peak in the spring and summer and a low in the autumn and winter. We further found that WRF slightly underpredicted the observed wind speed at the SODAR locations year-round but with near-zero bias in the summer, underpredicted the observed wind speed at the MET towers in winter and overpredicted it the rest of the year, and overpredicted the observed wind speed at the radiosonde locations year-round. However, in general, the WRF model reasonably reproduced the statistics of the observed winds across Bangladesh at 80 m AGL.
- Installation, maintenance, and data-collection activities for nine MET stations with diverse geographical positioning around Bangladesh.
- Generation of a set of high-quality data products:
 - Raw MET data set
 - Quality-controlled MET data set
 - Final modeled long-term correlated wind data set
 - Validated high-resolution wind resource maps
- Customized GIS-based tool called the RE Data Explorer, which graphically represents the Bangladesh data for users (<https://www.re-explorer.org/bangladesh-data.html>).
- Conducted a workshop in Bangladesh that presented final project results and provided training on the RE Data Explorer, wind resource modeling, and wind development process.

The preliminary technical potential analysis calculates gross potential and does not filter out already-developed land, environmentally sensitive land, or land unsuitable for other reasons. However, these preliminary results demonstrate that, for wind speeds of 5.75–7.75 m/s, there are more than 20,000 km² of land with a gross wind potential of over 30,000 MW. Although this estimate is not realistic when proper filters are applied to screen out undesirable land for wind development, it suggests that Bangladesh’s 10% renewable target by 2021 is achievable.

Can wind energy compete with the local wholesale energy market? It is the first question asked after every wind resource assessment presentation. Although this work is an important first step, other data inputs are needed to answer this question, including turbine selection (i.e., power curve assumed) and knowledge of the unsubsidized cost of wholesale power.

Recommendations for further work by the GOB are to analyze installation and financing costs for wind energy and compare against current 20-year forecasts for Bangladesh’s cost of power, assemble more

land-use layers in GIS format to enable more detailed filters to be applied within the technical potential tool, and continue to find opportunities to disseminate the data set and tools developed within this scope of work. Additionally, a detailed introduction to best practices for grid-integration strategies would support decision making for investors and power system planners as they look for renewable energy integration solutions.

In summary, the most important project deliverable is the collection of the data products highlighted in the report, the RE Data Explorer, and the public access to both. With the continued dissemination of these data products and complementary future analyses of others, the intended result will be more informed decision making, which will likely increase renewable investment and advance wind development in Bangladesh.

References

- AWS Truepower and NREL (National Renewable Energy Laboratory). 2010. “Colorado 80-Meter Wind Resource Map.” U.S. Department of Energy WINDEXchange. <https://windexchange.energy.gov/maps-data/15>.
- Carvalho, D., A. Rocha, M. Gómez-Gesteira, and C. Silva Santos. 2014. “WRF Wind Simulation and Wind Energy Production Estimates Forced by Different Reanalyses: Comparison With Observed Data for Portugal.” *Applied Energy* 01/2014 (117): 116–26.
- Carvalho, D., A. Rocha, C. Silva Santos, and R. Pereira. 2013. “Wind Resource Modelling in Complex Terrain Using Different Mesoscale–Microscale Coupling Techniques.” *Applied Energy* 108 (C): 493–504.
- Clifton, A., B.-M. Hodge, C. Draxl, J. Badger, and A. Habte. 2018. “Wind and Solar Resource Data Sets.” *WIREs Energy Environ* 7: e276. doi:10.1002/wene.276.
- DOE (U.S. Department of Energy). 2013. “Installed Wind Capacity.” http://apps2.eere.energy.gov/wind/windexchange/wind_installed_capacity.asp.
- Draxl, C., A. Clifton, B.-M. Hodge, and J. McCaa. 2015. “The Wind Integration National Dataset (WIND) Toolkit.” *Applied Energy*. <http://dx.doi.org/10.1016/j.apenergy.2015.03.121>.
- Draxl, C.; A.N. Hahmann, A. Peña, and G. Giebel. 2012. “Evaluating Winds and Vertical Wind Shear from Weather Research and Forecasting Model Forecasts Using Seven Planetary Boundary Layer Schemes.” *Wind Energy*. doi: 10.1002/we.1555.
- Draxl, C.; B.M. Hodge, K. Orwig, W. Jones, K. Searight, D. Getman, S. Harrold, J. McCaa, J. Cline, and C. Clark. 2013. *Advancements in Wind Integration Study Data Modeling: The Wind Integration National Dataset (WIND) Toolkit*. NREL/CP-5D00-60269. Golden, CO: National Renewable Energy Laboratory.
- Draxl, C., A. Purkayastha, and Z. Parker. 2014. *Wind Resource Assessment of Gujarat (India)*. NREL/TP-5000-61741. Golden, CO: National Renewable Energy Laboratory.
- Drechsel, S., G. J. Mayr, J. W. Messner, and R. Stauffer. 2012. “Wind Speeds at Heights Crucial for Wind Energy: Measurements and Verification of Forecasts.” *Journal of Applied Meteorology and Climatology* 51: 1602–17. <https://doi.org/10.1175/JAMC-D-11-0247.1>.
- Dvorak, M.J., B.A. Corcoran, J.E.T. Hovee, N.G. McIntyre, and M.Z. Jacobson. 2012. “US East Coast Offshore Wind Energy Resources and Their Relationship to Peak-Time Electricity Demand.” *Wind Energy* 16: 977–97. doi: 10.1002/we.1524.
- Elliott, D.L., C.G. Holladay, W.R. Barchet, H.P. Foote, and W.F. Sandusky. 1986. “Map 2-6 Annual Average Wind Resource Estimates in the Contiguous United States.” In *Wind Energy Resource Atlas of the United States*. Richland, WA: Pacific Northwest Laboratory. <https://rredc.nrel.gov/wind/pubs/atlas/maps/chap2/2-06m.html>.
- Garcia-Diez, M., J. Fernandez, L. Fita, M. Menendez, F.J. Mendez, J.M. Gutierrez. 2012. “Using WRF to Generate High Resolution Offshore Wind Climatologies.” Proceedings from the 8^o Congreso Internacional AEC, Salamanca, Spain, September 2012.

- Global Energy Concepts. 2005. *Indiana Energy Group Tall Towers Wind Study Final Project Report*. Indianapolis: Indiana Energy Group. https://www.in.gov/oed/files/Indiana_Final_Project_Report.pdf.
- Hewitson, B.C., and R.G. Crane. 2002. "Self-Organizing Maps: Applications to Synoptic Climatology." *Climate Research* 22: 13–26. <https://doi.org/10.3354/cr022013>.
- Keller, J.D., L. Delle Monache, and S. Alessandrini. 2017. "Statistical Downscaling of a High-Resolution Precipitation Reanalysis Using the Analog Ensemble Method." *Journal of Applied Meteorology and Climatology* 56: 2081–95. <https://doi.org/10.1175/JAMC-D-16-0380.1>.
- Kohonen, T. 1982. "Self-Organized Formation of Topologically Correct Feature Maps." *Biological Cybernetics* 43: 59–69. <https://doi.org/10.1007/BF00337288>.
- Li, Ji-Hang, Zhen-Hai Guo, and Hui-Jun Wang. 2014. "Analysis of Wind Power Assessment Based on the WRF Model." *Atmospheric and Oceanic Science Letters* 7 (2): 126–31.
- Liu, Y., F. Vandenbergh, S. Low-Nam, T. Warner, and S. Swerdlin. 2004. "Observation-Quality Estimation and Its Application in the NCAR/ATEC Real-Time FDDA and Forecast (RTFDDA) System." 16th Conf. on Numerical Weather Prediction, Seattle, WA. *Bulletin of the American Meteorological Society* 17. <https://ams.confex.com/ams/pdfpapers/71934.pdf>.
- Lundquist, J.K., A. Purkayastha, C. St. Martin, R. Newsom. 2014. *Estimating the Wind Resource in Uttarakhand: Comparison of Dynamic Downscaling with Doppler Lidar Wind Measurements*. NREL/TP-5000-61103. Golden, CO: National Renewable Energy Laboratory.
- Monaghan A. J., K. MacMillan, S. M. Moore, P. S. Mead, M. H. Hayden, and R. J. Eisen. 2012. "A Regional Climatology of West Nile, Uganda, to Support Human Plague Modeling." *Journal of Applied Meteorological Climatology* 51: 1201–1221. <https://doi.org/10.1175/JAMC-D-11-0195.1>.
- Power Division, Ministry of Power, Energy and Mineral Resources Government of the People's Republic of Bangladesh. 2016. "Power System Master Plan 2016 Summary." [https://powerdivision.portal.gov.bd/sites/default/files/files/powerdivision.portal.gov.bd/page/4f81bf4d_1180_4c53_b27c_8fa0eb11e2c1/\(E\)_FR_PSMP2016_Summary_revised.pdf](https://powerdivision.portal.gov.bd/sites/default/files/files/powerdivision.portal.gov.bd/page/4f81bf4d_1180_4c53_b27c_8fa0eb11e2c1/(E)_FR_PSMP2016_Summary_revised.pdf).
- Rasel, A.R. 2017. "2017 in review: Power generation continues to grow, and so does price." *Dhaka Tribune (online)*. <https://www.dhakatribune.com/bangladesh/power-energy/2017/12/27/power-generation-price>.
- Rife, D.L., E. Vanvyve, J.O. Pinto, A.J. Monaghan, C.A. Davis, and G. Poulos. 2013. "Selecting Representative Days for More Efficient Dynamical Climate Downscaling: Application to Wind Energy." *Journal of Applied Meteorology and Climatology* 52: 47–63. <https://doi.org/10.1175/JAMC-D-12-016.1>.
- Saha, S., S. Moorthi, X. Wu, J. Wang, S. Nadiga, P. Tripp, D. Behringer, Y. Hou, H. Chuang, M. Iredell, M. Ek, J. Meng, R. Yang, M. Peña Mendez, H. van den Dool, Q. Zhang, W. Wang, M. Chen, and E. Becker. 2014. "The NCEP Climate Forecast System Version 2." *Journal of Climate* 27: 2185–208. <https://doi.org/10.1175/JCLI-D-12-00823.1>.

- Santos-Alamillos, F.J., D. Pozo-Vázquez, J.A. Ruiz-Arias, V. Lara-Fanego, and J. Tovar-Pescador. 2013. “Analysis of WRF Model Wind Estimate Sensitivity to Physics Parameterization Choice and Terrain Representation in Andalusia (Southern Spain).” *Journal of Applied Meteorology and Climatology* 52: 1592–609. doi: <http://dx.doi.org/10.1175/JAMC-D-12-0204.1>.
- Skamarock, W.C., J.B. Klemp, J. Dudhia, D.O. Gill, D.M. Barker, M.G Duda, X.-Y. Huang, W. Wang, and J.G. Powers. 2008. “A Description of the Advanced Research WRF Version 3.” *NCAR Tech. Note NCAR/TN-475+STR*, 113 pp. doi:10.5065/D68S4MVH.
- Storm, B., and S. Basu. 2010. “The WRF Model Forecast-Derived Low-Level Wind Shear Climatology over the United States Great Plains.” *Energies* 3: 258–76. doi:10.3390/en3020258.
- Wood, A.W., L.R. Leung, V. Srtidhar, and D.P. Lettenmaier. 2004. “Hydrologic Implications of Dynamical and Statistical Approaches to Downscaling Climate Model Outputs.” *Climatic Change* 62: 189–216. <https://doi.org/10.1023/B:CLIM.0000013685.99609.9e>.
- Wyngaard, J.C. 2004. “Toward Numerical Modeling in the ‘Terra Incognita.’” *Journal of Atmospheric Sciences* 61, 1816–26. doi: [http://dx.doi.org/10.1175/1520-0469\(2004\)061<1816:TNMITT>2.0.CO; 2](http://dx.doi.org/10.1175/1520-0469(2004)061<1816:TNMITT>2.0.CO; 2).

Appendix

The following pages summarize the data collection in Bangladesh for the whole monitoring period. There are data for each of the seven MET towers as well as the SODAR unit, which was deployed at Inani Beach and then Rangpur.

For each site, the following information is included:

- Data set properties: general statistics from the site.
- Wind-speed and direction summary: six graphs that illustrate the average wind speed for each month, the directional properties of the wind, the average behavior relative to time of day, and the distribution of wind speeds (**NOTE: the plots include raw wind-speed measurements, not modeled or validated data, and should not be used for decision-making purposes**).
- Wind shear: four graphs characterize the wind shear at the site; the wind shear characterizes how the wind speed changes with height above the ground.
- Turbulence intensity: four graphs that characterize the turbulence intensity at the site; the turbulence intensity value is a measure of the “gustiness” of the wind at the site.
- Data column properties: each data field includes height, units, the recovery rate, and the average mean, minimum, maximum, and standard deviation for all of the data.

The following pages summarize the data collection in Bangladesh for the whole of the monitoring period. There are data for each of the seven met towers as well as the SODAR unit, which was deployed at Inanib Beach and then Rangpur.

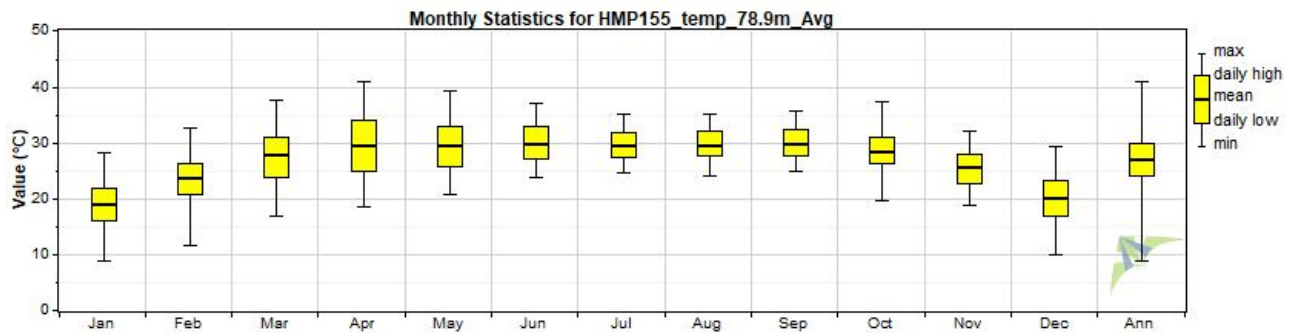
For each site, the following information is included:

- Data Set Properties – general statistics from the site
- Wind Speed and Direction Summary – six graphs which illustrate: the average wind speed for each month, the directional properties of the wind, the average behavior relative to time of day and the distribution of wind speeds (**NOTE: The plots include raw wind speed measurements, not modeled or validated data and should not be used for decision-making purposes**).
- Wind Shear – four graphs characterize the wind shear at the site. The wind shear characterizes how the wind speed changes with height above the ground.
- Turbulence Intensity – four graphs which characterize the turbulence intensity (TI) at the site. The turbulence intensity value is a measure of the “gustiness” of the wind at the site.
- Data Column Properties – each data field includes the following information: height, units, the recovery rate and the average: mean, min, max and standard deviation for all of the data.

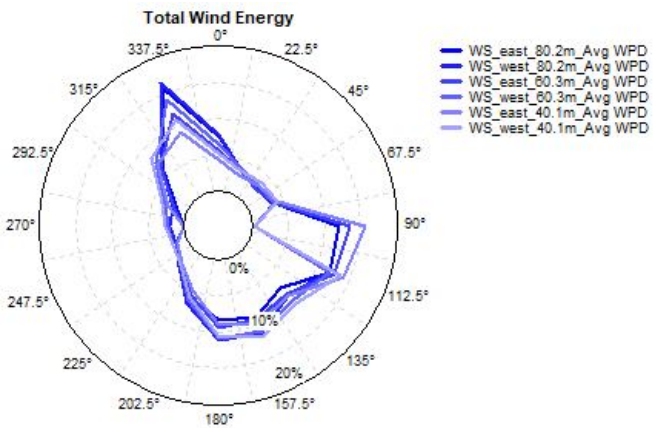
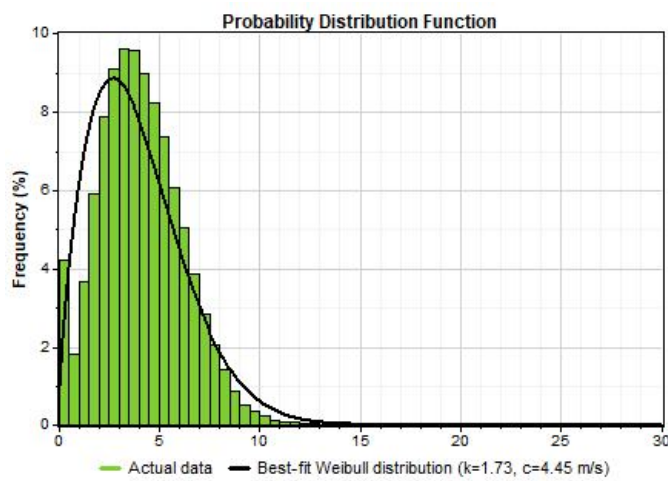
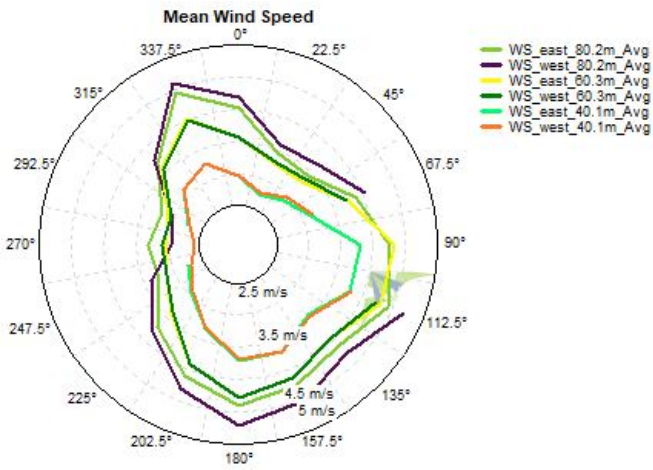
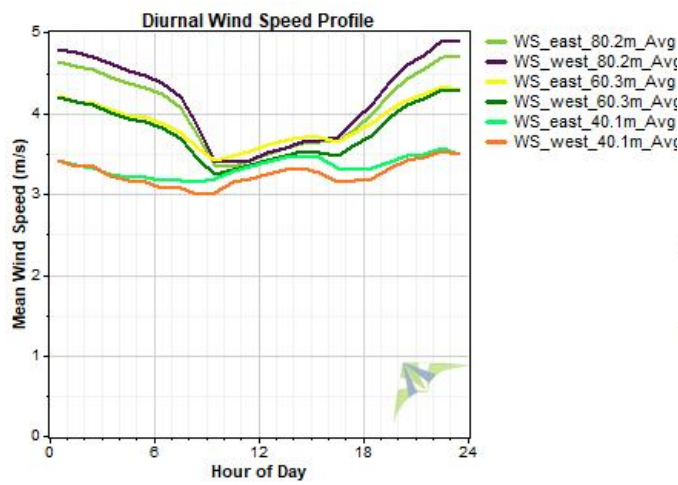
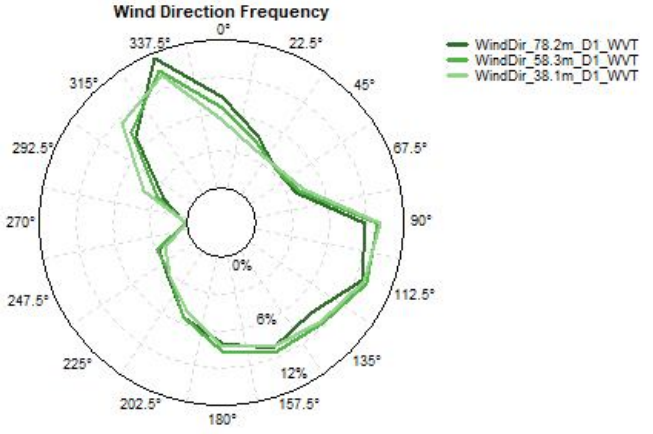
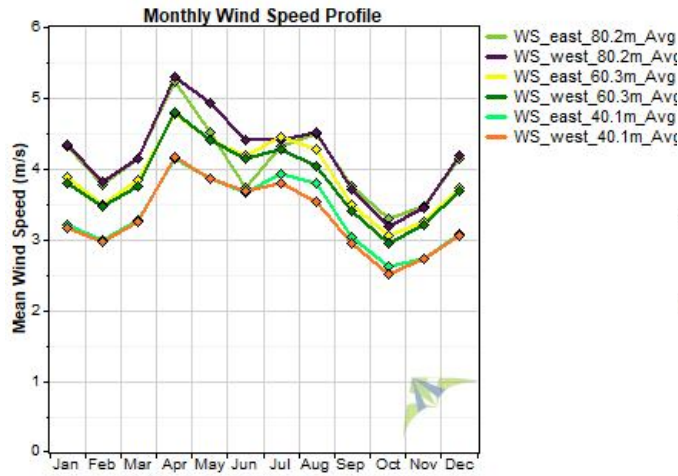
Data Set Properties

Report Created: 4/11/2018 10:34 using Windographer 3.3.10
 Filter Settings: <Unflagged data>

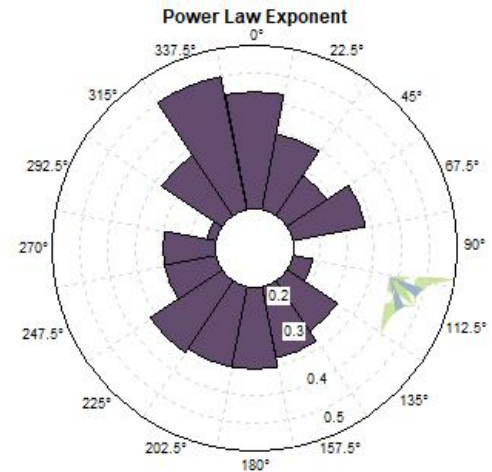
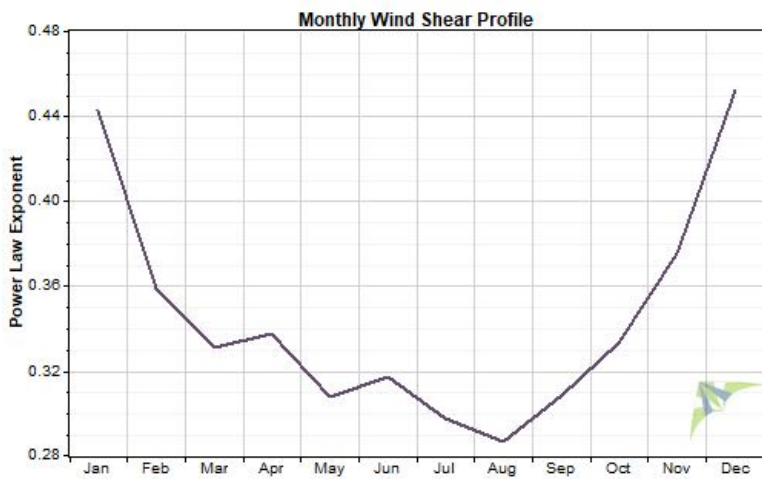
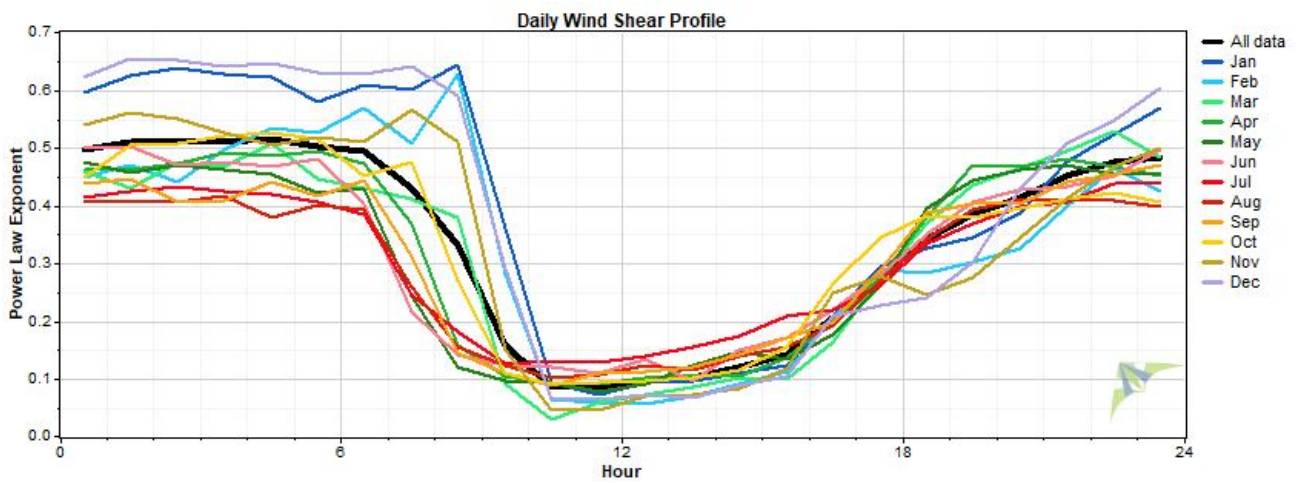
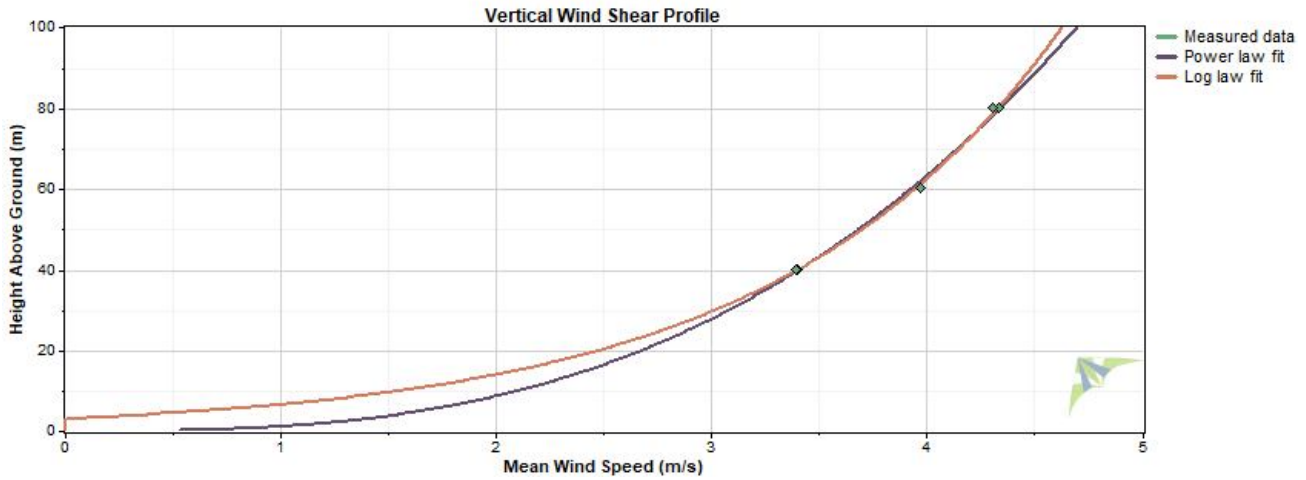
Variable	Value
Latitude	N 24.170350
Longitude	E 88.907340
Elevation	12 m
Start date	6/11/2014 15:10
End date	12/20/2017 14:30
Duration	3.5 years
Length of time step	10 minutes
Calm threshold	1 m/s
Mean temperature	27.2 °C
Mean pressure	998.5 mbar
Mean air density	1.179 kg/m ³
Power density at 50m	47 W/m ²
Wind power class	1
Power law exponent	0.35
Surface roughness	3.17 m
Roughness class	4.87



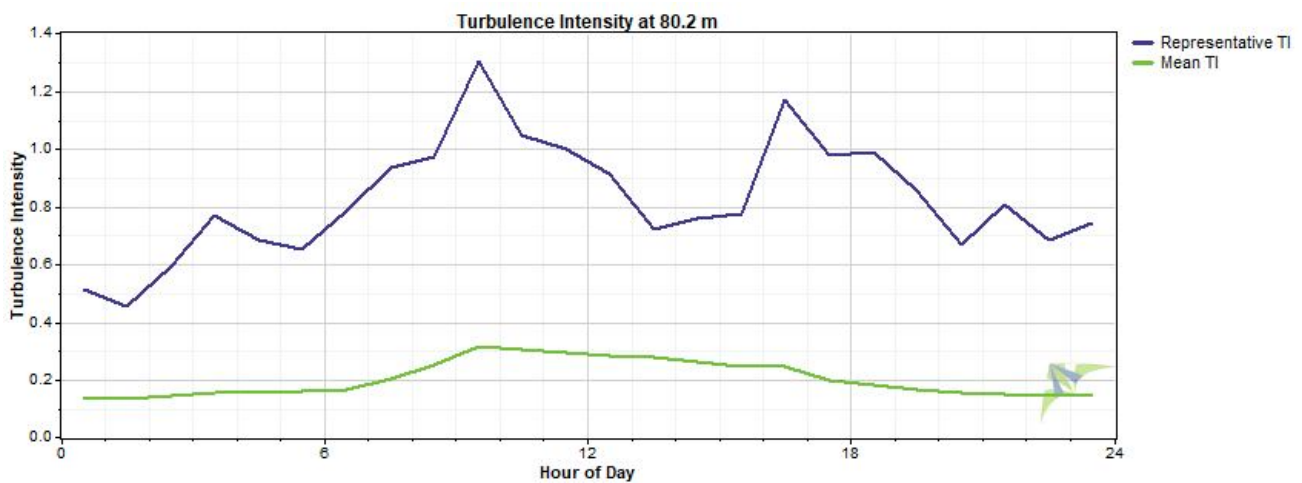
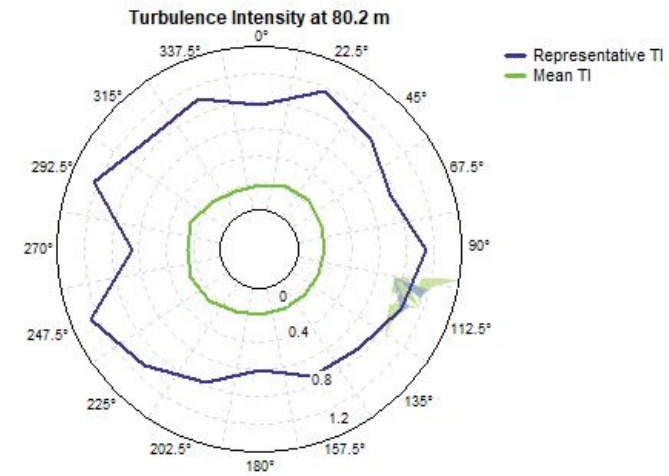
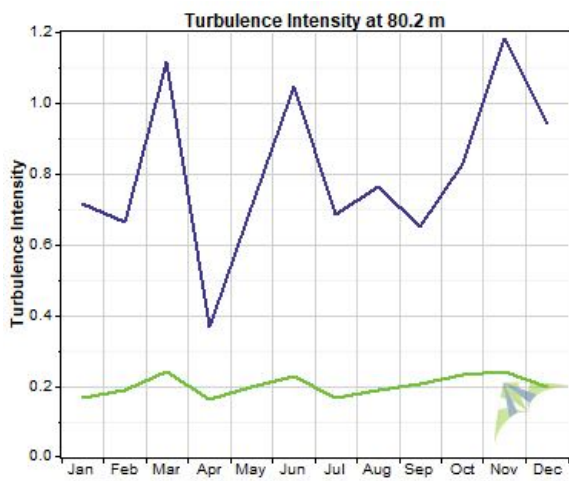
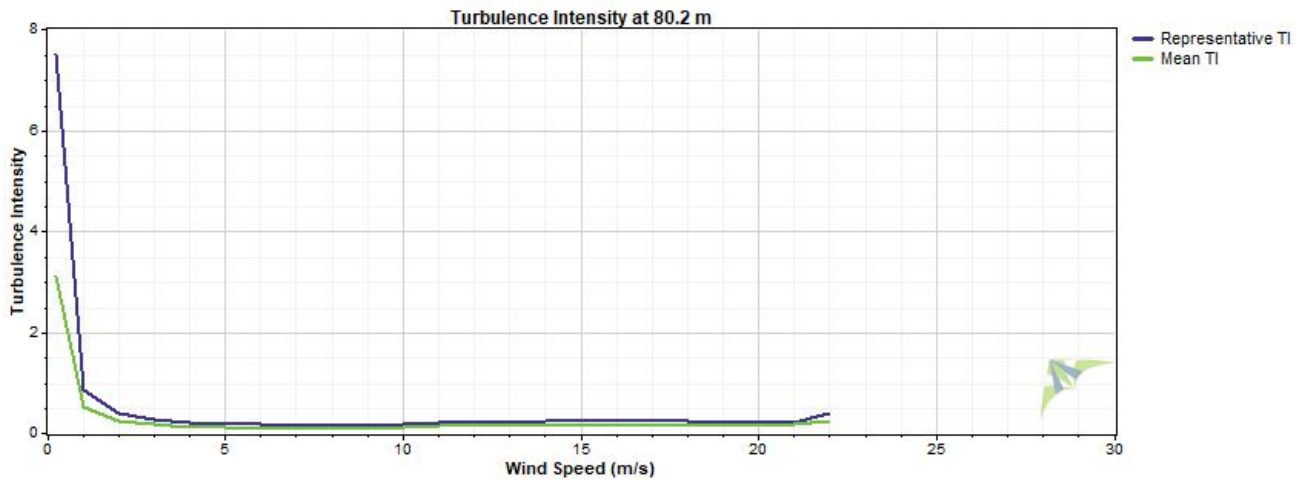
Wind Speed and Direction



Wind Shear



Turbulence Intensity



Data Column Properties

#	Label	Units	Height	Possible Data Points	Valid Data Points	Recovery Rate (%)	Mean	Min	Max	Std. Dev
1	RECORD	RN		185,468	175,418	94.58	38,479	0	102,881	28,330
2	WS_east_80.2m_Avg	m/s	80.2 m	185,468	156,625	84.45	4.060	0.000	25.670	2.106
3	WS_east_80.2m_Max	m/s	80.2 m	185,468	156,625	84.45	5.359	0.000	41.820	2.537
4	WS_east_80.2m_Min	m/s	80.2 m	185,468	156,625	84.45	2.735	0.000	15.610	1.871
5	WS_east_80.2m_Std	m/s	80.2 m	185,468	156,625	84.45	0.549	0.000	9.050	0.300
6	WS_west_80.2m_Avg	m/s	80.2 m	185,468	139,729	75.34	4.167	0.000	25.570	2.162
7	WS_west_80.2m_Max	m/s	80.2 m	185,468	139,729	75.34	5.531	0.000	40.320	2.578
8	WS_west_80.2m_Min	m/s	80.2 m	185,468	139,729	75.34	2.635	0.000	14.850	1.960
9	WS_west_80.2m_Std	m/s	80.2 m	185,468	139,729	75.34	0.597	0.000	8.540	0.350
10	WS_east_60.3m_Avg	m/s	60.3 m	185,468	167,785	90.47	3.880	0.000	24.690	1.782
11	WS_east_60.3m_Max	m/s	60.3 m	185,468	167,785	90.47	5.280	0.000	41.820	2.285
12	WS_east_60.3m_Min	m/s	60.3 m	185,468	167,785	90.47	2.469	0.000	14.070	1.512
13	WS_east_60.3m_Std	m/s	60.3 m	185,468	167,785	90.47	0.582	0.000	8.680	0.285
14	WS_west_60.3m_Avg	m/s	60.3 m	185,468	154,448	83.27	3.772	0.000	24.530	1.761
15	WS_west_60.3m_Max	m/s	60.3 m	185,468	154,448	83.27	5.135	0.000	41.010	2.229
16	WS_west_60.3m_Min	m/s	60.3 m	185,468	154,448	83.27	2.404	0.000	14.060	1.538
17	WS_west_60.3m_Std	m/s	60.3 m	185,468	154,448	83.27	0.569	0.000	8.730	0.282
18	WS_east_40.1m_Avg	m/s	40.1 m	185,468	165,813	89.40	3.342	0.000	23.450	1.557
19	WS_east_40.1m_Max	°C	40.1 m	185,468	165,813	89.40	4.809	0.000	40.240	2.180
20	WS_east_40.1m_Min	°C	40.1 m	185,468	165,813	89.40	1.905	0.000	10.980	1.221
21	WS_east_40.1m_Std	m/s	40.1 m	185,468	165,813	89.40	0.601	0.000	8.280	0.298
22	WS_west_40.1m_Avg	m/s	40.1 m	185,468	147,438	79.50	3.247	0.000	23.270	1.532
23	WS_west_40.1m_Max	m/s	40.1 m	185,468	147,438	79.50	4.676	0.000	40.160	2.128
24	WS_west_40.1m_Min	m/s	40.1 m	185,468	147,438	79.50	1.825	0.000	10.970	1.246
25	WS_west_40.1m_Std	m/s	40.1 m	185,468	147,438	79.50	0.593	0.000	8.110	0.302
26	WindDir_78.2m_D1_WVT	°	78.2 m	185,468	175,418	94.58	96.0	0.0	360.0	103.9
27	WindDir_78.2m_SD1_WVT	°	78.2 m	185,468	175,418	94.58	7.1	0.0	80.6	7.3
28	WindDir_58.3m_D1_WVT	°	58.3 m	185,468	175,418	94.58	106.5	0.0	360.0	103.9
29	WindDir_58.3m_SD1_WVT	°	58.3 m	185,468	175,418	94.58	8.1	0.0	79.7	7.7
30	WindDir_38.1m_D1_WVT	°	38.1 m	185,468	175,261	94.50	105.7	0.0	360.0	103.4
31	WindDir_38.1m_SD1_WVT	°	38.1 m	185,468	175,418	94.58	8.4	0.0	80.9	7.8
32	RTD_temp_C_78.4m_Avg	°C	78.4 m	185,468	175,418	94.58	26.0	7.9	39.4	4.3
33	RTD_temp_C_78.4m_Max	°C	78.4 m	185,468	175,418	94.58	26.1	8.0	39.7	4.3
34	RTD_temp_C_78.4m_Min	°C	78.4 m	185,468	175,418	94.58	25.8	7.8	39.0	4.3
35	RTD_temp_C_78.4m_Std	°C	78.4 m	185,468	175,418	94.58	0.1	0.0	6.0	0.1
36	RTD_temp_C_3.1m_Avg	°C	3.12 m	185,468	175,218	94.47	24.9	4.9	39.7	5.8
37	RTD_temp_C_3.1m_Max	°C	3.12 m	185,468	175,218	94.47	25.0	5.1	39.8	5.8
38	RTD_temp_C_3.1m_Min	°C	3.12 m	185,468	175,218	94.47	24.8	4.8	39.6	5.8
39	RTD_temp_C_3.1m_Std	°C	3.12 m	185,468	175,218	94.47	0.1	0.0	2.3	0.1
40	HMP155_temp_78.9m_Avg	°C	78.9 m	185,468	113,603	61.25	27.2	8.8	40.8	4.7
41	HMP155_temp_78.9m_Max	°C	78.9 m	185,468	113,603	61.25	29.0	10.3	60.4	4.7
42	HMP155_temp_78.9m_Min	°C	78.9 m	185,468	113,603	61.25	26.4	-21.8	39.9	4.7
43	HMP155_temp_78.9m_Std	°C	78.9 m	185,468	113,603	61.25	0.7	0.3	5.5	0.2
44	HMP155_RH_78.9m_Avg	%		185,468	175,406	94.57	75.9	-0.1	100.0	21.2
45	HMP155_RH_78.9m_Max	%		185,468	175,406	94.57	78.1	-0.1	100.0	20.8
46	HMP155_RH_78.9m_Min	%		185,468	175,406	94.57	74.2	-0.4	100.0	21.6
47	HMP155_RH_78.9m_Std	%		185,468	175,406	94.57	0.83	0.00	40.94	0.75
48	BP_78.7m_Avg	mbar	78.7 m	185,468	173,692	93.65	998.5	977.5	1,033.0	5.9
49	BP_78.7m_Max	mbar	78.7 m	185,468	173,692	93.65	998.7	978.5	1,034.0	5.9
50	BP_78.7m_Min	mbar	78.7 m	185,468	173,692	93.65	998.4	977.5	1,032.5	6.0
51	BP_78.7m_Std	mbar	78.7 m	185,468	173,692	93.65	0.1	0.0	15.7	0.2
52	BP_3.5m_Avg	mbar	3.49 m	185,468	154,700	83.41	1,006.9	990.0	1,021.5	6.0

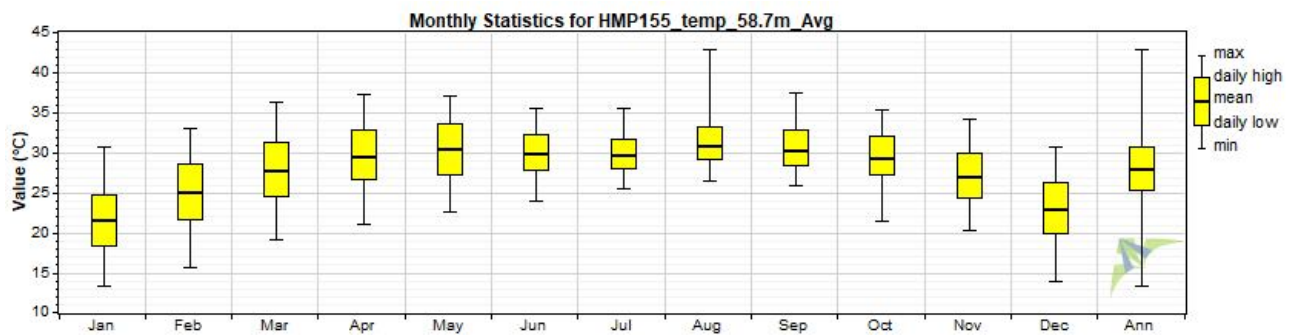
#	Label	Units	Height	Possible Data Points	Valid Data Points	Recovery Rate (%)	Mean	Min	Max	Std. Dev
53	BP_3.5m_Max	mbar	3.49 m	185,468	154,700	83.41	1,007.0	990.0	1,022.0	6.0
54	BP_3.5m_Min	mbar	3.49 m	185,468	154,700	83.41	1,006.8	989.5	1,021.5	6.0
55	BP_3.5m_Std	mbar	3.49 m	185,468	154,700	83.41	0.1	0.0	3.4	0.1
56	SlrW_Avg	W/m2		185,468	3,765	2.03	165	0	1,156	249
57	SlrW_Max	W/m2		185,468	3,765	2.03	199	0	1,332	302
58	SlrW_Min	W/m2		185,468	3,765	2.03	129	0	1,064	197
59	SlrW_Std	W/m2		185,468	3,765	2.03	20.6	0.0	426.4	47.3
60	VWC_Avg	m^3/m^3		185,468	173,692	93.65	14	0	7,999	337
61	VWC_Max			185,468	173,692	93.65	14	0	7,999	337
62	VWC_Min			185,468	173,692	93.65	14	0	7,999	336
63	VWC_Std			185,468	173,692	93.65	0	0	7,999	27
64	SoilT_Avg	°C	0 m	185,468	175,418	94.58	26.2	0.0	44.8	4.6
65	SoilT_Max	°C	0 m	185,468	175,418	94.58	26.2	0.0	44.8	4.6
66	SoilT_Min	°C	0 m	185,468	175,418	94.58	26.2	0.0	44.7	4.6
67	SoilT_Std	°C	0 m	185,468	175,418	94.58	0.0	0.0	16.0	0.1
68	LWmV_Avg	%		185,468	175,418	94.58	900.1	877.0	919.0	6.4
69	LWmV	%		185,468	175,418	94.58	900.1	877.0	919.0	6.4
70	HMP155_temp_3.75m_Avg	°C	3.75 m	185,468	171,613	92.53	25.0	5.2	40.0	5.8
71	HMP155_temp_3.75m_Max	°C	3.75 m	185,468	171,613	92.53	25.3	5.6	40.2	5.8
72	HMP155_temp_3.75m_Min	°C	3.75 m	185,468	171,613	92.53	24.9	5.0	39.9	5.8
73	HMP155_temp_3.75m_Std	°C	3.75 m	185,468	171,613	92.53	0.1	0.0	3.6	0.1
74	HMP155_RH_3.75m_Avg	%		185,468	173,588	93.59	80.37	-0.11	98.50	16.91
75	HMP155_RH_3.75m_Max	%		185,468	173,588	93.59	80.9	-0.1	108.6	16.8
76	HMP155_RH_3.75m_Min	%		185,468	173,588	93.59	79.92	-2.23	98.40	17.04
77	HMP155_RH_3.75m_Std	%		185,468	173,588	93.59	0.235	0.001	8.130	0.334
78	VBatt_Min	Volts		185,468	171,652	92.55	12.68	0.00	13.80	0.66
79	IBatt_Min	Amps		185,468	171,653	92.55	-0.008	-0.257	1.085	0.188
80	ILoad_Min			185,468	171,653	92.55	0.134	0.000	0.200	0.013
81	V_in_chg_Min			185,468	171,653	92.55	8.63	0.00	20.70	7.75
82	I_in_chg_Min			185,468	171,653	92.55	0.111	-0.004	1.174	0.158
83	Chg_TmpC_Avg	°C	2 m	185,468	171,653	92.55	27.3	0.0	46.6	7.7
84	Chg_State	Smp		185,468	171,653	92.55	0.923	0.000	3.000	1.153
85	Ck_Batt	Smp		185,468	171,653	92.55	0.016	0.000	1.000	0.126
86	BattV_Min	Volts		185,468	171,653	92.55	12.30	9.20	13.42	0.65
87	PTemp_C_Avg	°C	2 m	185,468	171,653	92.55	26.7	5.2	43.0	6.7
88	latitude_a	Smp		185,468	171,523	92.48	24	24	24	0
89	latitude_b	Smp		185,468	171,523	92.48	10.22	10.21	10.25	0.00
90	longitude_a	Smp		185,468	171,523	92.48	88	88	88	0
91	longitude_b	Smp		185,468	171,523	92.48	54.45	54.44	54.46	0.00
92	magnetic_variation	Smp		185,468	171,523	92.48	-0.4	-0.4	-0.4	0.0
93	fix_quality	Smp		185,468	171,523	92.48	2	1	2	0
94	nmbr_satellites	Smp		185,468	171,523	92.48	9.19	5.00	12.00	0.89
95	altitude	Smp		185,468	171,523	92.48	14.69	-53.20	43.30	5.85
96	max_clock_change			185,468	171,523	92.48	-87	-1,050	300	300
97	nmbr_clock_change	Smp		185,468	171,523	92.48	0.221	0.000	2.000	0.504
98	Air Density	kg/m³		185,468	185,468	100.00	1.179	1.099	1.246	0.032
99	WS_east_80.2m_Avg TI			185,468	151,777	81.83	0.20	0.02	20.25	0.50
100	WS_west_80.2m_Avg TI			185,468	135,084	72.83	0.23	0.02	23.33	0.67
101	WS_east_60.3m_Avg TI			185,468	167,097	90.09	0.20	0.02	19.50	0.33
102	WS_west_60.3m_Avg TI			185,468	153,755	82.90	0.21	0.02	20.00	0.36
103	WS_east_40.1m_Avg TI			185,468	163,714	88.27	0.25	0.03	23.67	0.53
104	WS_west_40.1m_Avg TI			185,468	144,783	78.06	0.26	0.03	24.00	0.60
105	WS_east_80.2m_Avg WPD	W/m²		185,468	156,625	84.45	74	0	9,929	131
106	WS_west_80.2m_Avg WPD	W/m²		185,468	139,729	75.34	79	0	9,814	141

#	Label	Units	Height	Possible Data Points	Valid Data Points	Recovery Rate (%)	Mean	Min	Max	Std. Dev
107	WS_east_60.3m_Avg WPD	W/m ²		185,468	167,785	90.47	58	0	8,835	100
108	WS_west_60.3m_Avg WPD	W/m ²		185,468	154,448	83.27	54	0	8,664	101
109	WS_east_40.1m_Avg WPD	W/m ²		185,468	165,813	89.40	38	0	7,570	71
110	WS_west_40.1m_Avg WPD	W/m ²		185,468	147,438	79.50	35	0	7,397	71

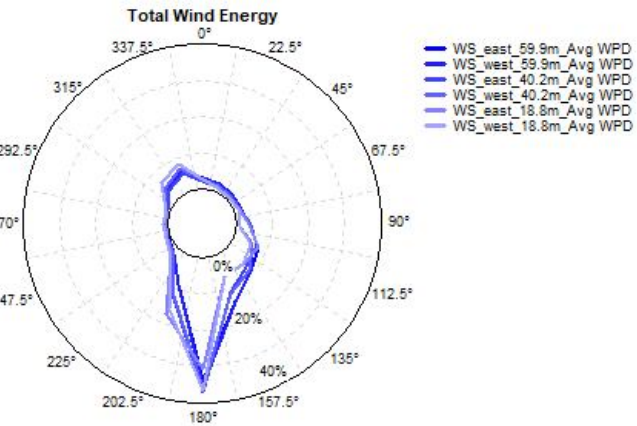
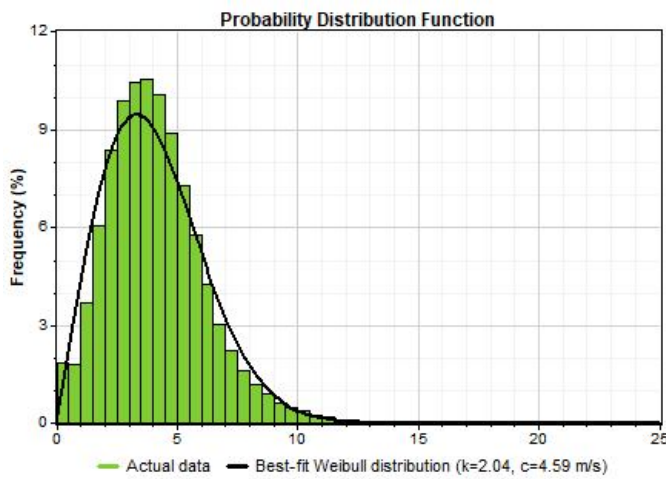
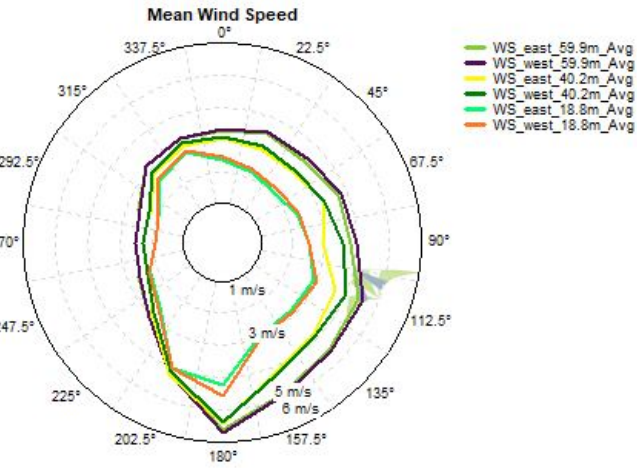
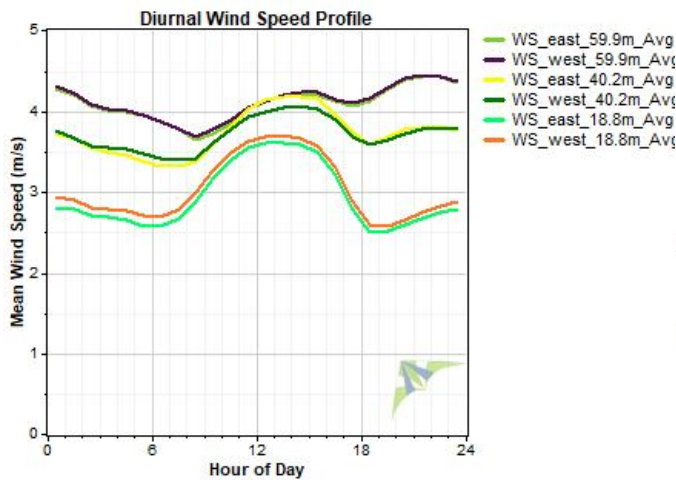
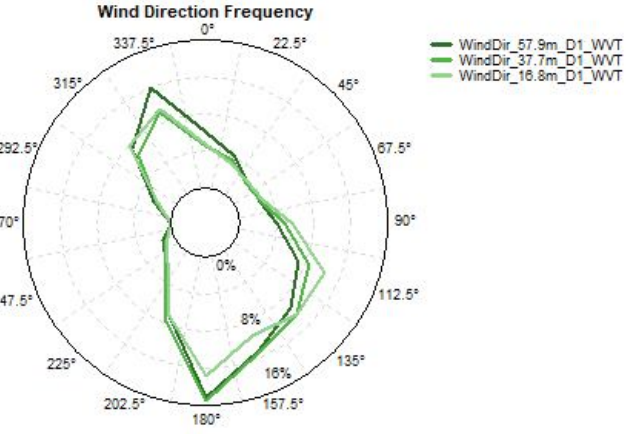
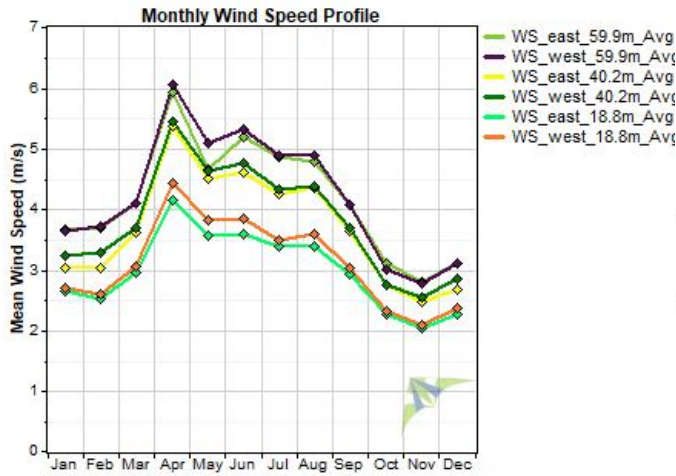
Data Set Properties

Report Created: 4/11/2018 10:11 using Windographer 3.3.10
 Filter Settings: <Unflagged data>

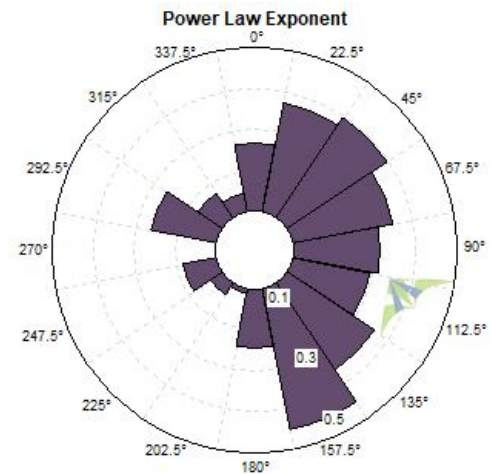
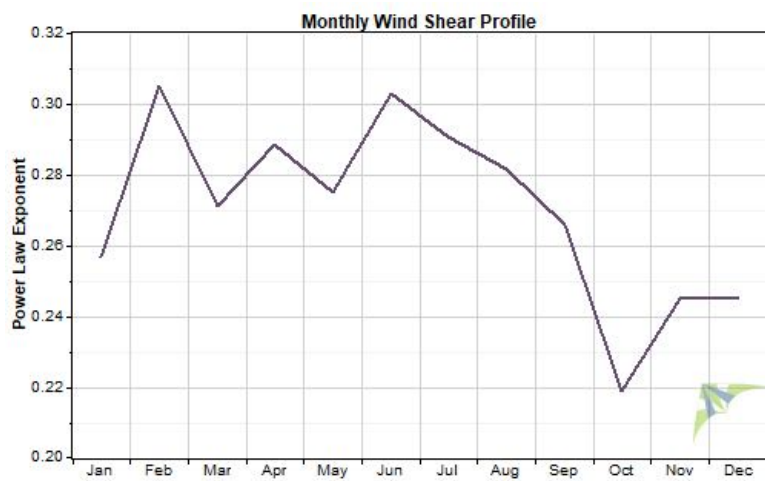
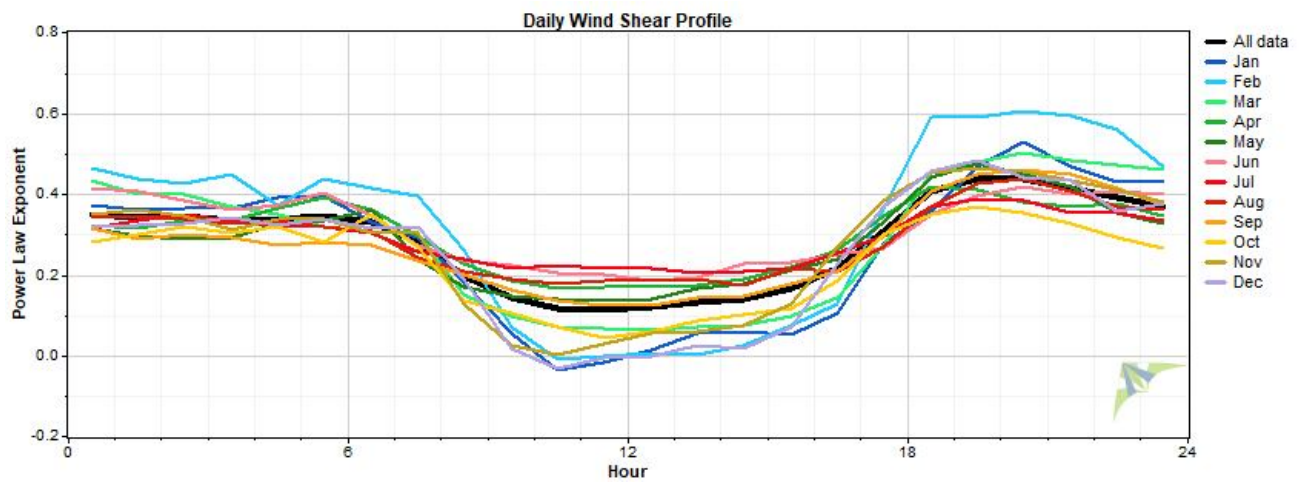
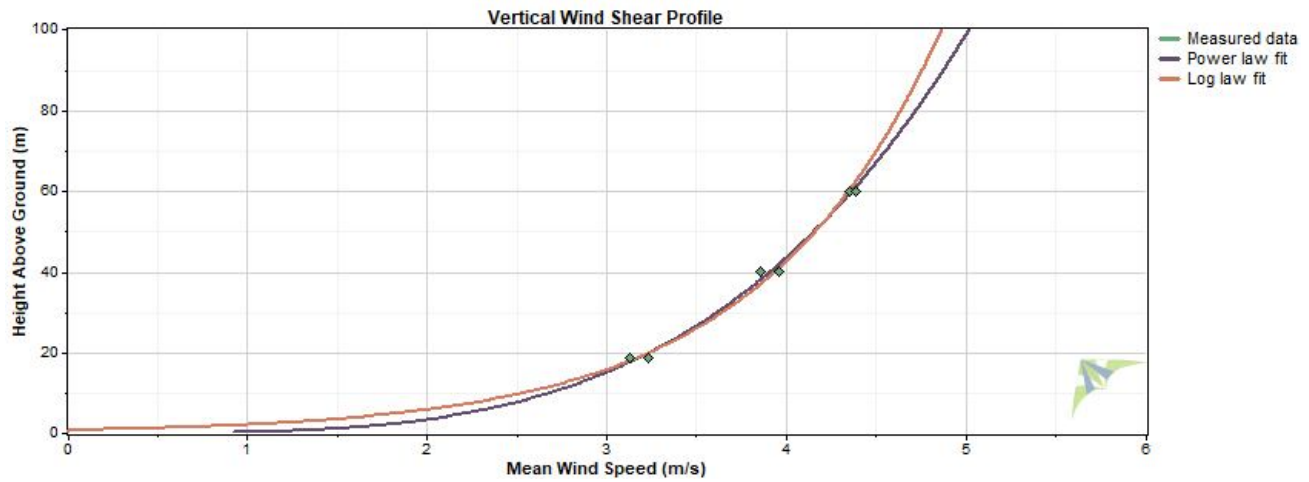
Variable	Value
Latitude	N 23.211160
Longitude	E 90.642370
Elevation	10 m
Start date	6/11/2014 00:10
End date	12/4/2017 12:00
Duration	3.5 years
Length of time step	10 minutes
Calm threshold	1 m/s
Mean temperature	27.9 °C
Mean pressure	1,002 mbar
Mean air density	1.171 kg/m ³
Power density at 50m	70 W/m ²
Wind power class	1
Power law exponent	0.273
Surface roughness	0.825 m
Roughness class	3.75



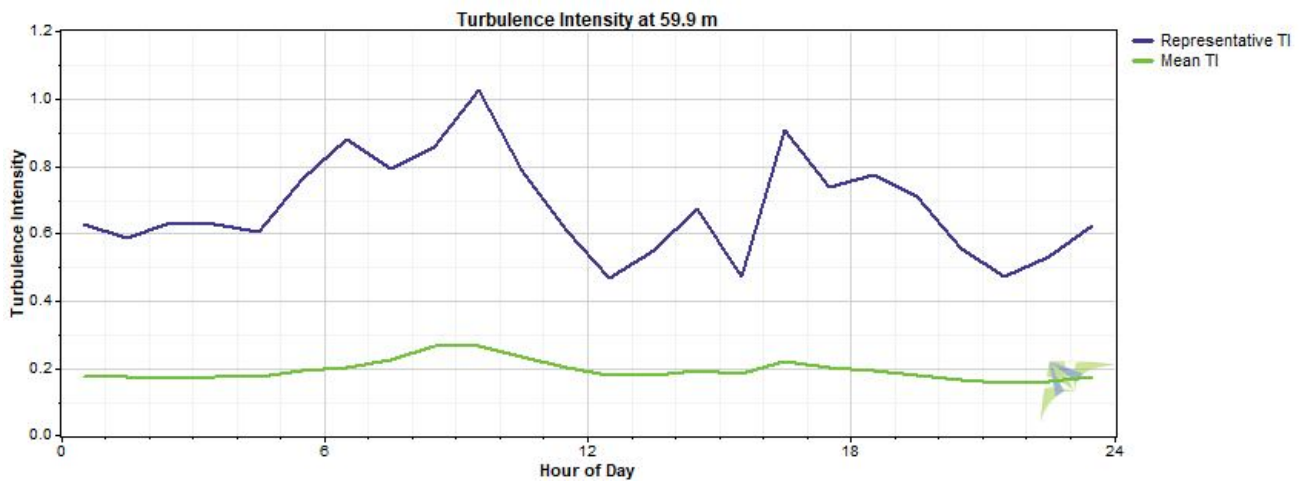
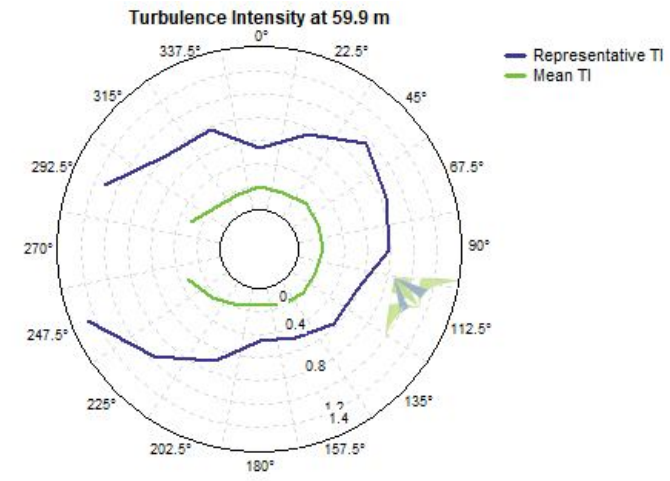
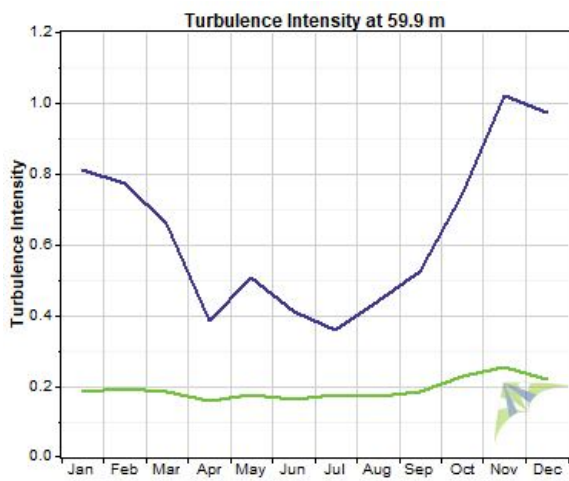
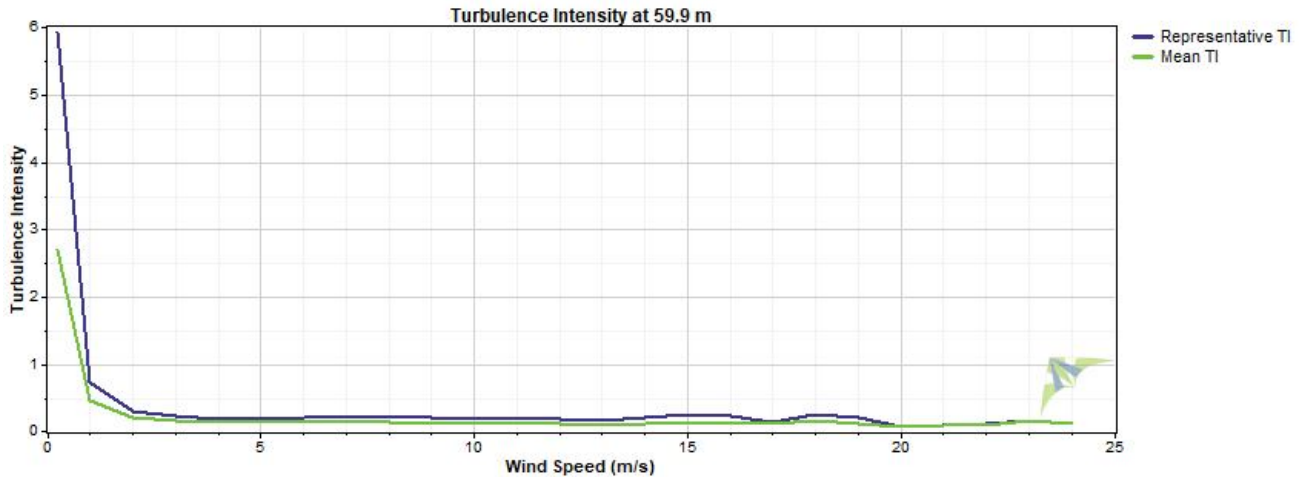
Wind Speed and Direction



Wind Shear



Turbulence Intensity



Data Column Properties

#	Label	Units	Height	Possible Data Points	Valid Data Points	Recovery Rate (%)	Mean	Min	Max	Std. Dev
1	RECORD	RN		183,239	146,725	80.07	24,627	0	58,583	16,934
2	WS_east_59.9m_Avg	m/s	59.9 m	183,239	141,776	77.37	4.093	0.000	23.920	2.042
3	WS_east_59.9m_Max	m/s	59.9 m	183,239	141,776	77.37	5.517	0.000	38.570	2.689
4	WS_east_59.9m_Min	m/s	59.9 m	183,239	141,776	77.37	2.631	0.000	17.860	1.577
5	WS_east_59.9m_Std	m/s	59.9 m	183,239	141,776	77.37	0.588	0.000	9.150	0.315
6	WS_west_59.9m_Avg	m/s	59.9 m	183,239	137,180	74.86	4.123	0.000	23.640	2.111
7	WS_west_59.9m_Max	m/s	59.9 m	183,239	137,180	74.86	5.539	0.000	37.000	2.753
8	WS_west_59.9m_Min	m/s	59.9 m	183,239	137,180	74.86	2.675	0.000	17.850	1.645
9	WS_west_59.9m_Std	m/s	59.9 m	183,239	137,180	74.86	0.584	0.000	9.030	0.316
10	WS_east_40.2m_Avg	m/s	40.2 m	183,239	117,312	64.02	3.728	0.000	23.220	2.028
11	WS_east_40.2m_Max	°C	40.2 m	183,239	117,312	64.02	5.310	0.000	34.760	2.787
12	WS_east_40.2m_Min	m/s	40.2 m	183,239	117,312	64.02	2.111	0.000	17.100	1.521
13	WS_east_40.2m_Std	°C	40.2 m	183,239	117,312	64.02	0.644	0.000	7.426	0.379
14	WS_west_40.2m_Avg	m/s	40.2 m	183,239	135,817	74.12	3.720	0.000	23.090	1.924
15	WS_west_40.2m_Max	m/s	40.2 m	183,239	135,817	74.12	5.200	0.000	36.350	2.623
16	WS_west_40.2m_Min	m/s	40.2 m	183,239	135,817	74.12	2.240	0.000	17.130	1.459
17	WS_west_40.2m_Std	°C	40.2 m	183,239	135,817	74.12	0.601	0.000	8.830	0.328
18	WS_east_18.8m_Avg	m/s	18.8 m	183,239	138,999	75.86	2.943	0.000	22.040	1.663
19	WS_east_18.8m_Max	m/s	18.8 m	183,239	138,999	75.86	4.596	0.000	32.370	2.446
20	WS_east_18.8m_Min	°C	18.8 m	183,239	138,999	75.86	1.350	0.000	16.290	1.164
21	WS_east_18.8m_Std	m/s	18.8 m	183,239	138,999	75.86	0.652	0.000	8.060	0.354
22	WS_west_18.8m_Avg	m/s	18.8 m	183,239	132,676	72.41	3.047	0.000	21.980	1.750
23	WS_west_18.8m_Max	m/s	18.8 m	183,239	132,676	72.41	4.641	0.000	32.590	2.496
24	WS_west_18.8m_Min	m/s	18.8 m	183,239	132,676	72.41	1.535	0.000	16.400	1.284
25	WS_west_18.8m_Std	m/s	18.8 m	183,239	132,676	72.41	0.627	0.000	7.951	0.342
26	WindDir_57.9m_D1_WVT	°	57.8 m	183,239	146,725	80.07	153.1	0.0	360.0	99.0
27	WindDir_57.9m_SD1_WVT	°	57.8 m	183,239	146,725	80.07	6.5	0.0	79.6	5.9
28	WindDir_37.7m_D1_WVT	°	37.7 m	183,239	146,725	80.07	155.9	-7,999.0	360.0	133.6
29	WindDir_37.7m_SD1_WVT	°	37.7 m	183,239	146,725	80.07	7.9	0.0	79.3	6.3
30	WindDir_16.8m_D1_WVT	°	16.8 m	183,239	146,725	80.07	153.2	0.0	360.0	98.2
31	WindDir_16.8m_SD1_WVT	°	16.8 m	183,239	146,725	80.07	9.4	0.0	79.8	7.4
32	RTD_temp_C_58m_Avg	°C	58 m	183,239	1,780	0.97	27.8	15.6	34.4	2.2
33	RTD_temp_C_58m_Max	°C	58 m	183,239	1,780	0.97	28.0	16.6	34.8	2.2
34	RTD_temp_C_58m_Min	°C	58 m	183,239	1,780	0.97	27.7	12.8	34.0	2.2
35	RTD_temp_C_58m_Std	°C	58 m	183,239	1,780	0.97	0.1	0.0	2.5	0.1
36	RTD_temp_C_3.7m_Avg	°C	3.65 m	183,239	103,119	56.28	23.8	9.5	33.8	4.4
37	RTD_temp_C_3.7m_Max	°C	3.65 m	183,239	103,119	56.28	23.9	9.9	34.1	4.4
38	RTD_temp_C_3.7m_Min	°C	3.65 m	183,239	103,119	56.28	23.6	9.3	33.5	4.4
39	RTD_temp_C_3.7m_Std	°C	3.65 m	183,239	103,119	56.28	0.1	0.0	2.8	0.1
40	HMP155_temp_58.7m_Avg	°C	58.7 m	183,239	146,723	80.07	27.9	13.2	42.9	3.9
41	HMP155_temp_58.7m_Max	°C	58.7 m	183,239	146,723	80.07	31.0	15.9	53.2	4.3
42	HMP155_temp_58.7m_Min	°C	58.7 m	183,239	146,723	80.07	26.7	-83.0	38.6	3.8
43	HMP155_temp_58.7m_Std	°C	58.7 m	183,239	146,723	80.07	1.1	0.8	12.7	0.3
44	HMP155_RH_58.7m_Avg	%		183,239	146,287	79.83	82.1	14.1	100.5	16.8
45	HMP155_RH_58.7m_Max	%		183,239	146,287	79.83	84.9	16.6	108.9	15.9
46	HMP155_RH_58.7m_Min	%		183,239	146,287	79.83	80.2	-0.0	100.0	17.5
47	HMP155_RH_58.7m_Std	%		183,239	146,287	79.83	1.00	0.00	33.70	0.81
48	Hmp155_temp_4.5m_Avg	°C	4.45 m	183,239	103,117	56.27	24.8	10.8	34.6	4.4
49	Hmp155_temp_4.5m_Max	°C	4.45 m	183,239	103,117	56.27	25.2	11.3	35.2	4.4
50	Hmp155_temp_4.5m_Min	°C	4.45 m	183,239	103,117	56.27	24.5	10.5	34.4	4.4
51	Hmp155_temp_4.5m_Std	°C	4.45 m	183,239	103,117	56.27	0.1	0.1	2.7	0.1
52	HMP155_RH_4.5m_Avg	%		183,239	146,725	80.07	85.9	15.3	100.0	12.4

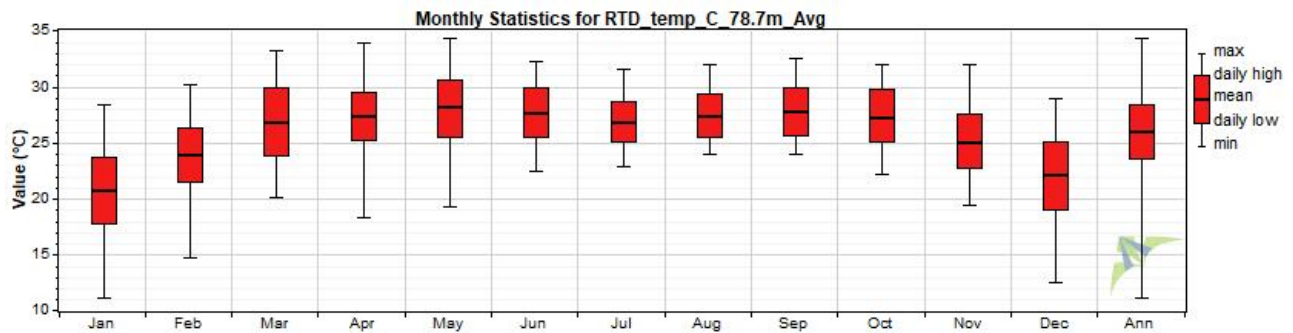
#	Label	Units	Height	Possible Data Points	Valid Data Points	Recovery Rate (%)	Mean	Min	Max	Std. Dev
53	HMP155_RH_4.5m_Max	%		183,239	146,725	80.07	87.4	17.2	100.0	11.4
54	HMP155_RH_4.5m_Min	%		183,239	146,725	80.07	84.5	-0.0	100.0	13.4
55	HMP155_RH_4.5m_Std	%		183,239	146,725	80.07	0.68	0.00	37.49	0.72
56	BP_58.2m_Avg	mbar	58.3 m	183,239	146,724	80.07	1,002.4	972.5	1,021.0	5.5
57	BP_58.2m_Max	mbar	58.3 m	183,239	146,724	80.07	1,002.5	974.5	1,022.0	5.4
58	BP_58.2m_Min	mbar	58.3 m	183,239	146,724	80.07	1,002.3	970.5	1,020.5	5.5
59	BP_58.2m_Std	mbar	58.3 m	183,239	146,724	80.07	0.1	0.0	18.1	0.2
60	BP_3.4m_Avg	mbar	3.4 m	183,239	146,724	80.07	1,008.0	989.5	1,022.0	5.6
61	BP_3.4m_Max	mbar	3.4 m	183,239	146,724	80.07	1,008.1	990.0	1,022.0	5.6
62	BP_3.4m_Min	mbar	3.4 m	183,239	146,724	80.07	1,007.9	989.5	1,022.0	5.6
63	BP_3.4m_Std	mbar	3.4 m	183,239	146,724	80.07	0.1	0.0	3.8	0.1
64	SlrW_Avg	W/m^2		183,239	14,383	7.85	16	-7,999	1,006	256
65	SlrW_Max			183,239	14,383	7.85	21	-7,999	1,218	265
66	SlrW_Min			183,239	14,383	7.85	12	-7,999	916	249
67	SlrW_Std			183,239	14,383	7.85	-4	-7,999	342	232
68	VWC_Avg	m^3/m^3		183,239	146,725	80.07	2.58	0.01	32.33	7.72
69	VWC_Max			183,239	146,725	80.07	2.58	0.09	32.35	7.73
70	VWC_Min			183,239	146,725	80.07	2.57	0.00	32.31	7.71
71	VWC_Std			183,239	146,725	80.07	0.00	0.00	11.02	0.03
72	SoilT_Avg	°C	0 m	183,239	146,725	80.07	92.8	0.5	903.0	230.3
73	SoilT_Max	°C	0 m	183,239	146,725	80.07	92.8	18.3	903.0	230.2
74	SoilT_Min	°C	0 m	183,239	146,725	80.07	25.8	0.0	36.5	4.8
75	SoilT_Std	°C	0 m	183,239	146,725	80.07	0.0	-0.2	12.3	0.1
76	LWmV_Avg	mV		183,239	146,725	80.07	832.0	0.0	914.0	238.1
77	LWmV	mV		183,239	146,725	80.07	832.6	0.0	914.0	235.9
78	VBatt_Min	Volts		183,239	144,709	78.97	12.25	-0.00	17.81	3.56
79	IBatt_Min	Amps		183,239	144,709	78.97	2.24	-0.20	39.10	7.94
80	ILoad_Min			183,239	144,709	78.97	0.199	0.000	3.000	0.476
81	V_in_chg_Min			183,239	144,709	78.97	8.87	0.00	21.33	8.55
82	I_in_chg_Min			183,239	144,709	78.97	1.05	-0.00	13.72	3.40
83	Chg_TmpC_Avg	°C	2 m	183,239	144,709	78.97	27.0	0.0	43.7	5.7
84	Chg_State	Smp		183,239	144,709	78.97	2.96	0.00	23.00	5.93
85	Ck_Batt	Smp		183,239	144,709	78.97	0.97	0.00	12.68	3.38
86	BattV_Min	Volts		183,239	144,709	78.97	18.83	11.87	90.00	20.52
87	PTemp_C_Avg	°C	2 m	183,239	144,709	78.97	27.7	10.8	43.0	6.0
88	latitude_a	Smp		183,239	144,709	78.97	21.20	-0.50	23.00	6.27
89	latitude_b	Smp		183,239	144,709	78.97	11.85	2.00	12.68	2.83
90	longitude_a	Smp		183,239	144,709	78.97	83.78	5.00	90.00	21.62
91	longitude_b	Smp		183,239	144,709	78.97	36.25	-12.70	38.55	8.10
92	magnetic_variation	Smp		183,239	144,709	78.97	225	-1	7,999	1,324
93	fix_quality	Smp		183,239	144,709	78.97	1.903	0.000	2.000	0.430
94	nubr_satellites	Smp		183,239	144,709	78.97	9.07	5.00	12.00	0.92
95	altitude	Smp		183,239	144,709	78.97	8.37	-28.60	36.60	6.08
96	max_clock_change			183,239	144,709	78.97	467	-1,020	7,999	2,464
97	nubr_clock_change	Smp		183,239	144,709	78.97	0.819	0.000	5.000	1.260
98	Air Density	kg/m³		183,239	183,239	100.00	1.171	1.095	1.231	0.029
99	WS_east_59.9m_Avg TI			183,239	140,765	76.82	0.19	0.03	20.00	0.39
100	WS_west_59.9m_Avg TI			183,239	136,263	74.36	0.20	0.03	20.50	0.42
101	WS_east_40.2m_Avg TI			183,239	113,461	61.92	0.24	0.03	19.50	0.57
102	WS_west_40.2m_Avg TI			183,239	135,121	73.74	0.22	0.04	20.00	0.42
103	WS_east_18.8m_Avg TI			183,239	136,257	74.36	0.32	0.05	19.50	0.61
104	WS_west_18.8m_Avg TI			183,239	131,440	71.73	0.30	0.05	20.00	0.59
105	WS_east_59.9m_Avg WPD	W/m²		183,239	141,776	77.37	73	0	8,049	142
106	WS_west_59.9m_Avg WPD	W/m²		183,239	137,180	74.86	77	0	7,764	153

#	Label	Units	Height	Possible Data Points	Valid Data Points	Recovery Rate (%)	Mean	Min	Max	Std. Dev
107	WS_east_40.2m_Avg WPD	W/m ²		183,239	117,312	64.02	61	0	7,363	134
108	WS_west_40.2m_Avg WPD	W/m ²		183,239	135,817	74.12	58	0	7,240	127
109	WS_east_18.8m_Avg WPD	W/m ²		183,239	138,999	75.86	32	0	6,297	87
110	WS_west_18.8m_Avg WPD	W/m ²		183,239	132,676	72.41	37	0	6,245	97

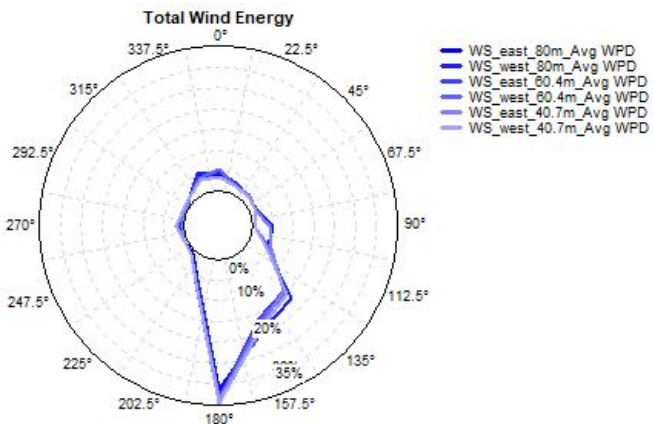
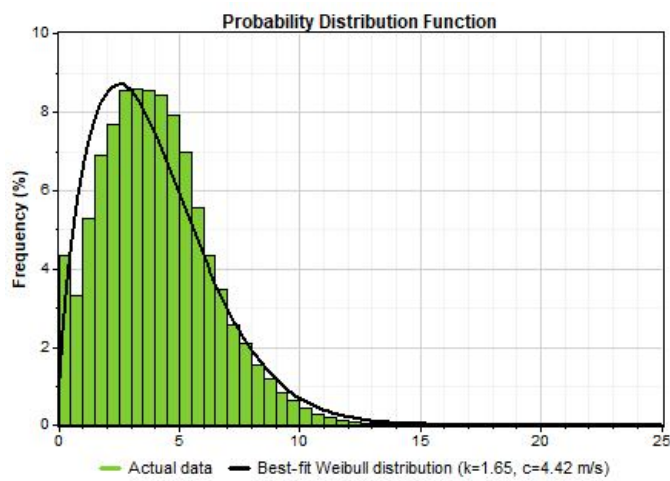
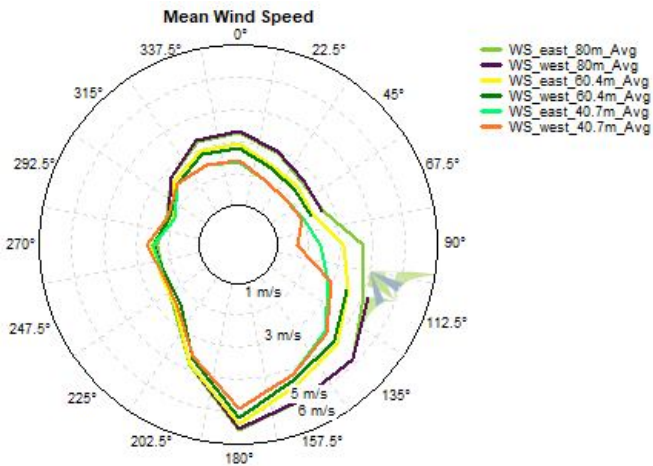
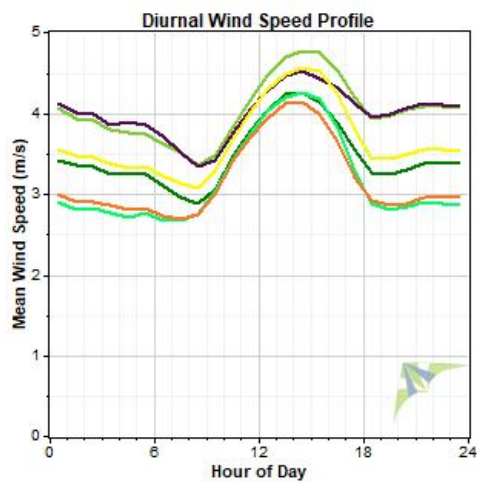
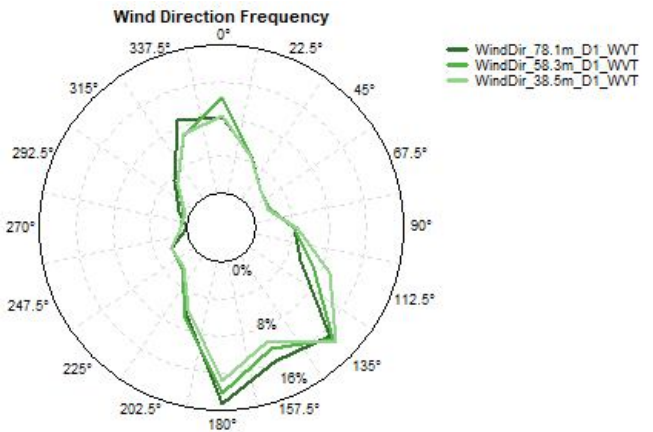
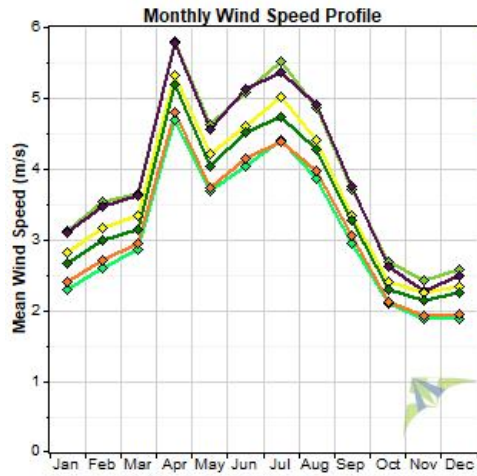
Data Set Properties

Report Created: 4/11/2018 10:43 using Windographer 3.3.10
 Filter Settings: <Unflagged data>

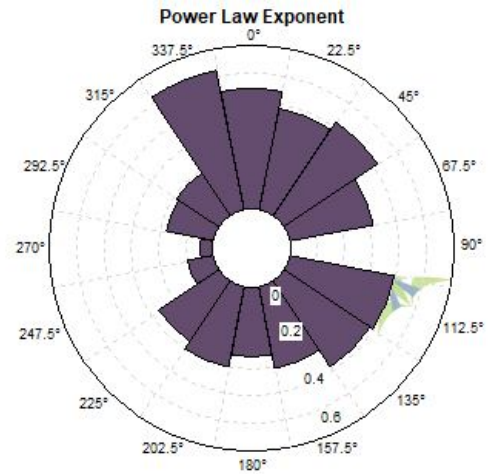
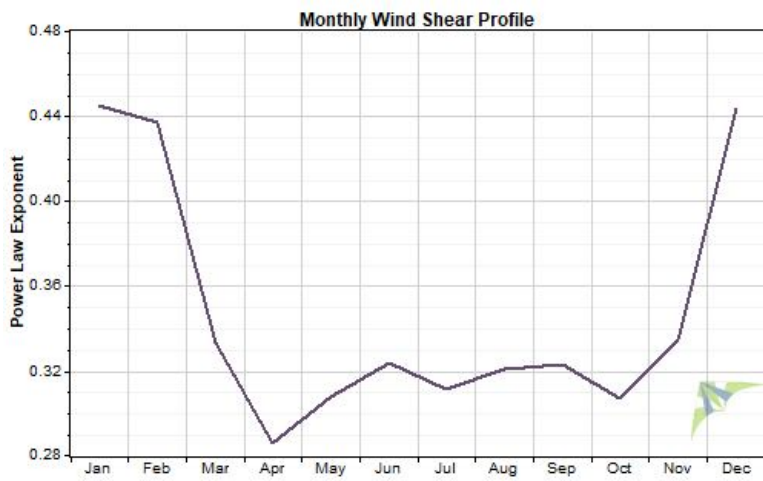
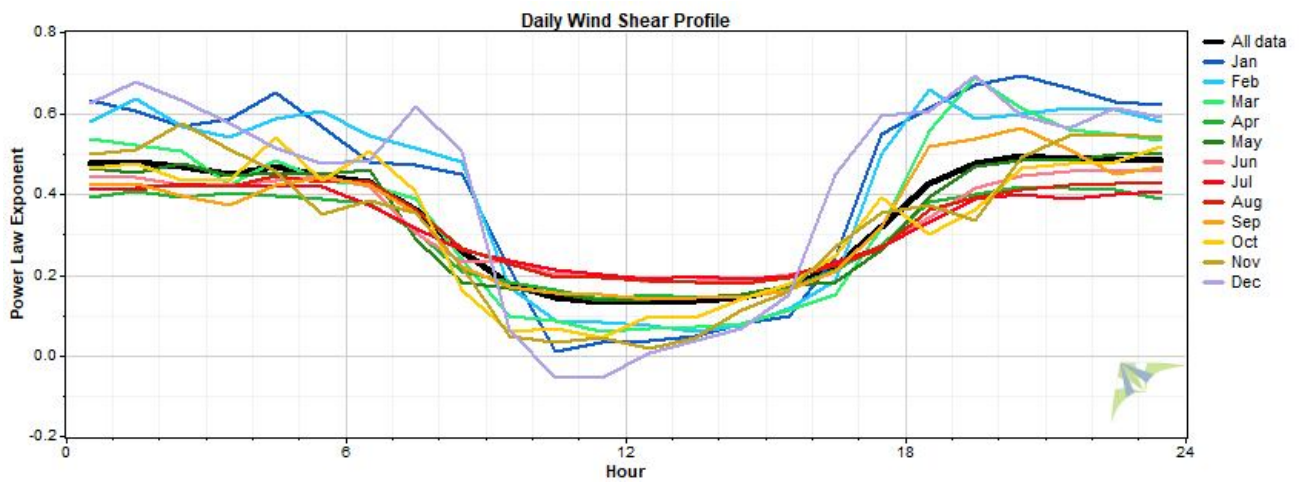
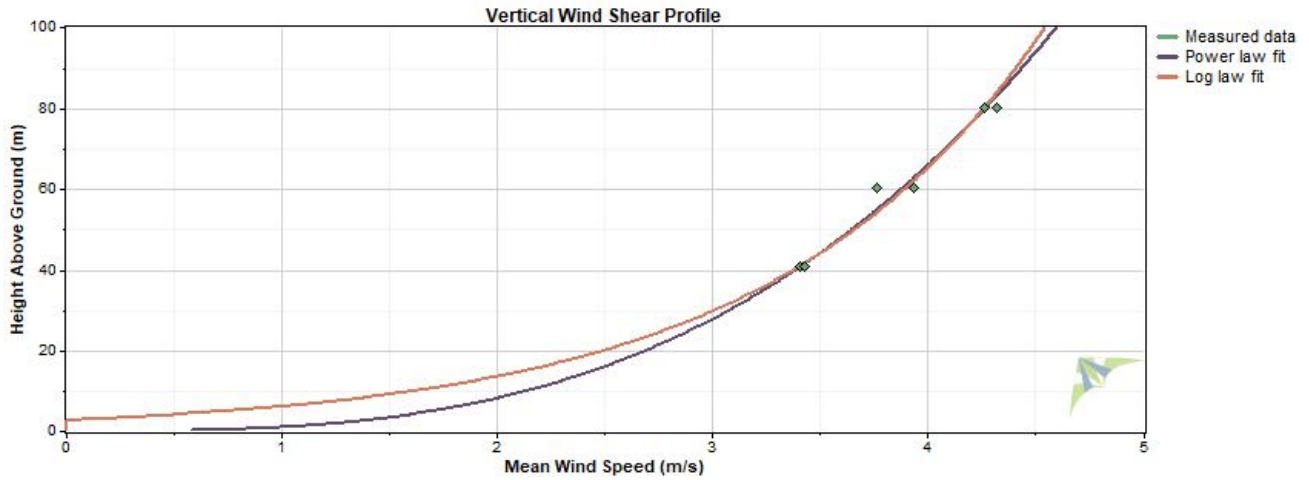
Variable	Value
Latitude	N 22.604160
Longitude	E 91.660100
Elevation	0 m
Start date	12/18/2014 09:50
End date	12/20/2016 00:10
Duration	24 months
Length of time step	10 minutes
Calm threshold	1 m/s
Mean temperature	26.0 °C
Mean pressure	999.9 mbar
Mean air density	1.169 kg/m ³
Power density at 50m	49 W/m ²
Wind power class	1
Power law exponent	0.334
Surface roughness	2.84 m
Roughness class	4.78



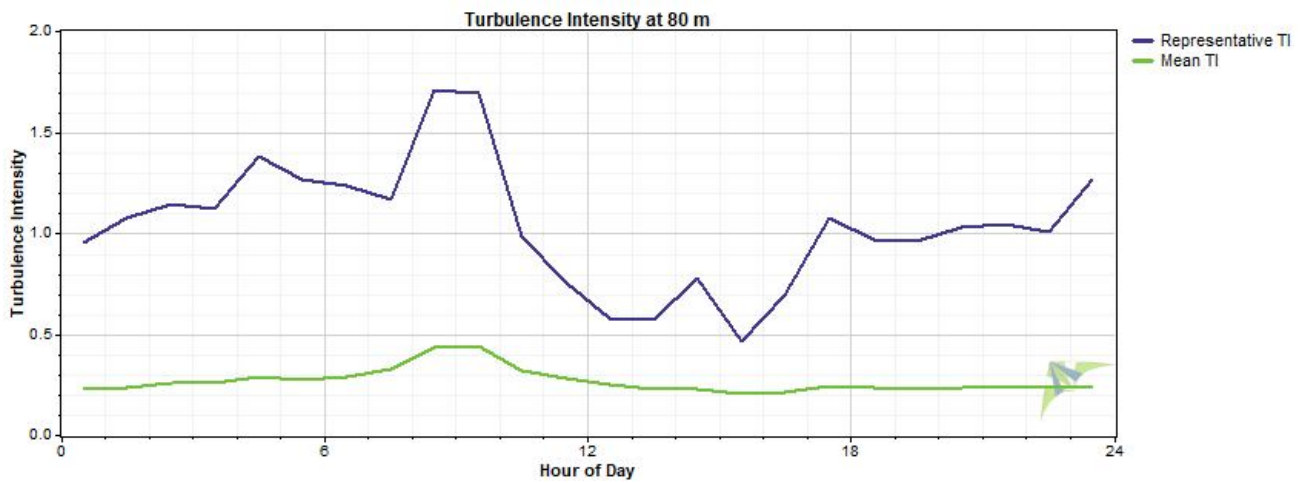
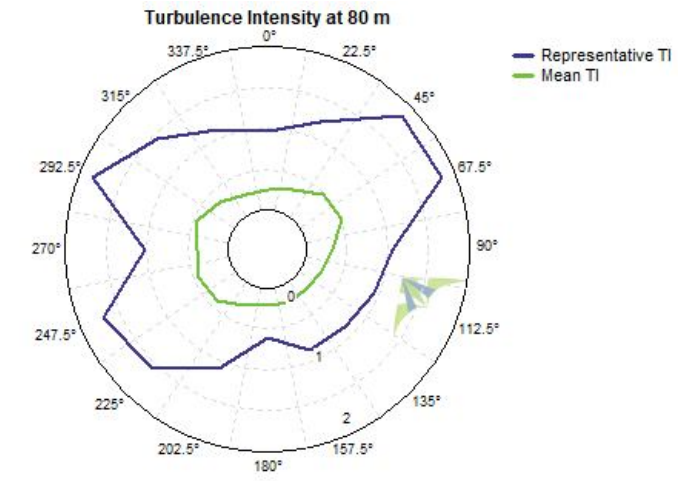
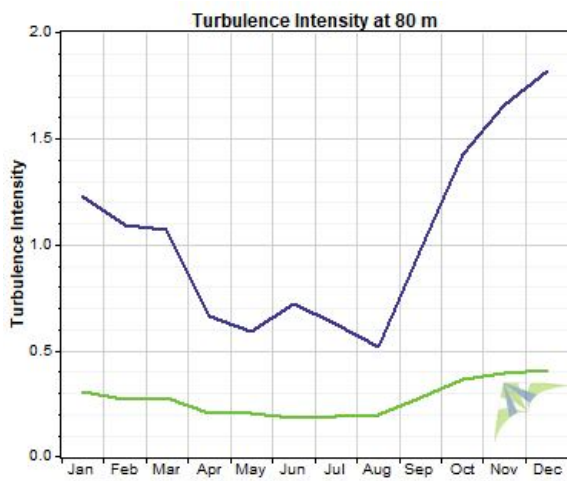
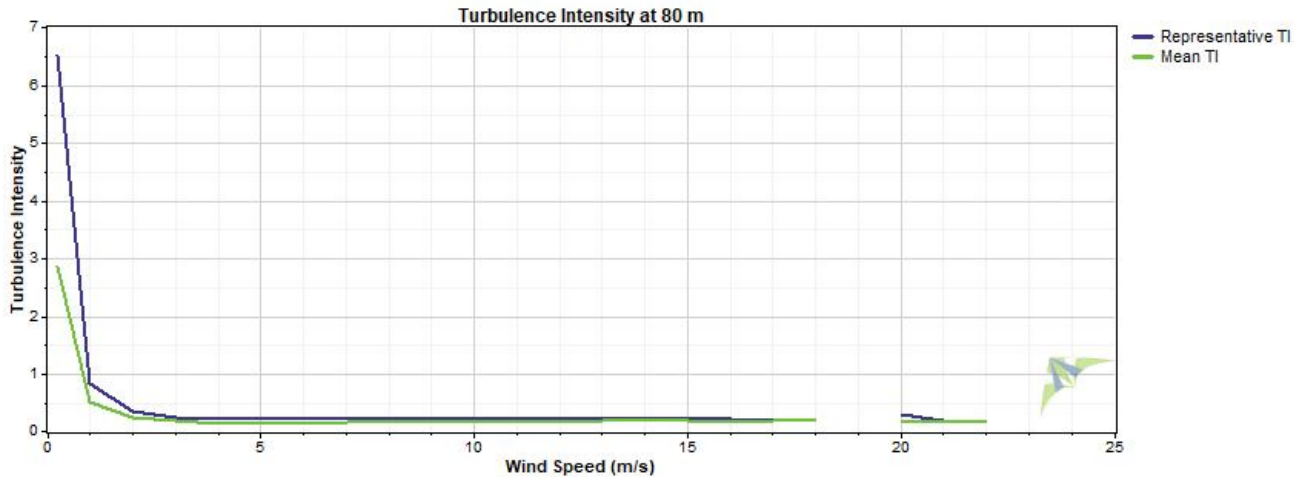
Wind Speed and Direction



Wind Shear



Turbulence Intensity



Data Column Properties

#	Label	Units	Height	Possible Data Points	Valid Data Points	Recovery Rate (%)	Mean	Min	Max	Std. Dev
1	RECORD	RN		105,494	96,567	91.54	22,630	0	53,062	14,763
2	WS_east_80m_Avg	m/s	80 m	105,494	91,476	86.71	4.015	0.000	21.730	2.296
3	WS_east_80m_Max	m/s	80 m	105,494	91,476	86.71	5.704	0.000	31.020	3.163
4	WS_east_80m_Min	m/s	80 m	105,494	91,476	86.71	2.350	0.000	14.070	1.575
5	WS_east_80m_Std	m/s	80 m	105,494	91,476	86.71	0.676	0.000	6.838	0.373
6	WS_west_80m_Avg	m/s	80 m	105,494	85,589	81.13	4.009	0.000	21.490	2.311
7	WS_west_80m_Max	m/s	80 m	105,494	85,589	81.13	5.720	0.000	31.010	3.170
8	WS_west_80m_Min	m/s	80 m	105,494	85,589	81.13	2.303	0.000	13.290	1.597
9	WS_west_80m_Std	m/s	80 m	105,494	85,589	81.13	0.687	0.000	6.486	0.386
10	WS_east_60.4m_Avg	m/s	60.4 m	105,494	92,008	87.22	3.638	0.000	20.430	2.125
11	WS_east_60.4m_Max	m/s	60.4 m	105,494	92,008	87.22	5.353	0.000	31.730	3.047
12	WS_east_60.4m_Min	m/s	60.4 m	105,494	92,008	87.22	1.987	0.000	12.510	1.385
13	WS_east_60.4m_Std	°C	60.4 m	105,494	92,008	87.22	0.678	0.000	6.575	0.373
14	WS_west_60.4m_Avg	m/s	60.4 m	105,494	89,834	85.16	3.480	0.000	19.600	2.115
15	WS_west_60.4m_Max	m/s	60.4 m	105,494	89,834	85.16	5.190	0.000	30.640	2.983
16	WS_west_60.4m_Min	m/s	60.4 m	105,494	89,834	85.16	1.818	0.000	11.700	1.397
17	WS_west_60.4m_Std	m/s	60.4 m	105,494	89,834	85.16	0.679	0.000	6.123	0.371
18	WS_east_40.7m_Avg	m/s	40.7 m	105,494	92,586	87.76	3.144	0.000	18.710	1.919
19	WS_east_40.7m_Max	m/s	40.7 m	105,494	92,586	87.76	4.918	0.000	36.860	2.939
20	WS_east_40.7m_Min	°C	40.7 m	105,494	92,586	87.76	1.477	0.000	10.230	1.095
21	WS_east_40.7m_Std	m/s	40.7 m	105,494	92,586	87.76	0.694	0.000	6.451	0.384
22	WS_west_40.7m_Avg	m/s	40.7 m	105,494	88,302	83.70	3.194	0.000	18.530	1.910
23	WS_west_40.7m_Max	m/s	40.7 m	105,494	88,302	83.70	4.977	0.000	30.230	2.913
24	WS_west_40.7m_Min	m/s	40.7 m	105,494	88,302	83.70	1.516	0.000	11.000	1.102
25	WS_west_40.7m_Std	m/s	40.7 m	105,494	88,302	83.70	0.699	0.000	6.059	0.381
26	WindDir_78.1m_D1_WVT	°	78.1 m	105,494	96,567	91.54	150.1	0.0	360.0	98.2
27	WindDir_78.1m_SD1_WVT	°	78.1 m	105,494	96,567	91.54	8.4	0.0	79.5	7.6
28	WindDir_58.3m_D1_WVT	°	58.3 m	105,494	96,567	91.54	149.5	0.0	360.0	99.6
29	WindDir_58.3m_SD1_WVT	°	58.3 m	105,494	96,567	91.54	9.3	0.0	80.1	7.9
30	WindDir_38.5m_D1_WVT	°	38.5 m	105,494	96,567	91.54	148.7	0.0	360.0	98.9
31	WindDir_38.5m_SD1_WVT	°	38.5 m	105,494	96,567	91.54	10.3	0.0	80.4	8.4
32	RTD_temp_C_78.7m_Avg	°C	78.7 m	105,494	96,567	91.54	26.0	11.2	34.3	3.2
33	RTD_temp_C_78.7m_Max	°C	78.7 m	105,494	96,567	91.54	26.3	11.3	34.4	3.2
34	RTD_temp_C_78.7m_Min	°C	78.7 m	105,494	96,567	91.54	25.7	11.0	34.1	3.2
35	RTD_temp_C_78.7m_Std	°C	78.7 m	105,494	96,567	91.54	0.1	0.0	2.4	0.1
36	RTD_temp_C_3.9m_Avg	°C	3.88 m	105,494	72,429	68.66	24.8	7.8	34.9	5.2
37	RTD_temp_C_3.9m_Max	°C	3.88 m	105,494	72,429	68.66	25.0	7.9	35.1	5.2
38	RTD_temp_C_3.9m_Min	°C	3.88 m	105,494	72,429	68.66	24.7	7.7	34.6	5.1
39	RTD_temp_C_3.9m_Std	°C	3.88 m	105,494	72,429	68.66	0.1	0.0	2.3	0.1
40	HMP155_temp_78.7m_Avg	°C	78.7 m	105,494	96,567	91.54	25.9	11.1	33.8	3.2
41	HMP155_temp_78.7m_Max	°C	78.7 m	105,494	96,567	91.54	26.0	11.1	34.0	3.2
42	HMP155_temp_78.7m_Min	°C	78.7 m	105,494	96,567	91.54	25.8	11.0	33.8	3.2
43	HMP155_temp_78.7m_Std	°C	78.7 m	105,494	96,567	91.54	0.1	0.0	2.2	0.1
44	HMP155_RH_78.7m_Avg	%		105,494	96,567	91.54	75.6	10.4	100.0	16.1
45	HMP155_RH_78.7m_Max	%		105,494	96,567	91.54	76.8	11.7	100.0	15.8
46	HMP155_RH_78.7m_Min	%		105,494	96,567	91.54	74.38	9.09	99.90	16.48
47	HMP155_RH_78.7m_Std	%		105,494	96,567	91.54	0.61	0.02	14.47	0.62
48	BP_79m_Avg	mbar	79 m	105,494	96,567	91.54	999.9	976.0	1,014.0	5.2
49	BP_79m_Max	mbar	79 m	105,494	96,567	91.54	1,000.1	976.0	1,015.0	5.2
50	BP_79m_Min	mbar	79 m	105,494	96,567	91.54	999.7	835.0	1,014.0	5.9
51	BP_79m_Std	mbar	79 m	105,494	96,567	91.54	0.1	0.0	27.4	0.2
52	BP_3.9m_Avg	mbar	3.88 m	105,494	96,567	91.54	1,008.3	984.0	1,022.0	5.4

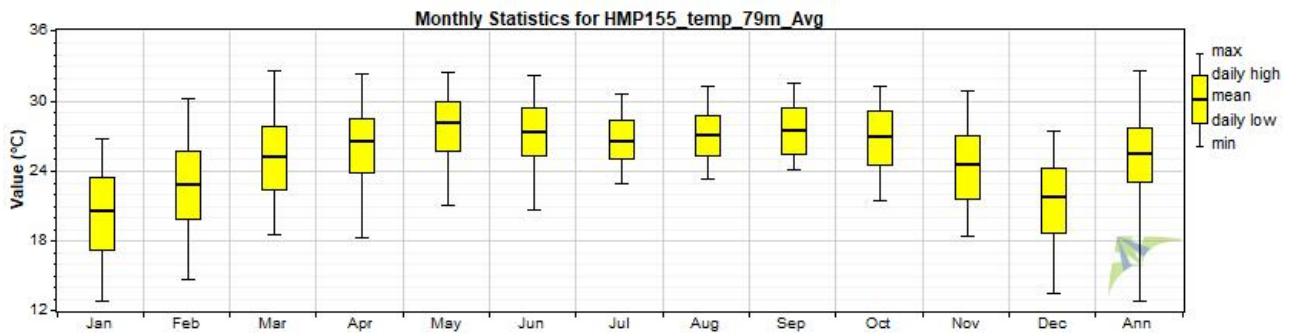
#	Label	Units	Height	Possible Data Points	Valid Data Points	Recovery Rate (%)	Mean	Min	Max	Std. Dev
53	BP_3.9m_Max	mbar	3.88 m	105,494	96,567	91.54	1,008.4	984.0	1,022.0	5.4
54	BP_3.9m_Min	mbar	3.88 m	105,494	96,567	91.54	1,008.2	983.0	1,021.0	5.4
55	BP_3.9m_Std	°C	2 m	105,494	96,567	91.54	0.0	0.0	1.0	0.0
56	SlrW_Avg	W/m2		105,494	31,255	29.63	999	980	1,014	6
57	SlrW_Max	W/m2		105,494	31,255	29.63	999	981	1,015	6
58	SlrW_Min	W/m2		105,494	31,255	29.63	999	835	1,014	6
59	SlrW_Std	W/m2		105,494	31,255	29.63	0.07	0.02	19.26	0.17
60	VWC_Avg	m^3/m^3		105,494	31,255	29.63	1,007	989	1,021	6
61	VWC_Max			105,494	31,255	29.63	1,007	990	1,021	6
62	VWC_Min			105,494	31,255	29.63	1,007	989	1,021	6
63	VWC_Std			105,494	31,255	29.63	0.0514	0.0200	0.9500	0.0312
64	SoilT_Avg	°C	0 m	105,494	31,255	29.63	320.4	246.4	840.0	98.3
65	SoilT_Max	°C	0 m	105,494	31,255	29.63	320.4	243.5	839.0	99.9
66	SoilT_Min	°C	0 m	105,494	31,255	29.63	12.9	0.0	13.7	0.5
67	SoilT_Std	°C	0 m	105,494	31,255	29.63	-0.0	-0.3	1.4	0.4
68	LWmV_Avg	%		105,494	96,567	91.54	217.8	0.0	737.6	168.0
69	LWmV	%		105,494	96,567	91.54	220.6	0.0	794.6	164.8
70	HMP155_temp_4.6m_Avg	°C	4.63 m	105,494	65,422	62.01	24.8	0.0	35.0	4.9
71	HMP155_temp_4.6m_Max	°C	4.63 m	105,494	65,422	62.01	25.0	8.3	35.2	4.9
72	HMP155_temp_4.6m_Min	°C	4.63 m	105,494	65,422	62.01	24.7	0.0	34.8	4.9
73	HMP155_temp_4.6m_Std	°C	4.63 m	105,494	65,422	62.01	0.1	0.0	2.0	0.1
74	HMP155_RH_4.6m_Avg	%		105,494	65,422	62.01	85.65	12.10	99.80	13.81
75	HMP155_RH_4.6m_Max	%		105,494	65,422	62.01	86.98	13.53	99.90	12.75
76	HMP155_RH_4.6m_Min	%		105,494	65,422	62.01	84.50	22.00	99.70	14.73
77	HMP155_RH_4.6m_Std	%		105,494	65,422	62.01	0.60	0.03	36.25	0.71
78	VBatt_Min	Volts		105,494	96,567	91.54	37.86	0.00	91.00	36.64
79	IBatt_Min	Amps		105,494	96,567	91.54	12.76	-0.35	39.61	18.51
80	ILoad_Min			105,494	96,567	91.54	-0.0058	-0.6000	0.3200	0.4098
81	V_in_chg_Min			105,494	96,567	91.54	6.53	0.00	19.96	7.55
82	I_in_chg_Min			105,494	96,567	91.54	3.11	-0.00	11.00	4.20
83	Chg_TmpC_Avg	°C	2 m	105,494	96,567	91.54	22.4	-28.5	46.8	12.8
84	Chg_State	Smp		105,494	96,567	91.54	-40	-1,350	340	308
85	Ck_Batt	Smp		105,494	96,567	91.54	0.169	0.000	2.000	0.487
86	BattV_Min	Volts		105,494	96,567	91.54	12.66	0.00	13.71	0.49
87	PTemp_C_Avg	°C	2 m	105,494	96,567	91.54	27.2	8.3	40.2	5.8
88	latitude_a	Smp		105,494	96,567	91.54	22	22	22	0
89	latitude_b	Smp		105,494	96,567	91.54	36.25	36.24	36.26	0.00
90	longitude_a	Smp		105,494	96,567	91.54	91	91	91	0
91	longitude_b	Smp		105,494	96,567	91.54	39.60	39.59	39.61	0.00
92	magnetic_variation	Smp		105,494	96,567	91.54	-0.6	-0.6	-0.6	0.0
93	fix_quality	Smp		105,494	96,567	91.54	2	1	2	0
94	nmbr_satellites	Smp		105,494	96,567	91.54	9.16	5.00	12.00	0.87
95	altitude	Smp		105,494	96,567	91.54	8.19	-37.50	37.00	6.38
96	max_clock_change			105,494	96,567	91.54	-156	-1,350	340	478
97	nmbr_clock_change	Smp		105,494	96,567	91.54	0.981	0.000	3.000	1.070
98	Air Density	kg/m³		105,494	105,494	100.00	1.169	1.126	1.234	0.021
99	WS_east_80m_Avg TI			105,494	89,873	85.19	0.27	0.03	20.00	0.64
100	WS_west_80m_Avg TI			105,494	82,399	78.11	0.28	0.04	20.25	0.70
101	WS_east_60.4m_Avg TI			105,494	90,318	85.61	0.30	0.03	20.00	0.70
102	WS_west_60.4m_Avg TI			105,494	86,721	82.20	0.38	0.03	25.00	1.04
103	WS_east_40.7m_Avg TI			105,494	91,288	86.53	0.36	0.05	20.00	0.81
104	WS_west_40.7m_Avg TI			105,494	87,343	82.79	0.35	0.04	20.50	0.75
105	WS_east_80m_Avg WPD	W/m²		105,494	91,476	86.71	79	0	5,880	147
106	WS_west_80m_Avg WPD	W/m²		105,494	85,589	81.13	78	0	5,687	141

#	Label	Units	Height	Possible Data Points	Valid Data Points	Recovery Rate (%)	Mean	Min	Max	Std. Dev
107	WS_east_60.4m_Avg WPD	W/m ²		105,494	92,008	87.22	61	0	4,891	117
108	WS_west_60.4m_Avg WPD	W/m ²		105,494	89,834	85.16	55	0	4,319	106
109	WS_east_40.7m_Avg WPD	W/m ²		105,494	92,586	87.76	42	0	3,757	86
110	WS_west_40.7m_Avg WPD	W/m ²		105,494	88,302	83.70	43	0	3,649	86

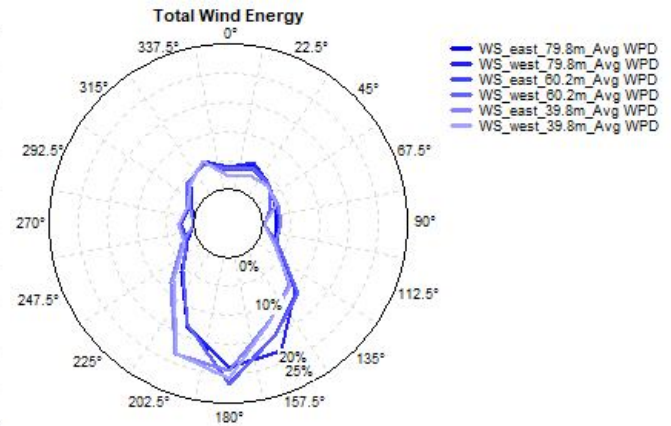
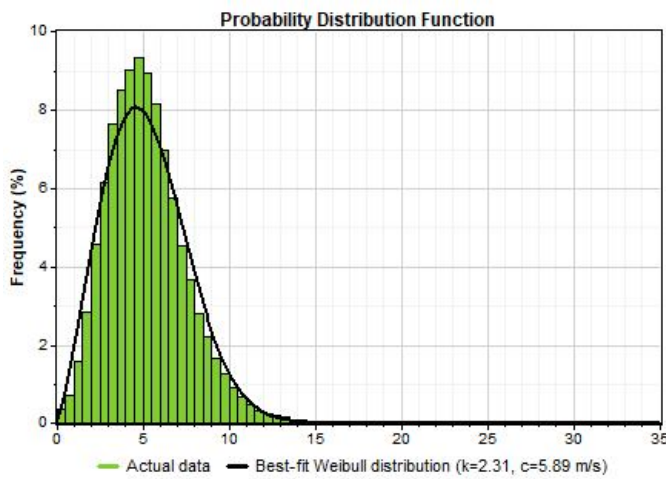
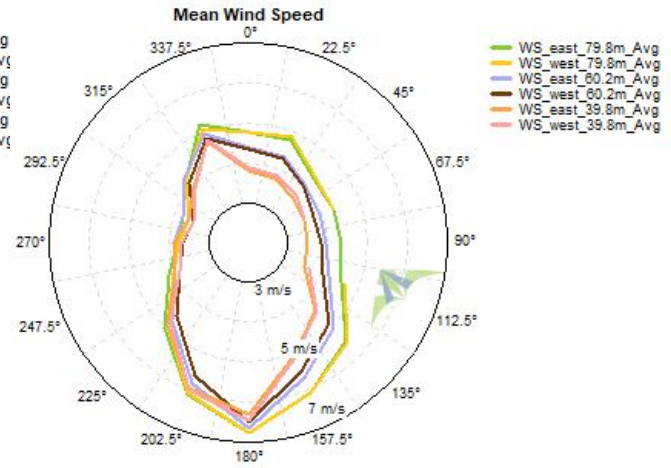
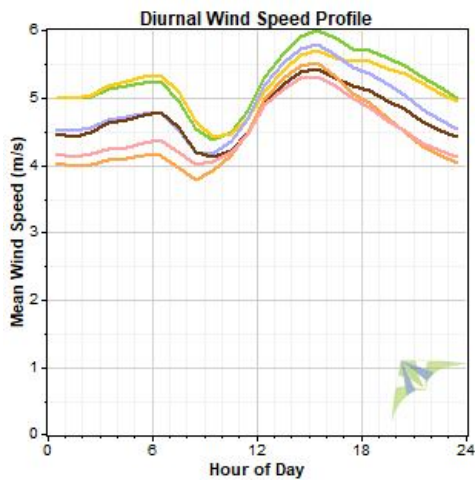
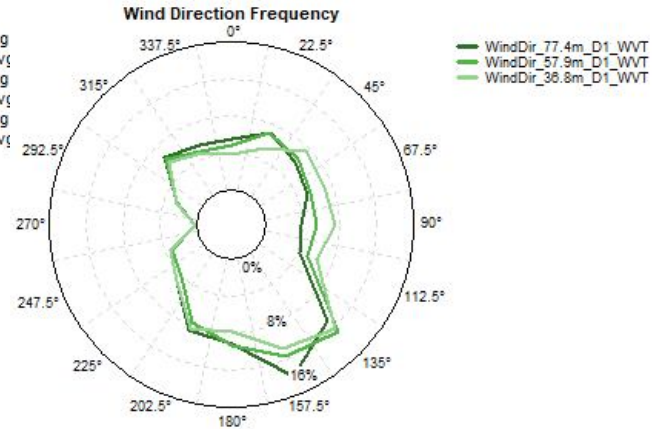
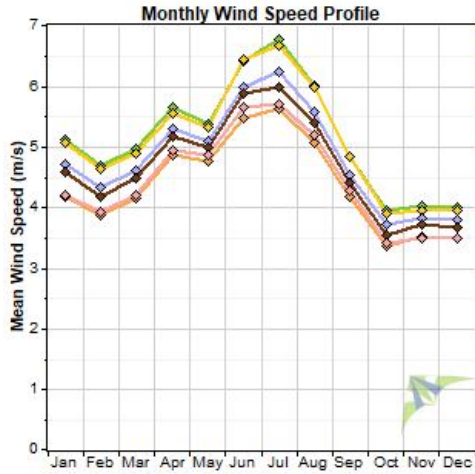
Data Set Properties

Report Created: 4/11/2018 10:23 using Windographer 3.3.10
 Filter Settings: <Unflagged data>

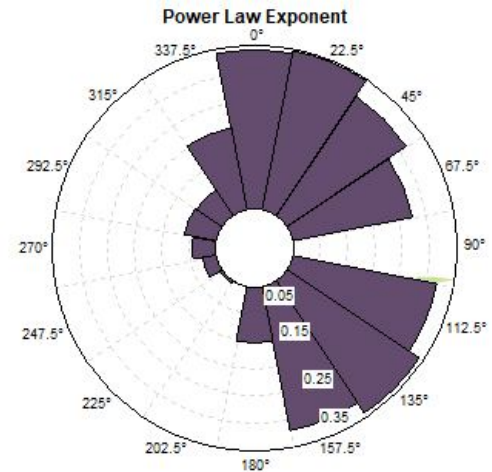
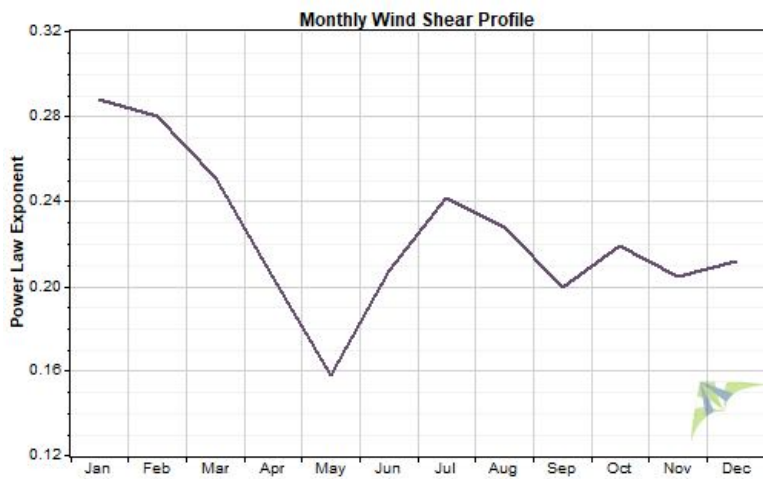
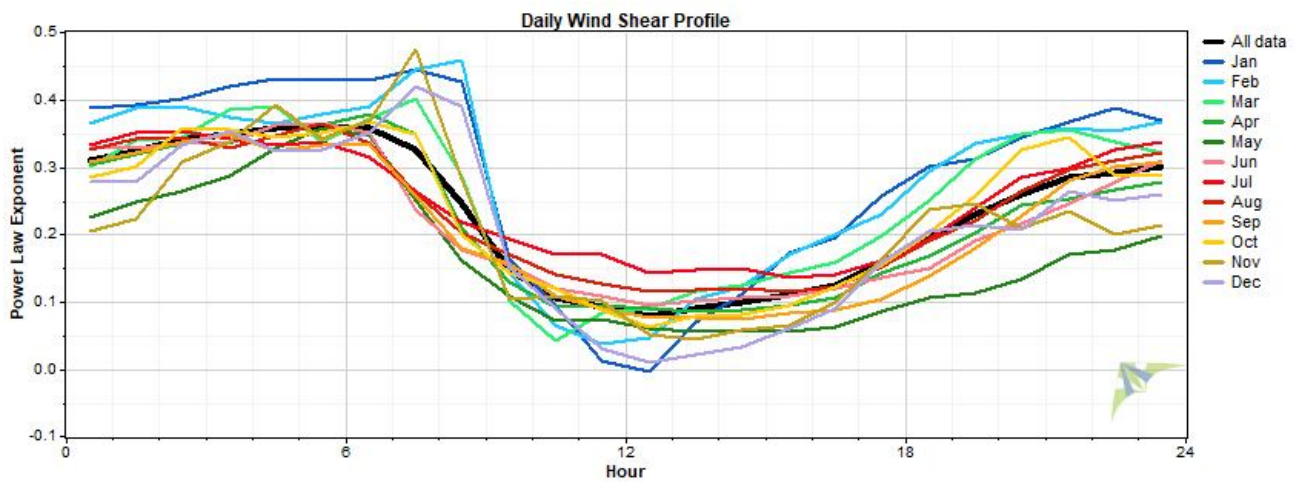
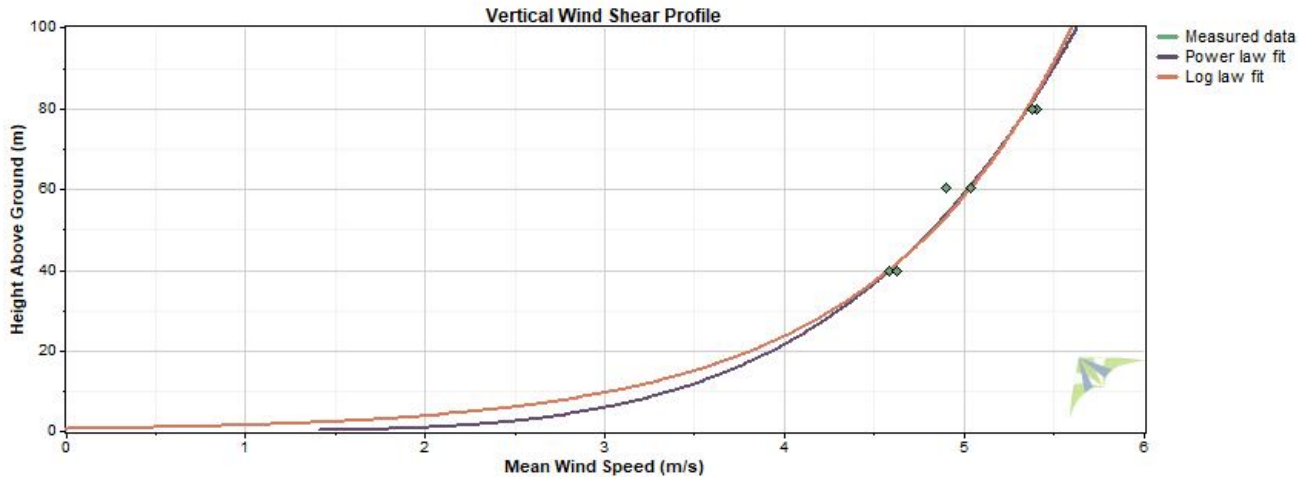
Variable	Value
Latitude	N 22.185130
Longitude	E 91.817670
Elevation	2 m
Start date	12/21/2014 19:50
End date	7/14/2017 08:50
Duration	31 months
Length of time step	10 minutes
Calm threshold	1 m/s
Mean temperature	25.5 °C
Mean pressure	1,000 mbar
Mean air density	1.172 kg/m ³
Power density at 50m	100 W/m ²
Wind power class	1
Power law exponent	0.223
Surface roughness	0.647 m
Roughness class	3.55



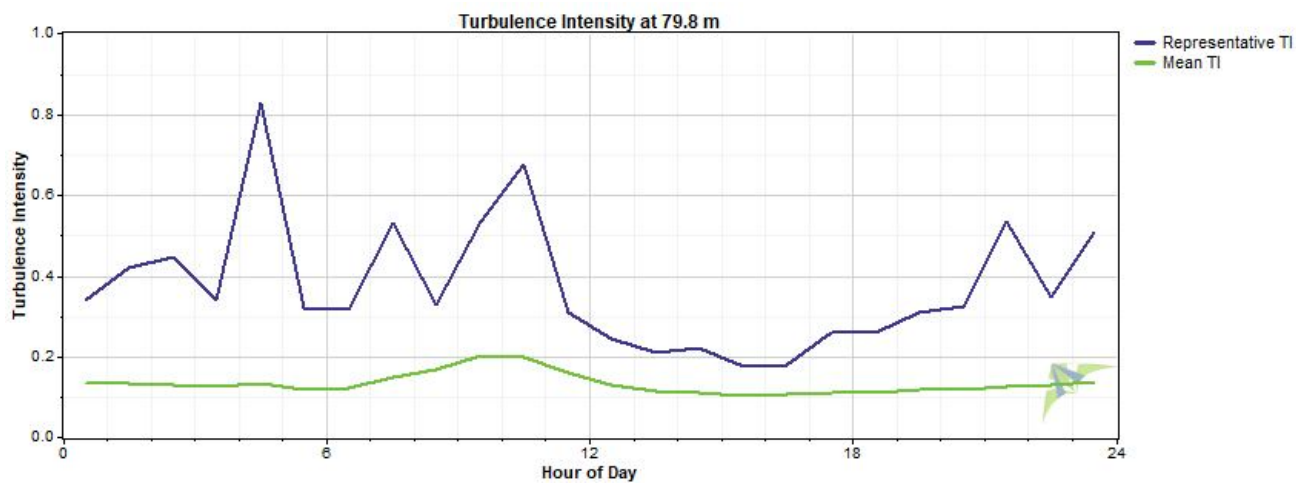
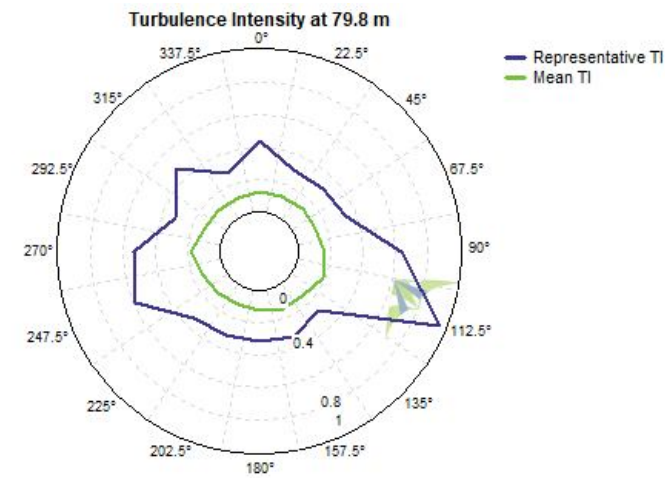
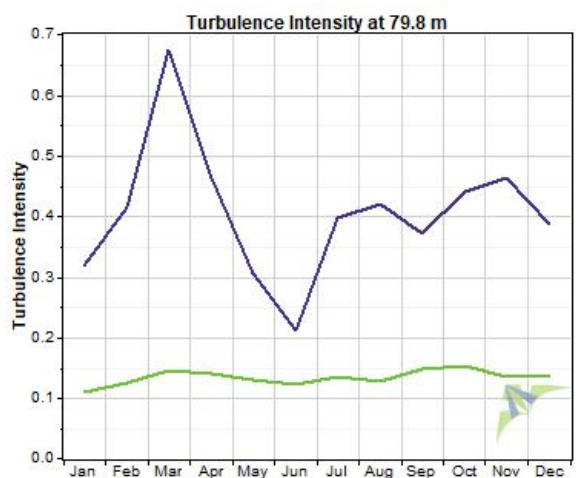
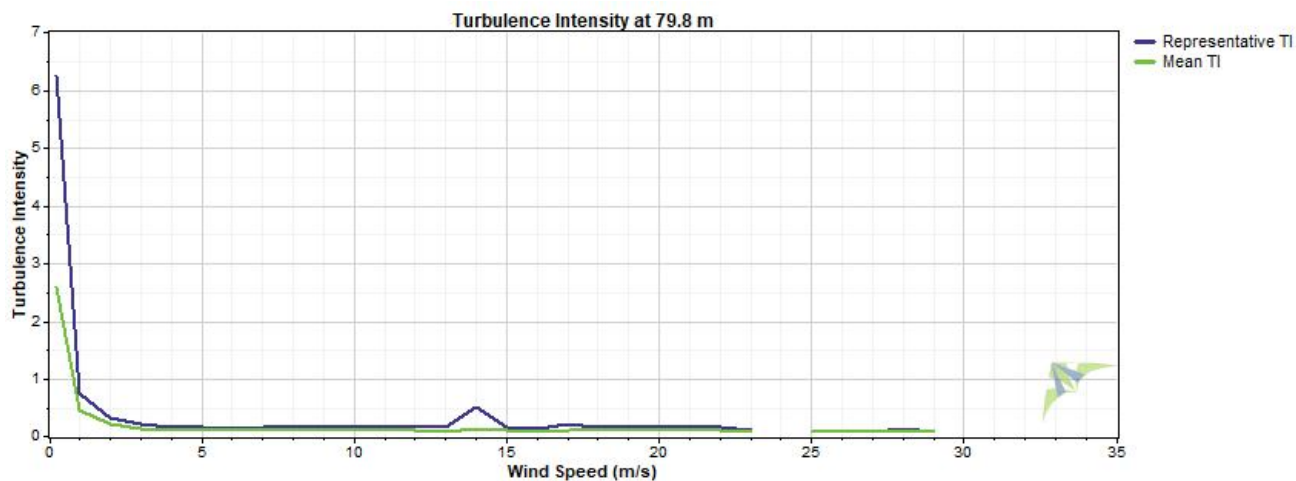
Wind Speed and Direction



Wind Shear



Turbulence Intensity



Data Column Properties

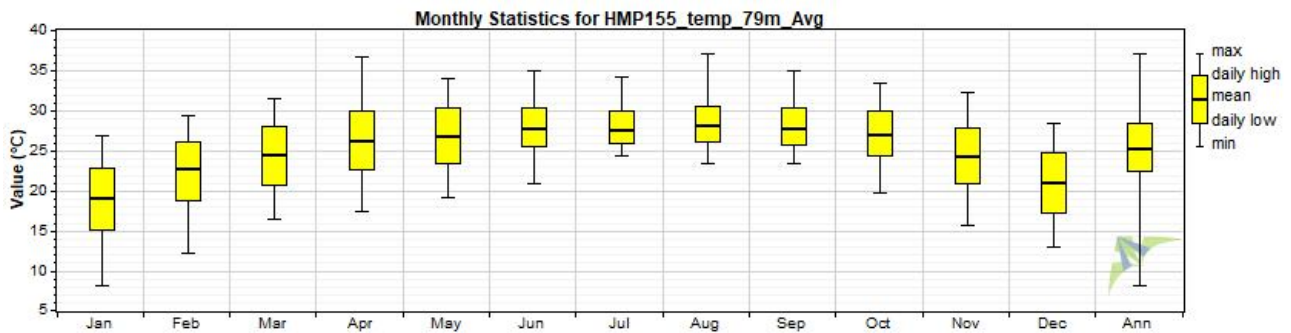
#	Label	Units	Height	Possible Data Points	Valid Data Points	Recovery Rate (%)	Mean	Min	Max	Std. Dev
1	RECORD	m/s		134,718	119,944	89.03	33,139	0	73,595	19,618
2	WS_east_79.8m_Avg	m/s	79.8 m	134,718	113,856	84.51	5.218	0.000	31.390	2.362
3	WS_east_79.8m_Max	m/s	79.8 m	134,718	113,856	84.51	6.611	0.000	769.500	3.697
4	WS_east_79.8m_Min	m/s	79.8 m	134,718	113,856	84.51	3.761	0.000	26.430	1.948
5	WS_east_79.8m_Std	m/s	79.8 m	134,718	113,856	84.51	0.577	0.000	54.960	0.343
6	WS_west_79.8m_Avg	m/s	79.8 m	134,718	114,124	84.71	5.167	0.000	31.320	2.374
7	WS_west_79.8m_Max	m/s	79.8 m	134,718	114,124	84.71	6.540	0.000	770.700	3.705
8	WS_west_79.8m_Min	m/s	79.8 m	134,718	114,124	84.71	3.728	0.000	25.690	1.949
9	WS_west_79.8m_Std	m/s	79.8 m	134,718	114,124	84.71	0.572	0.000	55.050	0.341
10	WS_east_60.2m_Avg	m/s	60.2 m	134,718	113,953	84.59	4.872	0.000	30.340	2.204
11	WS_east_60.2m_Max	m/s	60.2 m	134,718	113,953	84.59	6.316	0.000	406.800	3.046
12	WS_east_60.2m_Min	m/s	60.2 m	134,718	113,953	84.59	3.366	0.000	24.170	1.784
13	WS_east_60.2m_Std	m/s	60.2 m	134,718	113,953	84.59	0.595	0.000	28.840	0.325
14	WS_west_60.2m_Avg	m/s	60.2 m	134,718	111,431	82.71	4.745	0.000	29.420	2.235
15	WS_west_60.2m_Max	m/s	60.2 m	134,718	111,431	82.71	6.179	0.000	36.930	2.800
16	WS_west_60.2m_Min	m/s	60.2 m	134,718	111,431	82.71	3.233	0.000	23.200	1.850
17	WS_west_60.2m_Std	m/s	60.2 m	134,718	111,431	82.71	0.594	0.000	6.682	0.315
18	WS_east_39.8m_Avg	m/s	39.8 m	134,718	114,410	84.93	4.434	0.000	28.520	2.029
19	WS_east_39.8m_Max	m/s	39.8 m	134,718	114,410	84.93	5.970	0.000	729.200	3.430
20	WS_east_39.8m_Min	m/s	39.8 m	134,718	114,410	84.93	2.833	0.000	21.850	1.616
21	WS_east_39.8m_Std	m/s	39.8 m	134,718	114,410	84.93	0.623	0.000	52.080	0.366
22	WS_west_39.8m_Avg	m/s	39.8 m	134,718	109,067	80.96	4.522	0.000	29.000	2.088
23	WS_west_39.8m_Max	m/s	39.8 m	134,718	109,067	80.96	6.062	0.000	759.400	3.567
24	WS_west_39.8m_Min	m/s	39.8 m	134,718	109,067	80.96	2.921	0.000	23.370	1.667
25	WS_west_39.8m_Std	m/s	39.8 m	134,718	109,067	80.96	0.623	0.000	54.250	0.375
26	WindDir_77.4m_D1_WVT	°	77.4 m	134,718	119,944	89.03	150.7	0.0	360.0	97.5
27	WindDir_77.4m_SD1_WVT	°	77.4 m	134,718	119,944	89.03	5.2	0.0	78.5	5.0
28	WindDir_57.9m_D1_WVT	°	57.9 m	134,718	119,944	89.03	145.3	0.0	360.0	96.4
29	WindDir_57.9m_SD1_WVT	°	57.9 m	134,718	119,944	89.03	5.9	0.0	80.0	5.2
30	WindDir_36.8m_D1_WVT	°	36.8 m	134,718	119,944	89.03	146.7	0.0	360.0	94.2
31	WindDir_36.8m_SD1_WVT	°	36.8 m	134,718	119,944	89.03	6.9	0.0	79.9	5.6
32	RTD_temp_C_78m_Avg	°C	78 m	134,718	119,944	89.03	26.6	13.6	33.8	3.1
33	RTD_temp_C_78m_Max	°C	78 m	134,718	119,944	89.03	26.9	14.0	35.4	3.1
34	RTD_temp_C_78m_Min	°C	78 m	134,718	119,944	89.03	26.3	13.3	33.5	3.1
35	RTD_temp_C_78m_Std	°C	78 m	134,718	119,944	89.03	0.1	0.0	2.9	0.1
36	RTD_temp_C_4.9m_Avg	°C	4.9 m	134,718	119,944	89.03	25.4	11.1	37.1	4.0
37	RTD_temp_C_4.9m_Max	°C	4.9 m	134,718	119,944	89.03	25.5	11.2	37.2	4.0
38	RTD_temp_C_4.9m_Min	°C	4.9 m	134,718	119,944	89.03	25.2	11.0	36.9	4.0
39	RTD_temp_C_4.9m_Std	°C	4.9 m	134,718	119,944	89.03	0.1	0.0	3.6	0.1
40	HMP155_temp_79m_Avg	°C	79 m	134,718	119,300	88.56	25.5	12.7	32.6	3.1
41	HMP155_temp_79m_Max	°C	79 m	134,718	119,300	88.56	25.6	12.8	32.7	3.1
42	HMP155_temp_79m_Min	°C	79 m	134,718	119,300	88.56	25.4	12.7	32.5	3.1
43	HMP155_temp_79m_Std	°C	79 m	134,718	119,300	88.56	0.1	0.0	3.1	0.1
44	HMP155_RH_79m_Avg	%		134,718	119,944	89.03	80.8	0.4	100.0	16.6
45	HMP155_RH_79m_Max	%		134,718	119,944	89.03	82.2	0.5	100.0	16.0
46	HMP155_RH_79m_Min	%		134,718	119,944	89.03	79.31	0.41	99.90	17.24
47	HMP155_RH_79m_Std	%		134,718	119,944	89.03	0.75	0.01	13.79	0.84
48	HMP155_temp_5.7m_Avg	°C	5.65 m	134,718	118,371	87.87	25.4	11.2	35.8	4.0
49	HMP155_temp_5.7m_Max	°C	5.65 m	134,718	118,371	87.87	25.5	11.3	36.0	4.0
50	HMP155_temp_5.7m_Min	°C	5.65 m	134,718	118,371	87.87	25.2	-79.3	35.6	4.0
51	HMP155_temp_5.7m_Std	°C	5.65 m	134,718	118,371	87.87	0.1	0.0	8.6	0.1
52	HMP155_RH_5.7m_Avg	%		134,718	119,061	88.38	84.0	0.4	100.0	13.0

#	Label	Units	Height	Possible Data Points	Valid Data Points	Recovery Rate (%)	Mean	Min	Max	Std. Dev
53	HMP155_RH_5.7m_Max	%		134,718	119,061	88.38	85.3	0.4	100.0	12.3
54	HMP155_RH_5.7m_Min	%		134,718	119,061	88.38	82.82	0.39	99.90	13.73
55	HMP155_RH_5.7m_Std	%		134,718	119,061	88.38	0.61	0.00	49.55	0.88
56	BP_78.6m_Avg	mbar	78.6 m	134,718	119,944	89.03	1,000.4	962.0	1,018.0	5.2
57	BP_78.6m_Max	mbar	78.6 m	134,718	119,944	89.03	1,000.5	971.0	1,019.0	5.2
58	BP_78.6m_Min	mbar	78.6 m	134,718	119,944	89.03	1,000.2	809.0	1,017.0	5.9
59	BP_78.6m_Std	mbar	78.6 m	134,718	119,944	89.03	0.1	0.0	84.6	0.3
60	BP_4.1m_Avg	mbar	4.1 m	134,718	119,944	89.03	1,007.8	978.0	1,020.0	5.3
61	BP_4.1m_Max	mbar	4.1 m	134,718	119,944	89.03	1,007.9	979.0	1,021.0	5.3
62	BP_4.1m_Min	mbar	4.1 m	134,718	119,944	89.03	1,007.7	929.0	1,020.0	5.3
63	BP_4.1m_Std	mbar	4.1 m	134,718	119,944	89.03	0.0	0.0	5.0	0.0
64	LWmV_Avg	Avg		134,718	119,944	89.03	291	119	1,076	141
65	LWmV	Smp		134,718	119,944	89.03	291	118	1,076	141
66	VBatt_Min	Volts		134,718	119,943	89.03	12.71	0.00	14.03	0.56
67	IBatt_Min	Amps		134,718	119,944	89.03	-0.000	-0.491	3.455	0.433
68	ILoad_Min			134,718	119,944	89.03	0.260	0.000	0.383	0.052
69	V_in_chg_Min			134,718	119,944	89.03	8.34	0.00	20.42	8.22
70	I_in_chg_Min			134,718	119,944	89.03	0.234	-0.003	3.503	0.362
71	Chg_TmpC_Avg	°C	2 m	134,718	119,944	89.03	29.5	0.3	64.0	6.4
72	Chg_State	Smp		134,718	119,944	89.03	1.074	0.000	3.000	1.319
73	Ck_Batt	Smp		134,718	119,944	89.03	0.002	0.000	1.000	0.043
74	BattV_Min	Volts		134,718	119,944	89.03	12.33	9.23	13.63	0.54
75	PTemp_C_Avg	°C	2 m	134,718	119,944	89.03	27.3	10.7	38.4	4.9
76	latitude_a	Smp		134,718	119,944	89.03	22	22	22	0
77	latitude_b	Smp		134,718	119,944	89.03	11.11	11.10	11.12	0.00
78	longitude_a	Smp		134,718	119,944	89.03	91	91	91	0
79	longitude_b	Smp		134,718	119,944	89.03	49.06	49.05	49.07	0.00
80	magnetic_variation	Smp		134,718	119,944	89.03	-0.7	-0.7	-0.7	0.0
81	fix_quality	Smp		134,718	119,944	89.03	2.000	1.000	2.000	0.006
82	nmbr_satellites	Smp		134,718	119,944	89.03	9.12	5.00	12.00	0.88
83	altitude	Smp		134,718	119,944	89.03	12.38	-61.80	35.80	6.16
84	max_clock_change			134,718	119,944	89.03	2,782	-4,210	7,999	4,027
85	nmbr_clock_change	Smp		134,718	119,944	89.03	1.88	0.00	41.00	4.59
86	Air Density	kg/m ³		134,718	134,718	100.00	1.172	1.122	1.230	0.022
87	WS_east_79.8m_Avg TI			134,718	113,797	84.47	0.13	0.02	20.50	0.22
88	WS_west_79.8m_Avg TI			134,718	114,029	84.64	0.14	0.02	20.00	0.22
89	WS_east_60.2m_Avg TI			134,718	113,839	84.50	0.15	0.03	20.00	0.25
90	WS_west_60.2m_Avg TI			134,718	110,850	82.28	0.18	0.02	22.50	0.47
91	WS_east_39.8m_Avg TI			134,718	114,318	84.86	0.16	0.04	20.50	0.23
92	WS_west_39.8m_Avg TI			134,718	108,950	80.87	0.16	0.04	20.50	0.22
93	WS_east_79.8m_Avg WPD	W/m ²		134,718	113,856	84.51	142	0	17,598	295
94	WS_west_79.8m_Avg WPD	W/m ²		134,718	114,124	84.71	139	0	17,447	305
95	WS_east_60.2m_Avg WPD	W/m ²		134,718	113,953	84.59	116	0	15,860	258
96	WS_west_60.2m_Avg WPD	W/m ²		134,718	111,431	82.71	111	0	14,461	259
97	WS_east_39.8m_Avg WPD	W/m ²		134,718	114,410	84.93	90	0	13,174	218
98	WS_west_39.8m_Avg WPD	W/m ²		134,718	109,067	80.96	96	0	13,850	240

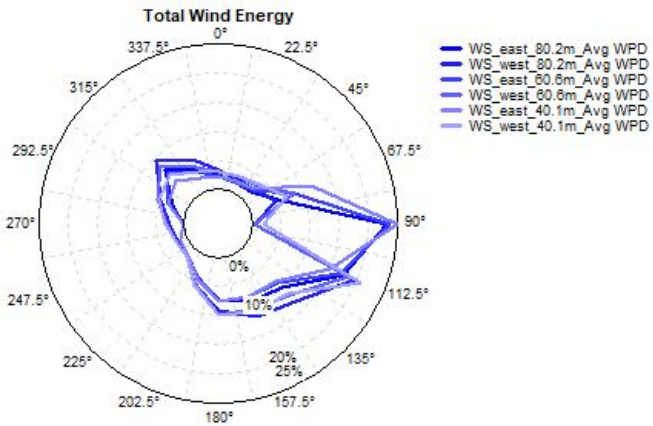
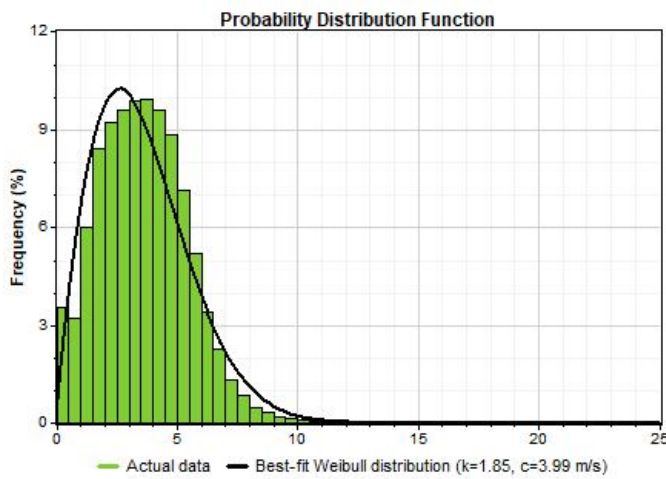
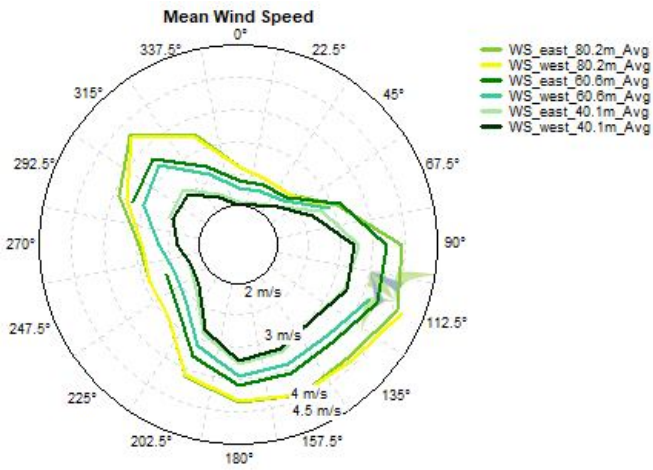
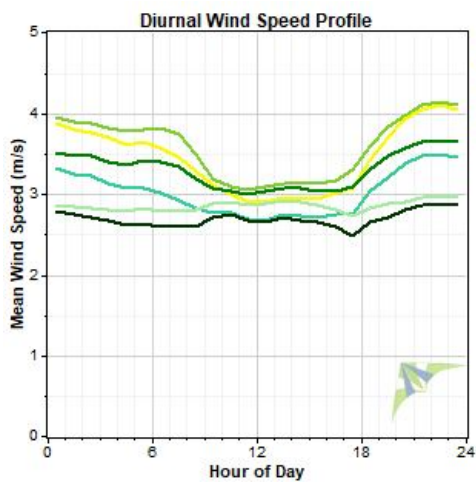
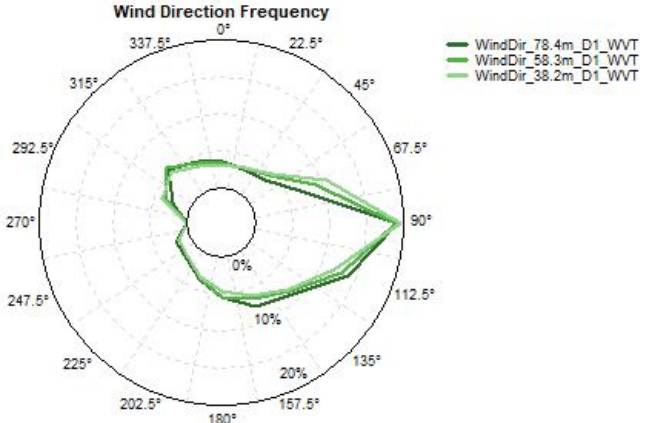
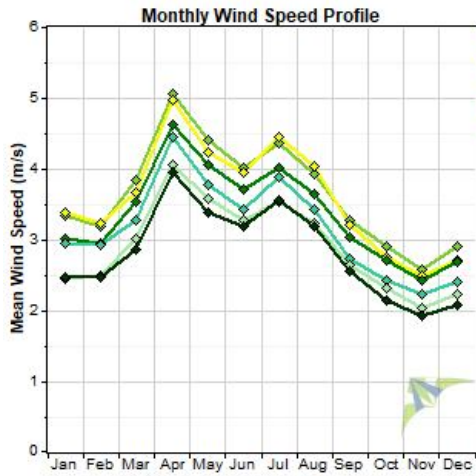
Data Set Properties

Report Created: 4/11/2018 10:21 using Windographer 3.3.10
 Filter Settings: <Unflagged data>

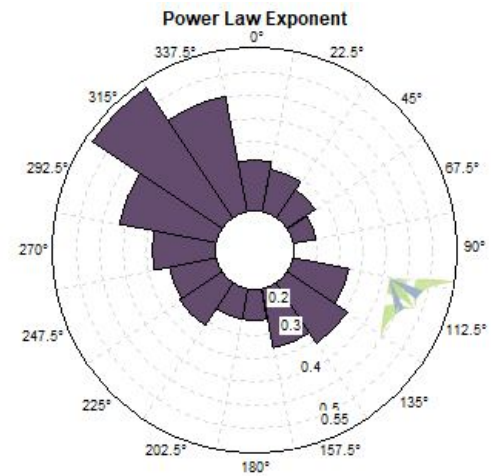
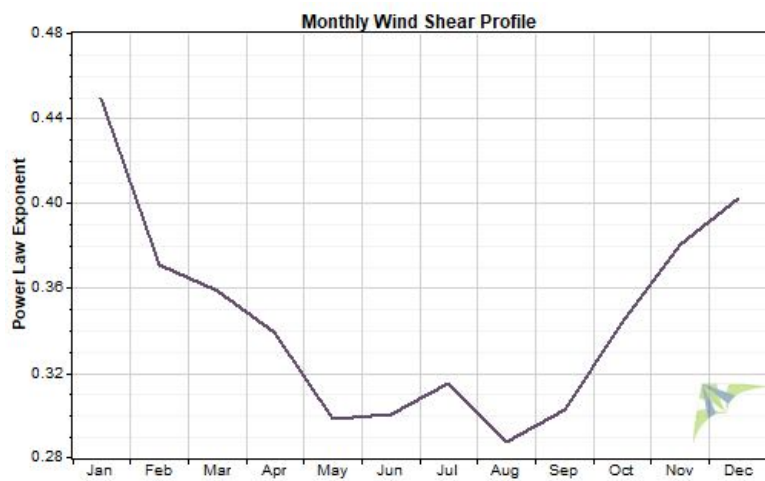
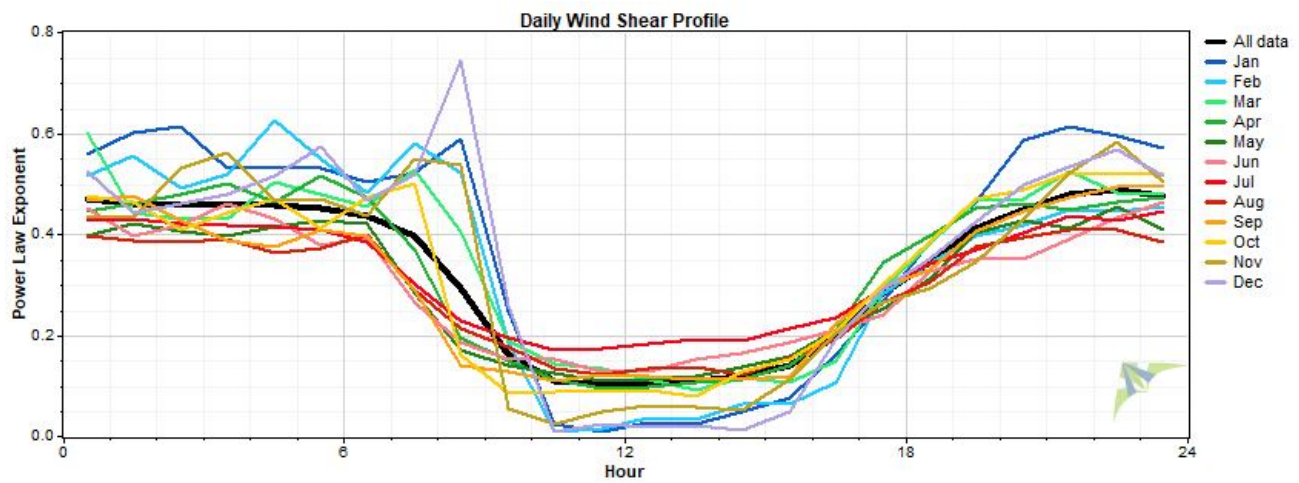
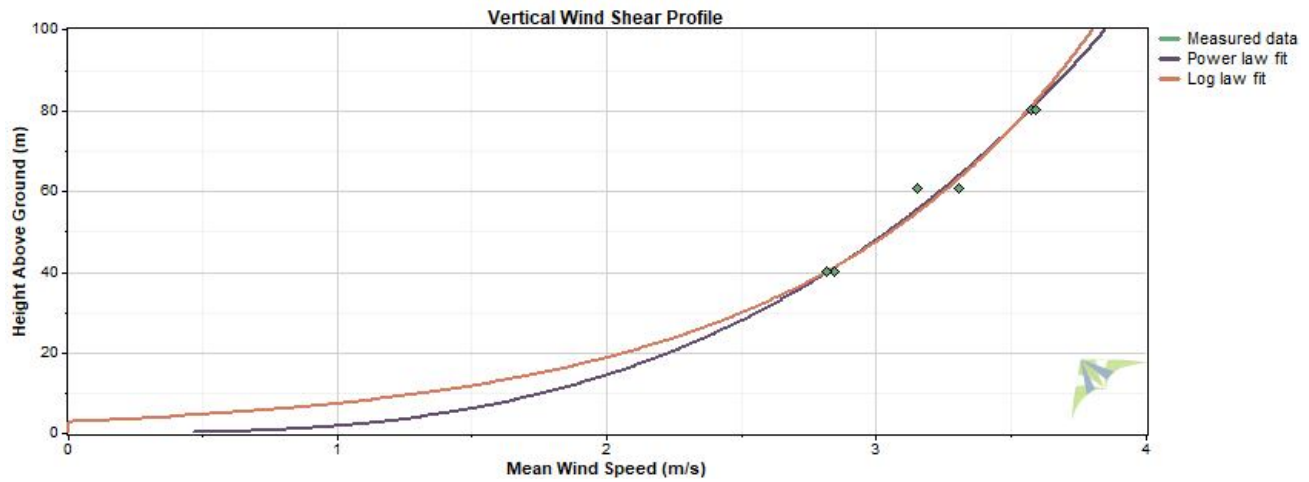
Variable	Value
Latitude	N 24.715460
Longitude	E 90.466800
Elevation	0 m
Start date	8/13/2015 14:50
End date	12/13/2017 00:10
Duration	28 months
Length of time step	10 minutes
Calm threshold	1 m/s
Mean temperature	25.4 °C
Mean pressure	999.6 mbar
Mean air density	1.168 kg/m ³
Power density at 50m	33 W/m ²
Wind power class	1
Power law exponent	0.34
Surface roughness	2.96 m
Roughness class	4.81



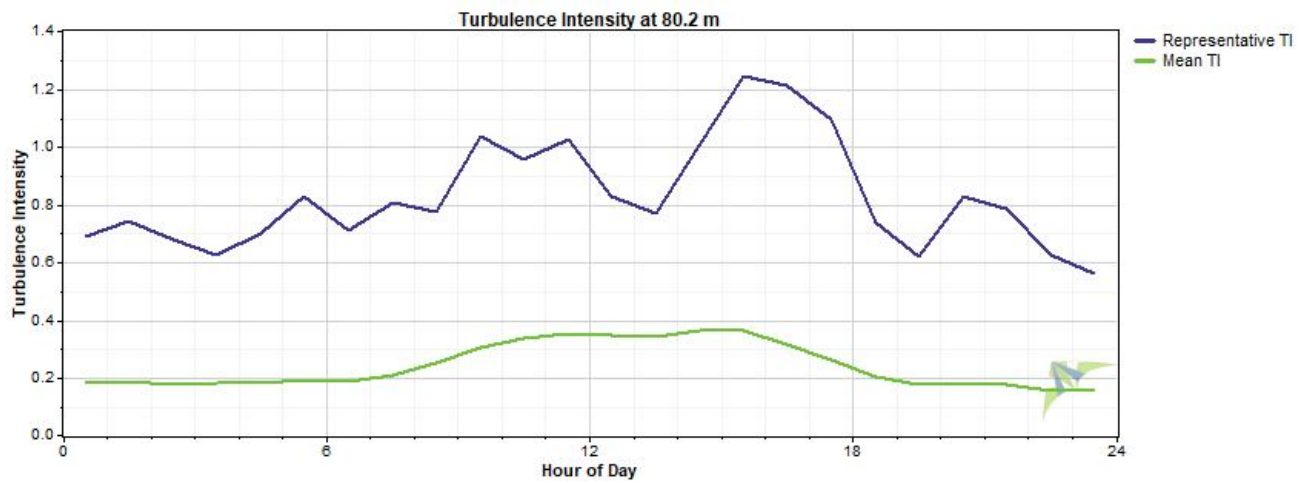
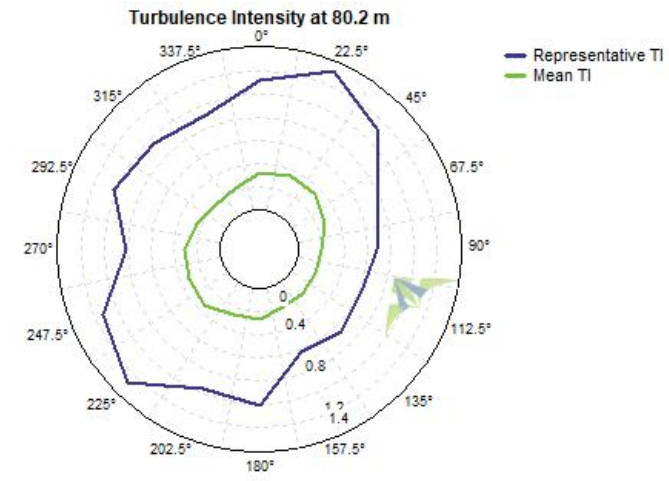
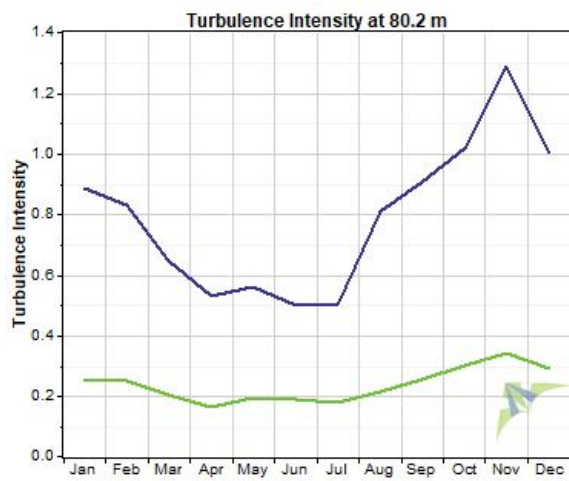
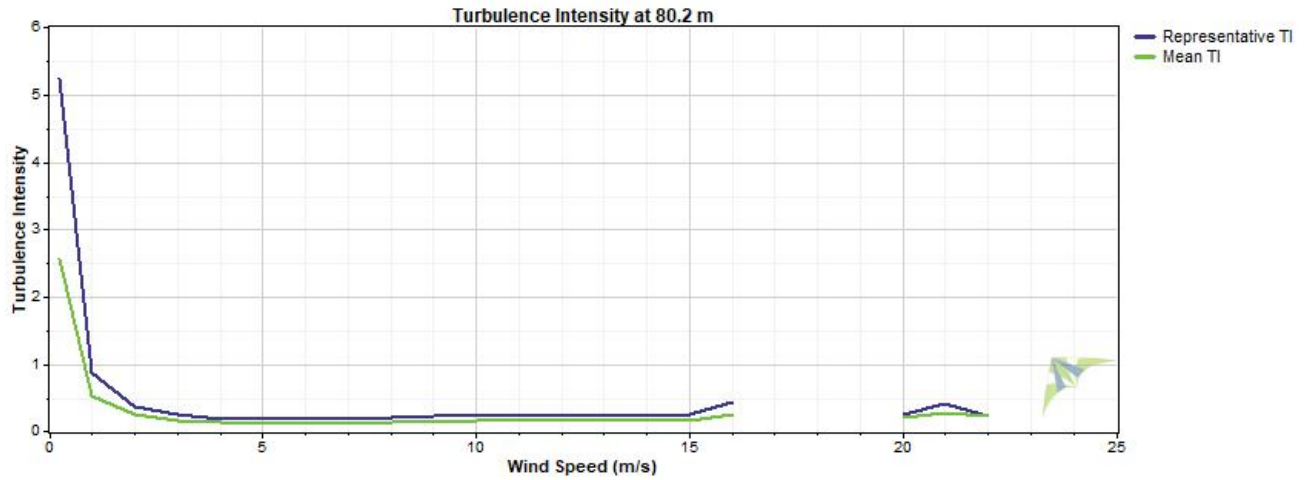
Wind Speed and Direction



Wind Shear



Turbulence Intensity



Data Column Properties

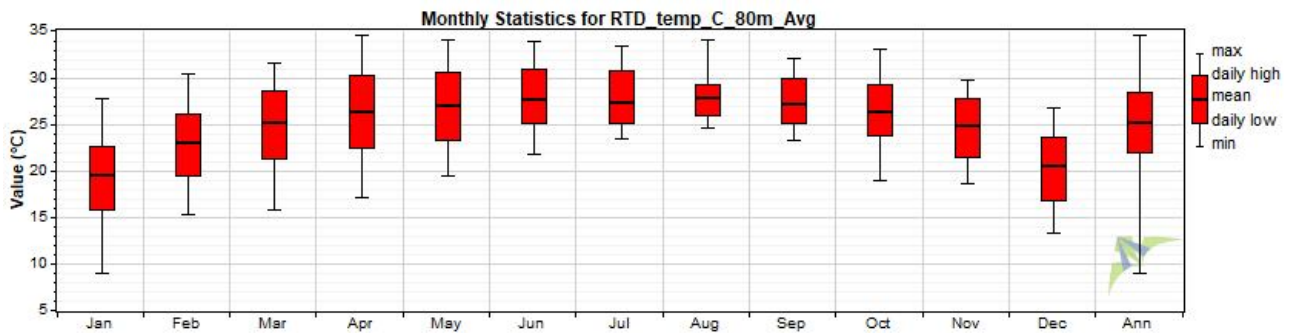
#	Label	Units	Height	Possible Data Points	Valid Data Points	Recovery Rate (%)	Mean	Min	Max	Std. Dev
1	RECORD			122,744	119,620	97.45	44,699	0	104,116	31,551
2	WS_east_80.2m_Avg	m/s	80.2 m	122,744	112,865	91.95	3.591	0.000	22.420	1.879
3	WS_east_80.2m_Max	m/s	80.2 m	122,744	112,865	91.95	4.885	0.000	38.730	2.362
4	WS_east_80.2m_Min	m/s	80.2 m	122,744	112,865	91.95	2.302	0.000	13.320	1.574
5	WS_east_80.2m_Std	m/s	80.2 m	122,744	112,865	91.95	0.548	0.000	8.780	0.278
6	WS_west_80.2m_Avg	m/s	80.2 m	122,744	91,254	74.34	3.461	0.000	22.330	1.880
7	WS_west_80.2m_Max	m/s	80.2 m	122,744	91,254	74.34	4.722	0.000	40.300	2.367
8	WS_west_80.2m_Min	m/s	80.2 m	122,744	91,254	74.34	2.226	0.000	13.320	1.579
9	WS_west_80.2m_Std	m/s	80.2 m	122,744	91,254	74.34	0.535	0.000	8.560	0.279
10	WS_east_60.6m_Avg	m/s	60.6 m	122,744	114,523	93.30	3.305	0.000	20.940	1.652
11	WS_east_60.6m_Max	m/s	60.6 m	122,744	114,523	93.30	4.615	0.000	34.850	2.190
12	WS_east_60.6m_Min	m/s	60.6 m	122,744	114,523	93.30	2.020	0.000	11.780	1.328
13	WS_east_60.6m_Std	m/s	60.6 m	122,744	114,523	93.30	0.550	0.000	8.280	0.269
14	WS_west_60.6m_Avg	m/s	60.6 m	122,744	91,141	74.25	3.025	0.000	20.570	1.707
15	WS_west_60.6m_Max	m/s	60.6 m	122,744	91,141	74.25	4.331	0.000	33.990	2.215
16	WS_west_60.6m_Min	m/s	60.6 m	122,744	91,141	74.25	1.755	0.000	12.570	1.391
17	WS_west_60.6m_Std	m/s	60.6 m	122,744	91,141	74.25	0.554	0.000	8.170	0.288
18	WS_east_40.1m_Avg	m/s	40.1 m	122,744	113,520	92.49	2.855	0.000	18.950	1.457
19	WS_east_40.1m_Max	m/s	40.1 m	122,744	113,520	92.49	4.204	0.000	34.140	2.086
20	WS_east_40.1m_Min	m/s	40.1 m	122,744	113,520	92.49	1.570	0.000	9.470	1.080
21	WS_east_40.1m_Std	m/s	40.1 m	122,744	113,520	92.49	0.557	0.000	7.923	0.266
22	WS_west_40.1m_Avg	m/s	40.1 m	122,744	91,969	74.93	2.693	0.000	18.640	1.450
23	WS_west_40.1m_Max	m/s	40.1 m	122,744	91,969	74.93	4.003	0.000	34.790	2.070
24	WS_west_40.1m_Min	m/s	40.1 m	122,744	91,969	74.93	1.453	0.000	9.450	1.076
25	WS_west_40.1m_Std	m/s	40.1 m	122,744	91,969	74.93	0.548	0.000	7.666	0.274
26	WindDir_78.4m_D1_WVT	°	78.4 m	122,744	119,618	97.45	107.6	0.0	360.0	93.6
27	WindDir_78.4m_SD1_WVT	°	78.4 m	122,744	119,620	97.45	7.3	0.0	79.4	7.8
28	WindDir_58.3m_D1_WVT	°	58.3 m	122,744	119,618	97.45	102.6	0.0	360.0	94.7
29	WindDir_58.3m_SD1_WVT	°	58.3 m	122,744	119,620	97.45	8.4	0.0	79.8	8.3
30	WindDir_38.2m_D1_WVT	°	38.2 m	122,744	119,618	97.45	99.9	0.0	360.0	95.0
31	WindDir_38.2m_SD1_WVT	°	38.2 m	122,744	119,620	97.45	9.5	0.0	80.2	8.7
32	RTD_temp_C_78.3m_Avg	°C	78.3 m	122,744	119,599	97.44	25.4	7.8	37.0	3.7
33	RTD_temp_C_78.3m_Max	°C	78.3 m	122,744	119,599	97.44	25.7	7.9	37.1	3.7
34	RTD_temp_C_78.3m_Min	°C	78.3 m	122,744	119,599	97.44	25.1	7.7	36.7	3.8
35	RTD_temp_C_78.3m_Std	°C	78.3 m	122,744	119,599	97.44	0.1	0.0	3.1	0.1
36	RTD_temp_C_3.7m_Avg	°C	3.72 m	122,744	119,514	97.37	24.6	8.0	37.0	5.0
37	RTD_temp_C_3.7m_Max	°C	3.72 m	122,744	119,514	97.37	24.7	8.1	37.2	5.0
38	RTD_temp_C_3.7m_Min	°C	3.72 m	122,744	119,514	97.37	24.4	8.0	36.8	5.0
39	RTD_temp_C_3.7m_Std	°C	3.72 m	122,744	119,514	97.37	0.1	0.0	2.3	0.1
40	HMP155_temp_79m_Avg	°C	79 m	122,744	119,480	97.34	25.4	8.0	37.1	3.8
41	HMP155_temp_79m_Max	°C	79 m	122,744	119,480	97.34	25.5	8.1	37.5	3.8
42	HMP155_temp_79m_Min	°C	79 m	122,744	119,480	97.34	25.2	7.9	36.6	3.8
43	HMP155_temp_79m_Std	°C	79 m	122,744	119,480	97.34	0.1	0.0	2.5	0.1
44	HMP155_RH_79m_Avg	%		122,744	119,619	97.45	78.6	14.4	100.0	16.1
45	HMP155_RH_79m_Max	%		122,744	119,619	97.45	79.9	16.4	100.0	15.7
46	HMP155_RH_79m_Min	%		122,744	119,619	97.45	77.46	-0.03	99.90	16.47
47	HMP155_RH_79m_Std	%		122,744	119,619	97.45	0.64	0.01	18.70	0.70
48	HMP155_temp_4.5m_Avg	°C	4.49 m	122,744	119,361	97.24	24.6	7.8	37.2	5.0
49	HMP155_temp_4.5m_Max	°C	4.49 m	122,744	119,361	97.24	24.7	7.9	37.2	5.1
50	HMP155_temp_4.5m_Min	°C	4.49 m	122,744	119,361	97.24	24.4	7.8	37.1	5.0
51	HMP155_temp_4.5m_Std	°C	4.49 m	122,744	119,361	97.24	0.1	0.0	2.1	0.1
52	HMP155_RH_4.5m_Avg	%		122,744	119,226	97.13	86.9	-22.7	100.0	13.9

#	Label	Units	Height	Possible Data Points	Valid Data Points	Recovery Rate (%)	Mean	Min	Max	Std. Dev
53	HMP155_RH_4.5m_Max	%		122,744	119,226	97.13	88.3	-20.6	100.0	12.7
54	HMP155_RH_4.5m_Min	%		122,744	119,226	97.13	85.77	-23.44	99.90	14.88
55	HMP155_RH_4.5m_Std	%		122,744	119,226	97.13	0.60	0.01	33.71	0.72
56	BP_78.7m_Avg	mbar	78.7 m	122,744	119,605	97.44	999.6	982.0	1,025.0	5.3
57	BP_78.7m_Max	mbar	78.7 m	122,744	119,605	97.44	999.8	983.0	1,026.0	5.3
58	BP_78.7m_Min	mbar	78.7 m	122,744	119,605	97.44	999.4	814.0	1,025.0	5.5
59	BP_78.7m_Std	mbar	78.7 m	122,744	119,605	97.44	0.1	0.0	11.3	0.1
60	BP_4.7m_Avg	mbar	4.69 m	122,744	119,620	97.45	1,007.2	992.0	1,021.0	5.4
61	BP_4.7m_Max	mbar	4.69 m	122,744	119,620	97.45	1,007.3	992.0	1,021.0	5.4
62	BP_4.7m_Min	mbar	4.69 m	122,744	119,620	97.45	1,007.1	958.0	1,020.0	5.4
63	BP_4.7m_Std	mbar	4.69 m	122,744	119,620	97.45	0.1	0.0	5.0	0.0
64	LWmV_Avg	Avg		122,744	119,620	97.45	326.1	167.8	968.0	88.4
65	LWmV	Smp		122,744	119,620	97.45	326.1	167.4	959.0	89.1
66	VBatt_Min	Volts		122,744	119,620	97.45	12.41	0.00	13.75	0.89
67	IBatt_Min	Amps		122,744	119,620	97.45	0.045	-0.430	3.389	0.501
68	ILoad_Min			122,744	119,620	97.45	0.283	0.000	0.350	0.019
69	V_in_chg_Min			122,744	119,620	97.45	8.34	0.00	20.44	8.21
70	I_in_chg_Min			122,744	119,620	97.45	0.285	-0.004	3.163	0.411
71	Chg_TmpC_Avg	°C	2 m	122,744	119,620	97.45	30.0	9.2	64.4	8.4
72	Chg_State	Smp		122,744	119,620	97.45	1.095	0.000	3.000	1.296
73	Ck_Batt	Smp		122,744	119,620	97.45	0.017	0.000	1.000	0.130
74	BattV_Min	Volts		122,744	119,618	97.45	12.01	9.24	13.39	0.92
75	PTemp_C_Avg	°C	2 m	122,744	119,618	97.45	27.2	8.8	47.1	6.5
76	latitude_a	Smp		122,744	119,620	97.45	24	24	24	0
77	latitude_b	Smp		122,744	119,620	97.45	42.92	42.92	42.93	0.00
78	longitude_a	Smp		122,744	119,620	97.45	90	90	90	0
79	longitude_b	Smp		122,744	119,620	97.45	28.01	28.00	28.02	0.00
80	magnetic_variation	Smp		122,744	119,620	97.45	-0.4	-0.4	-0.4	0.0
81	fix_quality	Smp		122,744	119,620	97.45	2	1	2	0
82	nubr_satellites	Smp		122,744	119,620	97.45	9.13	5.00	12.00	0.89
83	altitude	Smp		122,744	119,620	97.45	8.42	-33.80	45.70	6.11
84	max_clock_change			122,744	119,620	97.45	221	-1,000	7,999	1,969
85	nubr_clock_change	Smp		122,744	119,620	97.45	1.346	0.000	7.000	2.009
86	Air Density	kg/m ³		122,744	122,744	100.00	1.168	1.113	1.250	0.021
87	WS_east_80.2m_Avg TI			122,744	111,111	90.52	0.24	0.03	20.50	0.48
88	WS_west_80.2m_Avg TI			122,744	90,198	73.48	0.24	0.03	20.00	0.46
89	WS_east_60.6m_Avg TI			122,744	113,916	92.81	0.24	0.03	20.50	0.44
90	WS_west_60.6m_Avg TI			122,744	89,147	72.63	0.34	0.03	22.50	0.77
91	WS_east_40.1m_Avg TI			122,744	112,690	91.81	0.28	0.04	20.00	0.47
92	WS_west_40.1m_Avg TI			122,744	90,947	74.09	0.31	0.04	20.50	0.58
93	WS_east_80.2m_Avg WPD	W/m ²		122,744	112,865	91.95	52	0	6,597	102
94	WS_west_80.2m_Avg WPD	W/m ²		122,744	91,254	74.34	48	0	6,518	100
95	WS_east_60.6m_Avg WPD	W/m ²		122,744	114,523	93.30	39	0	5,375	80
96	WS_west_60.6m_Avg WPD	W/m ²		122,744	91,141	74.25	34	0	5,095	76
97	WS_east_40.1m_Avg WPD	W/m ²		122,744	113,520	92.49	26	0	3,984	60
98	WS_west_40.1m_Avg WPD	W/m ²		122,744	91,969	74.93	23	0	3,791	57

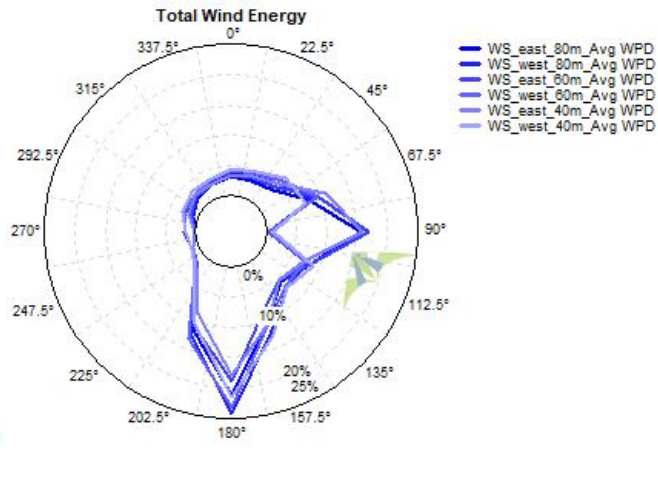
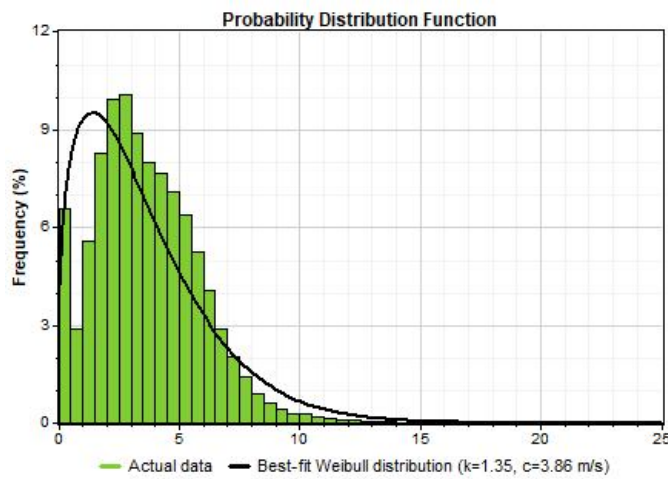
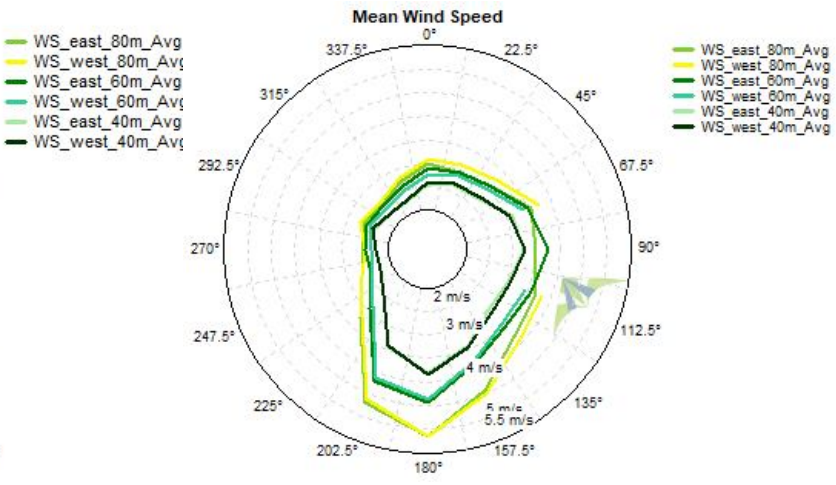
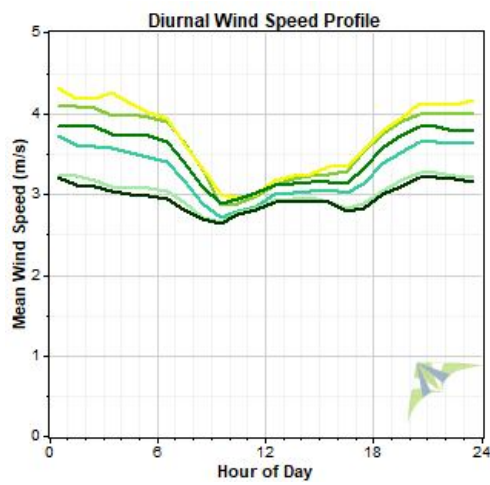
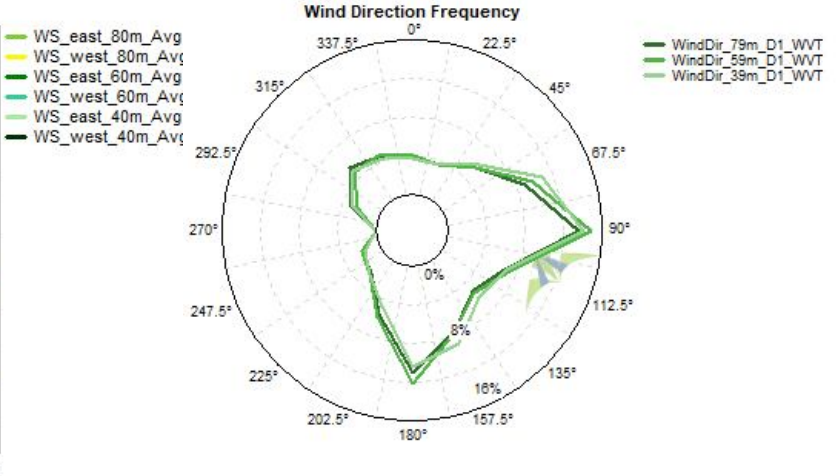
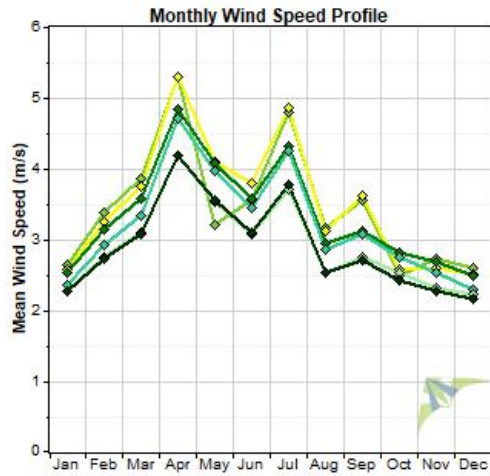
Data Set Properties

Report Created: 4/11/2018 10:14 using Windographer 3.3.10
 Filter Settings: <Unflagged data>

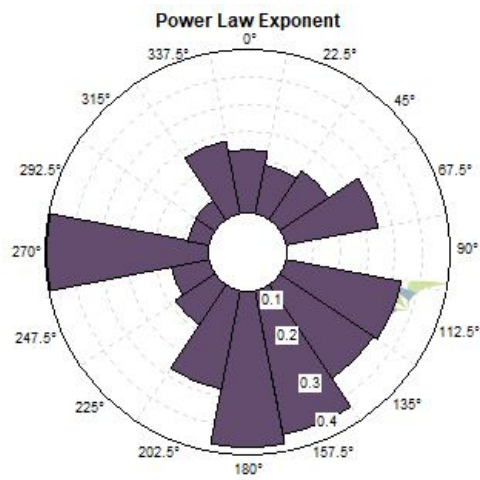
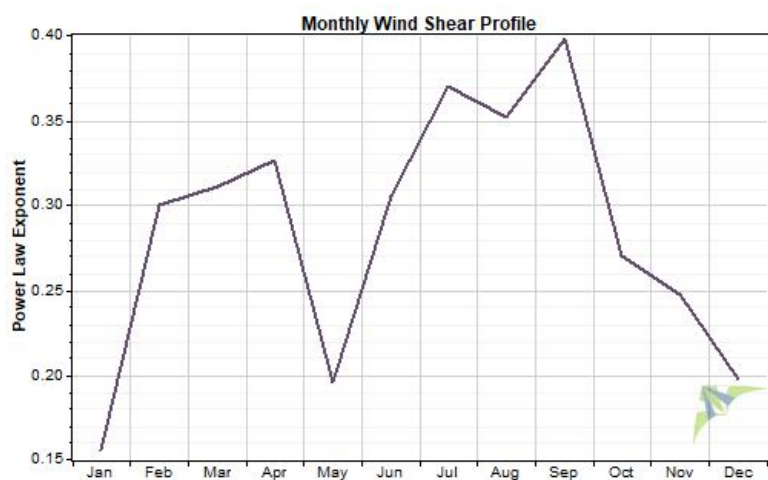
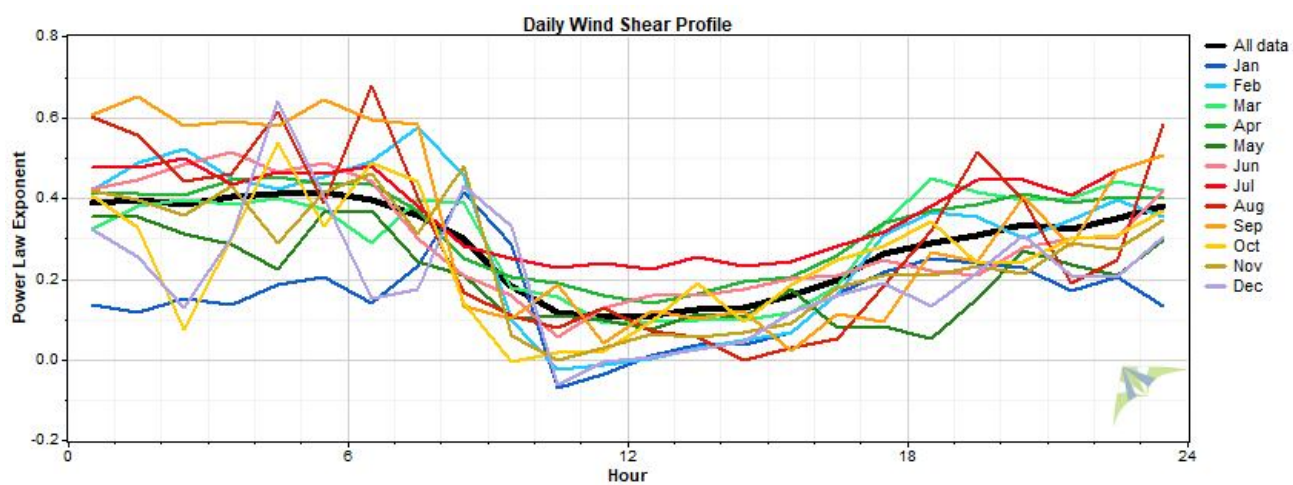
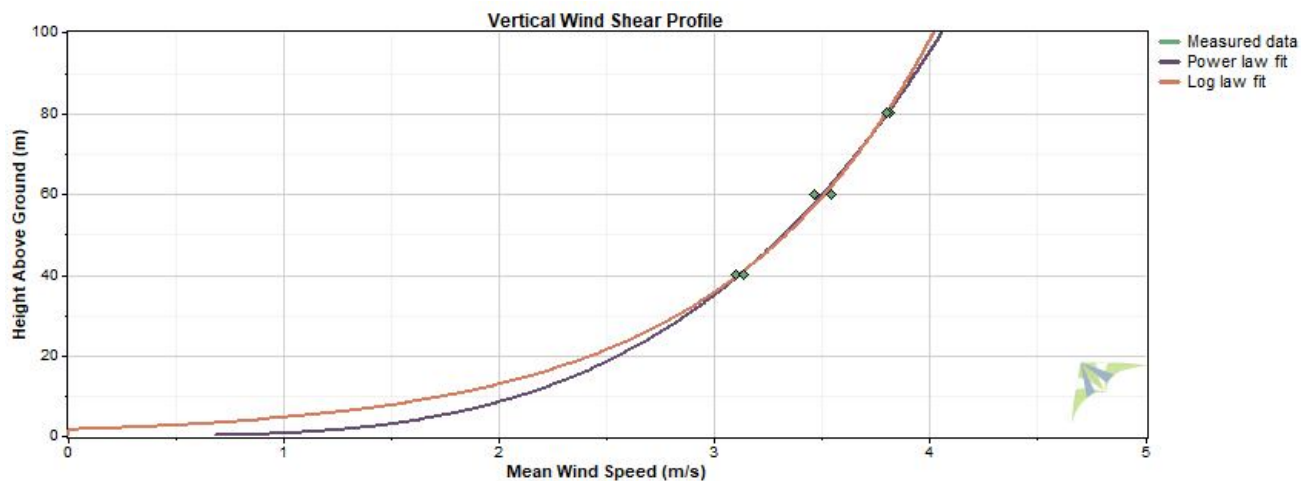
Variable	Value
Latitude	N 24.377780
Longitude	E 91.574620
Elevation	35 m
Start date	10/19/2015 16:50
End date	11/22/2017 10:10
Duration	25 months
Length of time step	10 minutes
Calm threshold	1 m/s
Mean temperature	25.3 °C
Mean pressure	997.4 mbar
Mean air density	1.175 kg/m ³
Power density at 50m	35 W/m ²
Wind power class	1
Power law exponent	0.288
Surface roughness	1.72 m
Roughness class	4.36



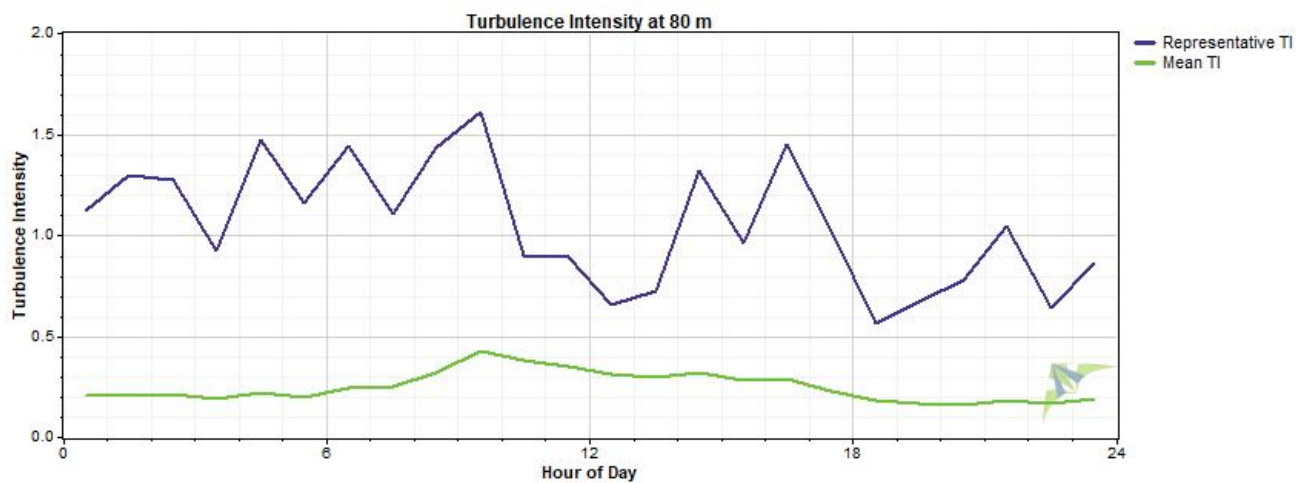
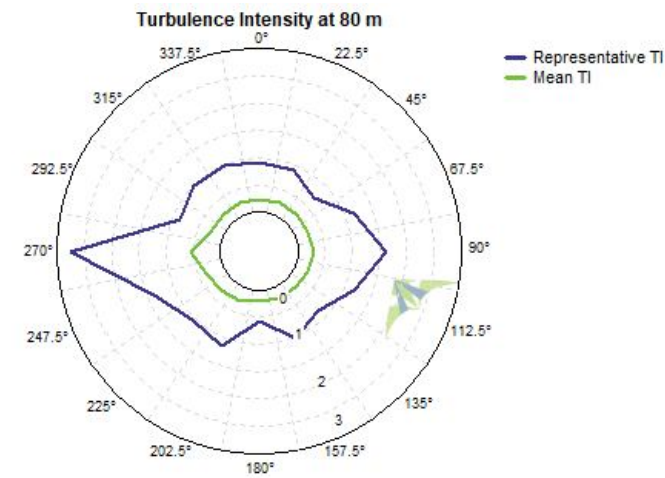
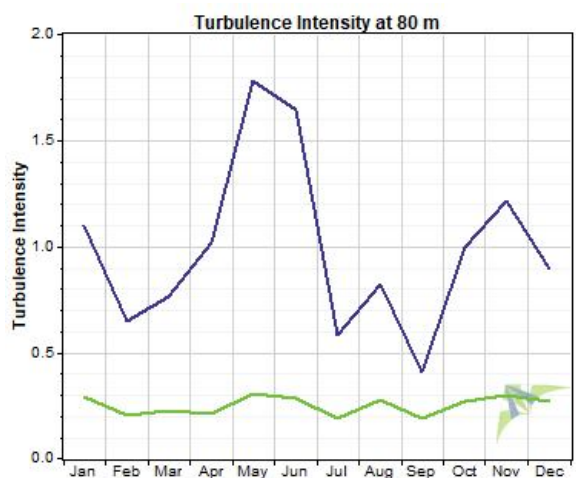
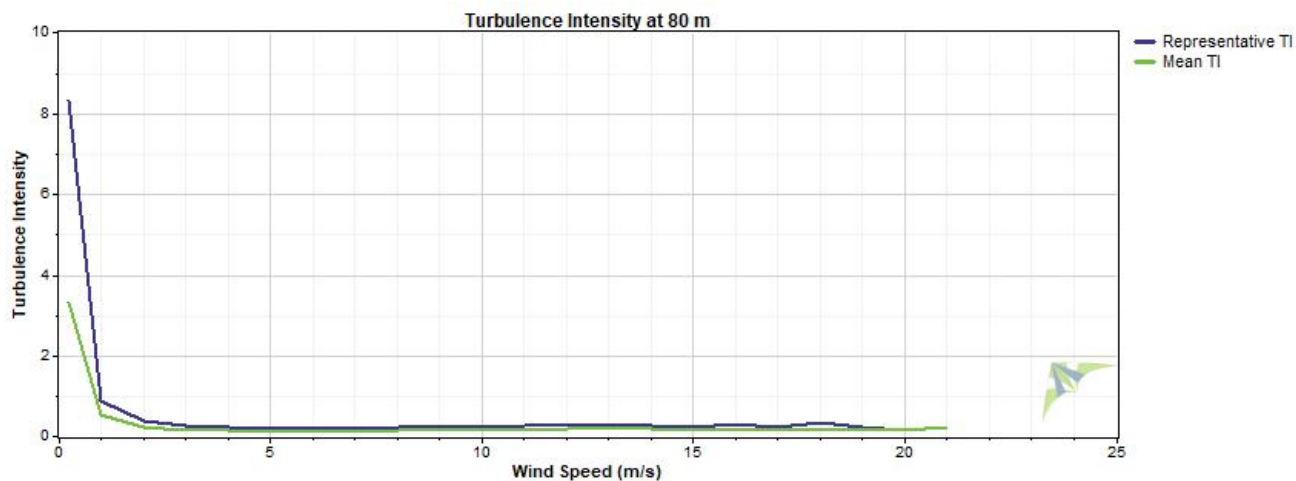
Wind Speed and Direction



Wind Shear



Turbulence Intensity



Data Column Properties

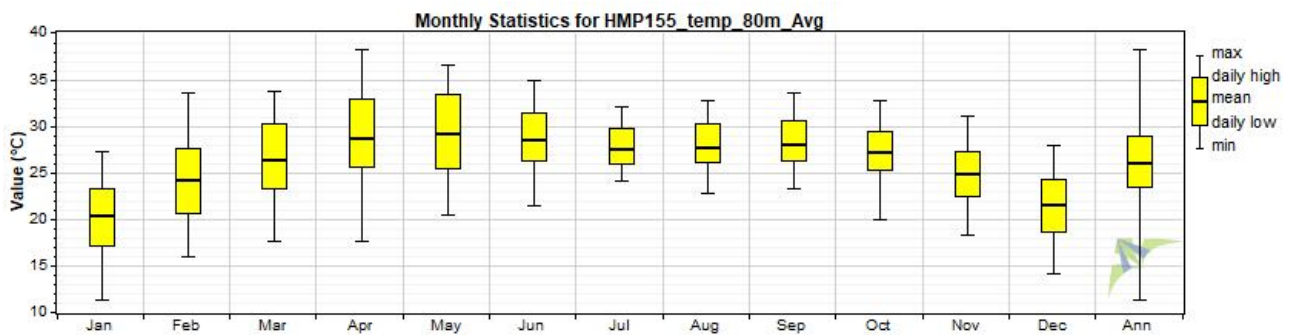
#	Label	Units	Height	Possible Data Points	Valid Data Points	Recovery Rate (%)	Mean	Min	Max	Std. Dev
1	RECORD	%		110,120	69,819	63.40	17,410	0	44,208	12,698
2	WS_east_80m_Avg	m/s	80 m	110,120	51,649	46.90	3.630	0.000	20.810	2.182
3	WS_east_80m_Max	m/s	80 m	110,120	51,649	46.90	4.991	0.000	34.000	2.891
4	WS_east_80m_Min	m/s	80 m	110,120	51,649	46.90	2.268	0.000	14.030	1.713
5	WS_east_80m_Std	m/s	80 m	110,120	51,649	46.90	0.572	0.000	7.954	0.377
6	WS_west_80m_Avg	m/s	80 m	110,120	45,830	41.62	3.700	0.000	20.980	2.186
7	WS_west_80m_Max	m/s	80 m	110,120	45,830	41.62	5.221	0.000	34.840	2.905
8	WS_west_80m_Min	m/s	80 m	110,120	45,830	41.62	2.143	0.000	12.550	1.716
9	WS_west_80m_Std	m/s	80 m	110,120	45,830	41.62	0.652	0.000	8.120	0.417
10	WS_east_60m_Avg	m/s	60 m	110,120	65,759	59.72	3.471	0.000	19.670	1.824
11	WS_east_60m_Max	m/s	60 m	110,120	65,759	59.72	4.920	0.000	34.020	2.535
12	WS_east_60m_Min	m/s	60 m	110,120	65,759	59.72	2.032	0.000	11.750	1.420
13	WS_east_60m_Std	m/s	60 m	110,120	65,759	59.72	0.604	0.000	7.544	0.352
14	WS_west_60m_Avg	m/s	60 m	110,120	57,070	51.83	3.289	0.000	19.360	1.850
15	WS_west_60m_Max	m/s	60 m	110,120	57,070	51.83	4.758	0.000	34.430	2.561
16	WS_west_60m_Min	m/s	60 m	110,120	57,070	51.83	1.844	0.000	10.960	1.435
17	WS_west_60m_Std	m/s	60 m	110,120	57,070	51.83	0.612	0.000	7.416	0.362
18	WS_east_40m_Avg	m/s	40 m	110,120	67,320	61.13	3.015	0.000	17.230	1.524
19	WS_east_40m_Max	m/s	40 m	110,120	67,320	61.13	4.526	0.000	33.290	2.333
20	WS_east_40m_Min	m/s	40 m	110,120	67,320	61.13	1.555	0.000	9.450	1.098
21	WS_east_40m_Std	m/s	40 m	110,120	67,320	61.13	0.617	0.000	7.676	0.344
22	WS_west_40m_Avg	m/s	40 m	110,120	54,879	49.84	2.968	0.000	17.130	1.549
23	WS_west_40m_Max	m/s	40 m	110,120	54,879	49.84	4.483	0.000	34.730	2.390
24	WS_west_40m_Min	m/s	40 m	110,120	54,879	49.84	1.523	0.000	9.450	1.102
25	WS_west_40m_Std	m/s	40 m	110,120	54,879	49.84	0.618	0.000	7.780	0.353
26	WindDir_79m_D1_WVT	°	79 m	110,120	69,641	63.24	123.2	0.0	360.0	96.2
27	WindDir_79m_SD1_WVT	°	79 m	110,120	69,695	63.29	8.5	0.0	78.8	9.0
28	WindDir_59m_D1_WVT	°	59 m	110,120	69,641	63.24	118.7	0.0	360.0	95.6
29	WindDir_59m_SD1_WVT	°	59 m	110,120	69,695	63.29	9.2	0.0	80.2	9.3
30	WindDir_39m_D1_WVT	°	39 m	110,120	67,417	61.22	113.5	0.0	360.0	94.9
31	WindDir_39m_SD1_WVT	°	39 m	110,120	67,471	61.27	10.3	0.0	79.3	9.5
32	RTD_temp_C_80m_Avg	°C	80 m	110,120	69,632	63.23	25.3	8.9	34.5	3.7
33	RTD_temp_C_80m_Max	°C	80 m	110,120	69,632	63.23	25.5	9.6	52.3	3.7
34	RTD_temp_C_80m_Min	°C	80 m	110,120	69,632	63.23	25.0	7.6	34.4	3.7
35	RTD_temp_C_80m_Std	°C	80 m	110,120	69,632	63.23	0.1	0.0	3.6	0.1
36	RTD_temp_C_4m_Avg	°C	4 m	110,120	69,554	63.16	24.6	7.9	35.9	4.8
37	RTD_temp_C_4m_Max	°C	4 m	110,120	69,554	63.16	24.8	8.0	36.3	4.8
38	RTD_temp_C_4m_Min	°C	4 m	110,120	69,554	63.16	24.3	7.9	35.6	4.7
39	RTD_temp_C_4m_Std	°C	4 m	110,120	69,554	63.16	0.1	0.0	2.4	0.1
40	HMP155_temp_80m_Avg	°C	80 m	110,120	69,673	63.27	25.2	8.9	34.4	3.7
41	HMP155_temp_80m_Max	°C	80 m	110,120	69,673	63.27	25.3	9.0	34.5	3.7
42	HMP155_temp_80m_Min	°C	80 m	110,120	69,673	63.27	25.1	8.5	34.4	3.7
43	HMP155_temp_80m_Std	°C	80 m	110,120	69,673	63.27	0.1	0.0	3.3	0.1
44	RH_80m_Avg	%		110,120	69,695	63.29	77.0	23.0	99.9	15.5
45	RH_80m_Max	%		110,120	69,695	63.29	78.3	24.0	100.0	15.1
46	RH_80m_Min	%		110,120	69,695	63.29	75.60	17.23	99.90	15.85
47	RH_80m_Std	%		110,120	69,695	63.29	0.74	0.01	14.99	0.80
48	HMP155_temp_4m_Avg	°C	4 m	110,120	69,654	63.25	24.5	7.8	35.5	4.7
49	HMP155_temp_4m_Max	°C	4 m	110,120	69,654	63.25	24.7	7.9	36.0	4.7
50	HMP155_temp_4m_Min	°C	4 m	110,120	69,654	63.25	24.3	7.7	35.3	4.7
51	HMP155_temp_4m_Std	°C	4 m	110,120	69,654	63.25	0.1	0.0	2.4	0.1
52	RH_4m_Avg	%		110,120	69,764	63.35	82.7	21.5	100.0	14.7

#	Label	Units	Height	Possible Data Points	Valid Data Points	Recovery Rate (%)	Mean	Min	Max	Std. Dev
53	RH_4m_Max	%		110,120	69,765	63.35	84.0	-29.9	100.0	14.0
54	RH_4m_Min	%		110,120	69,765	63.35	81.45	-54.29	99.90	15.35
55	RH_4m_Std	%		110,120	69,765	63.35	0.65	0.02	10.65	0.63
56	BP_80m_Avg	mbar	2 m	110,120	69,681	63.28	997.4	975.0	1,013.0	5.0
57	BP_80m_Max	mbar	2 m	110,120	69,681	63.28	997.6	976.0	1,013.0	5.0
58	BP_80m_Min	mbar	2 m	110,120	69,681	63.28	997.2	828.0	1,012.0	5.4
59	BP_80m_Std	mbar	2 m	110,120	69,681	63.28	0.1	0.0	44.9	0.3
60	BP_4m_Avg	mbar	2 m	110,120	69,695	63.29	1,005.4	986.0	1,018.0	5.1
61	BP_4m_Max	mbar	2 m	110,120	69,695	63.29	1,005.5	987.0	1,018.0	5.1
62	BP_4m_Min	mbar	2 m	110,120	69,695	63.29	1,005.3	834.0	1,018.0	5.2
63	BP_4m_Std	mbar	2 m	110,120	69,695	63.29	0.1	0.0	42.2	0.2
64	LWmV_Avg	Avg		110,120	69,765	63.35	229	-1,205	845	271
65	LWmV	Smp		110,120	69,765	63.35	229	-1,209	763	271
66	VBatt_Min	Volt		110,120	69,819	63.40	12.87	0.00	13.75	0.51
67	IBatt_Min	Amp		110,120	69,819	63.40	0.017	-0.482	1.273	0.323
68	ILoad_Min	m/s		110,120	69,819	63.40	0.215	0.000	0.550	0.087
69	V_in_chg_Min	m/s		110,120	69,819	63.40	8.70	0.00	20.44	8.54
70	I_in_chg_Min	°		110,120	69,819	63.40	0.199	-0.003	1.289	0.267
71	Chg_TmpC_Avg	°C	2 m	110,120	69,818	63.40	28.2	0.7	45.5	7.0
72	Chg_State	Smp		110,120	69,819	63.40	1.247	0.000	3.000	1.391
73	Ck_Batt	Smp		110,120	69,819	63.40	0	0	0	0
74	BattV_Min	Min		110,120	69,765	63.35	12.53	10.87	13.44	0.51
75	PTemp_C_Avg	°C	2 m	110,120	69,765	63.35	26.4	9.7	43.0	5.8
76	latitude_a	Smp		110,120	69,692	63.29	24	24	24	0
77	latitude_b	Smp		110,120	69,692	63.29	22.67	22.66	22.68	0.00
78	longitude_a	Smp		110,120	69,692	63.29	91	91	91	0
79	longitude_b	Smp		110,120	69,692	63.29	34.48	34.47	34.48	0.00
80	magnetic_variation	Smp		110,120	69,692	63.29	-0.5	-0.5	-0.5	0.0
81	fix_quality	Smp		110,120	69,819	63.40	1.996	0.000	2.000	0.085
82	nubr_satellites	Smp		110,120	69,819	63.40	9.09	0.00	12.00	0.96
83	altitude	Smp		110,120	69,692	63.29	32.70	14.20	51.10	3.84
84	max_clock_change	°	39 m	110,120	67,471	61.27	-44.9	-5,970.0	310.0	248.5
85	nubr_clock_change	Smp		110,120	69,819	63.40	0.604	0.000	4.000	1.161
86	Air Density	kg/m ³		110,120	110,120	100.00	1.175	1.106	1.231	0.031
87	WS_east_80m_Avg TI			110,120	49,106	44.59	0.25	0.03	23.67	0.67
88	WS_west_80m_Avg TI			110,120	44,813	40.69	0.29	0.03	20.25	0.66
89	WS_east_60m_Avg TI			110,120	64,971	59.00	0.25	0.03	20.50	0.53
90	WS_west_60m_Avg TI			110,120	55,968	50.82	0.33	0.03	23.00	0.82
91	WS_east_40m_Avg TI			110,120	66,825	60.68	0.29	0.04	20.00	0.62
92	WS_west_40m_Avg TI			110,120	54,369	49.37	0.30	0.04	21.00	0.62
93	WS_east_80m_Avg WPD	W/m ²		110,120	51,649	46.90	62	0	5,277	133
94	WS_west_80m_Avg WPD	W/m ²		110,120	45,830	41.62	65	0	5,407	143
95	WS_east_60m_Avg WPD	W/m ²		110,120	65,759	59.72	47	0	4,456	100
96	WS_west_60m_Avg WPD	W/m ²		110,120	57,070	51.83	43	0	4,249	96
97	WS_east_40m_Avg WPD	W/m ²		110,120	67,320	61.13	30	0	2,995	68
98	WS_west_40m_Avg WPD	W/m ²		110,120	54,879	49.84	30	0	2,943	70

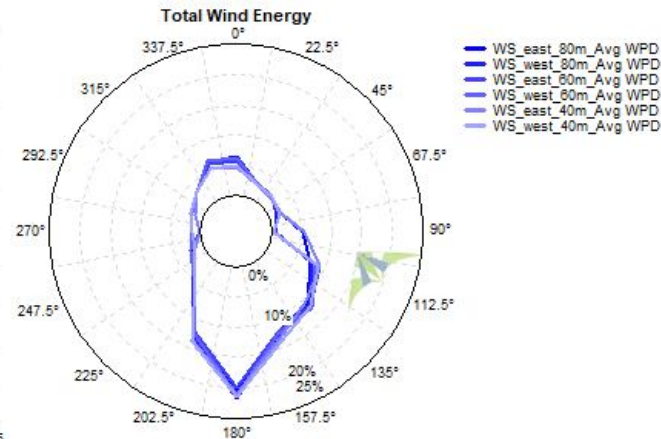
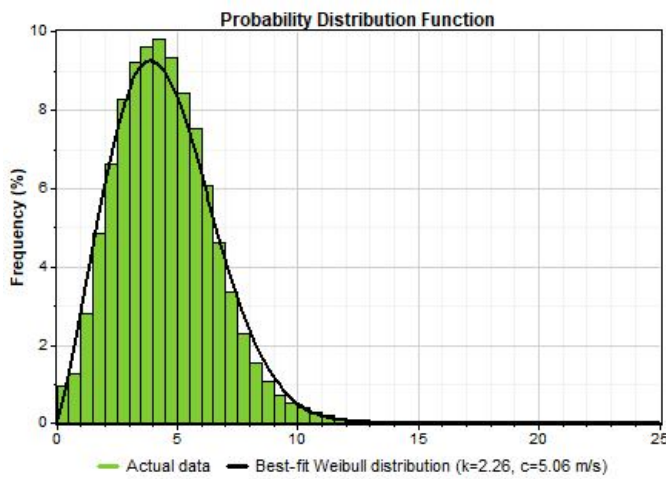
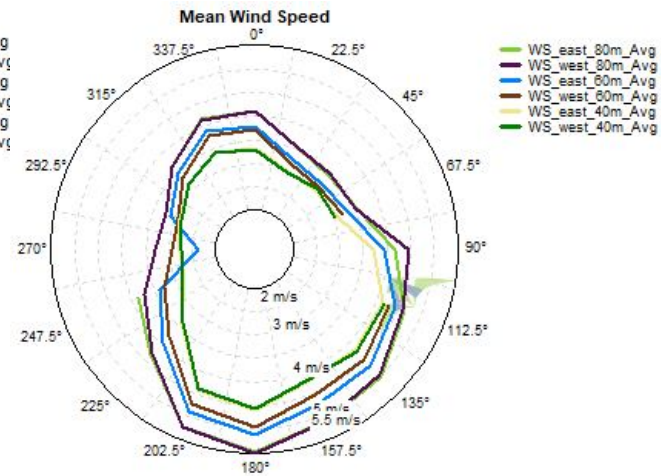
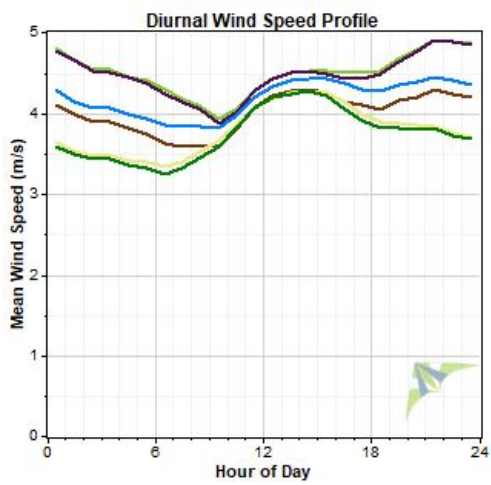
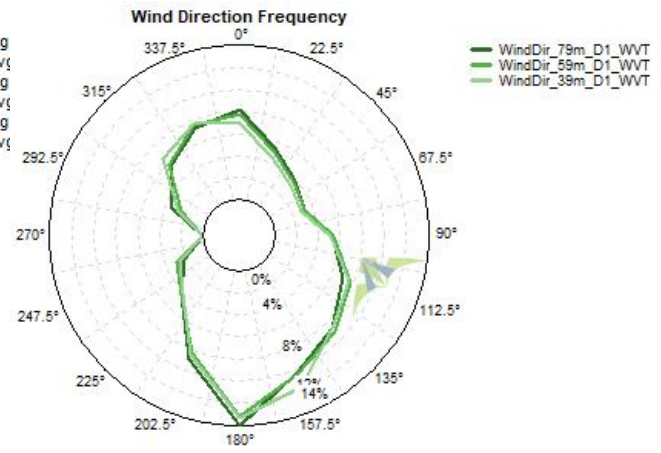
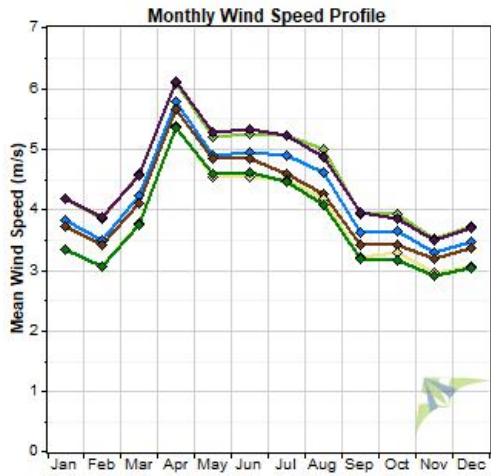
Data Set Properties

Report Created: 4/11/2018 10:16 using Windographer 3.3.10
 Filter Settings: <Unflagged data>

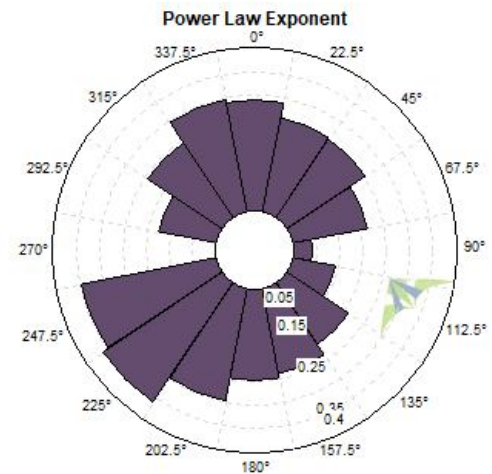
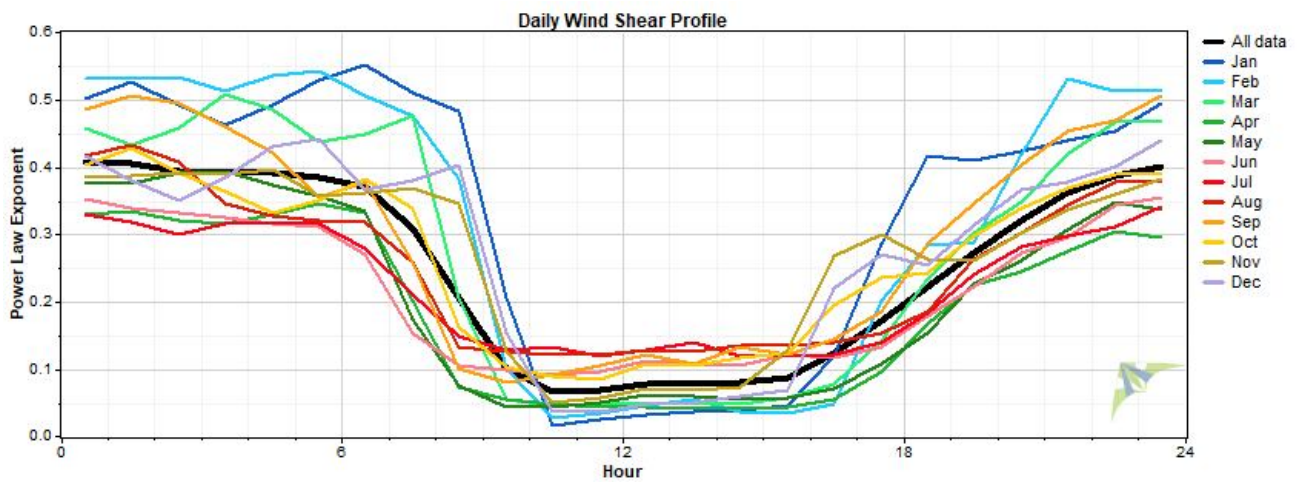
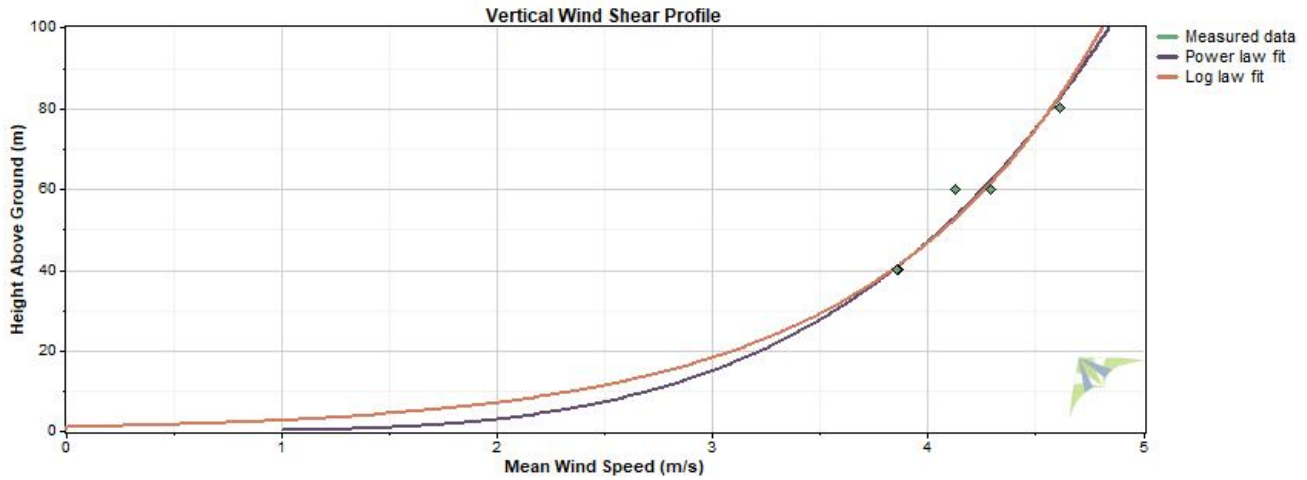
Variable	Value
Latitude	N 22.473420
Longitude	E 89.568260
Elevation	3.05 m
Start date	10/31/2015 13:20
End date	12/25/2017 10:50
Duration	26 months
Length of time step	10 minutes
Calm threshold	1 m/s
Mean temperature	26.1 °C
Mean pressure	1,000 mbar
Mean air density	1.165 kg/m ³
Power density at 50m	67 W/m ²
Wind power class	1
Power law exponent	0.253
Surface roughness	1.1 m
Roughness class	3.99



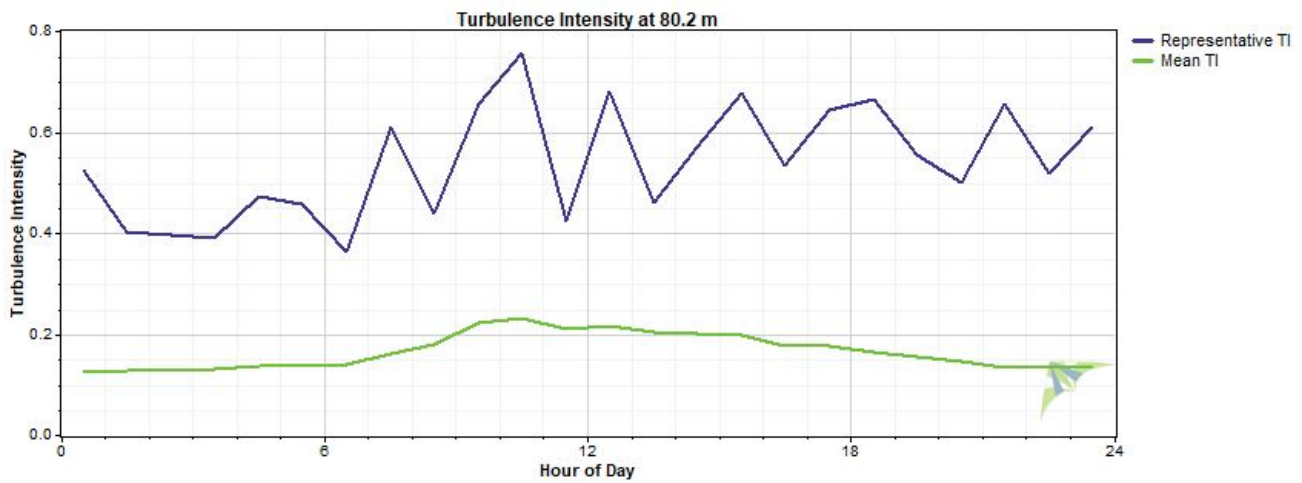
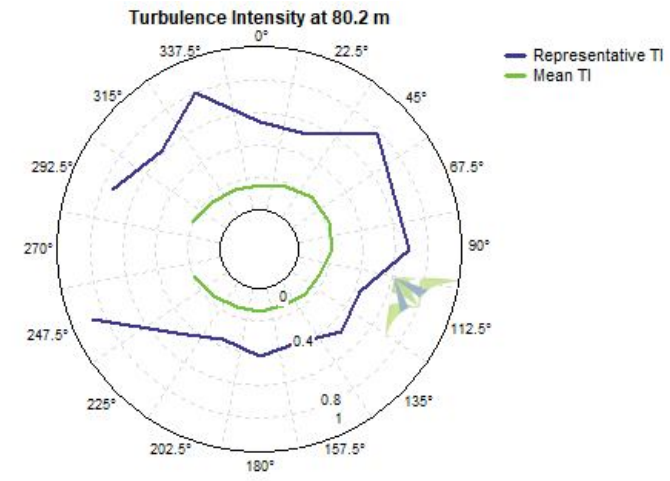
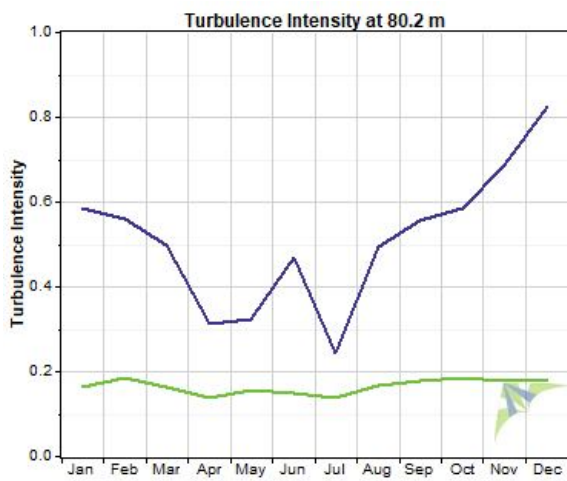
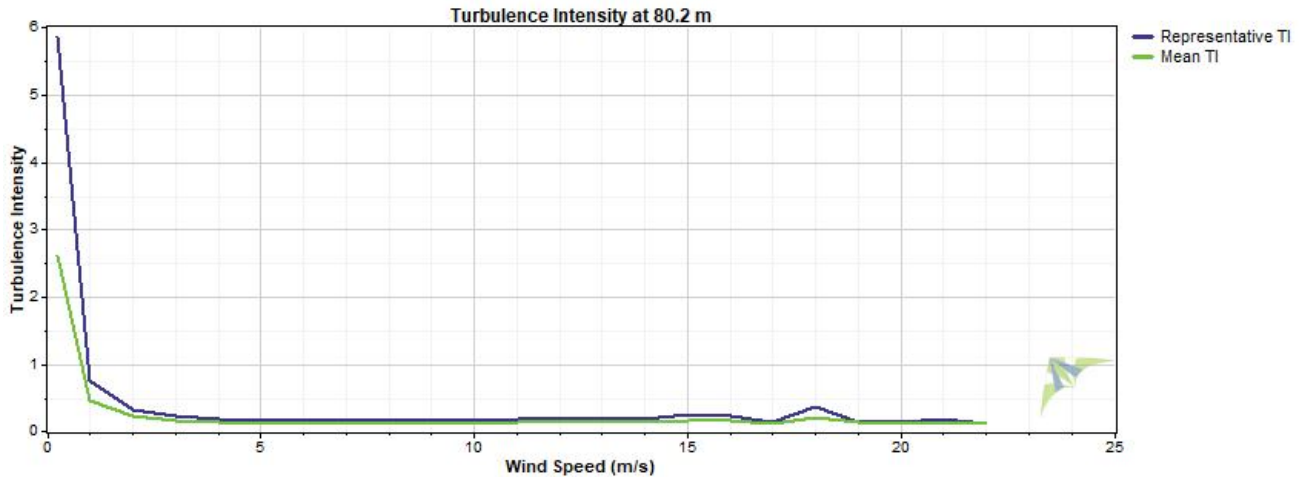
Wind Speed and Direction



Wind Shear



Turbulence Intensity



Data Column Properties

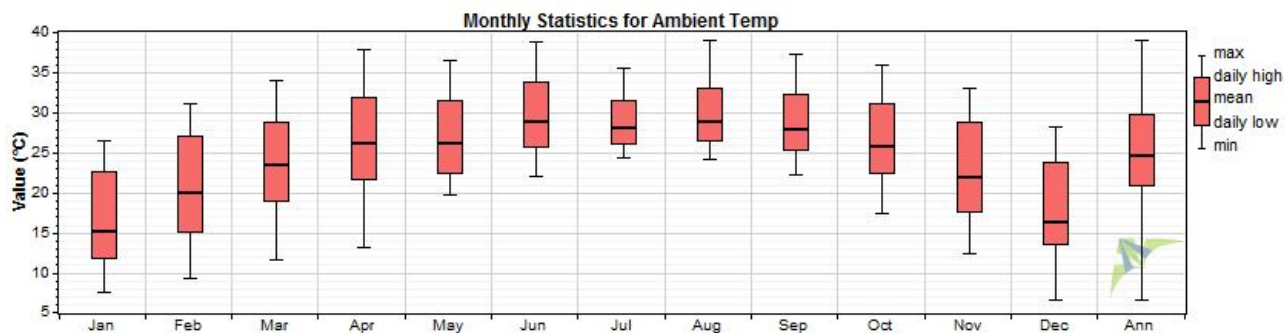
#	Label	Units	Height	Possible Data Points	Valid Data Points	Recovery Rate (%)	Mean	Min	Max	Std. Dev
1	RECORD	m/s		113,169	111,576	98.59	50.232	0	105.680	31.681
2	WS_east_80m_Avg	m/s	80.2 m	113,169	107,141	94.67	4.494	0.000	23.920	2.069
3	WS_east_80m_Max	m/s	80.2 m	113,169	107,141	94.67	5.891	0.000	40.280	2.615
4	WS_east_80m_Min	m/s	80.2 m	113,169	107,141	94.67	3.097	0.000	15.640	1.702
5	WS_east_80m_Std	m/s	80.2 m	113,169	107,141	94.67	0.575	0.000	7.920	0.280
6	WS_west_80m_Avg	m/s	80.2 m	113,169	104,972	92.76	4.470	0.000	24.000	2.062
7	WS_west_80m_Max	m/s	80.2 m	113,169	104,972	92.76	5.847	0.000	39.500	2.604
8	WS_west_80m_Min	m/s	80.2 m	113,169	104,972	92.76	3.096	0.000	15.630	1.705
9	WS_west_80m_Std	m/s	80.2 m	113,169	104,972	92.76	0.568	0.000	7.912	0.281
10	WS_east_60m_Avg	m/s	60 m	113,169	106,845	94.41	4.186	0.000	23.050	1.956
11	WS_east_60m_Max	m/s	60 m	113,169	106,845	94.41	5.612	0.000	39.640	2.564
12	WS_east_60m_Min	m/s	60 m	113,169	106,845	94.41	2.785	0.000	14.910	1.542
13	WS_east_60m_Std	m/s	60 m	113,169	106,845	94.41	0.581	0.000	8.110	0.280
14	WS_west_60m_Avg	m/s	60 m	113,169	103,243	91.23	4.009	0.000	22.370	1.955
15	WS_west_60m_Max	m/s	60 m	113,169	103,243	91.23	5.419	0.000	36.900	2.531
16	WS_west_60m_Min	m/s	60 m	113,169	103,243	91.23	2.610	0.000	14.040	1.581
17	WS_west_60m_Std	m/s	60 m	113,169	103,243	91.23	0.579	0.000	7.878	0.283
18	WS_east_40m_Avg	m/s	40 m	113,169	106,770	94.35	3.781	0.000	21.690	1.843
19	WS_east_40m_Max	m/s	40 m	113,169	106,770	94.35	5.224	0.000	40.280	2.507
20	WS_east_40m_Min	m/s	40 m	113,169	106,770	94.35	2.393	0.000	14.870	1.387
21	WS_east_40m_Std	m/s	40 m	113,169	106,770	94.35	0.583	0.000	8.020	0.279
22	WS_west_40m_Avg	m/s	40 m	113,169	104,313	92.17	3.734	0.000	21.680	1.840
23	WS_west_40m_Max	m/s	40 m	113,169	104,313	92.17	5.165	0.000	38.970	2.510
24	WS_west_40m_Min	m/s	40 m	113,169	104,313	92.17	2.364	0.000	14.170	1.386
25	WS_west_40m_Std	m/s	40 m	113,169	104,313	92.17	0.579	0.000	8.100	0.282
26	WindDir_79m_D1_WVT	°	78 m	113,169	111,576	98.59	155.8	0.0	360.0	98.6
27	WindDir_79m_SD1_WVT	°	78 m	113,169	111,576	98.59	6.3	0.0	79.2	6.2
28	WindDir_59m_D1_WVT	°	57.9 m	113,169	111,576	98.59	152.8	0.0	360.0	98.5
29	WindDir_59m_SD1_WVT	°	57.9 m	113,169	111,576	98.59	6.5	0.0	79.2	6.3
30	WindDir_39m_D1_WVT	°	37.9 m	113,169	111,576	98.59	154.4	0.0	360.0	97.0
31	WindDir_39m_SD1_WVT	°	37.9 m	113,169	111,576	98.59	6.9	0.0	78.4	6.5
32	RTD_temp_C_80m_Avg	°C	78.4 m	113,169	111,575	98.59	26.2	11.7	38.3	3.6
33	RTD_temp_C_80m_Max	°C	78.4 m	113,169	111,575	98.59	26.4	11.8	38.7	3.6
34	RTD_temp_C_80m_Min	°C	78.4 m	113,169	111,575	98.59	26.0	11.1	38.0	3.6
35	RTD_temp_C_80m_Std	°C	78.4 m	113,169	111,575	98.59	0.1	0.0	4.1	0.1
36	RTD_temp_C_4m_Avg	°C	3.3 m	113,169	96,308	85.10	25.6	7.2	39.2	5.2
37	RTD_temp_C_4m_Max	°C	3.3 m	113,169	96,308	85.10	25.8	7.4	39.8	5.2
38	RTD_temp_C_4m_Min	°C	3.3 m	113,169	96,308	85.10	25.4	7.0	39.0	5.2
39	RTD_temp_C_4m_Std	°C	3.3 m	113,169	96,308	85.10	0.1	0.0	3.6	0.1
40	HMP155_temp_80m_Avg	°C	79.2 m	113,169	111,521	98.54	26.1	11.4	38.2	3.6
41	HMP155_temp_80m_Max	°C	79.2 m	113,169	111,521	98.54	26.2	11.4	38.7	3.6
42	HMP155_temp_80m_Min	°C	79.2 m	113,169	111,521	98.54	26.0	11.3	37.8	3.6
43	HMP155_temp_80m_Std	°C	79.2 m	113,169	111,521	98.54	0.1	0.0	3.8	0.1
44	RH_80m_Avg	%		113,169	111,576	98.59	76.2	17.2	99.9	16.9
45	RH_80m_Max	%		113,169	111,576	98.59	77.5	17.6	100.0	16.5
46	RH_80m_Min	%		113,169	111,576	98.59	74.99	15.65	99.90	17.37
47	RH_80m_Std	%		113,169	111,576	98.59	0.65	0.03	16.50	0.70
48	HMP155_temp_4m_Avg	°C	4.1 m	113,169	111,459	98.49	25.5	7.9	39.1	5.1
49	HMP155_temp_4m_Max	°C	4.1 m	113,169	111,459	98.49	25.6	8.1	39.5	5.1
50	HMP155_temp_4m_Min	°C	4.1 m	113,169	111,459	98.49	25.3	7.7	38.9	5.1
51	HMP155_temp_4m_Std	°C	4.1 m	113,169	111,459	98.49	0.1	0.0	3.4	0.1
52	RH_4m_Avg	Avg		113,169	111,576	98.59	84.0	19.0	100.0	15.6

#	Label	Units	Height	Possible Data Points	Valid Data Points	Recovery Rate (%)	Mean	Min	Max	Std. Dev
53	RH_4m_Max	Max		113,169	111,576	98.59	85.4	21.4	100.0	14.7
54	RH_4m_Min	Min		113,169	111,576	98.59	82.76	16.34	99.90	16.40
55	RH_4m_Std	Std		113,169	111,576	98.59	0.64	0.02	10.65	0.67
56	BP_80m_Avg	mbar	78.7 m	113,169	111,576	98.59	1,000.4	978.0	1,015.0	5.6
57	BP_80m_Max	mbar	78.7 m	113,169	111,576	98.59	1,000.5	978.0	1,016.0	5.6
58	BP_80m_Min	mbar	78.7 m	113,169	111,576	98.59	1,000.2	804.0	1,014.0	5.8
59	BP_80m_Std	mbar	78.7 m	113,169	111,576	98.59	0.1	0.0	12.2	0.1
60	BP_4m_Avg	mbar	3.9 m	113,169	111,576	98.59	1,008.1	986.0	1,022.0	5.7
61	BP_4m_Max	mbar	3.9 m	113,169	111,576	98.59	1,008.2	986.0	1,022.0	5.7
62	BP_4m_Min	mbar	3.9 m	113,169	111,576	98.59	1,007.9	985.0	1,022.0	5.7
63	BP_4m_Std	mbar	3.9 m	113,169	111,576	98.59	0.0	0.0	1.1	0.0
64	LWmV_Avg	Avg		113,169	111,576	98.59	290.1	151.0	910.0	69.3
65	LWmV	Smp		113,169	111,576	98.59	290.1	150.6	966.0	70.1
66	VBatt_Min	°C		113,169	111,576	98.59	12.80	0.00	13.73	0.47
67	IBatt_Min	°C		113,169	111,576	98.59	0.000	-0.376	1.935	0.380
68	ILoad_Min	m/s		113,169	111,576	98.59	0.282	0.000	0.330	0.010
69	V_in_chg_Min	m/s		113,169	111,576	98.59	8.40	0.00	20.15	8.33
70	I_in_chg_Min	kW		113,169	111,576	98.59	0.249	-0.004	1.884	0.310
71	Chg_TmpC_Avg	m/s		113,169	111,576	98.59	29.93	8.62	47.51	7.39
72	Chg_State	m/s		113,169	111,576	98.59	1.194	0.000	3.000	1.367
73	Ck_Batt	Smp		113,169	111,576	98.59	0	0	0	0
74	BattV_Min	°C		113,169	111,576	98.59	12.44	11.12	13.41	0.49
75	PTemp_C_Avg	m/s		113,169	111,576	98.59	27.31	8.27	42.52	5.83
76	latitude_a	Smp		113,169	111,576	98.59	22	22	22	0
77	latitude_b	m/s		113,169	111,576	98.59	28.40	28.40	28.41	0.00
78	longitude_a	Smp		113,169	111,576	98.59	89	89	89	0
79	longitude_b	m/s		113,169	111,576	98.59	34.10	34.09	34.10	0.00
80	magnetic_variation	Smp		113,169	111,576	98.59	-0.6	-0.6	-0.6	0.0
81	fix_quality	Smp		113,169	111,576	98.59	2	2	2	0
82	nubr_satellites	m/s		113,169	111,576	98.59	9.29	6.00	12.00	0.87
83	altitude	m/s		113,169	111,576	98.59	5.05	-51.30	24.70	4.26
84	max_clock_change	m/s		113,169	111,576	98.59	-528	-1,000	980	486
85	nubr_clock_change	Smp		113,169	111,576	98.59	1.855	0.000	6.000	1.731
86	Air Density	kg/m ³		113,169	113,169	100.00	1.165	1.110	1.238	0.020
87	WS_east_80m_Avg TI			113,169	106,844	94.41	0.17	0.02	20.50	0.30
88	WS_west_80m_Avg TI			113,169	104,642	92.47	0.17	0.02	20.50	0.30
89	WS_east_60m_Avg TI			113,169	106,525	94.13	0.18	0.03	19.00	0.28
90	WS_west_60m_Avg TI			113,169	102,227	90.33	0.21	0.03	22.00	0.49
91	WS_east_40m_Avg TI			113,169	106,273	93.91	0.20	0.03	20.50	0.36
92	WS_west_40m_Avg TI			113,169	103,755	91.68	0.20	0.03	20.50	0.40
93	WS_east_80m_Avg WPD	W/m ²		113,169	107,141	94.67	90	0	8,018	154
94	WS_west_80m_Avg WPD	W/m ²		113,169	104,972	92.76	89	0	8,098	150
95	WS_east_60m_Avg WPD	W/m ²		113,169	106,845	94.41	74	0	7,174	133
96	WS_west_60m_Avg WPD	W/m ²		113,169	103,243	91.23	67	0	6,558	123
97	WS_east_40m_Avg WPD	W/m ²		113,169	106,770	94.35	57	0	5,978	111
98	WS_west_40m_Avg WPD	W/m ²		113,169	104,313	92.17	56	0	5,969	110

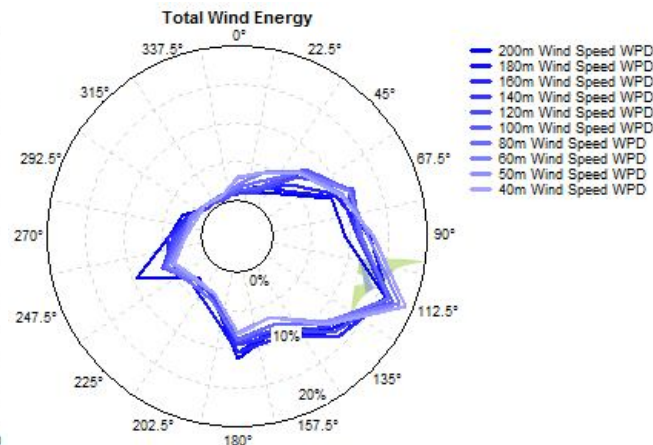
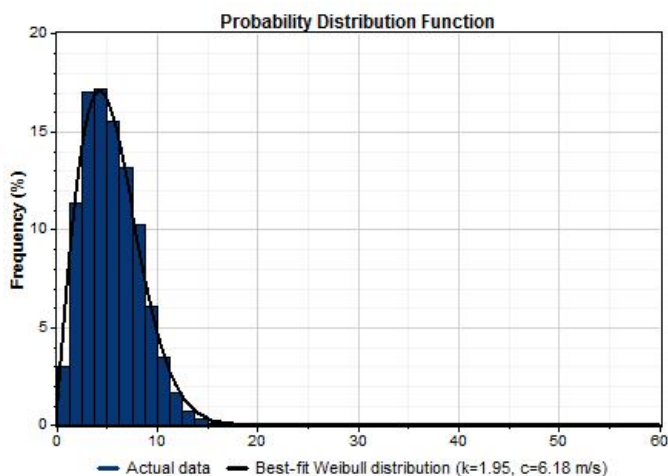
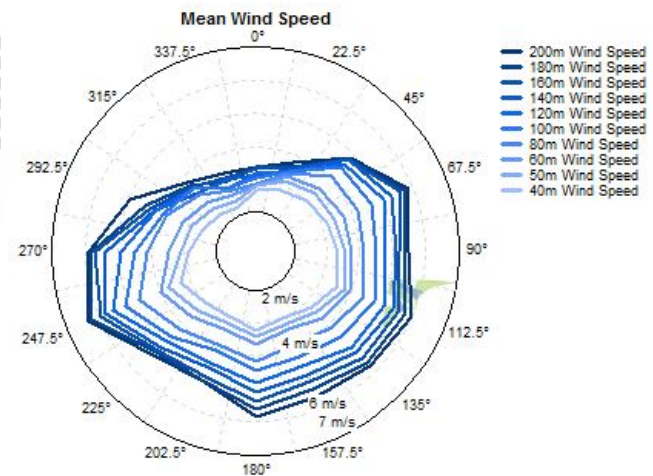
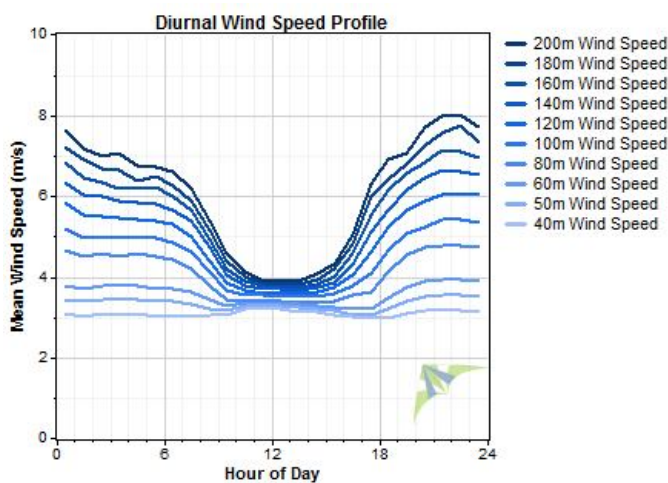
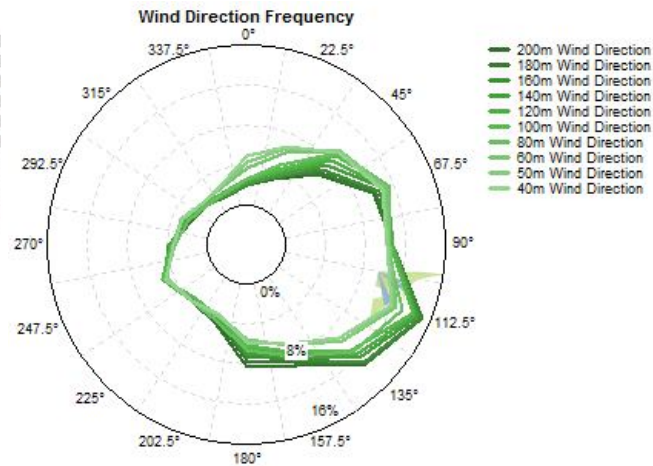
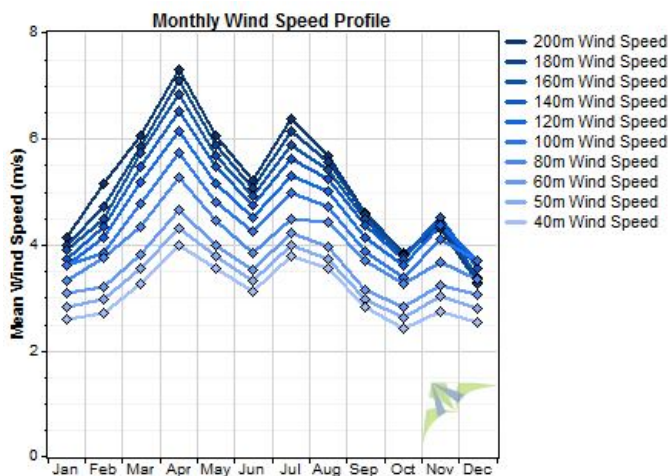
Data Set Properties

Report Created: 7/14/2017 16:14 using Windographer 3.3.10
 Filter Settings: <Unflagged data>

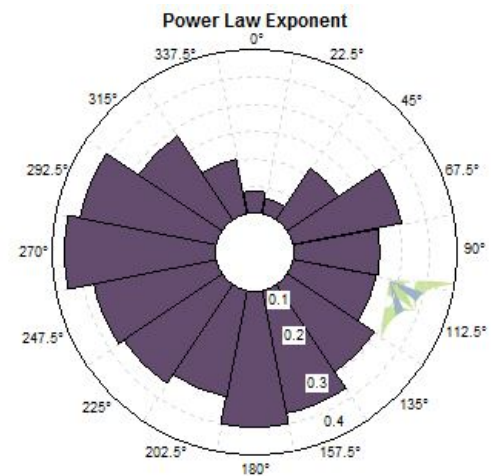
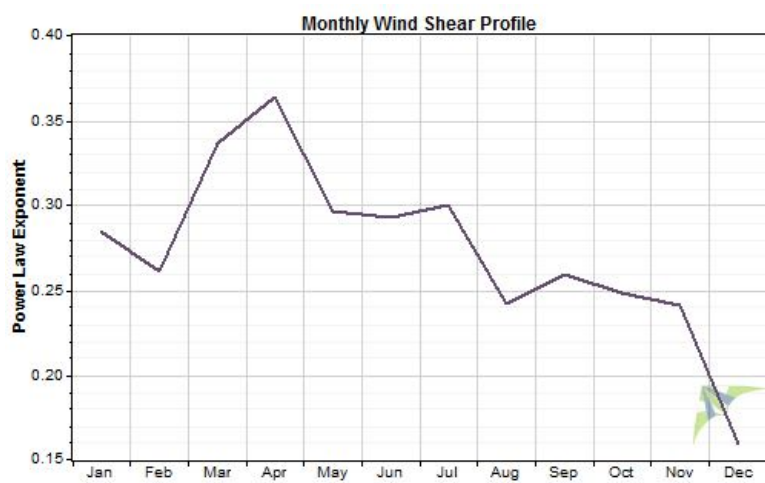
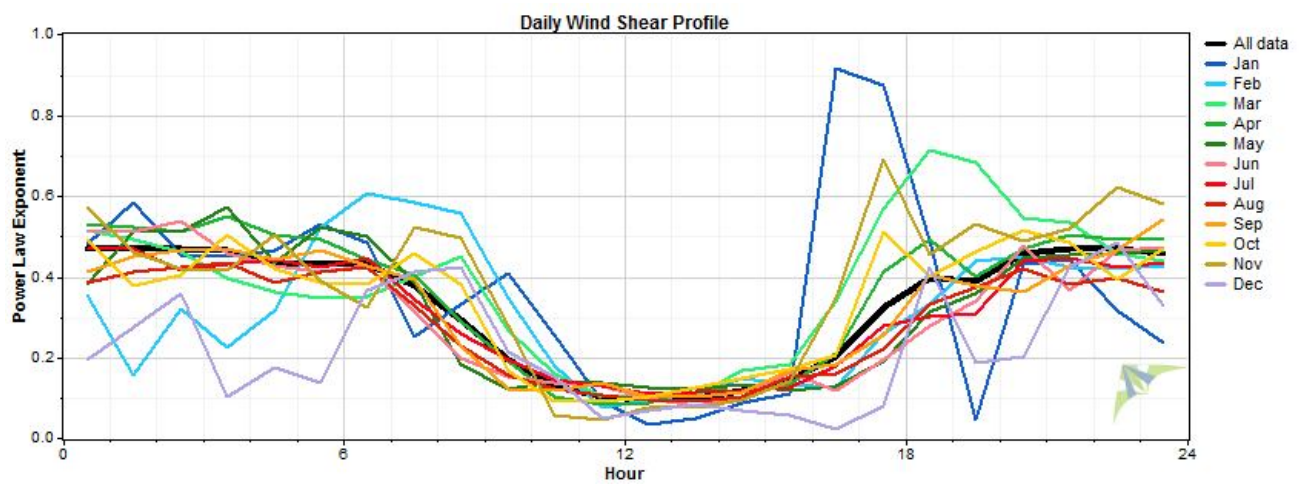
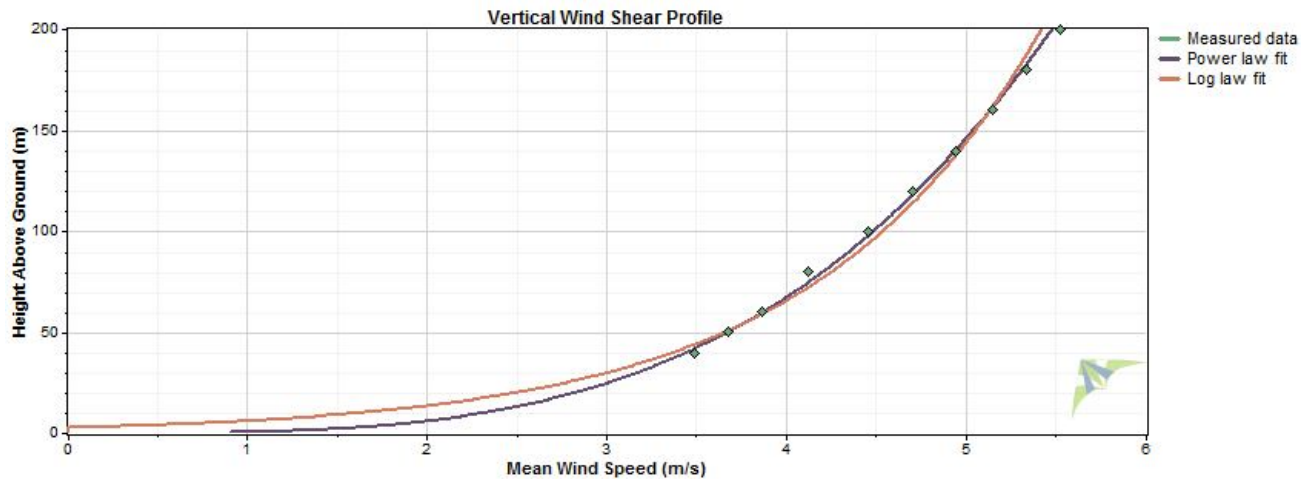
Variable	Value
Latitude	N 25° 36' 22.968"
Longitude	E 89° 4' 7.752"
Elevation	32 m
Start date	8/4/2015 19:10
End date	4/19/2017 06:10
Duration	20 months
Length of time step	10 minutes
Calm threshold	0 m/s
Mean temperature	24.7 °C
Mean pressure	1,590 mbar
Mean air density	1.688 kg/m ³
Power density at 50m	58 W/m ²
Wind power class	1
Power law exponent	0.289
Surface roughness	2.87 m
Roughness class	4.79



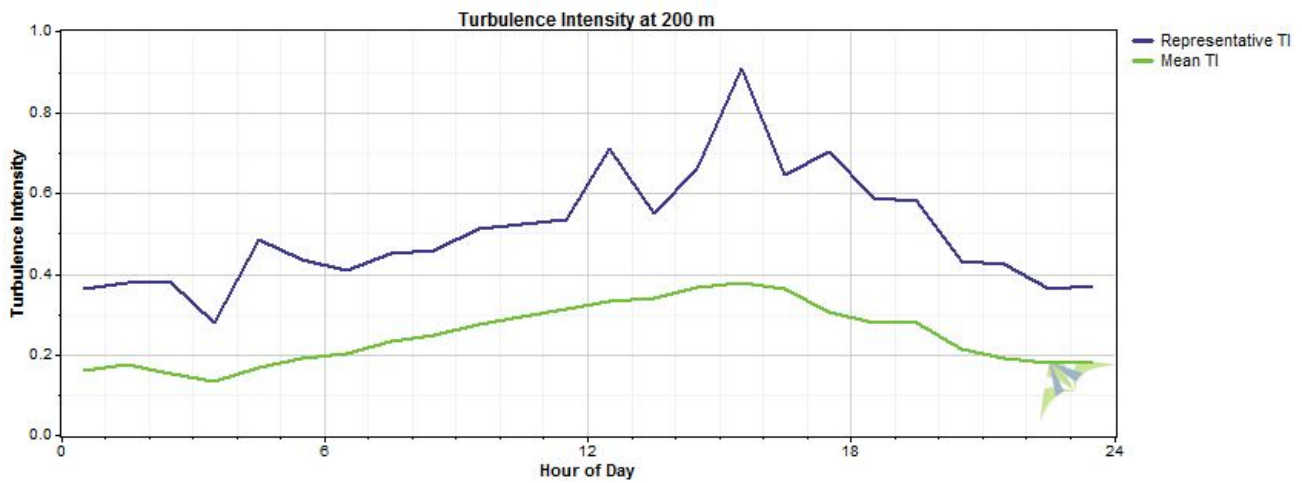
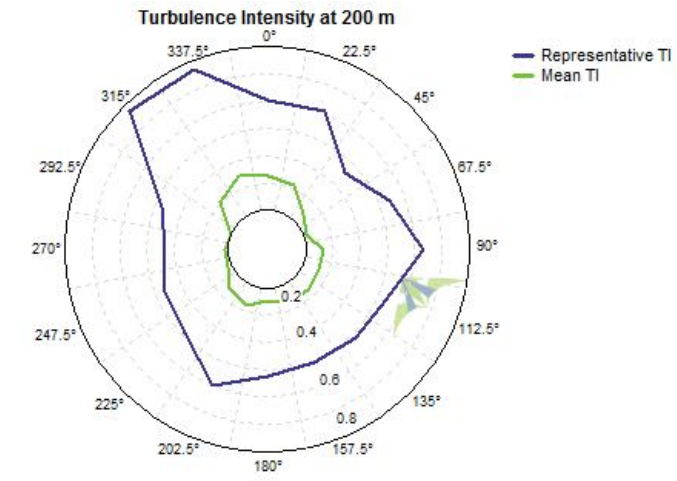
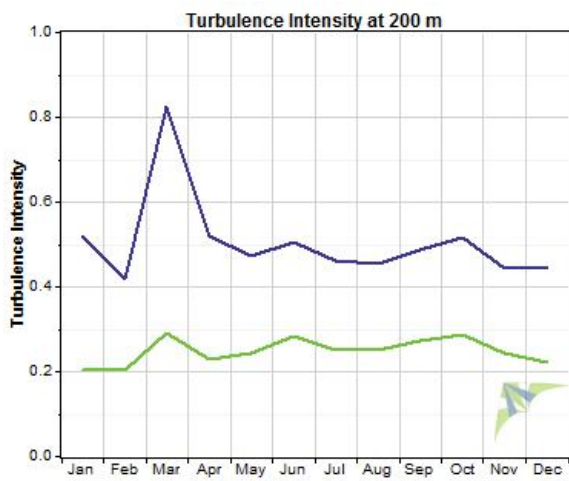
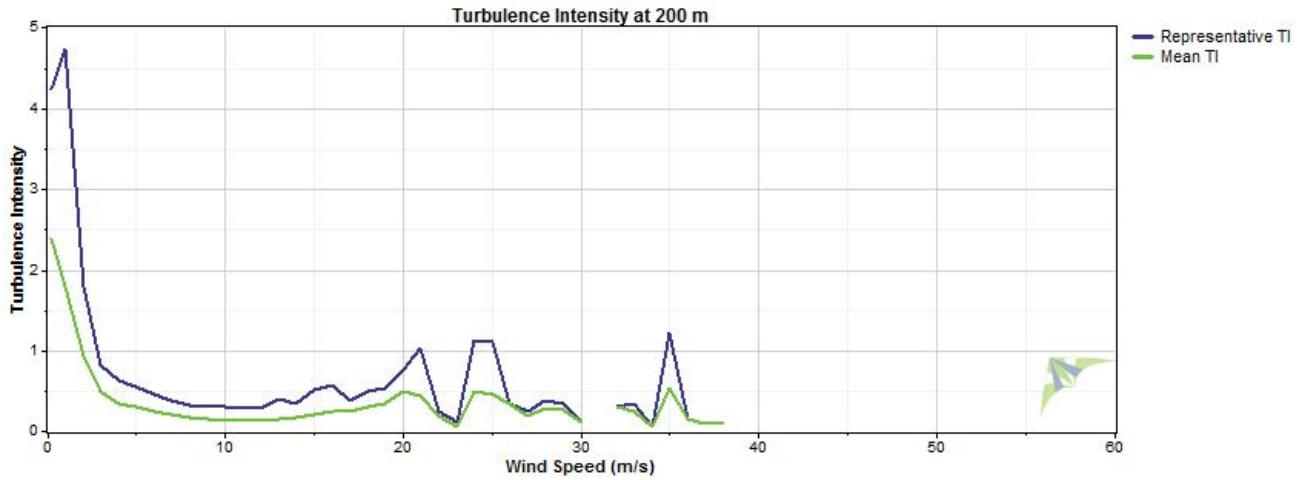
Wind Speed and Direction



Wind Shear



Turbulence Intensity



Data Column Properties

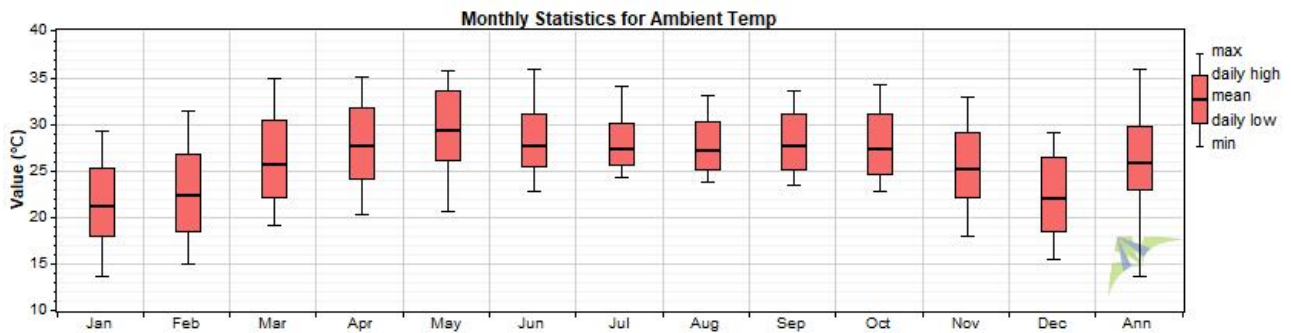
#	Label	Units	Height	Possible Data Points	Valid Data Points	Recovery Rate (%)	Mean	Min	Max	Std. Dev
1	40m Wind Direction	°	40 m	89,778	64,338	71.66	101.4	0.0	360.0	92.0
2	40m Wind Speed	m/s	40 m	89,778	64,338	71.66	3.09	0.01	15.19	1.41
3	40m Wind Vert	m/s	40 m	89,778	64,338	71.66	-0.20	-9.36	0.50	0.94
4	Quality (Station Height 40m)	%		89,778	64,469	71.81	97.3	31.0	100.0	1.6
5	50m Wind Direction	°	50 m	89,778	63,385	70.60	101.5	0.0	360.0	90.9
6	50m Wind Speed	m/s	50 m	89,778	63,385	70.60	3.33	0.02	15.42	1.52
7	50m Wind Vert	m/s	50 m	89,778	63,385	70.60	-0.20	-9.33	0.50	0.94
8	Quality (Station Height 50m)	%		89,778	63,632	70.88	97.3	22.0	100.0	1.9
9	60m Wind Direction	°	60 m	89,778	61,846	68.89	102.9	0.1	360.0	89.6
10	60m Wind Speed	m/s	60 m	89,778	61,846	68.89	3.56	0.02	16.39	1.63
11	60m Wind Vert	m/s	60 m	89,778	61,846	68.89	-0.21	-9.32	0.50	0.94
12	Quality (Station Height 60m)	%		89,778	62,210	69.29	97.3	19.0	100.0	2.1
13	80m Wind Direction	°	80 m	89,778	53,356	59.43	114.5	0.0	360.0	82.6
14	80m Wind Speed	m/s	80 m	89,778	53,356	59.43	4.04	0.02	19.70	1.87
15	80m Wind Vert	m/s	80 m	89,778	53,356	59.43	-0.25	-9.36	0.50	0.94
16	Quality (Station Height 80m)	%		89,778	53,927	60.07	96.7	0.0	100.0	4.4
17	100m Wind Direction	°	100 m	89,778	52,660	58.66	113.0	0.0	360.0	83.9
18	100m Wind Speed	m/s	100 m	89,778	52,660	58.66	4.38	0.01	30.41	2.07
19	100m Wind Vert	m/s	100 m	89,778	52,660	58.66	-0.23	-9.33	0.50	0.89
20	Quality (Station Height 100m)	%		89,778	53,476	59.56	96.8	0.0	100.0	4.1
21	120m Wind Direction	°	120 m	89,778	47,792	53.23	117.2	0.0	360.0	81.9
22	120m Wind Speed	m/s	120 m	89,778	47,792	53.23	4.70	0.03	27.96	2.25
23	120m Wind Vert	m/s	120 m	89,778	47,792	53.23	-0.23	-9.33	0.50	0.84
24	Quality (Station Height 120m)	%		89,778	48,812	54.37	96.4	0.0	100.0	5.3
25	140m Wind Direction	°	140 m	89,778	43,048	47.95	120.4	0.0	360.0	80.3
26	140m Wind Speed	m/s	140 m	89,778	43,048	47.95	4.95	0.05	45.08	2.46
27	140m Wind Vert	m/s	140 m	89,778	43,048	47.95	-0.22	-9.35	0.50	0.76
28	Quality (Station Height 140m)	%		89,778	44,241	49.28	96.0	0.0	100.0	6.3
29	160m Wind Direction	°	160 m	89,778	38,563	42.95	123.1	0.0	360.0	79.5
30	160m Wind Speed	m/s	160 m	89,778	38,563	42.95	5.15	0.04	40.06	2.64
31	160m Wind Vert	m/s	160 m	89,778	38,563	42.95	-0.21	-9.33	0.50	0.67
32	Quality (Station Height 160m)	%		89,778	39,843	44.38	95.5	0.0	100.0	7.3
33	180m Wind Direction	°	180 m	89,778	34,105	37.99	125.5	0.0	360.0	78.2
34	180m Wind Speed	m/s	180 m	89,778	34,105	37.99	5.32	0.04	54.53	2.79
35	180m Wind Vert	m/s	180 m	89,778	34,105	37.99	-0.20	-9.31	0.50	0.58
36	Quality (Station Height 180m)	%		89,778	35,492	39.53	94.9	0.0	100.0	8.2
37	200m Wind Direction	°	200 m	89,778	29,553	32.92	127.4	0.0	360.0	77.1
38	200m Wind Speed	m/s	200 m	89,778	29,553	32.92	5.48	0.04	56.06	2.94
39	200m Wind Vert	m/s	200 m	89,778	29,553	32.92	-0.21	-9.31	0.50	0.57
40	Quality (Station Height 200m)	%		89,778	31,023	34.56	94.1	0.0	100.0	9.5
41	40m Wind Turbulence	m/s	40 m	89,778	23,199	25.84	0.16	0.04	2.37	0.12
42	50m Wind Turbulence	m/s	50 m	89,778	28,017	31.21	0.16	0.03	7.90	0.14
43	60m Wind Turbulence	m/s	60 m	89,778	31,086	34.63	0.16	0.03	6.36	0.15
44	80m Wind Turbulence	m/s	80 m	89,778	31,554	35.15	0.17	0.03	9.57	0.17
45	100m Wind Turbulence	m/s	100 m	89,778	33,352	37.15	0.19	0.02	4.97	0.17
46	120m Wind Turbulence	m/s	120 m	89,778	32,050	35.70	0.20	0.03	34.48	0.26
47	140m Wind Turbulence	m/s	140 m	89,778	29,666	33.04	0.22	0.02	20.64	0.22
48	160m Wind Turbulence	m/s	160 m	89,778	26,856	29.91	0.23	0.00	4.07	0.19
49	180m Wind Turbulence	m/s	180 m	89,778	24,047	26.78	0.24	0.02	9.45	0.23
50	200m Wind Turbulence	m/s	200 m	89,778	21,030	23.42	0.25	0.00	10.00	0.22
51	Turbu. Quality (Station Height 40m)	%		89,778	23,214	25.86	96.0	7.0	100.0	7.5
52	Turbu. Quality (Station Height 50m)	%		89,778	28,045	31.24	96.5	3.0	100.0	6.6

#	Label	Units	Height	Possible Data Points	Valid Data Points	Recovery Rate (%)	Mean	Min	Max	Std. Dev
53	Turbu. Quality (Station Height 60m)	%		89,778	31,143	34.69	96.8	2.0	100.0	6.0
54	Turbu. Quality (Station Height 80m)	%		89,778	31,678	35.28	96.1	0.0	100.0	7.5
55	Turbu. Quality (Station Height 100m)	%		89,778	33,570	37.39	96.5	0.0	100.0	6.5
56	Turbu. Quality (Station Height 120m)	%		89,778	32,374	36.06	96.0	0.0	100.0	7.4
57	Turbu. Quality (Station Height 140m)	%		89,778	30,108	33.54	95.5	0.0	100.0	8.4
58	Turbu. Quality (Station Height 160m)	%		89,778	27,351	30.47	94.9	0.0	100.0	9.5
59	Turbu. Quality (Station Height 180m)	%		89,778	24,611	27.41	94.2	0.0	100.0	10.5
60	Turbu. Quality (Station Height 200m)	%		89,778	21,647	24.11	93.4	0.0	100.0	11.9
61	Ambient Temp	°C	2 m	89,778	66,250	73.79	24.7	6.6	39.0	5.7
62	Barometric Pressure	mbar	2 m	89,778	66,252	73.80	1,590.1	341.7	6,397.9	1,152.2
63	TiltX	°		89,778	66,252	73.80	-0.6503	-0.9000	0.0000	0.0733
64	Azimuth	°		89,778	66,252	73.80	0	0	0	0
65	TiltY	°		89,778	66,252	73.80	0.638	0.500	1.000	0.057
66	Humidity	%		89,778	66,252	73.80	79.4	30.0	97.0	10.8
67	Noise Level-A	dB		89,778	66,252	73.80	12.44	5.00	18.40	2.68
68	Noise Level-B	dB		89,778	66,252	73.80	12.48	5.00	18.20	2.69
69	Noise Level-C	dB		89,778	66,252	73.80	12.44	5.00	18.50	2.69
70	Solar Power	W		89,778	66,252	73.80	0	0	0	0
71	Core Power	W		89,778	66,252	73.80	2.786	2.400	3.400	0.083
72	CPU Power	W		89,778	66,252	73.80	2.379	2.000	3.200	0.169
73	Modem Power	W		89,778	66,252	73.80	0.064	0.000	0.600	0.122
74	Speaker Power	W		89,778	66,252	73.80	4.57	0.10	25.20	3.01
75	PWM Power	W		89,778	66,252	73.80	1.209	0.900	2.500	0.201
76	CPU Temp	°C	2 m	89,778	66,252	73.80	0.0	0.0	0.0	0.0
77	Internal Temp	°C	2 m	89,778	66,252	73.80	28.6	7.3	53.4	8.2
78	Mirror Temp	°C	2 m	89,778	66,252	73.80	27.8	5.5	68.6	9.2
79	Heater Temp	°C	2 m	89,778	66,252	73.80	0.0	0.0	0.0	0.0
80	VibrationX	g		89,778	66,252	73.80	0	0	0	0
81	VibrationY	g		89,778	66,252	73.80	0	0	0	0
82	Battery	Volts		89,778	66,252	73.80	12.84	11.70	14.90	0.68
83	Beep Volume	dB		89,778	66,252	73.80	89.4	0.0	100.0	30.8
84	Status	Mask		89,778	0	0.00				
85	Air Density	kg/m ³		89,778	89,778	100.00	1.688	0.398	7.438	1.173
86	200m Wind Speed WPD	W/m ²		89,778	29,553	32.92	357	0	300,922	2,571
87	180m Wind Speed WPD	W/m ²		89,778	34,105	37.99	304	0	282,466	2,058
88	160m Wind Speed WPD	W/m ²		89,778	38,563	42.95	259	0	98,921	1,160
89	140m Wind Speed WPD	W/m ²		89,778	43,048	47.95	218	0	159,700	1,041
90	120m Wind Speed WPD	W/m ²		89,778	47,792	53.23	171	0	30,641	386
91	100m Wind Speed WPD	W/m ²		89,778	52,660	58.66	136	0	22,164	288
92	80m Wind Speed WPD	W/m ²		89,778	53,356	59.43	104	0	14,644	215
93	60m Wind Speed WPD	W/m ²		89,778	61,846	68.89	71	0	11,159	142
94	50m Wind Speed WPD	W/m ²		89,778	63,385	70.60	58	0	5,237	118
95	40m Wind Speed WPD	W/m ²		89,778	64,338	71.66	48	0	5,897	105

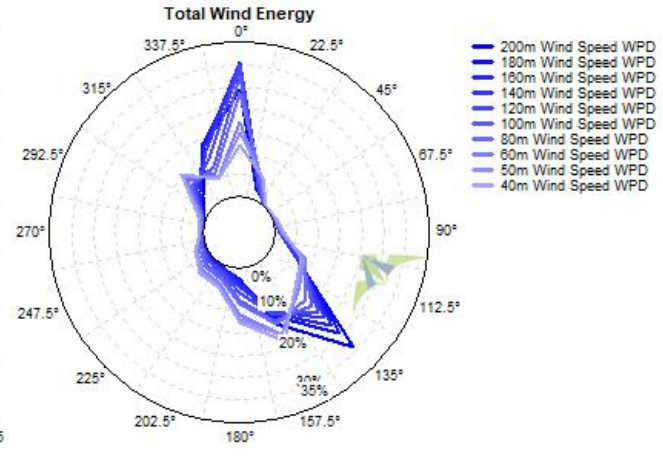
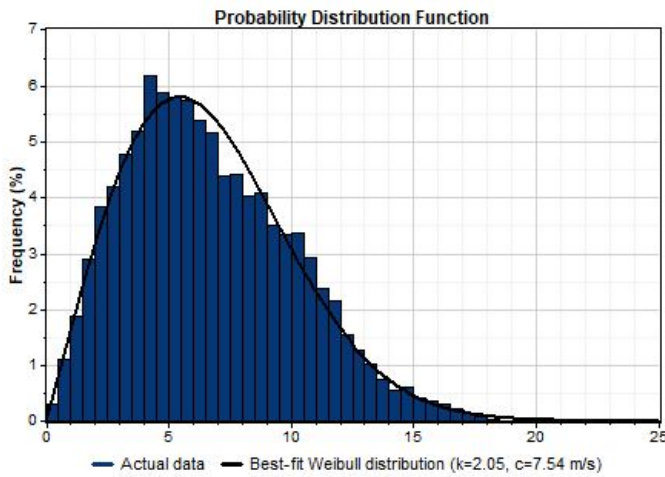
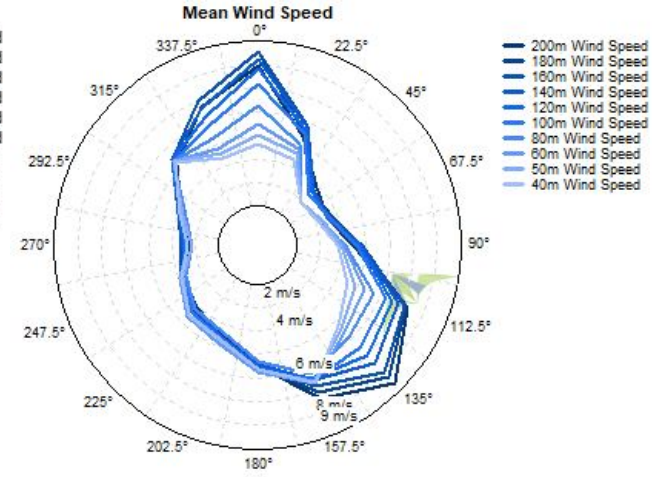
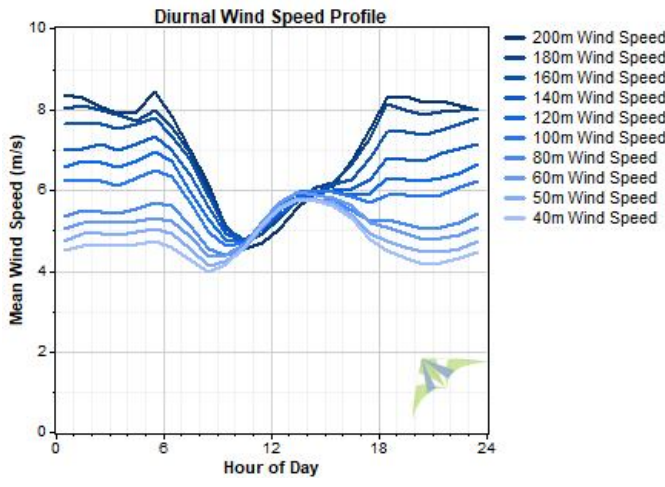
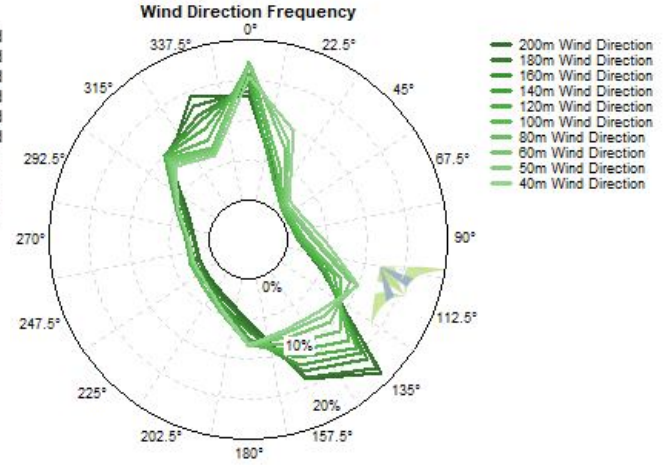
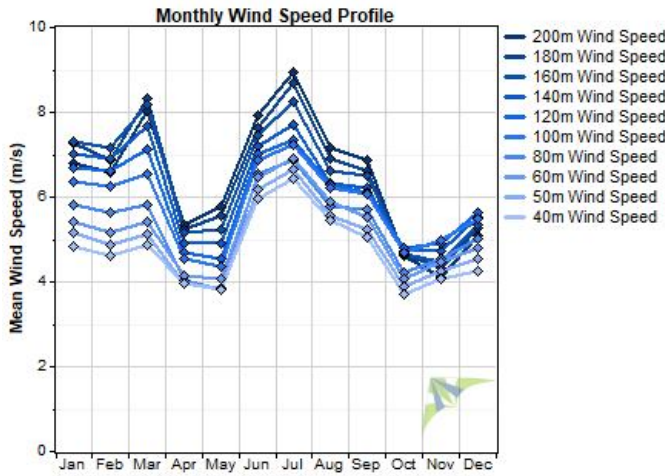
Data Set Properties

Report Created: 4/11/2018 10:40 using Windographer 3.3.10
 Filter Settings: <Unflagged data>

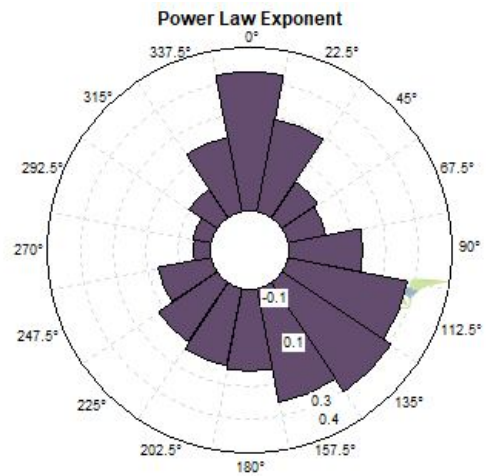
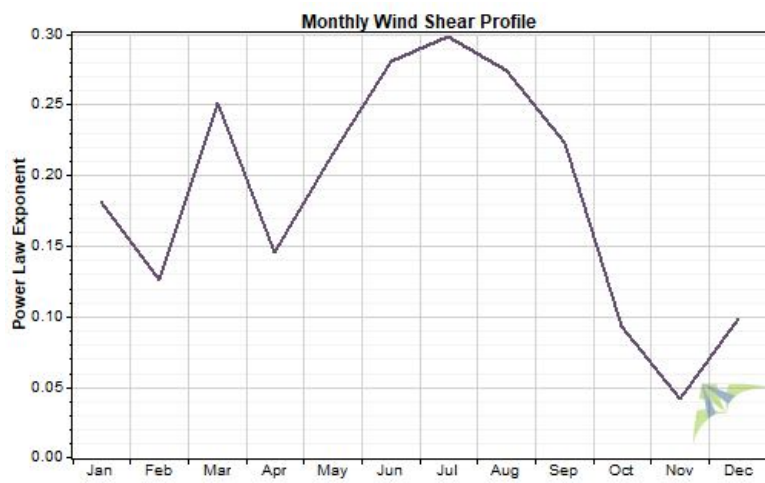
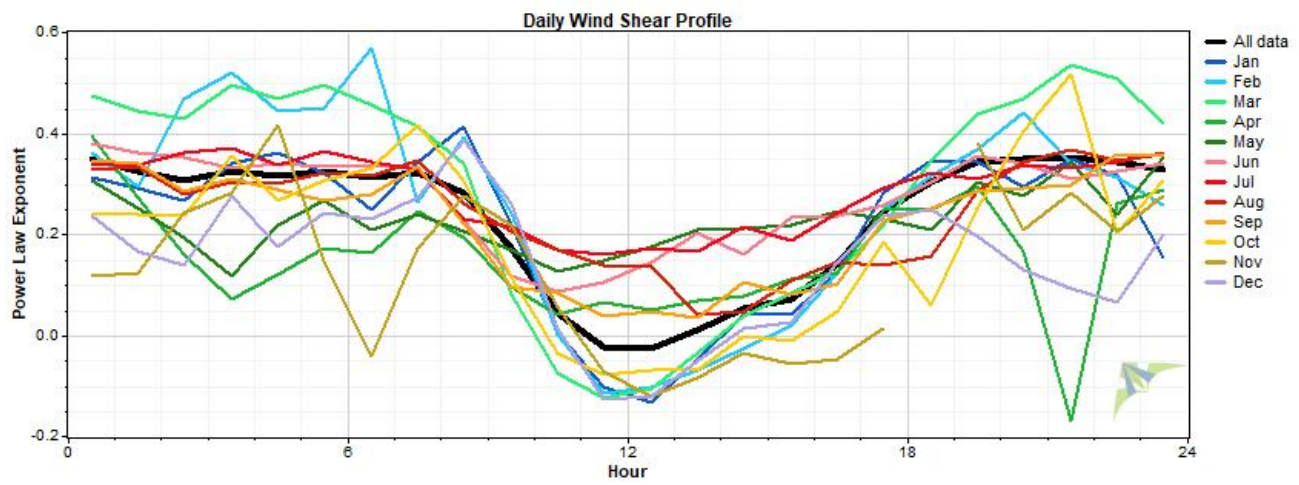
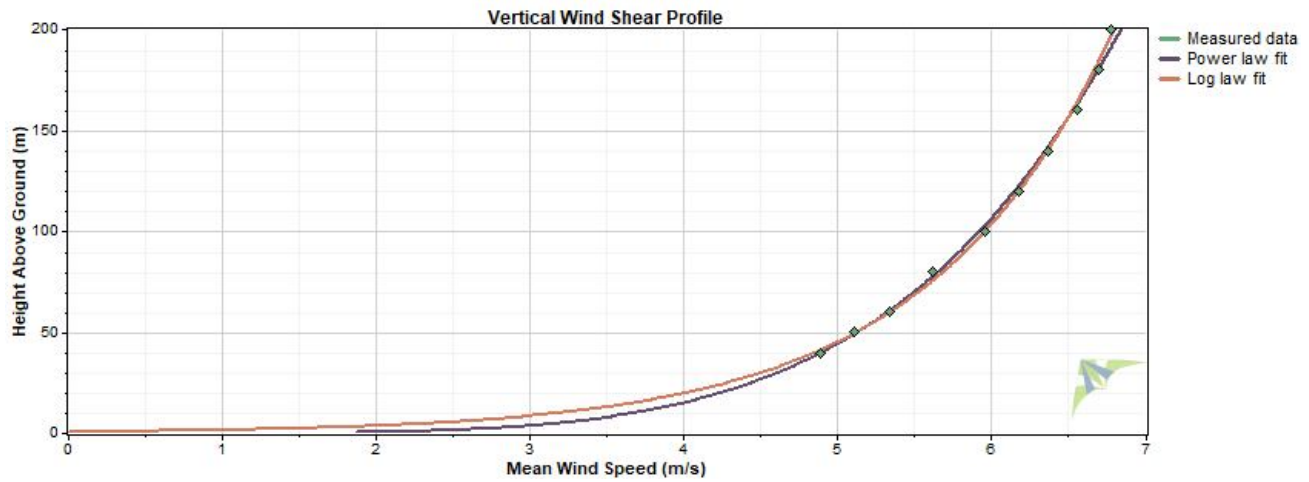
Variable	Value
Latitude	N 21° 8' 50.352"
Longitude	E 92° 4' 32.700"
Elevation	14 m
Start date	7/25/2014 13:30
End date	8/2/2015 10:30
Duration	12 months
Length of time step	10 minutes
Calm threshold	0 m/s
Mean temperature	26.0 °C
Mean pressure	1,009 mbar
Mean air density	1.177 kg/m ³
Power density at 50m	120 W/m ²
Wind power class	1
Power law exponent	0.209
Surface roughness	0.739 m
Roughness class	3.66



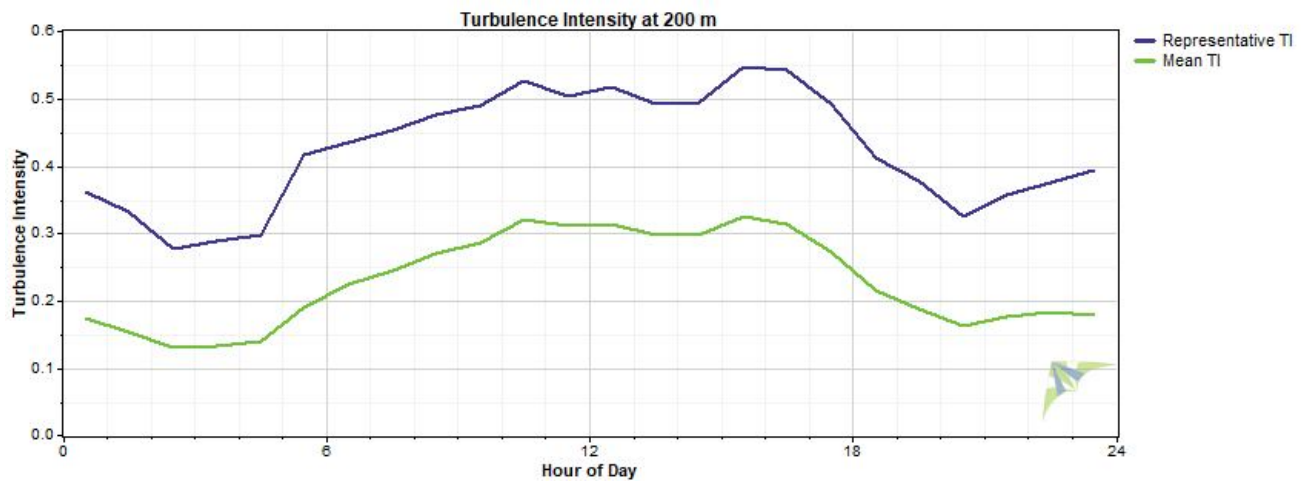
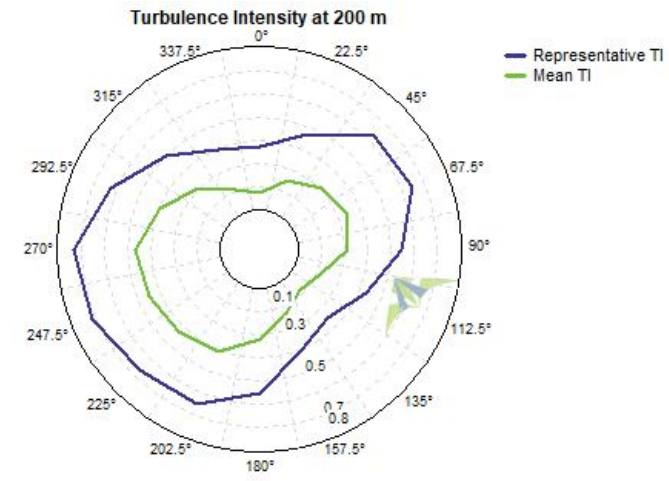
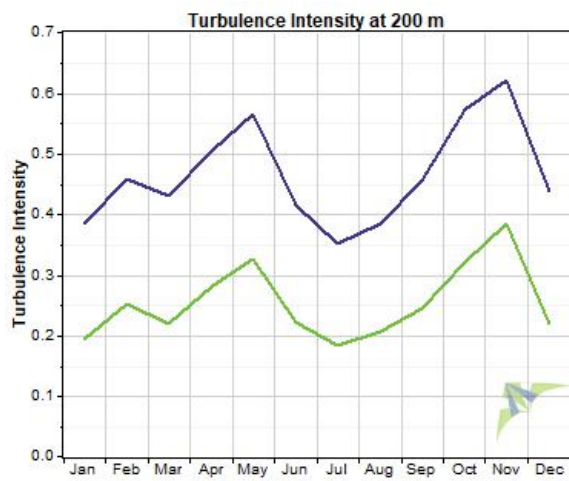
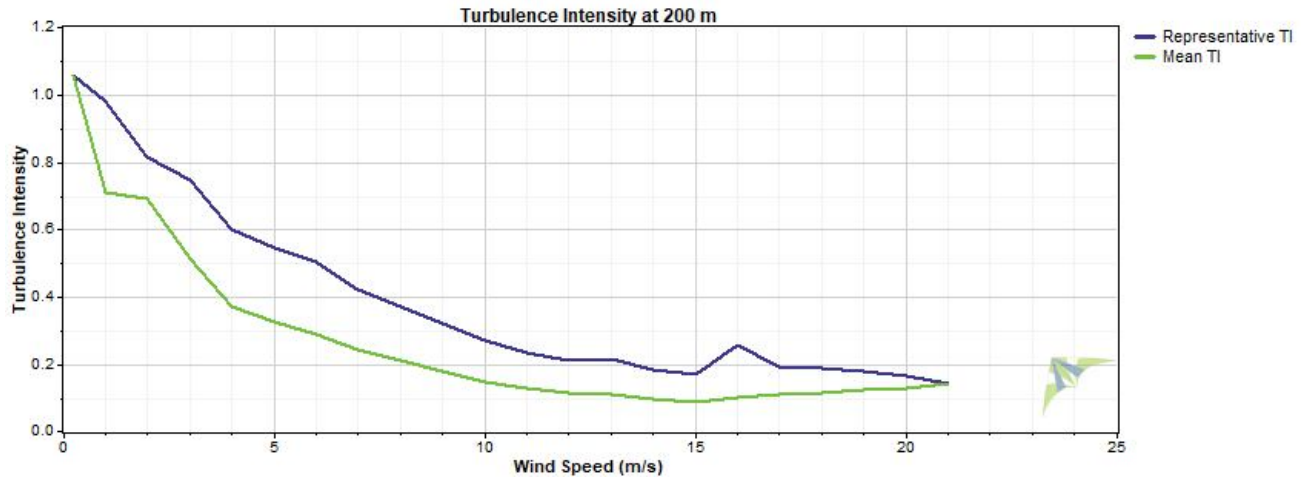
Wind Speed and Direction



Wind Shear



Turbulence Intensity



Data Column Properties

#	Label	Units	Height	Possible Data Points	Valid Data Points	Recovery Rate (%)	Mean	Min	Max	Std. Dev
1	40m Wind Direction	°	40 m	53,694	50,865	94.73	66.7	0.0	360.0	114.6
2	40m Wind Speed	m/s	40 m	53,694	50,865	94.73	4.713	0.070	17.730	2.210
3	40m Wind Vert	m/s	40 m	53,694	50,865	94.73	-0.278	-9.050	0.500	1.087
4	Quality (Station Height 40m)	%		53,694	51,077	95.13	98.2	90.0	100.0	1.2
5	50m Wind Direction	°	50 m	53,694	50,348	93.77	59.6	0.0	360.0	114.8
6	50m Wind Speed	m/s	50 m	53,694	50,348	93.77	4.902	0.020	20.010	2.297
7	50m Wind Vert	m/s	50 m	53,694	50,348	93.77	-0.278	-8.970	0.500	1.080
8	Quality (Station Height 50m)	%		53,694	50,760	94.54	98.1	90.0	100.0	1.4
9	60m Wind Direction	°	60 m	53,694	49,795	92.74	57.9	0.0	360.0	114.3
10	60m Wind Speed	m/s	60 m	53,694	49,795	92.74	5.148	0.030	19.790	2.402
11	60m Wind Vert	m/s	60 m	53,694	49,795	92.74	-0.274	-8.950	0.500	1.065
12	Quality (Station Height 60m)	%		53,694	50,409	93.88	98.0	90.0	100.0	1.6
13	80m Wind Direction	°	80 m	53,694	48,147	89.67	48.3	0.0	360.0	112.4
14	80m Wind Speed	m/s	80 m	53,694	48,147	89.67	5.282	0.030	18.310	2.599
15	80m Wind Vert	m/s	80 m	53,694	48,147	89.67	-0.266	-9.040	0.500	1.025
16	Quality (Station Height 80m)	%		53,694	48,994	91.25	97.5	90.0	100.0	2.1
17	100m Wind Direction	°	100 m	53,694	43,176	80.41	51.8	0.0	360.0	110.7
18	100m Wind Speed	m/s	100 m	53,694	43,176	80.41	5.804	0.050	18.610	2.711
19	100m Wind Vert	m/s	100 m	53,694	43,176	80.41	-0.269	-9.140	0.500	0.998
20	Quality (Station Height 100m)	%		53,694	44,666	83.19	97.0	90.0	100.0	2.5
21	120m Wind Direction	°	120 m	53,694	38,645	71.97	51.2	0.0	360.0	108.9
22	120m Wind Speed	m/s	120 m	53,694	38,645	71.97	6.022	0.020	18.660	2.870
23	120m Wind Vert	m/s	120 m	53,694	38,645	71.97	-0.256	-8.880	0.500	0.924
24	Quality (Station Height 120m)	%		53,694	39,915	74.34	96.4	90.0	100.0	2.8
25	140m Wind Direction	°	140 m	53,694	33,172	61.78	58.0	0.0	360.0	108.2
26	140m Wind Speed	m/s	140 m	53,694	33,172	61.78	6.254	0.090	18.690	3.041
27	140m Wind Vert	m/s	140 m	53,694	33,172	61.78	-0.243	-8.830	0.500	0.826
28	Quality (Station Height 140m)	%		53,694	34,272	63.83	95.9	90.0	100.0	2.9
29	160m Wind Direction	°	160 m	53,694	26,555	49.46	69.7	0.0	360.0	108.9
30	160m Wind Speed	m/s	160 m	53,694	26,555	49.46	6.539	0.030	19.750	3.246
31	160m Wind Vert	m/s	160 m	53,694	26,555	49.46	-0.241	-8.800	0.500	0.740
32	Quality (Station Height 160m)	%		53,694	27,678	51.55	95.5	90.0	100.0	3.0
33	180m Wind Direction	°	180 m	53,694	20,819	38.77	83.1	0.0	360.0	108.8
34	180m Wind Speed	m/s	180 m	53,694	20,819	38.77	6.681	0.070	21.590	3.371
35	180m Wind Vert	m/s	180 m	53,694	20,819	38.77	-0.232	-8.530	0.500	0.597
36	Quality (Station Height 180m)	%		53,694	21,870	40.73	95.2	90.0	100.0	2.9
37	200m Wind Direction	°	200 m	53,694	16,279	30.32	96.4	0.0	360.0	109.4
38	200m Wind Speed	m/s	200 m	53,694	16,279	30.32	6.672	0.090	21.100	3.418
39	200m Wind Vert	m/s	200 m	53,694	16,279	30.32	-0.227	-8.020	0.500	0.463
40	Quality (Station Height 200m)	%		53,694	17,219	32.07	94.7	90.0	100.0	2.8
41	40m Wind Turbulence	m/s	40 m	53,694	35,763	66.61	0.14	0.05	1.22	0.09
42	50m Wind Turbulence	m/s	50 m	53,694	36,175	67.37	0.14	0.04	1.35	0.09
43	60m Wind Turbulence	m/s	60 m	53,694	36,885	68.69	0.14	0.04	1.42	0.10
44	80m Wind Turbulence	m/s	80 m	53,694	34,400	64.07	0.15	0.04	1.32	0.11
45	100m Wind Turbulence	m/s	100 m	53,694	33,128	61.70	0.17	0.03	1.71	0.13
46	120m Wind Turbulence	m/s	120 m	53,694	29,850	55.59	0.19	0.03	1.77	0.15
47	140m Wind Turbulence	m/s	140 m	53,694	25,975	48.38	0.21	0.03	1.52	0.16
48	160m Wind Turbulence	m/s	160 m	53,694	21,168	39.42	0.22	0.03	1.40	0.16
49	180m Wind Turbulence	m/s	180 m	53,694	16,671	31.05	0.23	0.03	1.40	0.17
50	200m Wind Turbulence	m/s	200 m	53,694	12,807	23.85	0.24	0.03	1.68	0.17
51	Turbu. Quality (Station Height 40m)	%		53,694	35,890	66.84	98.2	90.0	100.0	1.8
52	Turbu. Quality (Station Height 50m)	%		53,694	36,430	67.85	98.2	90.0	100.0	1.8

#	Label	Units	Height	Possible Data Points	Valid Data Points	Recovery Rate (%)	Mean	Min	Max	Std. Dev
53	Turbu. Quality (Station Height 60m)	%		53,694	37,231	69.34	98.2	90.0	100.0	1.8
54	Turbu. Quality (Station Height 80m)	%		53,694	34,897	64.99	97.9	90.0	100.0	2.1
55	Turbu. Quality (Station Height 100m)	%		53,694	34,073	63.46	97.3	90.0	100.0	2.5
56	Turbu. Quality (Station Height 120m)	%		53,694	30,710	57.19	96.7	90.0	100.0	2.8
57	Turbu. Quality (Station Height 140m)	%		53,694	26,777	49.87	96.2	90.0	100.0	3.0
58	Turbu. Quality (Station Height 160m)	%		53,694	21,983	40.94	95.7	90.0	100.0	3.0
59	Turbu. Quality (Station Height 180m)	%		53,694	17,462	32.52	95.3	90.0	100.0	3.0
60	Turbu. Quality (Station Height 200m)	%		53,694	13,484	25.11	94.8	90.0	100.0	2.9
61	Ambient Temp	°C	2 m	53,694	51,503	95.92	26.0	13.7	35.9	3.6
62	Barometric Pressure	mbar	2 m	53,694	51,503	95.92	1,008.8	982.6	1,097.6	4.9
63	TiltX	°		53,694	51,503	95.92	-0.3670	-0.6000	0.0000	0.0788
64	TiltY	°		53,694	51,503	95.92	0.4301	0.3000	0.7000	0.0596
65	Azimuth	°		53,694	51,503	95.92	0	0	0	0
66	Humidity	%		53,694	51,503	95.92	77.2	19.0	98.0	11.7
67	Noise Level-A	dB		53,694	51,503	95.92	13.00	5.00	18.30	2.18
68	Noise Level-B	dB		53,694	51,503	95.92	13.01	5.00	18.10	2.18
69	Noise Level-C	dB		53,694	51,503	95.92	12.98	5.00	18.20	2.18
70	PWM Power	W		53,694	51,503	95.92	1.250	0.900	2.400	0.212
71	CPU Power	W		53,694	51,503	95.92	2.348	2.100	3.000	0.123
72	Core Power	W		53,694	51,503	95.92	2.802	2.500	3.100	0.076
73	Solar Power	W		53,694	51,503	95.92	0	0	0	0
74	Modem Power	W		53,694	51,503	95.92	0.036	0.000	0.600	0.076
75	Speaker Power	W		53,694	51,503	95.92	5.13	0.10	21.80	2.99
76	CPU Temp	°C	2 m	53,694	51,503	95.92	0.0	0.0	0.0	0.0
77	Internal Temp	°C	2 m	53,694	51,503	95.92	28.9	14.2	46.7	5.9
78	Heater Temp	°C	2 m	53,694	51,503	95.92	0.0	0.0	0.0	0.0
79	Mirror Temp	°C	2 m	53,694	51,503	95.92	28.3	13.3	62.5	6.9
80	VibrationX	g		53,694	51,503	95.92	0	0	0	0
81	VibrationY	g		53,694	51,503	95.92	0	0	0	0
82	Battery	Volts		53,694	51,503	95.92	12.92	11.60	14.70	0.63
83	Beep Volume	dB		53,694	51,503	95.92	90.1	0.0	100.0	29.8
84	Air Density	kg/m ³		53,694	53,694	100.00	1.177	1.129	1.311	0.020
85	200m Wind Speed WPD	W/m ²		53,694	16,279	30.32	325	0	5,531	465
86	180m Wind Speed WPD	W/m ²		53,694	20,819	38.77	322	0	5,926	463
87	160m Wind Speed WPD	W/m ²		53,694	26,555	49.46	298	0	4,539	416
88	140m Wind Speed WPD	W/m ²		53,694	33,172	61.78	255	0	3,791	348
89	120m Wind Speed WPD	W/m ²		53,694	38,645	71.97	223	0	3,775	291
90	100m Wind Speed WPD	W/m ²		53,694	43,176	80.41	195	0	3,725	252
91	80m Wind Speed WPD	W/m ²		53,694	48,147	89.67	155	0	3,576	218
92	60m Wind Speed WPD	W/m ²		53,694	49,795	92.74	138	0	4,506	212
93	50m Wind Speed WPD	W/m ²		53,694	50,348	93.77	121	0	4,658	196
94	40m Wind Speed WPD	W/m ²		53,694	50,865	94.73	108	0	3,217	182

www.nrel.gov/usaid-partnership



USAID
FROM THE AMERICAN PEOPLE

United States Agency for International Development
1300 Pennsylvania Avenue NW • Washington, DC 20523
+1-202-712-0000
www.usaid.gov

Jennifer E. Leisch, Ph.D.
USAID-NREL Partnership Manager
U.S. Agency for International Development
Tel: +1-303-913-0103
Email: jleisch@usaid.gov

Shayan Shafi
Bangladesh Mission Energy Contact
U.S. Agency for International Development (USAID)/Bangladesh
Tel: +8801713031078
Email: sshafi@usaid.gov



National Renewable Energy Laboratory
15013 Denver West Parkway • Golden, CO 80401
+1-303-275-3000
www.nrel.gov

Andrea Watson
USAID Portfolio Manager
National Renewable Energy Laboratory (NREL)
Tel: +1-303-275-4234
Email: andrea.watson@nrel.gov

NREL is a national laboratory of the U.S. Department of Energy, Office of Energy Efficiency & Renewable Energy, operated by the Alliance for Sustainable Energy, LLC.
NREL/TP-5000-71007 • September 2018